Thermalisation and Relaxation

of Quantum Systems

Dissertation

zur Erlangung des Grades

des Doktors der Naturwissenschaften

der Naturwissenschaftlich- Technischen Fakultät

der Universität des Saarlandes

und

der Université de Lorraine

von

Sascha Sebastian Wald

Saarbrücken/Nancy

2017

Eidesstattliche Versicherung

Hiermit versichere ich an Eides statt, dass ich die vorliegende Arbeit selbstständig und ohne Benutzung anderer als der angegebenen Hilfsmittel angefertigt habe. Die aus anderen Quellen oder indirekt übernommenen Daten und Konzepte sind unter Angabe der Quelle gekennzeichnet. Die Arbeit wurde bisher weder im In- noch im Ausland in gleicher oder ähnlicher Form in einem Verfahren zur Erlangung eines akademischen Grades vorgelegt.

Saarbrücken, den ....

....
(Sascha Sebastian Wald)

Tag des Kolloquiums:	28.09.2017
Dekan:	Prof. Dr. Guido Kickelbick
Mitglieder des Prüfungsausschusses:	Prof. Dr. Dragi Karevski
	Prof. Dr. Malte Henkel
	Prof. Dr. Giovanna Morigi
	Prof. Dr. Tomaz Prosen
	Dr. Anna Minguzzi
	Prof. Dr. Frank Wilhelm

„Irrend lernt man."

Goethe, Briefe. An August von Goethe

Acknowledgement

Contents

Summaries

Summary - english

This study deals with the dynamic properties of open quantum systems far from equilibrium in d dimensions. The focus is on a special, exactly solvable model, the spherical model (SM), which is technically simple. The analysis is of interest, since the critical behaviour in and far from equilibrium not of mean-field type. We begin with a résumé of the statistical mechanics of phase transitions and treat especially the quantum version of the SM. The quantum dynamics (QD) of the model cannot be described by phenomenological Langevin equation and must be formulated with Lindblad equations.First we examine the dynamic phase diagram of a single spherical quantum spin and interpret the solution as a mean-field approximation of the N-body problem. Hereby, we find a quantum mechanical 'freezing by heating' effect. After that, we extend the formalism to the N-body problem, determining first the form of the Lindblad equation from consistency conditions. The SM then allows the reduction to a single integro-differential equation whose asymptotic solution shows, that the effective QD in the semi-classical limit is fully classical. For a deep quench in the ordered phase, we show that the QD strongly and non-trivially depends on d and derive the dynamic scaling behaviour and its corrections. The mathematical tools for this analysis are new results on the asymptotic behaviour of certain confluent hypergeometric functions in two variables.

Zusammenfassung - deutsch

Diese Studie behandelt dynamische Eigenschaften offener Quantensysteme fern vom Gleichgewicht (GG) in d Dimensionen. Der Fokus liegt auf einem speziellen exakt lösbaren Modell, dem sphärischen Modell (SM), welches einfach zu behandeln ist. Die Analyse ist von Interesse, da das kritische Verhalten im und fern vom GG nicht vom Molekularfeldtypus ist. Wir beginnen mit einem Résumé zur statistischen Mechanik von Phasenübergängen und behandeln speziell die Quantenversion des SM. Die Quantendynamik (QD) des Modells kann nicht durch phänomenologische Langevingleichungen beschrieben werden und muss mit Lindbladgleichungen (LG) formuliert werden. Zunächst untersuchen wir das dynamische Phasendiagramm eines einzelnen sphärischen Quantenspins und deuten die Lösung als Molekularfeldnäherung des N-Körperproblems. Dabei finden wir einen quantenmechanischen „Einfrieren durch Aufheizen"-Effekt. Danach erweitern wir den Formalismus auf das N-Körperproblem, wobei zuerst die Form der LG aus Konsistenzbedingungen hergeleitet wird. Das SM erlaubt dann die Reduktion auf eine einzige Integrodifferentialgleichung, deren asymptotische Lösung zeigt, dass im halbklassischen Grenzfall die effektive QD klassisch ist. Für ein tiefes Abschrecken in die geordnete Phase zeigen wir, dass die QD stark und nicht-trivial von d abhängt und stellen das dynamische Skalenverhalten und zugehörige Korrekturen dar. Mathematisches Hilfsmittel dabei sind neue Ergebnisse zur Asymptotik hypergeometrischer Funktionen in zwei Variablen.

Résumé - français

Cette thèse traite la dynamique hors équilibre des systèmes quantiques ouverts couplés à un réservoir externe. Un modèle spécifique exactement soluble, le modèle sphérique, sert comme exemple paradigmatique. Ce modèle se résout exactement en toute dimension spatiale et pour des interactions très générales. Malgré sa simplicité technique, ce modèle est intéressant car ni son

comportement critique d'équilibre ni celui hors équilibre est du genre champ moyen. La présentation débute avec une revue sur la mécanique statistique des transitions de phases classique et quantique, et sur les propriétés du modèle sphérique. Sa dynamique quantique ne se décrit point à l'aide d'une équation de Langevin phénoménologique. Une description plus complète à l'aide de la théorie de l'équation de Lindblad est nécessaire. Les équations de Lindblad décrivent la relaxation d'un système quantique vers son état d'équilibre. En tant que premier exemple, le diagramme de phases dynamique d'un seul spin sphérique quantique est étudié. Réinterprétant cette solution en tant qu'une approximation champ moyen d'un problème de N corps, le diagramme de phases quantique est établi et un effet « congeler en réchauffant » quantique est démontré. Ensuite, le formalisme de Lindblad est généralisé au modèle sphérique quantique de N particules: primo, la forme précise de l'équation de Lindblad est obtenue des conditions que (i) l'état quantique d'équilibre exacte est une solution stationnaire de l'équation de Lindblad et (ii) dans le limite classique, l'équation Langevin de mouvement est retrouvée. Secundo, le modèle sphérique permet la réduction exacte du problème de N particules à une seule équation intégro-différentielle pour le paramètre sphérique. Tertio, en résolvant pour le comportement asymptotique des temps longs de cette équation, nous démontrons que dans la limite semi-classique, la dynamique quantique effective redevient équivalente à une dynamique classique, à une renormalisation quantique de la température T près. Quarto, pour une trempe quantique profonde dans la phase ordonnée, nous démontrons que la dynamique quantique dépend d'une manière non triviale de la dimension spatiale. L'émergence du comportement d'échelle dynamique et des corrections logarithmiques est discutée en détail. Les outils mathématiques de cette analyse sont des nouveaux résultats sur le comportement asymptotique de certaines fonctions hypergéométriques confluentes en deux variables.

Chapter 1

Introduction

In physics, *phases of matter* are defined as *uniform* states in which important *collective* properties of a many-body system coincide and one observes *macroscopic laws* which hold true throughout the entire phase and usually change sharply when the system crosses over from one phase to another one [Nis11, Yeo92, Dom96, Car96b, Voj03, Sac01]. Such transitions between different phases are omnipresent in nature and well-known from our daily life experience. Probably the best-known example is water which is liquid under standard conditions for pressure and temperature but freezes at low temperatures turning into a solid (lakes in winter, polar ice caps) or vaporises at high temperatures turning into vapour. Although the microscopic interactions between individual water molecules do not change, the macroscopic behaviour (mechanic, optic, ...) changes drastically in response to changes in thermodynamics parameters such as temperature or pressure. A qualitative phase diagram of water[1] shown in fig 1.1 reveals that there are three main phases: liquid, solid and vapour [Bri37, Pre04, Pap07].

Another daily life example is the structural transition of graphite and diamond that allows us to write with a pencil (graphite) while the same material in a different phase is amongst the hardest materials on earth (diamond) [Bun55, Hol01].

One of the best-studied classes of phase transitions is the one between ferro- and paramagnetic states. The high critical temperatures in many ferromagnets, including the classical examples of iron and nickel, can only be understood from quantum mechanics, although the transition mechanism itself is classical [Jäg96]. On the other hand, the ferromagnetic transition in dipolar-coupled chains in a transverse magnetic field are model examples of *quantum phase transitions* [Bit96, Kra12, Bab16].

Moreover, *superconductors* which allow to transport electrical currents without any dissipation (Joule heat) at very low temperatures (a material that is superconducting around ~ 100 [K] is considered to be a high-T superconductor) have attracted attention for their vast range of technical applications since their discovery by *H.K. Onnes* in 1911 [Onn11]. This discovery was "the first time, quantum phenomena were showing up at low temperature" in history [vD10] and while these materials still conduct electrical current at normal temperatures what their low temperature behaviour differs drastically from their "usual" characteristics. This implies that superconductivity is nothing but a phase of the conductor. Recently there has been a new high temperature record achieved for sulphur hydride H_2S which transforms under high pressure ~ 100 [GPa] to a superconductor. The critical temperature measured is 203 [K] [Dro15, Hei15] which is significantly higher than the previous record of 164 [K] in cuprates [Gao94]. This sort of hydrogen-based materials can even be expected to lead to room temperature superconductivity as the hydrogen atoms provide the high frequency phonon modes and strong electron-phonon coupling [Dro15].

Even our universe is believed to have undergone a series of different phase transitions which lead to the building of defects by crossing the phase boundaries (planets) [Kib80].

All these transitions and many others (see tab 1.1) occur if certain *external driving parameters*

---

[1]Contrary to widely hold beliefs, the thermodynamics of liquid water, and not only of solid ice, is complex. For instance, two distinct phases of liquid water have experimentally been seen to co-exist at a temperature of 125 [K] and a pressure of 1 [bar] [Per17].
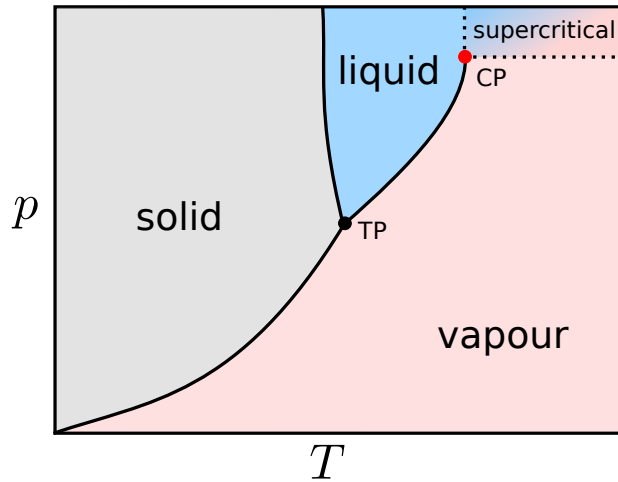
Figure 1.1: Schematic phase diagram of water with 3 different phases: solid, liquid and vapour. We mark the triple point where all these phases coexist with TP and the critical point where the system undergoes a continuous phase transition with CP.

like the temperature, pressure, density etc. reach a *critical value* and the point where the transition occurs is called a *critical point*. This specific point was first observed by *Cagniard de la Tour* as early as 1822 [dlT22] and he is therefore rightfully considered as the discoverer of *critical phenomena* [Ber09] although the name was attributed only much later by *T. Andrews* in 1869 [And69]. De la Tour heated a sealed glass tube filled with liquid alcohol until the whole volume vaporised and became transparent. He then cooled the tube down again and observed a thick cloud which is now acknowledged as the observation of the critical opacity and thus the discovery of the critical point. Despite the distinction between gas and liquid was already established by earlier experiments performed by Jean-François Clouet (1751 – 1801) and Gaspard Monge (1746 – 1818) the critical point had never been observed before.

We thus see that phase transitions influence not just our daily life but the concepts are rather general and being applied to a lot of different fields of research. This makes the theory of critical phenomena a flourishing and thriving discipline on the one hand while being a well-established and classical discipline on the other hand.

We shall now review the modern description of critical phenomena and put special emphasis on the quantum counterpart. As paradigmatic examples, we shall use the Ising and the spherical models. We shall then analyse the statistical behaviour of a quantum system close to criticality explicitly. In order to describe collective dynamical quantum properties we shall then introduce the Lindblad equation as a formalism that describes a true quantum relaxation with the semi-group property [Lin76, Bre07, Sch14].

1.1   A brief summary of phase transitions

This section recalls the main features of both classical and quantum phase transitions and critical phenomena. We therefore start by introducing general concepts of phase transitions and then focus later on quantum properties.

The literature on this topic is vast and any list of references is somewhat incomplete. Hence, there exist many good older and more recent sources that we consulted for this brief summary and to which we refer for further details [Yeo92, Car96b, DF97, Hen99, Ma00, Nis11, Pap07, Sac01].

We shall focus in this section on the classical formulation of statistical mechanics and the description of critical points and refer the reader to the following reviews of *selected* more modern topics in the field.

Table 1.1: Examples of phase transitions, see [Yeo92, Ma00, Dro15], and references therein.

transition	order parameter	example
ferromagnetic	magnetisation	Fe
antiferromagnetic	sublattice magnetisation	MnO
ferrimagnetic	sublattice magnetisation	Fe_3O_4
structural	atomic displacements	$SrTiO_3$
ferroelectric	electric polarization	$BaTiO_3$
order-disorder	sublattice atomic concentration	CuZn
phase separation	concentration difference	$CCl_4 + C_7F_{16}$
superfluid	condensate wave function	liquid He
superconductivity	ground state wave function	Al, Nb_3Sn
high-T_c superconductivity	ground state wave function	H_2S

1. The statistical mechanics of *complex networks* has attracted a lot of interest in the last decades since it reveals collective properties of very different systems as e.g. cells, the Internet, chemical reactions or different aspects of society. Consequently, this field is not just of pure scientific but as well of a high technological interest and thus highly dynamic. We refer to [Alb02, Wac07] and references therein for a recent review.

2. The transitions with which we shall be dealing in the present work rely on the mechanism of symmetry breaking. A class of different transitions is studied in the field of *topological insulators*: the quantum Hall effect has led to a fundamentally new classification based on topological order. For recent reviews on the field of topological insulators see [Has10, And13] and references therein.

3. The theory of *dynamical critical phenomena* deals with the description of systems that are out of and relax towards equilibrium. It is concerned with the change of material properties over time and studies effects as e.g. ageing. For recent reviews we consult e.g. [Hen09, Hen10, Hoh77] and mention that we shall be concerned in the later chapters with quantum relaxation processes.

4. Experiments in *ultracold atoms* have turned out to provide an excellent testing ground to study many-body physics due to the high tunability of the interactions in these systems. For a review on recent progress in the field of statistical mechanics of ultracold atoms we refer to [Blo08, Pet02, Pit03, Leg01, Leg03, Dal99] and references therein.

1.1.1 General properties of phase transitions

Any physical system made up of a large number of degrees of freedom is said to undergo a *phase transition* if its macroscopic properties undergo an important qualitative change [Yeo92]. For example, a liquid can vaporise or freeze, an isolator can become a conductor or a superconductor, a metal can become a magnet etc. as we discussed in the preceding section.

Such a change can occur in *different physical quantities* like the electric conductivity, the magnetisation or the viscosity to name a few and is routinely driven by an *external* control parameter (temperature, pressure, density, ...). In tab 1.1 we list some examples of phase transitions occurring in nature and name their *order parameter*. This is a quantity that distinguishes the different phases between which the transition occurs and thus quantifies the qualitative change of the physical properties of the system.
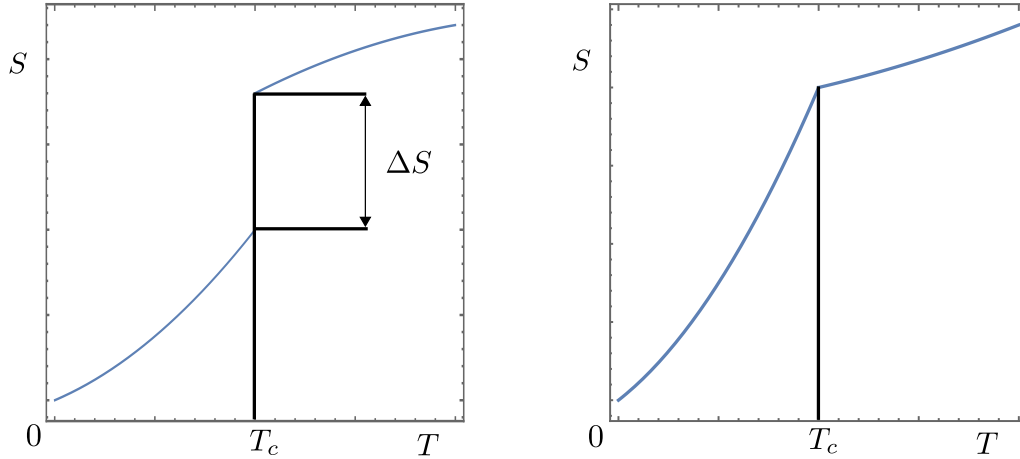
Figure 1.2: Entropy S as a function of temperature for a first-order phase transition (left panel) and for a continuous phase transition (right panel). In the first order transition the entropy has a jump at the critical temperature T_c which results in a *latent heat* due to the difference ΔS. In the continuous case there is no latent heat and the entropy has a continuous non-analyticity at T_c.

Generally, one distinguishes *first-order* and *continuous* phase transitions[2] as follows [Hua01]

- at a first-order transition, the different phases co-exist at the critical point and the phases are distinguishable, e.g. by a finite difference in entropy, see left panel of fig 1.2.

- at a continuous transition, the different phases become indistinguishable. First derivatives of the thermodynamics potentials (free energy), e.g. the entropy, the latent heat of the spontaneous magnetization, are continuous.

In this introduction we are mainly concerned with continuous transition and thus use from now on the term phase transition referring to continuous transitions. A non-analyticity as pictured in the right panel of fig 1.2 for continuous phase transitions, leads to diverging physical quantities (thermodynamic derivatives) as e.g. the correlation length. This on the other hand implies that *all length scales* become important at criticality and that long-range correlations are dynamically created throughout the entire system [Hen99]. This process leads to the birth of large clusters of macroscopic size and stretching across the entire system, typically washing out microscopic details. Indeed, the transition is found to depend only on a few properties of the system such as its (spatial) dimension, the range of interactions (short vs. long range interaction) or the symmetry of the system [Nis11]. This fact is called *universality* and it is probably the most fundamental principle in the theory of phase transitions since it allows us to model complicated macroscopic systems into highly simplified microscopic models and still describe the same universal features. The statement of universality emerges from elaborate arguments in the so-called *Renormalisation Group Theory* [Wil75] where one can show the irrelevance of these microscopic properties explicitly by applying scale transformations to the system[3] [Nis11].

The *textbook model* studied to illustrate continuous phase transitions is the $2D$ isotropic Ising model which consists of a $2D$ regular square lattice where every vertex is occupied by a binary spin variable $\sigma \in \{\pm 1\}$ (a configuration is illustrated in fig 1.3 by arrow up and down). The Hamilton function with short range nearest-neighbour interaction reads

$$H_{\text{Ising}} = -J \sum_{\langle n,m \rangle} \sigma_n \sigma_m \tag{1.1.1}$$

where J is the exchange energy which is in general of quantum mechanical origin[4] [Jäg96]. This model was proposed in the 1920's by *Wilhelm Lenz* who was Ernst Ising's supervisor and who

---

[2]Historically the term n-th order phase transition was introduced to distinguish different orders of divergences but from a physical point of view the most relevant ingredient is the (dis-) continuity.

[3]We shall give a brief overview of concepts of the Renormalisation Group later in the text.

[4]We shall rescale the exchange energy in the following sections as $J = 1$.
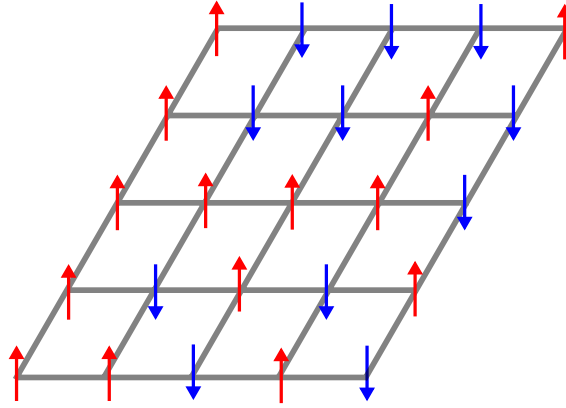
Figure 1.3: Schematic representation of a configuration of the $2D$ Ising model on a square lattice.

never really insisted to be recognised as the inventor of the model. In his thesis, Ising studied the partition function of the Ising model in one dimension and showed that there exists *no* ordered phase and thus the model did not seem suitable to explain ferromagnetism [Bru67]. As a simple explanation Ising proposed to imagine an ordered state $\left| \uparrow \uparrow \uparrow \ \dots \uparrow \uparrow \right\rangle$ which under thermal fluctuations can be spontaneously split into two regions $\left| \uparrow \ \dots \uparrow \downarrow \uparrow \dots \uparrow \right\rangle$. Then there is no mechanism in the system that would prevent either site from spontaneously collectively flip and thus the ordered state is not stable. In his argument Ising missed the fact that it applies exclusively in one spatial dimension and moreover, this exact result is in contrast with the so-called mean-field approximation, which predicts a continuous phase transition at some critical temperature $T_c > 0$ in any dimension d.

In the early 1930s Ising, as a German-Jewish scientist, lost his position at a public schools as Hitler came to power [Kob00]. He "*survived the war in a small town in Luxembourg*" but "*was there completely shut of from scientific and social life.*" [Bru67]. After having left Germany in 1939 and having arrived to USA "*Ising became aware of the first and the only contemporary citation of his paper by Heisenberg*" [Kob00] who developed the *Heisenberg model* [Hei28] as a generalisation of the Ising model. By introducing a more sophisticated interaction between nearest-neighbour spins, he tried to explain ferromagnetism which Ising was not able to do in his system. In this manner it took Ising until 1949 to become aware of the fact that his model became widely known [Kob00].

The existence of a phase transition in the Ising model, in $d \geq 2$ dimensions, was proven rigorously by Peierls in 1936 [Pei36] and the $2D$ Ising model was solved exactly in 1944 [Ons44] showing indeed a phase transition between a disordered and an ordered phase at the transition temperature

$$T_c^{(\text{2D Ising})} = \frac{2J}{\log\left(1 + \sqrt{2}\right)} \ .$$
(1.1.2)

Above this temperature the macroscopic order, triggered by nearest-neighbour interaction is destroyed by *thermal fluctuations*. Such a transition is said to be *classical* because it is driven by temperature. There exists another ensemble of transitions that are *not* thermally driven and take place at zero temperature as a function of a non-thermal driving parameter and the macroscopic order is destroyed by *quantum fluctuations*. Despite posing a mathematically well-defined problem such transitions raise immediately the fundamental question:

Why should one study a transition phenomena that occurs at an experimentally non-accessible temperature?

The study of these phenomena is vastly motivated by different aspects. On the one hand quantum

criticality occurs in large portions of the phase diagram and the asymptotic critical behaviour can be influenced by quantum fluctuations as we shall see later on. On the other hand quantum properties can indeed influence measurable quantities in these regions (e.g. superconductivity) and thus, quantum critical behaviour has solved many prominent puzzles of classical physics as rare-earth magnetic insulators [Bit96], high-temperature superconductivity [Dag94, Map98] or two dimensional electron gases [Son97, Kra95], which is probably the strongest argument in favour of studies concerning quantum criticality. Today, such quantum phase transitions can be studied experimentally, for example in certain dipolar-coupled magnets in either $1D$ or $2D$ and in a transverse field [Bit96, Kra12, Bab16], compare section 1.2.3 and e.g. [Sac11].

It is thus necessary to give a qualitative overview where quantum effects arise and when they are relevant. Therefore, we have to introduce the basic notions of scaling theory at a continuous phase transition and come back later to an explicit comparison between classical and quantum properties.

1.1.2   Statistical mechanics of phase transitions

As we discussed briefly in the previous section, phase transitions are *universal* and therefore it is possible to formulate the whole theory in the language of ferromagnetic phase transitions since the Ising model is available as a simple toy model.

Our starting point is the *canonical partition function*[5]

$$\mathcal{Z} = \sum_{\{\sigma\}} \mathrm{e}^{-H[\{\sigma\}]/T} \tag{1.1.3}$$

where the sum runs over all possible configurations $\{\sigma\}$ of the system, H is the Hamilton function and T the temperature of a reservoir which is in contact with the system[6]. From the partition function the *Gibbs free energy* $\mathcal{G}$ and the *free energy* $\mathcal{F}$ are defined as

$$\mathcal{G} = \mathcal{G}(T, h) = -T \log \mathcal{Z} \tag{1.1.4}$$

$$\mathcal{F} = \mathcal{F}(T, M) = -T \log \mathcal{Z} \ . \tag{1.1.5}$$

The distinction between these potential amounts to the fact that in magnets, one uses either an ensemble with fixed magnetic field and the Gibbs free energy as associated thermodynamic potential or else an ensemble with fixed magnetisation and the free energy. These two thermodynamic potentials are related in the large-system limit $\mathcal{N} \to \infty$ by a Legendre transformation as we remind now briefly, following [Hen09].

Consider the Ising model on a lattice with $\mathcal{N}$ sites and write down the partition functions $\mathcal{Z} = \mathcal{Z}(T, h) = \exp(-\mathcal{G}(T, h)/T)$ and $\tilde{\mathcal{Z}} = \tilde{\mathcal{Z}}(T, M) = \exp(-\mathcal{F}(T, M)/T)$ for fixed field h and fixed magnetisation M, respectively. The Ising model Hamilton function is $H = -\sum_{\langle n,m \rangle} \sigma_n \sigma_m - h \sum_{n \in \Lambda} \sigma_n$, where the first sum is over pairs of nearest neighbours. For a fixed magnetisation $M = \sum_{n \in \Lambda} \sigma_n$, the partition function is, with $\delta_{n,0} = \frac{1}{2\pi} \int_{-\pi}^{\pi} \mathrm{d}\alpha \, e^{i\alpha n}$

$$\tilde{\mathcal{Z}}(T, M) = \sum_{\{\sigma\}} \mathrm{e}^{-H/T} \delta_{M, \sum_n \sigma_n}$$

$$= \frac{1}{2\pi} \int_{-\pi}^{\pi} \mathrm{d}\alpha \, e^{-i\alpha M} \sum_{\{\sigma\}} \exp\left[T^{-1} \sum_{(n,n')} \sigma_n \sigma_{n'} + i\alpha \sum_n \sigma_n \right].$$

Writing $M = \mathcal{N}m$, $\mathcal{F}(T, M) = \mathcal{N} f(T, m)$ and $\mathcal{G}(T, h) = \mathcal{N} g(T, h)$, the relationship between f and g is given by

$$\exp\left[-\frac{\mathcal{N}}{T} f(T, m) \right] = \frac{1}{2\pi} \int_{-\pi}^{\pi} \mathrm{d}\alpha \, \exp\left[-\mathcal{N} \left(\frac{1}{T} g(T, i\alpha T) + i\alpha m \right) \right]. \tag{1.1.6}$$

---

[5]Throughout the whole text we shall use units in which the Boltzmann constant $k_b = 1$.

[6]In the canonical ensemble the system and the reservoir exchange energy while *not* exchanging particles.
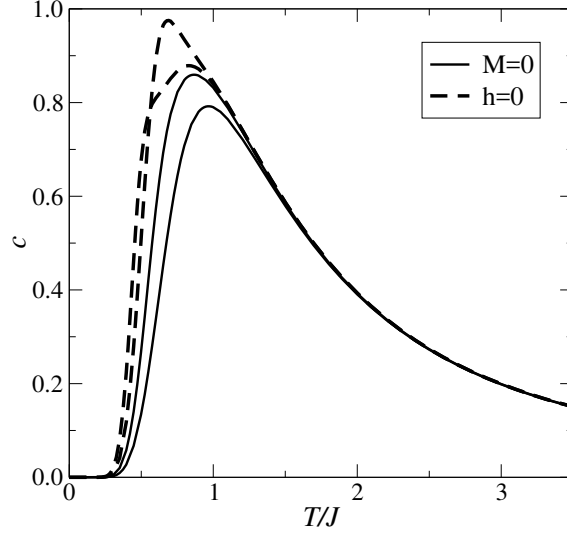
Figure 1.4: Specific heat, as defined in eq (1.1.11), of the Ising model on a periodic chain. The full lines give the case $M = 0$ for 30 sites (lower curve) and 60 sites (upper curve). The dashed lines give the case $h = 0$ for 30 sites (upper curve) and 60 sites (lower curve). Reprinted from [Hen09] with permission by *Springer*.

For $\mathcal{N}$ large, integrals of this kind can be estimated from the saddle-point method, which in this simple case amounts to the identity

$$\int_{\mathbb{R}} \mathrm{d}x\, e^{-\lambda f(x)} \simeq e^{-\lambda f(x_0)} \sqrt{\frac{2\pi}{\lambda f''(x_0)}} \left(1 + \mathrm{O}(\lambda^{-2})\right) \quad ; \quad f'(x_0) = 0 \tag{1.1.7}$$

Applied to eq (1.1.6), the extremal condition $\partial_\alpha\left(T^{-1}g + \mathrm{i}\alpha m\right) \overset{!}{=} 0$ leads to the standard thermodynamic relation $m = -\partial g/\partial h$, as it should be. The estimate of the integral in eq (1.1.6) gives

$$\exp\left[-\frac{\mathcal{N}}{T} f(T, m)\right] = \exp\left[-\frac{\mathcal{N}}{T}\left(g + hm\right) + \frac{1}{2}\ln\left(\frac{2\pi}{\mathcal{N}T\chi}\right)\right] \left(1 + \mathrm{O}(\mathcal{N}^{-2})\right) \tag{1.1.8}$$

where $\chi = \partial m/\partial h$ is the susceptibility. Hence

$$f(T, m) = g(T, h) + hm + \mathrm{O}\left(\frac{\ln \mathcal{N}}{\mathcal{N}}\right) \tag{1.1.9}$$

reproduces in the limit $\mathcal{N} \to \infty$ the standard equilibrium thermodynamics, where the two thermodynamic potentials $f = f(T, m)$ and $g = g(T, h)$ are related by a *Legendre transformation*. For illustration, one may calculate the mean energy $\langle E \rangle = \mathcal{Z}^{-1}\partial\mathcal{Z}/\partial(1/T)$. Writing $\langle E \rangle = \mathcal{N}\varepsilon$, from the above it is easily seen that $\varepsilon|_m = \varepsilon|_h + \mathrm{O}(\mathcal{N}^{-1})$. For an explicit check in the $1D$ Ising model, one may calculate the two partition functions on a periodic chain of $\mathcal{N} = 2N$ sites, for $h = 0$ and $M = 0$, respectively. The result is [Hen09]

$$\mathcal{Z}(T, 0) = (2\cosh 1/T)^{2N} + (2\sinh 1/T)^{2N} \qquad\qquad ; \text{if } h = 0$$

$$\tilde{\mathcal{Z}}(T, 0) = (2\sinh 2/T)^N \left[P_N(\coth 2/T) - P_{N-1}(\coth 2/T)\right] \qquad ; \text{if } M = 0 \tag{1.1.10}$$

where P_n is the nth Legendre polynomial [Abr64]. In 1.4 the specific heats, calculated from either $\tilde{\mathcal{Z}}(T, 0)$ (fixed magnetisation – full curves) or $\mathcal{Z}(T, 0)$ (fixed field – dashed curves) are shown for two periodic lattices of different size. We see that for fixed magnetisation, the specific heat is lower than for a fixed magnetic field (as it should be for an equilibrium system) and that for $N \to \infty$, the two sets of curves converge towards each other. This convergence is very rapid for sufficiently large

Table 1.2: Critical exponents in the language of a continuous magnetic order-disorder transition: h is the external magnetic field and $\mathfrak{r}$ is the reduced driving parameter.

Physical Observable	Exponent	Definition
specific heat	α	$c_{h=0}(\mathfrak{r} \to 0) \propto |\mathfrak{r}|^{-\alpha}$
order parameter	β	$m_{h=0}(\mathfrak{r} \to 0^-) \propto (-\mathfrak{r})^{\beta}$
susceptibility	γ	$\chi_{h=0}(\mathfrak{r} \to 0) \propto |\mathfrak{r}|^{-\gamma}$
critical isotherm	δ	$h_{\mathfrak{r}=0} \propto |m|^{\delta}\mathrm{sign}\,(m)$
correlation function	η	$G_{h=0,\mathfrak{r}=0}(r) \propto |r|^{-d+2-\eta}$
correlation length	ν	$\xi_{h=0}(\mathfrak{r} \to 0) \propto |\mathfrak{r}|^{-\nu}$
relaxation time	z	$\tau^c_{h=0}(\mathfrak{r} \to 0) \propto \xi^z$
anisotropic correlation length	θ	$\xi_{||} \propto \xi_{\perp}^{\theta}$

temperatures but becomes notably more slow for more small values of T and evolves in opposite directions for $M = 0$ fixed and $h = 0$ fixed.

Having specified the associated thermodynamic potentials for the canonical ensemble, they allow us to compute physical quantities as thermodynamic derivatives

$$\text{specific heat} \qquad c = -\partial_T|_h \partial_T \mathcal{G} \ , \tag{1.1.11}$$

$$\text{magnetisation} \qquad m = -\partial_h|_T \mathcal{G} \ , \tag{1.1.12}$$

$$\text{susceptibility} \qquad \chi = -\partial_h^2|_T \mathcal{G} \ . \tag{1.1.13}$$

These macroscopic quantities quantify the behaviour of the system as a unit. In order to characterise the system on finite scales one has to introduce the *spin-spin correlation function* and the correlation function for the *energy density* $\varepsilon(\boldsymbol{x})$

$$G_\sigma(\boldsymbol{x}, \boldsymbol{y}) := \langle \sigma_{\boldsymbol{x}} \sigma_{\boldsymbol{y}} \rangle = \frac{1}{\mathcal{Z}} \sum_{\{\sigma\}} \sigma_{\boldsymbol{x}} \sigma_{\boldsymbol{y}} \mathrm{e}^{-H[\{\sigma\}]/T} \tag{1.1.14}$$

$$G_\varepsilon(\boldsymbol{x}, \boldsymbol{y}) := \langle \varepsilon_{\boldsymbol{x}} \varepsilon_{\boldsymbol{y}} \rangle = \frac{1}{\mathcal{Z}} \sum_{\{\sigma\}} \varepsilon_{\boldsymbol{x}} \varepsilon_{\boldsymbol{y}} \mathrm{e}^{-H[\{\sigma\}]/T} \tag{1.1.15}$$

where $\boldsymbol{x}$ and $\boldsymbol{y}$ define two positions in the lattice. Each of these correlators has its individual correlation length $\xi_{\sigma/\varepsilon}$ and corresponding amplitude $\mathcal{A}_{\sigma/\varepsilon}$

$$G_\sigma(\boldsymbol{x}, \boldsymbol{y}) \propto \mathcal{A}_\sigma \mathrm{e}^{-\frac{|\boldsymbol{x}-\boldsymbol{y}|}{\xi_\sigma}}, \qquad G_\varepsilon(\boldsymbol{x}, \boldsymbol{y}) \propto \mathcal{A}_\varepsilon \mathrm{e}^{-\frac{|\boldsymbol{x}-\boldsymbol{y}|}{\xi_\varepsilon}} \ . \tag{1.1.16}$$

However, ξ_σ and ξ_ε are known to be asymptotically proportional [Car96b] and one thus writes a single *correlation length* ξ as

$$G(\boldsymbol{x}, \boldsymbol{y}) \propto \mathrm{e}^{-\frac{|\boldsymbol{x}-\boldsymbol{y}|}{\xi}} \tag{1.1.17}$$

It has already been argued in section 1.1.1 that a phase transition can be characterised as a point of divergences in thermodynamic quantities. It is therefore desirable to characterise these divergences by the so called *critical exponents*. These are defined in terms of the reduced temperature

$$\mathfrak{r} = \frac{T - T_c}{T_c} \tag{1.1.18}$$

and are given in tab 1.2.
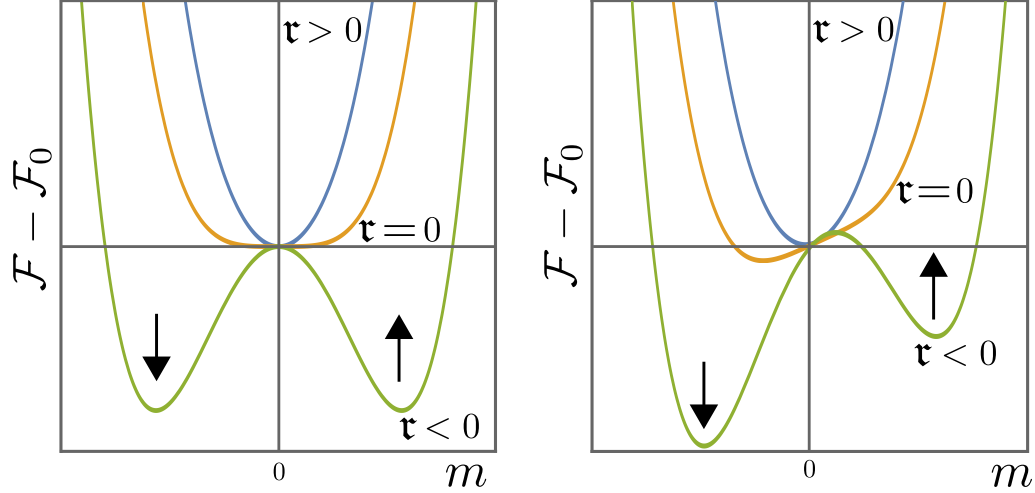
Figure 1.5: Ginzburg-Landau free energy in zero field $h = 0$ (left panel) and in a magnetic field $h \neq 0$ (right panel).

Ginzburg-Landau theory

The Ginzburg-Landau (GL) theory is a simple phenomenological approach to describe transition phenomena built from the non-fluctuating average value of the order parameter (magnetisation m in magnetic systems). Our presentation loosely follows [Yeo92] and recalls the basic concepts and elementary results of the theory. For further details, see e.g. [Hoh15, Kad09, Bax71] for further reading.

The basic assumption is that the free energy can be developed in a power series of the order parameter m according to

$$\mathcal{F} = \mathcal{F}_0 + \mathfrak{r}a_2 m^2 + a_4 m^4 + hm \tag{1.1.19}$$

We show the form of the free energy in fig 1.5 and observe immediately

1. The coefficient of m^2 is chosen to be proportional to $\mathfrak{r}$. In this manner, the global minimum changes for the cases $\mathfrak{r} > 0$ and $\mathfrak{r} < 0$ and the theory is able to describe a transition phenomena

2. Since the curves transform continuously in one another as a function of temperature, the GL theory describes a continuous phase transition. For the external field $h \neq 0$ the transition is of first order.

3. For $\mathfrak{r} < 0$ and $h = 0$ the ground state is two-fold degenerated due to a symmetry $m \mapsto -m$ in the free energy. The phase transition is therefore said to be a *spontaneous symmetry breaking.*

4. The magnetic field h cancels the degeneracy and selects the state orientated along its direction as energetically favourable.

5. At the critical point $\mathfrak{r} = 0$ the Ginzburg Landau free energy becomes flat around $m = 0$ and thus thermal fluctuations around the value $m = 0$ can spread throughout the entire system.

Apart from providing a clear physical insight into the physics behind transition phenomena, the GL theory allows to calculate the critical exponents exactly and we list them in tab 1.3 [Yeo92, Bax71] (along with the values of the spherical model). The exponents α, β, γ and δ are obtained by straightforward calculations from eq (1.1.19). In order to obtain the mean-field values of ν and η which describe the behaviour of the correlation function, the *Ornstein-Zernike extension* to GL theory [Yeo92] is needed. This extension allows the magnetisation of the system to vary with position and up to lowest order in m the free energy in zero field $h = 0$ reads

$$\mathcal{F} = \mathcal{F}_0 + \mathfrak{r}a_2 \int \mathrm{d}\boldsymbol{r} \; m(\boldsymbol{r})^2 + g \int \mathrm{d}\boldsymbol{r} \; (\nabla m(\boldsymbol{r}))^2 \; . \tag{1.1.20}$$

Table 1.3: Critical exponents of the Ginzburg-Landau theory and the spherical model in $d < 4$ spatial dimensions.

	α	β	γ	δ	η	ν	z
GL theory	0	$\frac{1}{2}$	1	3	0	$\frac{1}{2}$	2
SM $d < 4$	$\frac{d-4}{d-2}$	$\frac{1}{2}$	$\frac{2}{d-2}$	$\frac{d+2}{d-2}$	0	$\frac{1}{d-2}$	2

In this approximation the Fourier modes $\boldsymbol{k}$ decouple and one can calculate the correlation function in Fourier space [Yeo92]. To conclude this overview, we want to give some closing remarks.

1. The GL theory unifies a number of classical mean-field studies, of which the most prominent one may be the molecular field theory. This theory derives an effective mean-field Hamilton function by replacing the exact Hamiltonian H by a member $H_0(\kappa)$ of a family of Hamiltonians which depend on a variational parameter κ. The Bogoliubov inequality

$$\mathcal{F}[H] - \mathcal{F}[H_0] \le \langle H - H_0 \rangle_0 \tag{1.1.21}$$

   then allows to find the optimal $H_0(\kappa^\star)$ from a minimisation problem. This allows e.g. to replace an interacting Hamiltonian by a free one

$$\sum_{n,m} J_{nm} \sigma_n \sigma_m \to \kappa^\star \sum_n \sigma_n \tag{1.1.22}$$

2. For most systems, especially in low dimensions, the prediction of the GL theory are *wrong*. The reason can be easily seen from our remark 1: since every spin interacts in the trial Hamiltonian solely with the average of all other spins, fluctuations are neglected. Thus, *the GL theory is valid iff fluctuations are unimportant.*

3. Ginzburg criterion: The unimportance of fluctuations can be quantified as follows. Fluctuations have a typical energy associated with the temperature T and they can affect the system on the length scale of the correlation length, thus in a volume ξ^d. Their contribution to the free energy should consequently be

$$\mathcal{F}_{\text{fluc}} \simeq \frac{T}{\xi^d} \sim |\mathfrak{r}|^{\nu d} . \tag{1.1.23}$$

   This contribution must be negligible for the GL theory to be applicable. The free energy itself behaves as

$$\mathcal{F} \sim |\mathfrak{r}|^{2-\alpha} . \tag{1.1.24}$$

   By comparing the exponents and substituting the mean-field values from tab 1.3, condition

$$d > 4 \tag{1.1.25}$$

   is deduced. $d = 4$ is therefore called the upper critical dimension above which GL theory is applicable.

4. All models with the same GL expansion share the same critical exponents and therefore lay in the same universality class.

5. Generally, a mean-field theory is a good starting point for a treatment of any complicated problem. It usually gives a qualitative idea of the phase diagram and helps to greatly simplify complicated problems. Moreover, despite numerical approaches get harder as the dimensionality increases, mean-field studies improve while not increasing technical difficulties.

Exactly solvable models

In general, calculating the partition function is a difficult if not impossible challenge and numerical methods often have their own flaws. Therefore, it is useful to study models that allow to determine $\mathcal{Z}$ explicitly and hence test generic expectations analytically. In general this is possible in the following scenarios

- $2D$ systems that are *integrable* (e.g. Onsager's solution of the 2D classical Ising model [Ons44], Baxter's solution of the hard hexagon/eight-vertex model [Bax71] and similarly solutions of the quantum Ising chain in a transverse magnetic field [Zam89] or Bethe's celebrated solution of the quantum Heisenberg chain [Bet31])

- *free fields* that usually lead to mean-field descriptions,

- the *spherical model* [Ber52, Lew52] which in spite of an underlying free-field theory cannot be reduced to a simple mean-field description.

We shall be mainly concerned here with the study of the spherical model which will be introduced later properly since it is **not** a mean-field theory **and** allows generalisations to higher dimensions, for very general interactions and external fields.

The value of lattice models and especially exactly solvable models has always been questioned, since they seem to simplify nature drastically. It is certainly helpful and even advisable to always critically question the validity of an abstract description but the integrability of a model alone cannot serve as justification to dismiss this model as useless. We quote the preface to [Bax71] where Baxter categorically dismissed all contentions that exactly solvable models were intrinsically pathological: "*There are 'down-to-earth' physicists and chemists who reject lattice models as being unrealistic. In its most extreme form, their argument is that if a model can be solved exactly, then it must be pathological. I think this is defeatist nonsense: [. . .] There is probably also a feeling that the models are 'too hard' mathematically. This does not bear close examination: Ruelle (1969) rightly says in the preface to his book that if a problem is worth looking at at all, then no mathematical technique is to be judged too sophisticated. Basically, I suppose the justification for studying these lattice models is very simple: they are relevant and they can be solved, so why not do so and see what they tell us?*"

General scaling theory

While not all models are exactly solvable and mean-field theories usually only give qualitative insight into the phase diagram one has to go beyond mean-field studies in order to describe scenarios where fluctuation effects are not negligible. The scaling theory we want to outline in this section is the *renormalisation group theory* (RG). The literature on this topic is vast but as well this field of research is constantly growing what makes it hard, if not impossible for a single reference to provide a more or less complete overview on this topic. Our presentation is mainly inspired by [Nis11, Car96b, Ma00].

The basic idea is illustrated in fig 1.6 and consists of tracing out iteratively microscopic degrees of freedom in a lattice model (here ■). This procedure of rescaling a coarse grained system is the essence of the basic renormalisation group operation and changes amongst other quantities especially the number of lattice sites $N \mapsto N'$ and the temperature $T \mapsto T'$. Of course, explicit real-space renormalisations will generate additional couplings (green links in fig 1.6), beyond simple nearest-neighbour interactions (blue links in fig 1.6). The usual assumption is that these extra couplings should not affect the critical behaviour, e.g. the values of the exponents, in an essential way. Hence, a priori the Hamilton function of the system will transform indirectly under the RG procedure as well $H \mapsto H'$. The general hypothesis is that such a transformation should not affect the physics of the critical point due to universality. This manifests in the following postulate.

Postulate: After a *renormalisation step*[7] R_b which maps all quantities $\mathcal{O}$ to $R_b(\mathcal{O}) =: \mathcal{O}'$ and rescales the lengths in the system by a factor $b > 1$, the partition function does **not** change

$$\mathcal{Z} \mapsto R_b(\mathcal{Z}) = \mathcal{Z}' \stackrel{!}{=} \mathcal{Z} \tag{1.1.26}$$

---

[7]In general such a step is an involved non-linear transformation.
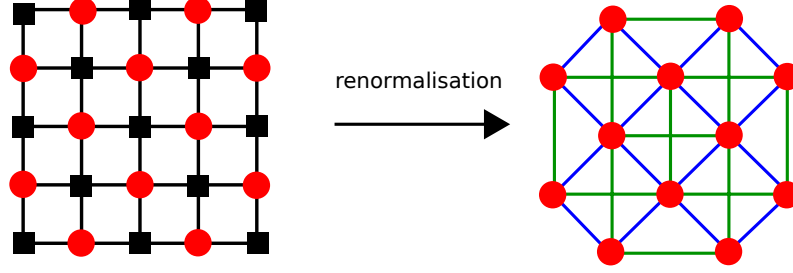
Figure 1.6: Schematic representation of the real space renormalisation group.

By applying such a transformation the system effectively loses information about its microscopic configuration since such a map R_b is non-invertible. The physical assumption underlying this mathematical statement is the existence of a single diverging length scale near to criticality. This turns out to be effectively correct in many systems. However, if several such length scales exist, the simple picture presented here will not hold [Car96b, Nis11] .

The repetition of such a transformation will thus reveal the macroscopical critical behaviour of the system since such a series accounts for fluctuations on all length scales. We shall now briefly sketch how to derive the general RG procedure by first introducing a quantity that is commonly defined in the context of RG maps.

Definition: The **scaling dimension** $y_{\mathcal{O}}$ of a physical quantity $\mathcal{O}$ is defined as

$$R_b(\mathcal{O}) = b^y \mathcal{O} \tag{1.1.27}$$

and encodes how the quantity $\mathcal{O}$ scales under RG transformations.

We shall see later that the scaling dimension of a physical quantity contains information on whether this quantity is able to affect the critical behaviour of a system or not.

At criticality the system with the Hamilton function H_c is expected to remain essentially unchanged after many transformations R_b since fluctuations are present on all length scales. Thus, the series of Hamiltonians $(R_b^n(H_c))_{n \in \mathbb{N}}$ has to converge towards a *fixed point* $H^\star$ with

$$H^\star = R_b(H^\star) = \lim_{n \to \infty} R_b^n(H_c) \tag{1.1.28}$$

We now aim at giving a recipe for applying the RG to a general Hamiltonian

$$H = \sum_n u_n \mathcal{O}_n = \boldsymbol{u} \cdot \boldsymbol{\mathcal{O}} \tag{1.1.29}$$

where $\mathcal{O}_n$ are coarse-grained microscopic degrees of freedom, in field theory usually referred to as operators [Car96b], and $u_n \in \mathbb{C}$ are constants. In this language, the **renormalisation group equation** reads

$$\boldsymbol{u}' = R_b(\boldsymbol{u}) \tag{1.1.30}$$

and its successive application

$$\boldsymbol{u} \mapsto R_b(\boldsymbol{u}) \mapsto R_b^2(\boldsymbol{u}) \mapsto \ldots \mapsto R_b^n(\boldsymbol{u}) \mapsto \ldots \tag{1.1.31}$$

defines the so-called discrete **renormalisation group flow**. Fixed points of the renormalisation group, $u* = R_b(u*)$, play an essential role in what is going to follow. We now want to study the effects of this flow close to criticality. May $\boldsymbol{u}^\star$ be a fixed point, then one writes

$$\boldsymbol{u} = \boldsymbol{u}^\star + \delta \boldsymbol{u}, \qquad \boldsymbol{u}' = \boldsymbol{u}^\star + \delta \boldsymbol{u}' . \tag{1.1.32}$$

Linearising the recursion relation around the fixed point leads to

$$\delta \boldsymbol{u}' = T_b(\boldsymbol{u}^\star) \delta \boldsymbol{u} \qquad \text{with} \qquad [T_b(\boldsymbol{u}^\star)]_{ij} = \partial_{\boldsymbol{u}_j} \boldsymbol{u}'_i |_{\boldsymbol{u}^\star} \tag{1.1.33}$$

It is usually assumed that this matrix is diagonalisable and expand $\boldsymbol{u}$ and $\boldsymbol{u}'$ in terms of eigenvectors $\boldsymbol{\phi}_i$ with $T_b \boldsymbol{\phi}_i = b^{y_i} \boldsymbol{\phi}_i$ and find

$$\boldsymbol{u} = \boldsymbol{u}^\star + \sum_i g_i \boldsymbol{\phi}_i \qquad\qquad \boldsymbol{u}' = \boldsymbol{u}^\star + \sum_i g_i' \boldsymbol{\phi}_i \qquad (1.1.34)$$

with $g_i' = b^{y_i} g_i$. The behaviour of the system under renormalisation is now reduced to the study of the so-called **scaling fields** g_i around the fixed point. Here, the first major physical insight comes from the exponents y_i: if $y_i > 0$ the associated scaling field moves away from criticality and is thus said to be **relevant**. Otherwise $y_i < 0$ describes **irrelevant** scaling fields[8].

In ferromagnetic systems, critical behaviour can solely be observed if the temperature $\mathfrak{r} = 0$ and the magnetic field $h = 0$. This leads us to the conclusion that these are the only relevant scaling fields for the ferromagnetic phase transition. We write after a single renormalisation step

$$f(\mathfrak{r}, h) = b^{-d} f(\mathfrak{r} b^{y_\mathfrak{r}}, h b^{y_h}) \qquad (1.1.35)$$

$$G_\sigma(\boldsymbol{r}; \mathfrak{r}, h) = b^{-2x_\sigma} G_\sigma(\boldsymbol{r}/b; \mathfrak{r} b^{y_\mathfrak{r}}, h b^{y_h}) \qquad (1.1.36)$$

$$G_\varepsilon(\boldsymbol{r}; \mathfrak{r}, h) = b^{-2x_\varepsilon} G_\varepsilon(\boldsymbol{r}/b; \mathfrak{r} b^{y_\mathfrak{r}}, h b^{y_h}) \qquad (1.1.37)$$

Here, we refer to the connected versions of eqs (1.1.14, 1.1.15), viz.

$$G_\sigma(\boldsymbol{x}, \boldsymbol{y}) := \langle (\sigma_{\boldsymbol{x}} - \langle \sigma_{\boldsymbol{x}} \rangle)(\sigma_{\boldsymbol{y}} - \langle \sigma_{\boldsymbol{y}} \rangle) \rangle = \langle \sigma_{\boldsymbol{x}} \sigma_{\boldsymbol{y}} \rangle - \langle \sigma_{\boldsymbol{x}} \rangle \langle \sigma_{\boldsymbol{y}} \rangle \qquad (1.1.38)$$

$$G_\varepsilon(\boldsymbol{x}, \boldsymbol{y}) := \langle (\varepsilon_{\boldsymbol{x}} - \langle \varepsilon_{\boldsymbol{x}} \rangle)(\varepsilon_{\boldsymbol{y}} - \langle \varepsilon_{\boldsymbol{y}} \rangle) \rangle = \langle \varepsilon_{\boldsymbol{x}} \varepsilon_{\boldsymbol{y}} \rangle - \langle \varepsilon_{\boldsymbol{x}} \rangle \langle \varepsilon_{\boldsymbol{y}} \rangle \qquad (1.1.39)$$

in order to only account for fluctuations around the mean value. The renormalisation group exponents y_h and $y_\mathfrak{r}$ are now related to the critical exponents according to

$$\alpha = 2 - \frac{d}{y_\mathfrak{r}}, \quad \beta = \frac{d - y_h}{y_\mathfrak{r}}, \quad \gamma = \frac{2y_h - d}{y_\mathfrak{r}}, \quad \delta = \frac{y_h}{d - y_h}, \quad \nu = \frac{1}{y_\mathfrak{r}}, \quad \eta = d - 2y_h + 2 \qquad (1.1.40)$$

Thus, RG allows to *systematically* analyse critical phenomena and determine universality classes.

1.2 Quantum criticality

After having studied the classical theory of critical phenomena we want to turn our attention to quantum properties in this section. The studies of quantum criticality trace back to the 1970s and the main works of [Suz71, Fra78, Kog79] who established first correspondences between statistical mechanics and quantum mechanics in the Ising model and studied in great detail the connection between lattice gauge theories and the quantum Hamiltonian formalism.

First we shall recall the quantum-classical mapping that makes the theory of classical phase transitions up to some changes applicable in the quantum case. Then we shall discuss where in the phase diagram quantum effects are relevant and have to be taken into account. We then complete this part by reviewing several experimental examples of quantum phase transitions.

1.2.1 Correspondences between quantum and statistical systems

We want to briefly review the link between quantum systems and statistical systems that is introduced by *Feynman's path integration formalism* [Fey65]. For this purpose we explicitly keep the constant $\hbar$ in this section while it will be set to $\hbar = 1$ almost everywhere later.

The quantum transition amplitude $\mathcal{Z}$ between two distinct space-time configurations $(t_1, \boldsymbol{x}_1)$ and $(t_2, \boldsymbol{x}_2)$ of a quantum mechanical system with the (time-independent) Hamiltonian $\mathcal{H}$ can be expressed by the path integral

$$\mathcal{Z} = \int \prod_j U(t_{j+1}, t_j) \mathrm{d}x_j = \int \mathcal{D}\boldsymbol{x} \, \mathrm{e}^{-\frac{\mathrm{i}}{\hbar} S} \qquad (1.2.1)$$

---

[8]The case $y_i = 0$ is not treated here: usually the associated scaling fields are referred to as **marginal** and give rise to logarithmic corrections to the leading scaling behaviour.

Table 1.4: Correspondences between classical statistical system and quantum systems established by the notion of the transfer matrix [Hen99].

Statistical Systems		Quantum Systems	
temperature	T	$\hbar$	Planck's constant
cl. Hamilton function	H/T	$S/\hbar$	classical action
transfer matrix	$\mathcal{T} = \mathrm{e}^{-\tau\mathcal{H}}$	$U = \mathrm{e}^{-\frac{\mathrm{i}}{\hbar}t\mathcal{H}}$	time-evol. operator
equilibrium state		$|0\rangle$	ground state (GS)
ensemble average	$\langle\mathcal{O}\rangle_{\mathrm{ens}}$	$\langle 0|\,\mathcal{O}\,|0\rangle$	GS exp. value
correlation functions	G	$\Delta(t, \boldsymbol{r})$	propagators
inv. correlation lengths	ξ^{-1}	$E_1 - E_0$	energy gaps
free energy density	f	E_0/N	GS energy density
classical CP	$d + 1$	d	QCP

where the integral represents the sum over all possible paths that connect $(t_1, \boldsymbol{x}_1)$ and $(t_2, \boldsymbol{x}_2)$, $S(t_1, t_2) = \int_{t_1}^{t_2} \mathrm{d}t\,\mathcal{L}$ is the classical action and U is the quantum mechanical time evolution operator $U(t_{j+1}, t_j) = \mathrm{e}^{-\frac{\mathrm{i}}{\hbar}\mathcal{H}(t_{j+1}-t_j)}$. This expression for the transition amplitude can be easily related to the partition function: Consider a statistical system which is described on a hypercubic $d + 1$ dimensional lattice and single out one of the dimensions and name it "time". The remaining d dimensions are referred to as space and define the **transfer matrix** $\mathcal{T}$ as

$$\big\langle \{\sigma\}(t_1)\big|\mathcal{T}\big|\{\sigma\}(t_2)\big\rangle := \mathrm{e}^{-\tilde{H}(t_1,t_2)/T} \tag{1.2.2}$$

with $H = \sum_t \tilde{H}(t, t+1)$. It is a well-known result that the partition function can then be expressed as [Sch05, Hen99]

$$\mathcal{Z} = \mathrm{tr}\,\mathcal{T}^M \tag{1.2.3}$$

where M is the number of sites in the time direction (with periodic boundary conditions). Using the explicit expression and the Trotter product formula in the *extremely anisotropic limit*, in which the time-direction becomes continuous, one can formally relate eq (1.2.1) and (1.2.3) by an analytic continuation in time. This leads to the mapping described in tab 1.4.

The procedure we describe here distinguishes explicitly between 'time' and 'space' in order to go over from statistical mechanics to quantum mechanics. This leads to a potential anisotropy between space and time which may be characterised by the *anisotropy exponent* θ. It is most easily defined by amounting to both directions an individual correlation length exponent $\nu_{||}$ (time) and $\nu_{\perp}$ (space). The anisotropy exponent is then defined as[9]

$$\theta = \frac{\nu_{||}}{\nu_{\perp}} \tag{1.2.4}$$

and can be readily deduced from the low energy spectrum of the quantum Hamiltonian

$$E_k \overset{k\to 0}{\sim} k^\theta\ . \tag{1.2.5}$$

Here, $k = |\boldsymbol{k}|$ is the absolute value of the wave vector $\boldsymbol{k}$ of a collective excitation of the many-body Hamiltonian $\mathcal{H}$ which is assumed to be rotational and translational invariant.

There is an opinion that "there are deep reasons" for the analogies between quantum mechanics and statistical mechanics which seem to be related to the properties of space time [Pol87], though there is no real explanation as the author admits himself.

---

[9]Sometimes the anisotropy exponent is referred to as 'dynamical exponent' which is due to the name 'time' awarded to the anisotropic direction in the Hamiltonian limit. One must not confuse θ with z.

1.2.2 Thermal and quantum fluctuations

Our goal was to understand how quantum properties enter in the transition and in which regions of the phase diagram quantum effects are relevant. Therefore, the energy of typical quantum fluctuations has to be compared to the one of thermal fluctuations. The typical thermal energy scale is simply given by the temperature T while the quantum fluctuations have a typical energy scale of

$$\hbar\omega_{\text{char}} \propto \frac{\hbar}{\tau_c} \propto |\mathfrak{r}|^{\nu_\perp \theta} \ . \tag{1.2.6}$$

From here it is clear that every finite temperature transition is indeed classical, since the right hand side vanishes at the critical point. True quantum transitions can just be observed at $T = 0$. This can be readily understood since QPT occur due to a spontaneous symmetry breaking between two indistinguishable *ground* states. As long as $T \neq 0$ the system is thermally excited and can thus not show the pure GS transition. Nevertheless, the quantum critical region shown in fig 1.7 can give rise to unconventional physics like unconventional power law behaviour, non-Fermi liquid behaviour etc. which is caused by absence of conventional quasiparticle-like excitations [Voj03].
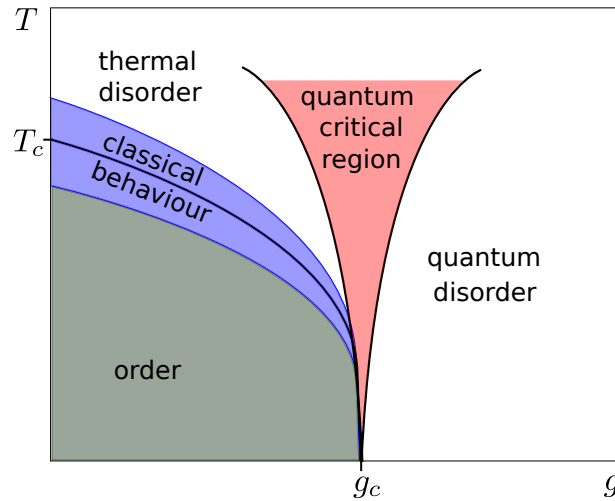
Figure 1.7: Comparison of classical and quantum contributions to the critical behaviour of a system that has a classical and a quantum phase transition.

1.2.3 Experimental examples

The field of experimentally observed or designed QPT is very active and vast. A full review would thus go beyond the scope of our theoretical work. Nevertheless, we think that it is essential to highlight at least a few important realisations and milestones in the field of experimental QPT because after all "*La théorie n'est que l'idée scientifique contrôlée par l'expérience.*" [Ber65].

CoNb$_2$O$_6$ and LiHoF$_4$: Model quantum Ising magnets

In both of these materials cobalt ions for $CoNb_2O_6$ and respectively holmium atoms for $LiHoF_4$ can order along a particular crystalline axis which leads to the two states $|\uparrow\rangle$ or $|\downarrow\rangle$ that can be canonically associated with the Ising spin states [Bit96, Col10]. The main difference between $CoNb_2O_6$ and $LiHoF_4$ is the type of interaction: while $LiHoF_4$ is dominated by magnetic dipolar interactions which are long-range, $CoNb_2O_6$ is dominated by nearest neighbour exchange interactions and thus provides an extraordinary testing ground for exact $1D$ results in the transverse field Ising model [Sac01]. In fig 1.8 the experimental results from [Bit96] for $LiHoF_4$ are shown. In this experiment the classical thermal transition can be converted into a QPT by a transverse
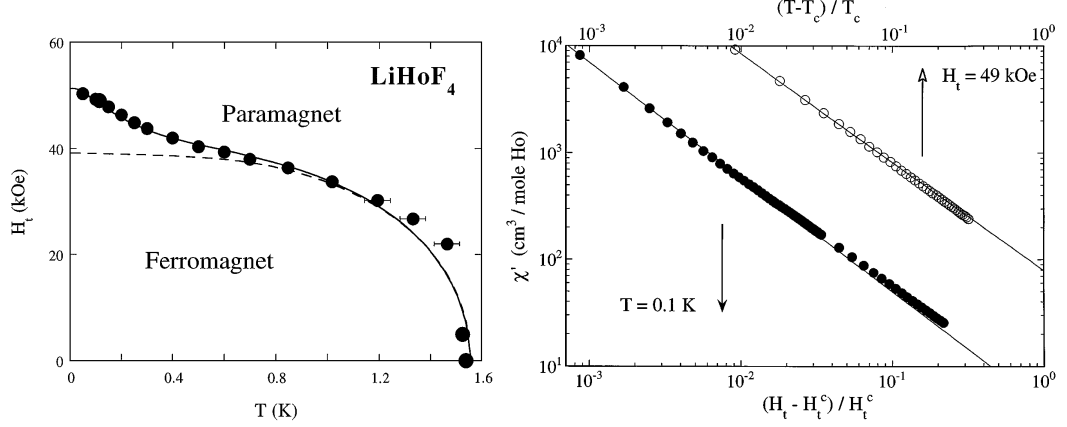
Figure 1.8: left panel: Mean-field critical behaviour of the magnetic susceptibility of LiHoF$_4$ in the $T \to 0$ limit as functions of reduced temperature (open circles, $T_c = 0.114$[K], $H_t = 49.0$[kOe]) and reduced transverse field (filled circles, $H_t^c = 49.3$[kOe], $T = 0.100$[K]). right panel: Experimental phase boundary (filled circles) for the ferromagnetic transition in the transverse field-temperature plane. Dashed line is a mean-field theory including only the electronic spin degrees of freedom; solid line is a full mean- field theory incorporating the nuclear hyperfine interaction. Reprinted from [Bit96] with permission by the *American Physical Society.*

magnetic field H_t. Using magnetic susceptibility measurement the phase boundary in $3D$ can be determined and can be compared to mean-field predictions with qualitative agreement.

LiErF$_4$ & LiYbF$_4$: Model antiferromagnets for classical-to-quantum crossover

A system where a phase diagram of the shape shown in fig 1.7 can be measured is LiErF$_4$. Its magnetic structure is shown in fig 1.9 and one can test the physics of dipolar-coupled systems explicitly in this system. The dipolar coupling is antiferromagnetic and implies a macroscopic bi-layer antiferromagnetic order for non-zero temperature as shown in fig 1.10 (Néel point: $T_N = 0.373(5)$[K], critical transverse field $h_c = 4.0(1)$[kOe]). By applying a transverse magnetic field, the antiferromagnetic order is suppressed and a quantum phase transition into a paramagnetic state is induced. Thus, one can explicitly study e.g. quantum fluctuations around a classical phase transition and determine different critical exponents [Kra12]. Although the experiment was carried out in a $3D$ system, its critical behaviour was more reminiscent of a $2D$ material as e.g. the critical exponents $\beta_T \approx 0.15(2)$, $\beta_H \approx 0.31(2)$ and $\alpha \approx -0.28(4)$ reveal. The value for the thermal transition β_T and α thermal are completely different from the mean-field predictions (tab 1.3) but rather agree with the ones of the classical $2D$ XY model with cubic anisotropy [Jos77, Jos78, Cal02, Tar08].[10] The value β_H for the quantum transition is close to the $2 + 1D$ value. This implies that the quantum transition is effectively $3D$ while the thermal transition is $2D$, explicitly verifying the classical-to-quantum map introduced in section 1.2.1.

Whether the dimensional reduction is characteristic for LiErF$_4$ due to rather close higher-lying crystal-field levels or weak hyperfine interactions, cannot be argued from [Kra12].

In recent studies, these kind of dimensional reductions have been shown to be universal to quantum dipolar antiferromagnets on a distorted diamond lattice [Bab16]. In this work susceptibility, specific heat, and neutron scattering measurements are carried out on LiYbF$_4$ in three spatial dimensions. The result of the susceptibility measurement is shown in fig 1.11: especially the cusps in fig 1.11(b) below the Néel temperature indicate a QPT according to the same mechanism as described for LiErF$_4$.

In this manner the dimensional reduction is verified in a system with a largely different crystal field environment, Néel temperature and hyperfine interactions. This experimentally establishes

---

[10]In order to give a more complete overview, we would like to mention that also materials like monolayer Fe/W(100) [Elm96] or layered ferromagnets like Rb$_2$CrCl$_4$ [AN93] and K$_2$CoF$_4$ [Hir82] belong to this universality class.
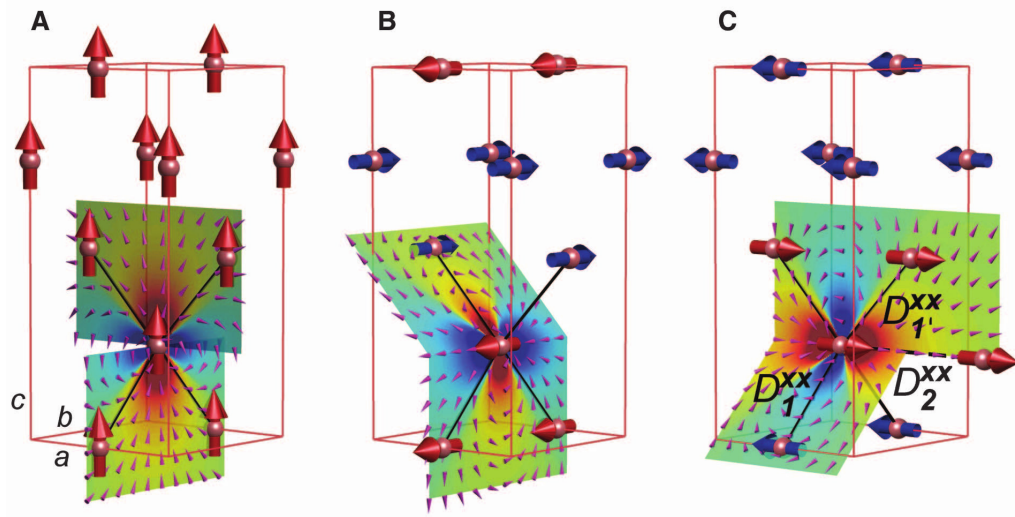
Figure 1.9: Different magnetic structures in LiErF$_4$. Reprinted from [Kra12] with permission by *The American Association for the Advancement of Science.*
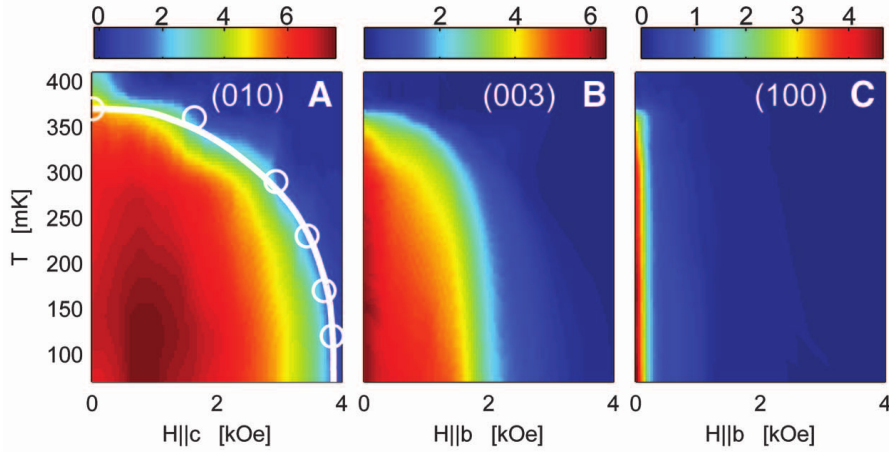
Figure 1.10: Field-temperature phase diagrams of LiErF$_4$ from the intensity of magnetic Bragg peaks: (010) with $H_{c||}$, (003) and (100) with $H_{b||}$, respectively. Reprinted from [Kra12] with permission by *The American Association for the Advancement of Science.*

that the mechanism of dimensional reduction is a universal feature of dipolar coupled quantum antiferromagnets and are applicable to a vast range of different systems [Bab16].

Ultracold atoms in optical lattices

Another celebrated realisation of a QPT was achieved by confining ultracold atoms in optical lattices [Gre02]. The experimental setup is shown in the left panel of fig 1.12: a cloud of bosonic ^{87}Rb atoms is cooled down until the atoms form a superfluid state. By applying a periodic potential, generated by an optical lattice, the experimentalists succeed to design a QPT to an insulating state, compare the right panel of fig 1.12.[11]

Another recent realisation of quantum phase transitions in $2D$ in ultracold atoms is given in [Lan16b]. In this experiment, the standard Bose Hubbard model [Ger63] has an additional long range interaction that favours an imbalance between different sublattices. Consequently, long and

---

[11] In fig 1.12 it is also visible that the quantum coherence is lost as the lattice depth is changed since for increasing lattice depth the interference pattern washes out (compare e) - h).
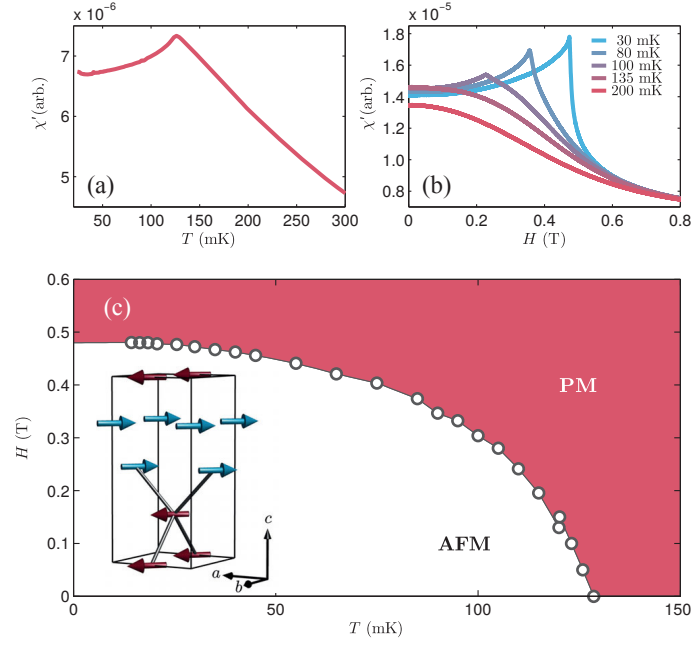
Figure 1.11: (a) Susceptibility for $H = 0$ as a function of temperature. (b) Susceptibility as a function of H for different temperatures (c) Resulting magnetic phase diagram with the bilayer magnetic structure of LiYbF$_4$ as inset. Reprinted from [Bab16] with permission of the *American Physical Society*.
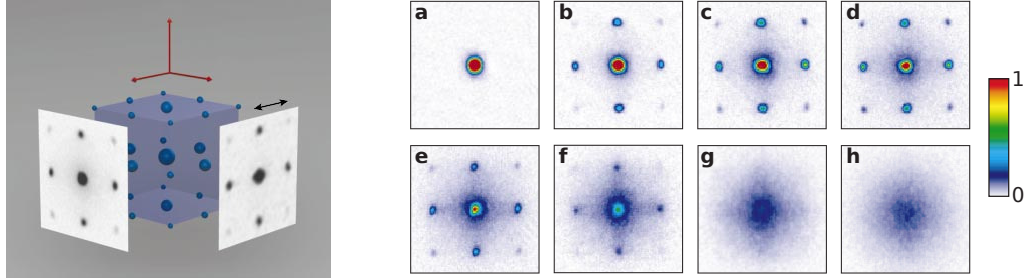
Figure 1.12: left panel: Schematic experimental setup. right panel: Absorption images of different matter wave interference patterns which were measured after suddenly releasing the atoms from the optical lattice potential with different potential depths V_0 after a time of flight of 15 ms. Values of V_0 were a) 0 E_r; b) 3 E_r; c) 7 E_r; d) 10 E_r; e) 13 E_r; f) 14 E_r; g) 16 E_r; and h) 20 E_r and E_r is the recoil energy. Reprinted from [Gre02] with permission of the *Nature Publishing Group*.

short range interactions compete with each other and produce four distinct phases: supersolid, superfluid, Mott insulator and charge density wave as shown in the right panel of fig 1.13.

1.3   The spherical model

In 1952, Berlin and Kac [Ber52] introduced the *spherical model* in order to '*investigate models which yield to exact analysis and show transition phenomena*'. In their opinion '*it is irrelevant that the models may be far removed from physical reality if they can illuminate some of the complexities of the transition phenomena*.' After the striking success of the exact analysis of the two dimensional Ising model, the spherical model was introduced to overcome the problem that the Ising model is (still) not solved in more than two spatial dimensions. In its origin, the spherical model is often considered as being exclusively theoretically motivated but the following properties will shed light on it from a different angle.
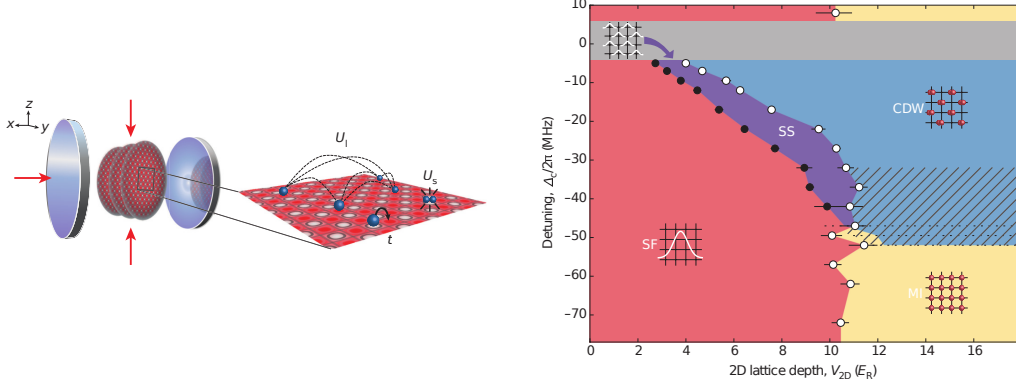
Figure 1.13: <u>left panel</u>: Schematic experimental setup. <u>right panel</u>: Phase diagram as function of the $2D$ lattice depth and the detuning $\Delta_c = \omega_z - \omega_c$ where ω_z is the frequency of the z-lattice beam and ω_c is the cavity resonance frequency. Reprinted from [Lan16b] with permission of the *Nature Publishing Group.*

1. The spherical model can also be obtained as the $n \to \infty$ limit of the classical $O(n)$ vector model [Sta68, Pea77] or the quantum $O(n)$ sigma model [Voj96] in the sense that the equilibrium bulk critical behaviour of the spherical model is *the same*. The $O(n)$ model is a more realistic spin model and thus one could hope to observe properties of the spherical model in setups that are described by sufficiently high-dimensional $O(n)$ models. In this context one also has to mention, that this map is limited as it does e.g. no longer hold true for the surface critical behaviour [Bin83, Die83].

2. In three dimensions, the specific heat exponent α in the $O(n)$ model is negative for $n \geq 2$ and $\alpha = -1$ in the spherical model (for $T \geq T_c$). In this sense, the spherical model can be considered as a much better approximation to $O(n)$-models with $n \geq 2$ than to the Ising model ($n = 1$), where in $\alpha \sim 0.1 > 0$ in $3D$.

3. In diluted magnets such as the family of $\mathrm{Eu}_x \mathrm{Sr}_{1-x} \mathrm{S}_{0.50}\mathrm{Se}_{0.50}$ [Wes86] or $\mathrm{Eu}_{0.65}\mathrm{La}_{0.35}\mathrm{S}$ critical exponents close to those of the $3D$ spherical model have been reported: $\alpha \approx -1$, $\beta = 0.5$, $\gamma \approx 2.1$, $\delta \approx 4.7$ [Wes87], compare tab 1.3 for $d = 3$.

Therefore the spherical model is widely considered as an useful analytical tool beyond GL theory that is well-justified in certain setups [Joy72, God02, Hen10].

1.3.1   The classical spherical model

The main idea of the spherical model is to *enlarge* the configuration space in a manner that helps to reduce the sums involved in the analysis of the Ising model. This is achieved by introducing a continuous description as shown in fig 1.14 for a system of two spins. Formally a spherical spin S is described by a real number $S \in \mathbb{R}$ with the constraint that each allowed $\mathcal{N}$-body configuration has to lay on a hypersphere.

Definition: The *(mean) spherical model* (SM) is defined on a d dimensional hyper-cubic lattice $\mathcal{L}$ with $|\mathcal{L}| = \mathcal{N}$ vertices by the interacting Hamiltonian [Ber52, Lew52]

$$H = -\sum_{\langle i,j \rangle} S_i S_j + \mathcal{S} \left(\sum_{i=1}^{\mathcal{N}} S_i^2 - \mathcal{N} \right) \tag{1.3.1}$$

with the real-valued variables $S_i \in \mathbb{R}$. The second term in the Hamiltonian is the so-called *(mean) spherical constraint* which is ensured by the Lagrange multiplier $\mathcal{S}$ via a thermodynamic derivative of the free energy density f

$$\sum_{i=1}^{\mathcal{N}} \langle S_i^2 \rangle = \mathcal{N} \iff \partial_{\mathcal{S}} f = \frac{1}{2} . \tag{1.3.2}$$
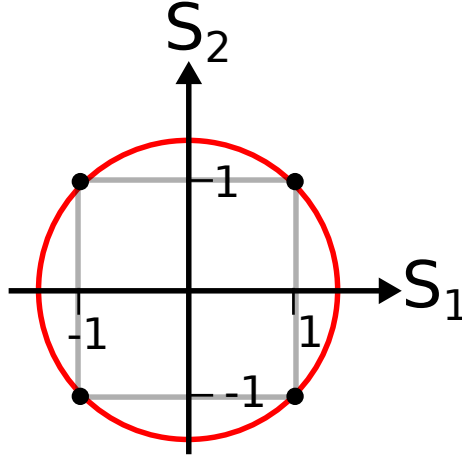
Figure 1.14: Visualisation of the *spherical configuration space* (red) compared to the Ising one (black) for two distinct spins.

Here, $\langle \cdot \rangle$ indicates the grand-canonical ensemble average.

Originally, the SM was introduced without the ensemble average in the constraint (1.3.2), thus not allowing for fluctuations [Ber52]. It turns out that this leads to an unnecessarily complicated description of the collective properties in the thermodynamic limit which are not effected by the exact nature of the constraint [Lew52]. This passage amounts merely to a change of thermodynamic ensembles and it comes as no surprise that the thermodynamics is the same for sufficiently short-range interactions [Lew52].[12] Furthermore, the classical dynamics of both model in the thermodynamic limit is equivalent[Fus02] but the SM as presented here and is much better adapted to studies of dynamical properties and to a quantum formulation than the original version.

1.3.2   The quantum spherical model

Motivation: classical SM in $3D$

We shall briefly show that Nernst theorem is violated in the $3D$ classical spherical model, without explicitly deriving all thermodynamic properties of the model. This will be done in section 1.3.3 for the quantum version and thus reveals as well the classical properties by means of the classical-quantum map we discussed in section 1.2.1

The Hamiltonian (1.3.1) with periodic boundary conditions can be easily diagonalised by a Fourier transform and reads in $3D$

$$H = \sum_{\boldsymbol{k} \in \mathcal{B}} \left(\mathcal{S} - \cos k_1 - \cos k_2 - \cos k_3 \right) |\mathcal{Q}_{\boldsymbol{k}}|^2 \tag{1.3.3}$$

where $\mathcal{Q}_{\boldsymbol{k}}$ is the Fourier transformed spin, $\boldsymbol{k} = (k_1, k_2, k_3)$ and $\mathcal{B}$ is the Brioullin zone. Thus, the free energy density in the thermodynamic limit reads

$$f = -T \log \sqrt{\pi T} + \frac{T}{2} \int_{\mathcal{B}} \frac{\mathrm{d}\boldsymbol{k}}{(2\pi)^3} \, \log \left(\mathcal{S} - \cos k_1 - \cos k_2 - \cos k_3 \right) \; . \tag{1.3.4}$$

From this expression it is a straightforward to derive the spherical constraint in the form

$$\frac{1}{T} = \int_0^\infty \mathrm{d}u \, \mathrm{e}^{-u\mathcal{S}} I_0^3(u) \tag{1.3.5}$$

where I_0 is the modified Bessel function of zeroth order [Abr64].

---

[12]For long-range interactions it is well-known that ensembles tend to be no longer equivalent in the thermodynamic limit [Dau02].
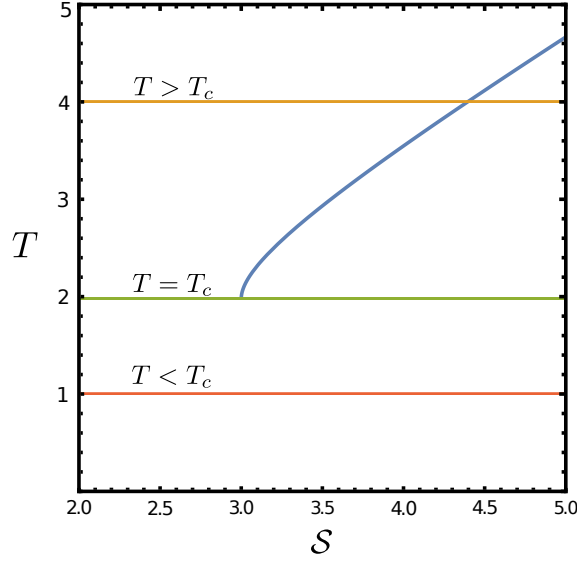
Figure 1.15: Solution of eq (1.3.5) for different temperatures: the blue line shows the inverse of the right-hand site of eq (1.3.5) and the horizontal lines indicate different temperatures. Above a critical temperature $T \geq T_c$ there is a unique solution while for $T < T_c$, the solution does not exist any more and the spherical parameter freezes at the critical value $\mathcal{S} = 3$.

Remarks:

- The right-hand site of eq (1.3.5) has a singularity occurring at $\mathcal{S} = 3$ below which the integral does no longer exist.

- This singularity coincides with the transition temperature $T_c \approx 1.97839$ [Oli06, Car03, Wal15].

- Below T_c there is no solution to eq (1.3.5) anymore and the partition function has to be evaluated with the best approximation, which is the critical value $\mathcal{S} = 3$. Consequently, the spherical parameter in the low temperature regime freezes and does *not* depend on the temperature anymore.

- We illustrate the graphical solution of eq (1.3.5) in fig 1.15.

Consequently, the expression for the internal energy u of the system in the low-temperature region, where $\mathcal{S}$ is no longer a function of the temperature, reads

$$u = -T^2 \partial_T \frac{f}{T} = \frac{T}{2} \tag{1.3.6}$$

and find for the specific heat in this regime

$$c = \partial_T u = \frac{1}{2} \ . \tag{1.3.7}$$

This result is in strong contradiction with the third law of thermodynamics which states that the specific heat has to vanish at absolute zero $T = 0$ and therefore, an extension of the SM to correct this deficiency is required. In fig 1.16 (blue line) we illustrate this fact and show already that the quantum approach will correct this behaviour as we shall show explicitly in the following section.

Formulation of the quantum spherical model

In order to correct the thermodynamic behaviour of the SM in the low-temperature phase, one has to take the quantum nature of the spins into account. The typical classical picture of a quantum mechanical spin is shown in fig 1.17 and consists of an charge distribution that is rotating around
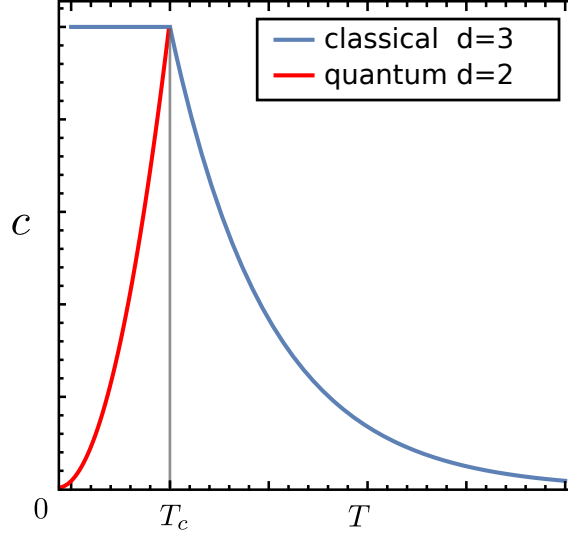
Figure 1.16: Specific heat in the classical SM in $d = 3$ spatial dimensions as a function of T. The specific heat freezes in the classical $3D$ system below the critical point while in the $2D$ quantum system, the specific heat vanishes with temperature.

an axis and thus generating an angular momentum that can be associated with a spin. This motivates the introduction of a kinetic part in the Hamiltonian that does not commute with the spin variables [Obe72].

Definition: The *quantum spherical model* (QSM) is defined on a d dimensional hyper-cubic lattice $\mathcal{L}$ with $|\mathcal{L}| = \mathcal{N}$ vertices by the interacting Hamiltonian[13]

$$\mathcal{H} = -\sum_{\langle i,j \rangle}^{\mathcal{N}} s_i s_j + \frac{\mathcal{S}}{2} \sum_{i=1}^{\mathcal{N}} s_i^2 + \frac{g}{2} \sum_{i=1}^{\mathcal{N}} p_i^2 \tag{1.3.8}$$

with the canonically conjugated variables s_i and p_j obeying the canonical commutation relation

$$[s_n, p_m] = i\delta_{nm} \tag{1.3.9}$$

and the thermodynamic derivative with respect to the spherical parameter $\mathcal{S}$ obeys the mean spherical constraint

$$\sum_{n \in \mathcal{L}} \langle s_n^2 \rangle = \mathcal{N} \ \Leftrightarrow \ \partial_{\mathcal{S}} f = \frac{1}{2} \ . \tag{1.3.10}$$

This model was first obtained from an extremely anisotropic limit of the classical SM [Sre79, Hen84b], before it was re-discovered as a quantum spin model [Voj96, Oli06].

In order to show that the quantum properties indeed cure the defect of the classical model, the Hamiltonian (1.3.8) has to be diagonalised. This procedure is shown in e.g. [Wal15, Bie13, Oli06] and is merely a question of finding an adequate canonical transformation. The free energy density in $2D$ reads[14]

$$\frac{f}{T} = \log 2 + \int_{\mathcal{B}} \frac{\mathrm{d}\boldsymbol{k}}{(2\pi)^d} \log \sinh \left(\sqrt{\frac{g}{4T^2}\left[\mathcal{S} - \cos k_1 - \cos k_2 \right]} \right) \tag{1.3.11}$$

---

[13]Whenever we refer to quantum operators we use s, p. Classical quantities are referred to in capital letters S.

[14]Since we calculated the specific heat in the classical $3D$ SM, we have to compare the results with the $2D$ QSM, see section 1.2.1
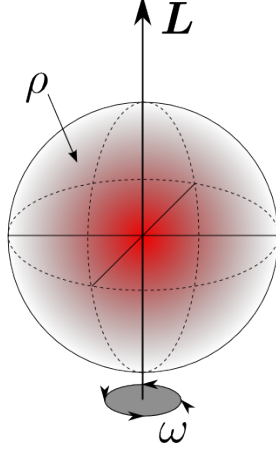
Figure 1.17: Classical view of a quantum mechanical spin: the magnetic momentum of the spin is generated by a rotational dynamics of a charge distribution ρ.

We want to study the temperature dependence in the ordered phase close to absolute $T = 0$ where[15] $\mathcal{S} = 2$. This leads immediately to

$$c = \frac{g}{2T^2} \int \frac{\mathrm{d}\boldsymbol{k}}{(2\pi)^2} \frac{\sqrt{\mathcal{S} - \cos k_1 - \cos k_2}}{\sinh^2\left(\sqrt{g/(4T^2)\,[\mathcal{S} - \cos k_1 - \cos k_2]}\right)} \tag{1.3.12}$$

Considering that the main contribution arises from the low-laying $k \simeq 0$ modes, one finds in $d = 2$ dimensions for $T \to 0^+$

$$c \simeq \frac{3}{2\pi g^3} T^2 \tag{1.3.13}$$

in agreement with the third law of thermodynamics. This is illustrated in fig 1.16.

1.3.3 Spin anisotropic extension of the QSM

In order to review the statistical properties of the QSM fully, we chose to work with a slight generalisation of the model that we suggested in [Wal15]. This new model lies (up to an isolated special case) in the same universality class as standard QSM and shows thus the same collective behaviour.

It is straightforward to recast the Hamiltonian (1.3.8) in terms of bosonic ladder operators $a_{\boldsymbol{n}}$ and $a_{\boldsymbol{n}}^\dagger$, defined as [Obe72]

$$s_{\boldsymbol{n}} = \left(\frac{g}{\mathcal{S}}\right)^{\frac{1}{4}} \frac{a_{\boldsymbol{n}} + a_{\boldsymbol{n}}^\dagger}{\sqrt{2}} \quad , \quad p_{\boldsymbol{n}} = -\mathrm{i}\left(\frac{\mathcal{S}}{g}\right)^{\frac{1}{4}} \frac{a_{\boldsymbol{n}} - a_{\boldsymbol{n}}^\dagger}{\sqrt{2}} \, . \tag{1.3.14}$$

These render the Hamiltonian (1.3.8) as follows

$$\mathcal{H} = \sum_{\boldsymbol{n}} \left[\sqrt{g\mathcal{S}} \left(a_{\boldsymbol{n}}^\dagger a_{\boldsymbol{n}} + \frac{1}{2} \right) - \frac{1}{2}\sqrt{\frac{g}{\mathcal{S}}} \sum_{j=1}^d \left[a_{\boldsymbol{n}}^\dagger a_{\boldsymbol{n}+\boldsymbol{e}_j} + a_{\boldsymbol{n}} a_{\boldsymbol{n}+\boldsymbol{e}_j}^\dagger + a_{\boldsymbol{n}}^\dagger a_{\boldsymbol{n}+\boldsymbol{e}_j}^\dagger + a_{\boldsymbol{n}} a_{\boldsymbol{n}+\boldsymbol{e}_j} \right] \right]$$
$$\tag{1.3.15}$$

We wish to point out an analogy with quantum Ising/XY chains (also called Ising/XY chains in a transverse field), with an anisotropy in spin space, and given by the Hamiltonian [Kat62, McC71]

$$\mathcal{H}_{\mathrm{XY}} = -\frac{1}{2} \sum_n \left[g\sigma_n^z + \frac{1+\lambda}{2}\sigma_n^x\sigma_{n+1}^x + \frac{1-\lambda}{2}\sigma_n^y\sigma_{n+1}^y \right] \tag{1.3.16}$$

$$= \sum_n \left[g\left(c_n^\dagger c_n - \frac{1}{2} \right) - \frac{1}{2}\left[c_n^\dagger c_{n+1} - c_n c_{n+1}^\dagger + \lambda\left(c_n^\dagger c_{n+1}^\dagger - c_n c_{n+1} \right) \right] \right] \tag{1.3.17}$$

---

[15]In the QSM the spherical parameter freezes in the ordered phase in the same fashion as in the classical SM

Table 1.5: Critical exponents for the quantum spherical model (1.3.18) at zero temperature, along the quantum critical isochore $h = 0$, in dependence on the dimension d and the coupling λ.

critical isochore		α	β	γ	ν	η	θ
$d < 3$	$\lambda \neq 0$	$\frac{d-3}{d-1}$	$\frac{1}{2}$	$\frac{2}{d-1}$	$\frac{1}{d-1}$	0	1
$d > 3$	$\lambda \neq 0$	0	$\frac{1}{2}$	1	$\frac{1}{2}$	0	1
$d > 0$	$\lambda = 0$	0	$\frac{1}{2}$	1	$--$	$--$	2

where the $\sigma_n^{x,y,z}$ denote the Pauli matrices attached to the nth site of a periodic chain of N sites and the c_n are fermionic operators obtained from a Jordan-Wigner transformation. The transverse field g measures the quantum fluctuations and λ is a spin-anisotropy coupling.

The ground-state of quantum Ising/XY chain (1.3.16) has a rich phase diagram with a disordered phase for $g > 1$, a line of second-order transitions at $g = 1$ which is in the universality class of the 2D Ising model for $\lambda \neq 0$, an ordered ferromagnetic phase for $\sqrt{1 - \lambda^2} < g < 1$ and an ordered oscillating phase for $g < \sqrt{1 - \lambda^2}$ [McC71, Hen87b, Bur87, Hof96, Cha96, Hen99, Kar00, Dut15]. The universality of the quantum critical behaviour at $T = 0$, including the universal amplitude combinations [Pri84, Pri93, Hen01, Cam14], with respect to $0 < \lambda \leq 1$ along the Ising critical line has been explicitly confirmed: for the chain for both the spin-$\frac{1}{2}$ as well as the the spin-1 representations of the Lie algebra of the rotation group [Hen87b, Bur87, Hof96], as well as in 2D for the spin-$\frac{1}{2}$ representation [Hen84a, Hen87a].

Comparing the fermionic Hamiltonian (1.3.17) with the bosonic one (1.3.15),[16] one observes that in the former the two-particle annihilation/creation processes are controlled by the parameter λ, whereas that parameter happens to be fixed to unity in the latter. Here, we shall inquire into what happens if an analogous rate is introduced into the Hamiltonian (1.3.15), and write [Wal15]

$$H = \sqrt{g\mathcal{S}} \sum_{\boldsymbol{n}} \left[a_{\boldsymbol{n}}^\dagger a_{\boldsymbol{n}} + \frac{1}{2} - \frac{1}{\mathcal{S}} \sum_{j=1}^d \left(a_{\boldsymbol{n}}^\dagger a_{\boldsymbol{n}+\boldsymbol{e}_j} + a_{\boldsymbol{n}} a_{\boldsymbol{n}+\boldsymbol{e}_j}^\dagger + \lambda \left(a_{\boldsymbol{n}}^\dagger a_{\boldsymbol{n}+\boldsymbol{e}_j}^\dagger + a_{\boldsymbol{n}} a_{\boldsymbol{n}+\boldsymbol{e}_j} \right) \right) \right]$$

$$= \sum_{\boldsymbol{n}} \left[\frac{g}{2} p_{\boldsymbol{n}}^2 + \frac{\mathcal{S}}{2} s_{\boldsymbol{n}}^2 - \sum_{j=1}^d \left(\frac{1+\lambda}{2} s_{\boldsymbol{n}} s_{\boldsymbol{n}+\boldsymbol{e}_j} + \frac{1-\lambda}{2\mathcal{S}} g\, p_{\boldsymbol{n}} p_{\boldsymbol{n}+\boldsymbol{e}_j} \right) \right] \tag{1.3.18}$$

The re-formulation in terms of the original spins and momenta shows that the Hamiltonian (1.3.18) introduces an interaction between the momenta, quite analogous to the spin anisotropies in the quantum XY chain (1.3.16).

The computation of the eigenvalues is carried out in [Wal15] and is as in the isotropic case a matter of finding the appropriate canonical transformation. After the diagonalisation process this model allows for analytic analysis of all physical quantities and the reader may again consult [Wal15] for an overview. Here, we first want to list the critical exponents in tab 1.5 and 1.6. These exponents do not depend on the anisotropy parameter $\lambda \neq 0$ and are identical to the exponents of the isotropic model which is an explicit manifestation of universality.

Quantum phase transition

In $d > 2$ dimensions, the spherical model undergoes a thermal phase transition at some critical temperature $T_c > 0$ [Voj96, Ma97, Sac01, Bra00, SG04, Oli06]. In general, one expects that this finite-temperature transition of the d-dimensional model should be in the same universality class as the one of the classical model (without quantum terms) [Kog79, Sac01, Bra00]. Here, we rather

---

[16]Alternatively, one can consider the fermionic degrees of freedom in (1.3.17) as *hard-core bosons*. Relaxing the 'hard-core/fermionic' constraint on the single-site occupation numbers $\langle n_i \rangle = \langle c_i^\dagger c_i \rangle \stackrel{!}{=} 0, 1$, towards $\sum_i \langle c_i c_i^\dagger \rangle \stackrel{!}{=} \bar{\nu}\mathcal{N}$, where $\bar{\nu} = \frac{1}{2}$ is a filling factor, one has a third way to replace (1.3.17) by a quantum spherical model [Ma97].

Table 1.6: Critical exponents for the quantum spherical model (1.3.18) at zero temperature, along the quantum critical 'isotherm' $\mathfrak{r}_g = 0$, in dependence on the dimension d and the coupling λ.

critical isotherm		α_c	γ_c	δ	ν_c
$d < 3$	$\lambda \neq 0$	$2\frac{d-3}{d+3}$	$\frac{4}{d+3}$	$\frac{d+3}{d-1}$	$\frac{2}{d+3}$
$d > 3$	$\lambda \neq 0$	0	$\frac{2}{3}$	3	$\frac{1}{3}$
$d > 0$	$\lambda = 0$	0	$-\frac{1}{3}$	3	$-$

focus on the quantum phase transition which occurs in the ground-state, that is, at temperature $T = 0$.

Generically, quantum phase transitions arise mathematically from a degeneracy in the ground state of the Hamiltonian. The diagonal Hamiltonian in zero field reads [Wal15]

$$H = \sqrt{2g/\mathcal{S}} \sum_{\boldsymbol{k} \in \mathcal{B}} \Lambda_{\boldsymbol{k}} \left(\widehat{b}_{\boldsymbol{k}}^{\dagger} \widehat{b}_{\boldsymbol{k}} + \frac{1}{2} \right) \quad , \text{ with} \tag{1.3.19}$$

$$\Lambda_{\boldsymbol{k}} := \sqrt{\mathcal{S} - \frac{1+\lambda}{2} \sum_{j=1}^{d} \cos k_j} \sqrt{\mathcal{S} - \frac{1-\lambda}{2} \sum_{j=1}^{d} \cos k_j} \tag{1.3.20}$$

and we can thereof deduce the smallest energy gap ΔE

$$\Delta E \propto \lim_{\boldsymbol{k} \to \boldsymbol{0}} \Lambda_{\boldsymbol{k}} = \sqrt{\mathcal{S} - \frac{1+\lambda}{2}d} \sqrt{\mathcal{S} - \frac{1-\lambda}{2}d} \tag{1.3.21}$$

This energy gap closes at the critical point

$$\mathcal{S}_c := \frac{1+|\lambda|}{2}d \tag{1.3.22}$$

such that the spherical parameter must satisfy $\mathcal{S} \geq (1+|\lambda|)d/2$. We can now evaluate the free energy density in the continuum limit

$$f = T \int_{\mathcal{B}} \frac{\mathrm{d}\boldsymbol{k}}{(2\pi)^d} \ln \sinh \left[\frac{1}{T} \sqrt{\frac{g}{2\mathcal{S}}} \, \Lambda_{\boldsymbol{k}} \right] \tag{1.3.23}$$

and deduce the ground-state thermodynamics from an analysis of the spherical constraint (1.3.10), which in the limit $T \to 0$ takes the form

$$1 = \sqrt{\frac{g\mathcal{S}}{8}} \int_{\mathcal{B}} \frac{\mathrm{d}\boldsymbol{k}}{(2\pi)^d} \, \Lambda_{\boldsymbol{k}}^{-1} \left(1 - \frac{1-\lambda^2}{4\mathcal{S}^2} \left[\sum_{j=1}^{d} \cos k_j \right]^2 \right) \tag{1.3.24}$$

This defines the function $\mathcal{S} = \mathcal{S}(g, \lambda, d, h)$, or alternatively its inverse $g = g(\mathcal{S}, \lambda, d, h)$. For a vanishing external field $h = 0$, this equation is symmetric under $\lambda \mapsto -\lambda$, hence it is then sufficient to consider the case $\lambda \geq 0$ only. We shall almost always restrict to this special case, and then write $g = g(\mathcal{S}, \lambda, d) := g(\mathcal{S}, \lambda, d, 0)$.

Physical observables near quantum criticality

The scaling of the thermodynamic observables follows from the free-energy density. Since we restrict ourselves to an analysis of the zero-temperature properties of our model, the quantum coupling g takes over the role of the temperature in classical spin systems, such that $\mathfrak{r}_g := \sqrt{\frac{8}{g_c} \frac{g_c - g}{g_c}}$ takes over the role of $T - T_c$ in classical phase transitions. Therefore, one expects the singular part f^{sin} of the free energy density to obey the following scaling behaviour

$$f^{\mathrm{sin}}(\mathfrak{r}_g, h) = A_1 |\mathfrak{r}_g|^{2-\alpha} W_{\pm} \left(A_2 h |\mathfrak{r}_g|^{-\beta-\gamma} \right) \tag{1.3.25}$$

where $W_\pm$ are universal scaling functions, associated with the sign of $\mathfrak{r}_g \gtrless 0$, and α, β, γ are the standard critical exponents. All non-universal information on the specific model can be absorbed into the two metric factors $A_{1,2}$. For isotropic classical phase transitions, a long-standing result of Privman and Fisher [Pri84] states that there exist only two independent non-universal metric factors, such as $A_{1,2}$. For quantum systems, anisotropies are possible between correlators along the spatial lattice and correlations in the (euclidean) 'time' direction and generated via the transfer matrix $\mathcal{T} = \exp\left(-\tau\mathcal{H}\right)$. One then must distinguish 'parallel' distances $r_\parallel$ along the 'time' direction and 'perpendicular' distances $\boldsymbol{r}_\perp$ along the space direction. The correlation length $\xi = \xi_\perp$ considered here is spatial, whereas the 'temporal' correlation length $\xi_\parallel \sim (\Delta E)^{-1}$ is related to the energy gap of H. The anisotropy between 'time' and 'space' introduces a further metric factor which in those cases where there is a classical analogue, and therefore the dynamical exponent $z = 1$, amounts simply to a further independent amplitude D_0 related to the freedom of normalisation of the quantum Hamiltonian $\mathcal{H}$. For such anisotropic or quantum systems (at $T = 0$), one expects a scaling form for a two-point correlator [Hen01, Cam14, Kir15]

$$C(R; \mathfrak{r}_g, B) = D_0 D_1 R^{2-d-z-\eta} X_\pm \left(|\boldsymbol{R}|/\xi; D_0 r_\parallel / \xi^z; D_2 B \, |\mathfrak{r}_g|^{-\beta-\gamma} \right) \qquad (1.3.26)$$

where in the situation under study here, we have $R = |\boldsymbol{R}| = |\boldsymbol{r}_\perp|$ and $r_\parallel = 0$. As before, $X_\pm$ are universal scaling functions with non-universal metric factors $D_{0,1,2}$. For isotropic systems, one has $z = 1$ such that the distinction between the scaling of $\boldsymbol{r}_\perp$ and $r_\parallel$ is no longer necessary and $D_0 = 1$ without restriction to the generality. Then, in that situation, only two of the four metric factors $A_{1,2}, D_{1,2}$ are independent, according to the long-standing Privman-Fisher hypothesis [Pri84]. This follows by tracing the metric factors as they occur in the thermodynamic observables and using the static fluctuation-dissipation theorem. For potentially anisotropic or quantum systems, even if $z = 1$, this argument has to be generalised in order to admit a potentially non-universal normalisation D_0. This leads to the following universal amplitude combinations $Q_{1,2,3}$ [Hen01]

$$Q_1 = A_1 \xi_0^{d+z} D_0^{-1}; \qquad Q_2 = D_2 A_2^{-1}; \qquad Q_3 = D_0^{\frac{\gamma}{\nu(d+z)}} D_1 A_1^{-1-\frac{\gamma}{\nu(d+z)}} A_2^{-2} \qquad (1.3.27)$$

where the amplitude ξ_0 is from $\xi \simeq \xi_0 \mathfrak{r}_g^{-\nu}$. Here, we shall use the dependence on the parameter $\lambda > 0$ to control explicitly the universality and hence to test the scaling forms (1.3.25, 1.3.26).

Returning to the quantum spherical model at $T = 0$, the analysis of the spherical constraint (1.3.24), see appendix C in [Wal15], gives us the dependence of the shift $\mathfrak{r}_g$ on the shifted spherical parameter $\sigma = \mathcal{S} - \mathcal{S}_c$. Including now the magnetic field h as well, we have to leading order in σ

$$\mathfrak{r}_g - \frac{h^2}{\sqrt{2g_c}} \frac{1}{\sigma^2} \simeq \begin{cases} A_< \, \sigma^{\frac{d-1}{2}} & ; \quad \text{if } d < 3 \\ A_3 \, \sigma \ln \sigma & ; \quad \text{if } d = 3 \\ A_> \, \sigma & ; \quad \text{if } d > 3 \end{cases} \qquad (1.3.28)$$

with explicitly known amplitudes $A_<$, A_3 and $A_>$. For a non-vanishing magnetic field $h \neq 0$ the magnetic contribution will always dominate the behaviour of the spherical constraint near criticality.

To begin with the investigation of the critical behaviour, we consider the spin-spin correlation $C(|\boldsymbol{r}|) = \langle s_{\boldsymbol{n}} s_{\boldsymbol{n}+\boldsymbol{r}} \rangle$ at zero temperature $T = 0$ in order to find the correlation length. As shown in [Wal15], we can use spatial translation- and rotation-invariance, and have for $\lambda > 0$

$$C(R) = (2\pi)^{-\frac{d+1}{2}} \sqrt{\frac{g}{\mathcal{S}}} \frac{\mathcal{S} - (1-\lambda)d}{\sqrt{\lambda(1+\lambda)d}} \left(\frac{1}{\xi R} \right)^{(d-1)/2} K_{\frac{d-1}{2}} \left(\frac{R}{\xi} \right) \qquad (1.3.29)$$

where we identify the correlation length, with $\mathcal{S} = (1+\lambda)d + 2\sigma$, as follows

$$\xi = \sqrt{\frac{1+\lambda}{4}} \, \sigma^{-1/2} \qquad (1.3.30)$$

and $K_\nu(x)$ is the other modified Bessel function [Abr64].

1. First, we treat the case $0 < \lambda < 1$ and $1 < d < 3$. From the Gibbs free energy, eq (1.3.23), we find for the magnetisation near criticality

$$m(\mathfrak{r}_g, h) = -\frac{\partial f(\mathfrak{r}_g, h)}{\partial h} = \frac{h}{2}\frac{1}{\sigma} \tag{1.3.31}$$

where the spherical constraint (1.3.28) must be used. The critical behaviour is extracted by moving along the quantum critical 'isochore' $h = 0$ or else the quantum critical 'isotherm' $\mathfrak{r}_g = 0$. We obtain

$$m(\mathfrak{r}_g, 0) \simeq \left[\frac{g_c}{8}\right]^{\frac{1}{4}}\sqrt{\mathfrak{r}_g} \, , \tag{1.3.32}$$

$$m(0, h) \simeq 2^{-\frac{d+2}{d+3}}A_<^{\frac{2}{d+3}}g_c^{\frac{1}{d+3}}h^{\frac{d-1}{d+3}} \tag{1.3.33}$$

where we used the non-universal amplitudes from (1.3.28) and the value of $g_c = g_c(\lambda, d)$, which are explicitly λ-dependent.

The analogue of the susceptibility is defined by $\chi(\mathfrak{r}_g, h) = \partial m(\mathfrak{r}_g, h)/\partial h$. Explicitly, we find

$$\chi(\mathfrak{r}_g, 0) = \frac{1}{2}A_<^{\frac{2}{d-1}}\mathfrak{r}_g^{-\frac{2}{d-1}} \, , \tag{1.3.34}$$

$$\chi(0, B) = 2^{-\frac{d+2}{d+3}}\frac{d-1}{d+3}A_<^{\frac{2}{d+3}}g_c^{\frac{1}{d+3}}h^{-\frac{4}{d+3}} \tag{1.3.35}$$

In general, the specific heat is given by the second derive of the free energy with respect to the temperature (here replaced by $\mathfrak{r}_g$). Here, we consider its analogue, where the role of T is taken over by $\mathfrak{r}_g$. Furthermore, in the spherical model, the spherical constraint requires a little more careful consideration as we have already discussed while introducing the QSM, which amounts to

$$c(\mathfrak{r}_g, B) = -\frac{\partial}{\partial \mathfrak{r}_g}\left(\frac{\partial f^{\mathrm{sin}}(\mathfrak{r}_g, h)}{\partial \mathfrak{r}_g}\bigg|_{\mathcal{S}}\right) \tag{1.3.36}$$

where the first derivative must be taken grand-canonically, with fixed spherical parameter, whereas the second derivative is an usual thermodynamic derivative, in the canonical ensemble, see e.g. [Ber52, Lew52, Bax82, Hen84b, Bra00, Bie13]. We find

$$c(\mathfrak{r}_g, 0) = c_0 + \frac{1}{d-1}\sqrt{\frac{g_c}{2}}A_<^{-\frac{2}{d-1}}\mathfrak{r}_g^{-\frac{d-3}{d-1}} \tag{1.3.37}$$

$$c(0, h) = c_0 + \frac{1}{d-1}g_c^{\frac{1}{d+3}}8^{\frac{d-2}{d+3}}A_<^{-\frac{2d}{d+3}}h^{2\frac{d-3}{d+3}} \tag{1.3.38}$$

where c_0 is an unimportant background constant.

The correlation length ξ, introduced in eq (1.3.30), reads near criticality

$$\xi(\mathfrak{r}_g, 0) = \sqrt{\frac{1+\lambda}{4}}A_<^{\frac{1}{d-1}}\cdot\mathfrak{r}_g^{1/(d-1)} \tag{1.3.39}$$

$$\xi(0, B) = \sqrt{1+\lambda}\left(\sqrt{\frac{g_c}{2}}A_<\right)^{\frac{1}{d+3}}2^{-\frac{d+2}{d+3}}\cdot B^{-\frac{2}{d+3}} \tag{1.3.40}$$

Here, the correlation length $\xi \sim 1/\Delta E$ is related to the lowest energy gap in the Hamiltonian H, such that the dynamical exponent $z = 1$.

Finally, for the correlation function, we have from (1.3.29) that at criticality, where $\sigma = 0$

$$C(R) = \langle s_0 s_R \rangle = \sqrt{\frac{g_c}{2}}\frac{\sqrt{\lambda}}{1+\lambda}\frac{\Gamma\left(\frac{d-1}{2}\right)}{\pi^{\frac{1+d}{2}}}R^{1-d} \tag{1.3.41}$$

In contrast to the thermodynamics observables considered before, this result[17] holds true for arbitrary dimensions and is not restricted to $d < 3$.

---

[17] Observe that the exponents of R in $C(R) \sim R^{-(d-1)}$ for $\xi \gg R$ and $C(R) \sim R^{-d/2}e^{-R/\xi}$ for $\xi \ll R$ are different. For $d = 2$, one recovers the Ornstein-Zernicke form.

For the interpretation of these results, we recall the conventional critical exponents and also the associated amplitudes, in the notation of [Pri93], along the quantum critical 'isochore' $h = 0$

$$m \simeq B\mathfrak{r}_g^\beta \; ; \; \chi \simeq \Gamma\mathfrak{r}_g^{-\gamma} \; ; \; c \simeq \frac{A}{\alpha}\mathfrak{r}_g^{-\alpha} + c_0 \; ; \; \xi \simeq \xi_0\mathfrak{r}_g^{-\nu} \; ; \; G(R) \sim R^{2-d-z-\eta} \; ; \; \Delta E \sim \xi^{-z} \quad (1.3.42)$$

The values of the exponents can be read off and are collected in tab 1.5. As expected they agree with those of the classical spherical model in $d + 1$ dimensions.

Along the quantum critical isotherm, $\mathfrak{r}_g = 0$, one can define

$$c \simeq c_0 + (A_c/\alpha_c)|h|^{-\alpha_c} \; ; \; \chi \simeq \Gamma_c|h|^{-\gamma_c} \; ; \; h \simeq D_c m|m|^{\delta-1} \; ; \; \xi \simeq \xi_c|h|^{-\nu_c} \quad (1.3.43)$$

and read off the exponents[18], collected in tab 1.6. The universality of this quantum phase transition is confirmed through the λ-independence of all these exponents.

In addition, the universality of full scaling scaling forms (1.3.25, 1.3.26) can be tested by working out at least three universal amplitude combinations [Pri93]. Considering the singular free energy and its derivatives, we considered three amplitude combinations which from (1.3.25) are expected to be universal. Explicitly, we give the results which follow from our explicit calculations above

$$R_c = A\Gamma/B^2 = \frac{3-d}{(d-1)^2} \qquad R_\chi = \Gamma D_c B^{\delta-1} = 1 \qquad \delta\Gamma_c D_c^{1/\delta} = 1 \; . \quad (1.3.44)$$

The λ-independence of these three amplitude ratios is an additional confirmation of the scaling form (1.3.25), with only two non-universal metric factors. In order to test the universality of the scaling form (1.3.26) of the spin-spin correlator, consider

$$Q_1 = 2^{2-d}\frac{\Gamma\left(\frac{1-d}{2}\right)}{\Gamma\left(\frac{d-1}{2}\right)}\frac{W_+''(0)^2}{W_+'(0)^2}X_+(0) \qquad\qquad\qquad (1.3.45)$$

$$Q_3 = 2^{\frac{2d}{d+1}}\left(\frac{\Gamma\left(\frac{d-1}{2}\right)}{\Gamma\left(\frac{1-d}{2}\right)X_+(0)}\right)^{\frac{2}{d+1}}\frac{W_+'(0)^{\frac{1-d}{d+1}}}{W_+''(0)^{\frac{4}{d+1}}} \qquad\qquad (1.3.46)$$

whose universality is likewise confirmed explicitly through the λ-independence. Observe that for $1 < d < 3$ all universal amplitude ratios in (1.3.44, 1.3.46) are finite, but that several of them they either vanish or diverge when $d \to 1$ or $d \to 3$. This indicates that the scaling behaviour is going to be different (or does not even exist) when $d \geq 3$ or $d \leq 1$.

For the spin-anisotropic quantum spherical model, we can conclude that *the scaling forms (1.3.25, 1.3.26), and their universality, have been fully confirmed at the quantum critical point at* $T = 0$, $g = g_c(\lambda, d)$, *with* $1 < d < 3$ *and* $0 < \lambda \leq 1$.[19] Since the scaling functions themselves are universal, they were already calculated explicitly in the classical spherical model in $d + 1$ dimensions, see e.g. [Bra00], and do not need to be repeated here.

2. For $0 < \lambda < 1$ and $d = 3$, we are working at the upper critical dimension. Therefore, we have to introduce logarithmic corrections to the scaling behaviour, see eq (1.3.28). In order to work with the logarithmic terms and the magnetic field, we introduce the dimensionless field $\widehat{B} := \frac{2B}{\sqrt{g_c}}$. In this manner, the expression $\ln\widehat{B}$ is well-defined viz. dimensionless. We find for the magnetisation

$$m(\mathfrak{r}_g, 0) \simeq \left[\frac{g_c}{8}\right]^{\frac{1}{4}} \cdot \mathfrak{r}_g^{\frac{1}{2}} \qquad\qquad\qquad (1.3.47)$$

$$m(0, \widehat{B}) \simeq \sqrt{\frac{g_c}{8}}\left(\frac{2}{3}A_3\right)^{\frac{1}{3}} \cdot |\widehat{B}|^{\frac{1}{3}}|\ln|\widehat{B}||^{\frac{1}{3}} \qquad\qquad (1.3.48)$$

and for the susceptibility

$$\chi(\mathfrak{r}_g, 0) \simeq \frac{A_3}{2} \cdot |\mathfrak{r}_g|^{-1}|\ln|\mathfrak{r}_g|| \qquad\qquad\qquad (1.3.49)$$

$$\chi(0, \widehat{B}) \simeq \frac{1}{2}\left(\frac{2A_3}{3}\right)^{\frac{1}{3}} \cdot |\widehat{B}|^{-\frac{2}{3}}|\ln|\widehat{B}||^{\frac{1}{3}} \qquad\qquad (1.3.50)$$

---

[18]These obey the standard scaling relations, such as $\alpha_c = \alpha/\beta\delta$, $\gamma_c = 1 - 1/\delta$, $\nu_c = \nu/\beta\delta$.

[19]The condition $0 < \lambda < 1$ comes from the techniques used to analyse the spherical constraint, see [Wal15] for details.

In the same manner as above, we calculate the specific heat and find

$$c(\mathfrak{r}_g, 0) \simeq \sqrt{\frac{2g_c}{A_3^2}} \cdot |\ln|\mathfrak{r}_g||^{-1} \tag{1.3.51}$$

$$c(0, \widehat{B}) \simeq 3\sqrt{\frac{g_c}{2A_3^2}} \cdot |\ln|\widehat{B}||^{-1} \tag{1.3.52}$$

Finally, the correlation length reads

$$\xi(\mathfrak{r}_g, 0) \simeq \sqrt{\frac{1+\lambda}{4A_3}} \cdot |\mathfrak{r}_g|^{-\frac{1}{2}} \cdot |\ln|\mathfrak{r}_g||^{\frac{1}{2}} \tag{1.3.53}$$

$$\xi(0, \widehat{B}) \simeq \sqrt{\frac{1+\lambda}{4}} \left(\frac{2A_3}{3}\right)^{\frac{1}{6}} \cdot |\widehat{B}|^{-\frac{1}{3}} |\ln|\widehat{B}||^{\frac{1}{6}} \tag{1.3.54}$$

This logarithmic behaviour can be described in terms of logarithmic sub-scaling exponents [Ken06a, Ken06b]

$$c \sim |\mathfrak{r}_g|^{-\alpha} |\ln|\mathfrak{r}_g||^{\widehat{\alpha}} \ ; \ m(\mathfrak{r}_g, 0) \sim |\mathfrak{r}_g|^{\beta} |\ln|\mathfrak{r}_g||^{\widehat{\beta}} \ ; \ \chi \sim |\mathfrak{r}_g|^{-\gamma} |\ln|\mathfrak{r}_g||^{\widehat{\gamma}} \ ;$$
$$\xi \sim |\mathfrak{r}_g|^{-\nu} |\ln|\mathfrak{r}_g||^{\widehat{\nu}} \ ; \ m(0, \widehat{B}) \sim \widehat{B}^{1/\delta} |\ln|\widehat{B}||^{\widehat{\delta}} \ ; \ C(R) \sim R^{-(d-2+z+\eta)} |\ln R|^{\widehat{\eta}} \tag{1.3.55}$$

and we simply read off their (universal, since λ-independent) values

$$\widehat{\alpha} = -1 \ ; \ \widehat{\beta} = 0 \ ; \ \widehat{\gamma} = 1 \ ; \ \widehat{\nu} = \frac{1}{2} \ ; \ \widehat{\delta} = \frac{1}{3} \ ; \ \widehat{\eta} = 0 \tag{1.3.56}$$

These values agree with those of the $4D$ $O(n)$-Heisenberg model in the limit $n \to \infty$ [Ken06a, Ken06b, Hen10].

3. In the case $0 < \lambda < 1$ and $3 < d$ we expect mean-field critical behaviour. Near criticality $0 < \mathfrak{r}_g \ll 1$, we find the observables in the same manner as in the previous parts, but with the 'linear' spherical constraint. We find the observables along the critical $B = 0$ line

$$m(\mathfrak{r}_g, 0) = \left[\frac{g_c}{8}\right]^{\frac{1}{4}} \mathfrak{r}_g^{\frac{1}{2}} \ ; \qquad\qquad \chi(\mathfrak{r}_g, 0) = \frac{A_>}{2}\mathfrak{r}_g^{-1} \ ; \tag{1.3.57}$$

$$c(\mathfrak{r}_g, 0) = \frac{\sqrt{g_c/2}}{A_>} \ ; \qquad\qquad \xi(\mathfrak{r}_g, 0) = \sqrt{\frac{1+\lambda}{4}A_>}\mathfrak{r}_g^{-\frac{1}{2}} \ ; \tag{1.3.58}$$

and along the quantum critical isotherm $\mathfrak{r}_g = 0$ they read

$$m(0, B) = \left[\frac{\sqrt{g_c/8}}{2A_>}\right]^{\frac{1}{3}} B^{\frac{1}{3}} \ ; \qquad \chi(0, B) = \frac{1}{2}\left[\frac{A_>}{\sqrt{g_c/2}}\right]^{-\frac{1}{3}} B^{-\frac{2}{3}} \ ; \tag{1.3.59}$$

$$c(0, B) = \frac{\sqrt{g_c}}{\sqrt{2}A_>} \ ; \qquad\qquad \xi(0, B) = \sqrt{\frac{1+\lambda}{4}} \left[\frac{\sqrt{2g_c}}{A_>}\right]^{\frac{1}{6}} B^{-\frac{1}{3}} \ ; \tag{1.3.60}$$

Reading off the critical exponents (see tab 1.5 and 1.6) yields the expected mean-field behaviour.

4. A different universality class is found for $\lambda = 0$, for any dimension d. The free energy density reads

$$f(\mathfrak{r}_g, B) = -\frac{B^2}{4}\frac{1}{\sigma} + \frac{\sqrt{g}}{2}\mathcal{S} \tag{1.3.61}$$

The magnetisation reads consequently

$$m(\mathfrak{r}_g, 0) \simeq \frac{1}{\sqrt{8}} \cdot \mathfrak{r}_g^{1/2} \tag{1.3.62}$$

$$m(0, B) \simeq (2d)^{-1/3} \cdot B^{1/3} \tag{1.3.63}$$

and the magnetic susceptibility becomes

$$\chi(\mathfrak{r}_g, 0) \simeq \frac{1}{2} \frac{\sqrt{8}}{d} \cdot \mathfrak{r}_g^{-1} \tag{1.3.64}$$

$$\chi(0, B) \simeq \left(\frac{d}{2}\right)^{1/3} \cdot B^{1/3} \tag{1.3.65}$$

The specific heat is found to be constant near criticality and along the quantum critical isotherm

$$c \simeq \frac{d^{\frac{3}{2}}}{2} \tag{1.3.66}$$

The critical exponents are listed in tab 1.5 and 1.6. They are distinct from those of the modified quantum spherical models defined in [Nie95, SG04], where the particle number N is conserved as well.

For the correlation function, we see a disconnected part from the zero temperature contribution. As derived in appendix D of [Wal15], we have to take thermal contributions into account. We then find

$$C(R) = \sqrt{\frac{g}{4\mathcal{S}}} + \sqrt{\frac{g}{\mathcal{S}}} \exp\left(-z\mathcal{S}\right) I_0(z)^{d-1} I_R(z) \tag{1.3.67}$$

with $z = \sqrt{g/T^2\mathcal{S}}$. At criticality, we can deduce to leading order in T (see appendix D in [Wal15] for details)

$$\begin{aligned}
C(R) &= \sqrt{\frac{g_c}{4d}} \delta_{R,0} + \sqrt{\frac{g_c}{d}} \left(\frac{T^2 d}{4\pi^2 g_c}\right)^{d/4} \exp\left(-\frac{R^2 T}{2} \sqrt{\frac{d}{g_c}}\right) \\
&= \frac{1}{2} T \xi_T^{-2} \delta_{R,0} + T \xi_T^{2-d} \exp\left(-\frac{1}{2}\left(\frac{R}{\xi_T}\right)^2\right)
\end{aligned} \tag{1.3.68}$$

with the thermal reference length $\xi_T^{-4} := T^2 d/g_c$ and where the critical coupling constant $g_c = g_c(0, d; T)$ has to be found from the spherical constraint in the non-vanishing zero-temperature limit. To leading order in T, this gives the condition

$$\sqrt{\frac{1}{g_c}} = \sqrt{\frac{1}{4d}} + \frac{d^{-1/2}}{(2\pi)^{d/2}} \left(\frac{d}{g_c}\right)^{d/4} T^{d/2} \tag{1.3.69}$$

hence $g_c \simeq 4d\left(1 - \frac{2/\sqrt{d}}{(4\pi)^{d/2}} T^{d/2} + \dots\right)$, which illustrates how finite-temperature effects renormalise the value of g_c. The behaviour (1.3.68) of the correlation function does not fit into the standard phenomenology, described by the conventional critical exponents [DF97, Hen99, Sac01, Bra00].

1.3.4   Phase diagram

We have studied the statistical properties of the spin anisotropic quantum spherical model and describes the physical observables fully. Now, we want to understand how the phase diagram of the QSM, which is somewhat similar fig 1.7, compare e.g. [Oli06], is modified at $T = 0$ as a function of λ.

A surprising feature of the model studied at thermal equilibrium for zero temperature is the presence of a re-entrant quantum phase transition for dimensions $d \lesssim 2.065$ and sufficiently small values of λ, see the right panel of fig 1.18 . This shape of the quantum critical line could not have been anticipated from previous studies of the classical spherical model. This makes it clear that interactions between the momenta cannot always be absorbed into a change of variables. Moreover, considering the leading finite-temperature corrections to the value of $g_c(\lambda, d)$, it can be shown that for T sufficiently small, the value of g_c is only slightly renormalised such that the re-entrant transition also occurs for finite (and small) temperatures $T > 0$.

In the left panel of fig 1.18 we compare the shape of the critical line $g_c = g_c(\lambda)$, normalised to the value at $g_c(0)$ at $\lambda = 0$, of the bosonic quantum spherical model (1.3.18), with the fermionic
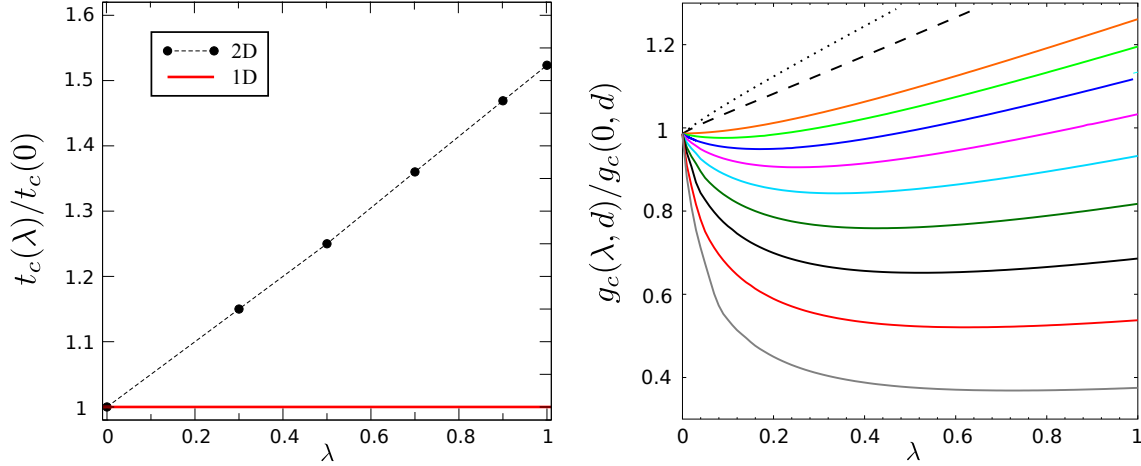
Figure 1.18: Left panel: normalised critical quantum coupling $g_c(\lambda)/g_c(0)$ in the quantum XY model (1.3.16), as a function of the coupling λ. In $1D$, one has $g_c(\lambda) = 1$. In $2D$, the numerically known estimates of $g_c(\lambda)$ [Hen84a, Hen87a] are given by the dots and the dashed line is a guide to the eye. Right panel: normalised critical coupling $g_c(\lambda, d)/g_c(0, d)$ in the quantum spherical model (1.3.18), as a function of λ and for dimensions $d = [1.3, 1.4, 1.5, 1.6, 1.7, 1.8, 1.9, 2.0, 2.1, 2.5, 3.0]$ from bottom to top in different colours.

quantum XY model. In $1D$, the latter model reduces to free fermions. Comparing the shapes of $g_c(\lambda, d)$, the re-entrant phase transition found in the bosonic case of the SAQSM does not appear in the analogous $1D$ fermionic model, where $g_c(\lambda) = 1$ is simply constant [McC71, Suz71]. In order to better appreciate the influence of dimensionality in the quantum XY chain on $g_c(\lambda)$, and in the absence of an analytic solution, the best what we can do is to compare with the few known numerical values of $g_c(\lambda)$ in extension of the spin Hamiltonian H_{XY} from (1.3.16) to $2D$ [Hen84a, Hen87a]. Although those few data shown in fig 1.18 seem to indicate that the approach of $g_c(\lambda)$ towards the $\lambda = 0$ case should be monotonous and hence no re-entrant transition is suggested, the available data are too few and too far apart for a final conclusion.

These results illustrate the non-trivial character of the quantum ground state of the SAQSM. Below, we shall impose the requirement that any quantum dynamics should relax towards it.

1.4   Langevin dynamics in classical systems

As early as 1827 *Robert Brown* studied the pollen of *Clarckia pulchella* immersed in water and he found "*many of them very evidently in motion*"[Bro28]. Finally he arrived to the conclusion that these motions "*arose neither from currents in the fluid, nor from its gradual evaporation, but belonged to the particle itself*". We thus assert that in the 1820s it was *not* at all evident to the scientific world whether the pollens were alive or what else was the origin of their motion.

As we know today, the so called *Brownian motion* has its origin in the constantly ongoing collisions with thermal particles in the liquid and thus it is not possible to describe the dynamics by means of classical mechanics, since there are simply too many liquid molecules present. Moreover, the dynamics of these molecules is irrelevant since on the one hand we are just interested in the dynamics of the suspended particle and on the other hand, the collective properties of the liquid remain unaffected by the suspension of the particles.

It took almost 80 years until the task, of describing the dynamics of a system (pollen) interacting with a bath (water) while neglecting the bath dynamics, was first accomplished by A. Einstein [Ein05]. In his work he derived the *diffusion equation* for the distribution function Υ of the dissolved particles from thermodynamic considerations on the osmotic pressure to be

$$\partial_t \Upsilon = D \partial_x^2 \Upsilon \tag{1.4.1}$$

with the diffusion coefficient D. By giving the exact solution for n dissolved particles

$$\Upsilon(x,t) = \frac{n}{\sqrt{4\pi D}} \frac{\mathrm{e}^{-\frac{x^2}{4Dt}}}{\sqrt{t}} \tag{1.4.2}$$

he succeeded in deriving the *mean displacement* of a suspended particle $\bar{\Delta}_x$: During a time interval τ, the mean displacement $\bar{\Delta}_x$ of a spherical particle with radius a suspended in a bath of temperature T with viscosity μ is

$$\bar{\Delta}_x^2 = \frac{RT}{N_A} \frac{\tau}{3\pi a \mu} \tag{1.4.3}$$

with the universal gas constant R and the Avogadro number N_A. Thus, this equation provides an excellent theoretical justification for experimental measures of N_A. Einstein himself did *not* claim the validity of molecular kinetic theory but rather pointed out that provided this formula, an experimental test will be a strong argument in favour or against the theory [New06].

It was *Jean Baptiste Perrin* [Per09] who studied the mean square displacement of Brownian motion for as many as 200 distinct granules and obtained $N_A = 7.15 \times 10^{23}$, compared to the CODATA value of $N_A \approx 6.022 \times 10^{23}$. In 1926 Perrin was awarded to Nobel prize in physics '*for his work on the discontinuous structure of matter, and especially for his discovery of sedimentation equilibrium*'. Perrin hereby settled the ongoing dispute concerning the molecular theory and together with Einstein's theoretical description, even Wilhelm Ostwald known as '*an old fighter against atomistics ... has been converted by the complete explanation of Brownian motion*' [Som49].

In 1908 Langevin proposed a *simplified approach* which aims at implementing the bath immediately into the equation of motion. By using the *long time limit* Stokes formula for the viscose force and introducing a random force ζ [Lan08]

$$m \frac{\mathrm{d}^2 x}{\mathrm{d}t^2} = -6\pi a \mu \frac{\mathrm{d}x}{\mathrm{d}t} + \zeta \tag{1.4.4}$$

He thus arrives in a very easy and straightforward fashion at the formula derived by Einstein. For completeness, we show the way described in [Lan08]. Multiplying eq (1.4.4) by x and remembering that

$$x \frac{\mathrm{d}^2 x}{\mathrm{d}t^2} = \frac{1}{2} \frac{\mathrm{d}^2 x^2}{\mathrm{d}t^2} - \left(\frac{\mathrm{d}x}{\mathrm{d}t}\right)^2 \tag{1.4.5}$$

leads to

$$\frac{m}{2} \frac{\mathrm{d}^2 x^2}{\mathrm{d}t^2} - m \left(\frac{\mathrm{d}x}{\mathrm{d}t}\right)^2 = -3\pi\mu a \frac{\mathrm{d}x^2}{\mathrm{d}t} + \zeta x \tag{1.4.6}$$

Averaging this equation over a large number of particles makes disappear the term ζx. Moreover, we use the equipartition theorem $m \left(\mathrm{d}x/\mathrm{d}t \right)^2 = RT/N_A$ and one arrives immediately at

$$\bar{\Delta}_x^2 = \frac{RT}{N_A} \frac{\tau}{3\pi a \mu} + K \mathrm{e}^{-6\pi r \eta / m} \tag{1.4.7}$$

which reduces to eq (1.4.3) in the limit of large times $t \to \infty$ (K is an integration constant).

We described this evolution to show on the one hand how the idea of a system interacting with a comparably large reservoir emerged and with what mathematical complications it was connected. But in the final formulation of Langevin's dynamics, it is sufficient to simply damp the amplitude of the dynamical process and implement the bath properties by a *random force* according to

$$m\ddot{x} = -\partial_x H - \gamma \dot{x} + \zeta(x,t) \quad \text{with} \quad \langle \zeta(x,t)\zeta(y,t') \rangle = T\delta(x-y)\delta(t-t') \tag{1.4.8}$$

In the 'over-damped limit' where γ is large enough, the inertial term $m\ddot{x}$ can be dropped if one is merely interested in the long-time evolution [Str07].

Eq (1.4.8) can be easily recast into a coupled system of first order differential equations with the definition $p = m\dot{x}$ as follows

$$\dot{x} = p/m \tag{1.4.9}$$

$$\dot{p} = -\partial_x H - \gamma \dot{x} + \zeta(x,t) \tag{1.4.10}$$

This system will serve us as a defective starting point for a phenomenological description of quantum dynamics.

1.5 Langevin dynamics in quantum systems?

In this section we want to describe a simple phenomenological approach to quantum dynamics, following the example of e.g. [Car99]. This approach will turn out to be defective and we want to discuss its flaws on the example of the quantum mechanical harmonic oscillator with mass m and frequency ω. The Hamiltonian of this system reads

$$\mathcal{H}_{\mathrm{HO}} = \frac{p^2}{2m} + \frac{m\omega^2}{2}x^2 \tag{1.5.1}$$

where the position operator x and the momentum operator p obey the canonical bosonic commutation relation $[x,p] = \mathrm{i}$. By interpreting x and p as Heisenberg operators, one deduces the equations of motion[20]

$$\partial_t x = -\mathrm{i}\left[x, \mathcal{H}_{\mathrm{HO}}\right] = m^{-1}p \tag{1.5.2}$$

$$\partial_t p = -\mathrm{i}\left[p, \mathcal{H}_{\mathrm{HO}}\right] = -m\omega^2 x \tag{1.5.3}$$

By analogy to the Langevin description of classical stochastic motion, it might appear tempting to add a phenomenological damping term $-\gamma p$ to the dynamics of the momentum operator[21]

$$\partial_t x = m^{-1}p \tag{1.5.4}$$

$$\partial_t p = -m\omega^2 x - \gamma p \tag{1.5.5}$$

This is not a satisfactory procedure, since equation of motion for the canonical commutator

$$\partial_t [x,p] = -\gamma [x,p] \tag{1.5.6}$$

implies an exponential decay of the Heisenberg uncertainty and thus a *classical* target state.

As we shall show in section 2.A this statement stays true in the more involved many-body quantum problem: a simple Langevin- or Kramers-like phenomenological equation of motion for

---

[20]In the proceeding text we will introduce thoroughly the notion of quantum dynamics. For now, the reader may take them as granted.

[21]The Langevin equation more precisely describes the so-called over-damped limit in which $\partial_t p = 0$.

the observables, *even if the system is initially in a quantum state*, will turn over rapidly (on a time-scale related to the dissipation constant) to an effectively classical dynamics and the quantum coherence will be lost. Therefore a *coherent* quantum dynamics is required.

The reason for the phenomenological Langevin approach to fail lays in the fact that one should consider the noise as an operator and the coupling between system and bath dictates the commutation relations of the system operators with the noise operator [Gar04].[22]

It remains to say that dissipation effects do not play a significant role in many traditional applications of quantum mechanics as the description of the hydrogen atom or the prediction of atomic spectra. Nonetheless, with advanced physical setups, especially in the field of quantum optics, the interaction of single atoms with lasers in leaky cavities is of fundamental relevance. Moreover, we already mentioned in section 1.2.3 that ultracold atoms in optical lattices can provide an excellent setting to study many-body properties and QPT. It thus seems natural that such a setup may also be suitable for dynamic out-of-equilibrium studies in many-body systems and one then has to use techniques that are able to account for true quantum effects. This is of particular importance as we have discussed in the previous section, that quantum effects are dominant in large portions of the phase diagram.

We shall see that such a description requires a more precise analysis than the one outlined here for classical systems. Particularly, we have to study in great detail the coupling of the "system" to the "bath".

1.6   Coherent quantum dynamics

Our main goal in this section is to derive the Lindblad equation [Lin76]

$$\partial_t \rho_S = -\mathrm{i}\left[\mathcal{H}_S, \rho_S\right] + \sum_\alpha \left(L_\alpha \rho L_\alpha^\dagger - \frac{1}{2} \left\{ L_\alpha^\dagger L_\alpha, \rho_S \right\} \right) \tag{1.6.1}$$

which describes the time evolution of the reduced system density matrix ρ_S of a quantum system interacting with a large environment. We shall first introduce the concepts of closed quantum dynamics and later study the extension to open quantum systems by taking the environment explicitly into account. This review follows mainly [Bre07, Sch14], where the first source follows a more physically motivated approach while the latter one follows a more mathematical path. We shall try here to shed some light from both of these approaches and thus give a complete picture of the Lindblad dynamics of open quantum systems.

Further aspects of the vast field of quantum dynamics are covered in [Car99, Eng02] and references therein. For exact methods in $1D$ quantum dynamics in equilibrium, we refer to [Lan15b, Lan17].

1.6.1   Evolution of closed quantum systems

The physical state of a quantum mechanical system S is described by a *state vector* $|\Psi\rangle$ which is an element of a *Hilbert space* that defines all possible states of S. There is a hermitian Hamiltonian $\mathcal{H}$ associated with the system, which defines the energy of S as well as the *time evolution* according to the *Schrödinger equation*

$$\partial_t |\Psi\rangle = -\mathrm{i}\,\mathcal{H}\,|\Psi\rangle \ . \tag{1.6.2}$$

Starting from this equation, we now introduce the so called *interaction picture* which is desirable to use if one wants to study the effect of a certain part V (usually an interaction) of the full Hamiltonian. One may write the full Hamiltonian in two parts $\mathcal{H} = \mathcal{H}_0 + V$, where $\mathcal{H}_0$ is a rather trivial Hamiltonian of (sub-)systems and V describes the interaction between the different (sub-)systems.

---

[22]Since we shall not be further concerned with *quantum Langevin equations*, we omit the explicit formulae here but rather state them briefly in the end of this section.

Theorem (Interaction Picture): For the quantum system S as described above, the time evolution can be equivalently expressed as

$$\partial_t \left| \tilde{\Psi} \right\rangle = -\mathrm{i}\, V(t) \left| \tilde{\Psi} \right\rangle \tag{1.6.3}$$

with the transformed interaction $V(t) = \mathrm{e}^{\mathrm{i}\mathcal{H}_0 t} V \mathrm{e}^{-\mathrm{i}\mathcal{H}_0 t}$ and the transformed state vector $\left| \tilde{\Psi} \right\rangle = \mathrm{e}^{\mathrm{i}\mathcal{H}_0 t} \left| \Psi \right\rangle$. We call this representation the *interaction picture*.
Proof: A standard calculation proves this theorem [Sch14, Bre07]. $\qquad\square$

We point out that the unitary time evolution of a closed quantum system *always* preserves the information about the initial state. In an out of equilibrium situation, where the system relaxes towards the *unique* equilibrium state such a type of dynamics is thus not applicable since *all* initial states must relax towards the same equilibrium state for sufficiently long times, consequently loosing information about the initial condition.

Another drawback of the closed dynamics is that one has to store the dynamical evolution of *all* degrees of freedom. If a quantum system interacts with a single isolated heat bath, the composed system is closed and one could try to tackle the problem with the unitary time evolution described above. But such heat baths are usually of macroscopic size, thus composed out of typically $\mathrm{O}(10^{23})$ degrees of freedom, for which (in the simplest case of 2-level systems as degrees of freedom) one has to store $\mathrm{O}(2^{10^{23}})$ bits: a task which is *impossible* by means of calculation power. Moreover, in most setups the changes in the baths are not only negligible but also not of interest for the physical questions asked (e.g. in the repeated interaction process, the bath is replaced by a new, identical copy after every interaction [Att06a, Kar09, Wen15]).

Thus, it is required and desirable to implement the bath properties in another way which allows to focus on the system itself.

1.6.2 Density matrix formalism

Density matrices are a convenient tool for the description of quantum dynamics of a system whose exact quantum state is not known but of which statistical information on an ensemble mixture $\{\left| \Psi_i \right\rangle | i \in \mathbb{N}\}$ of possible states is known. We begin by recalling some of their basic properties which will be required in what follows [Sch14, Bre07].

Definition: The **density matrix** ρ of a quantum system described by the Hilbert space $\mathscr{H}$ with the ensemble of possible states $\mathscr{H} \supset \mathscr{E} = \{\left| \Psi_i \right\rangle | i \in \mathbb{N}\}$ and the corresponding discrete probability distribution $\quad \mathcal{P}: \quad \mathscr{E} \to [0,1], \left| \Psi_i \right\rangle \mapsto p_i \quad$ is defined as

$$\rho = \sum_{i \in \mathbb{N}} p_i \left| \Psi_i \right\rangle \left\langle \Psi_i \right| \tag{1.6.4}$$

and canonically obeys the following properties

- $\rho^\dagger = \rho$ (*self adjointness*),

- $\operatorname{tr} \rho = 1$ (*normalisation*),

- $\forall \left| \Psi \right\rangle \in \mathscr{H} \; : \; \left\langle \Psi \right| \rho \left| \Psi \right\rangle \geq 0$ (*positivity*).

The (ensemble) **mean value** of a physical observable $\mathcal{O}$ is then defined as

$$\left\langle \mathcal{O} \right\rangle_{\mathscr{E}} := \operatorname{tr} \mathcal{O} \rho \;. \tag{1.6.5}$$

With the Schrödinger equation (1.6.2) it is straightforward to deduce the so-called *von-Neumann equation*

$$\partial_t \rho = -\mathrm{i} \left[\mathcal{H}, \rho \right] \tag{1.6.6}$$

which governs the dynamics of the density matrix and yields the same dynamics as an ensemble average of the Schrödinger equation.

In order to understand the time evolution of the density matrix, we are now interested in the most general time evolution that maps one density matrix ρ_0 to another density matrix ρ_t. Since the von-Neumann equation is linear, any time evolution can be written as

$$\rho_t = \sum_{\alpha,\beta} \gamma_{\alpha\beta} A_\alpha \rho_0 A_\beta^\dagger \tag{1.6.7}$$

The constraint that ρ_t is a density matrix restricts the evolution as follows

1. **self adjointness**: $\rho_t^\dagger = \rho_t$ implies that the matrix γ has to be hermitian.

2. **normalisation**: The condition $\operatorname{tr}\rho_t = 1$ requires that the evolution itself is a partition of the unity

$$\sum_{\alpha,\beta} \gamma_{\alpha\beta} A_\beta^\dagger A_\alpha = \mathbb{1} . \tag{1.6.8}$$

3. **positivity**: Since $\forall \left|\Psi\right\rangle \in \mathscr{H}$: $\left\langle\Psi\right| \rho_t \left|\Psi\right\rangle$ the matrix γ has to be positive definite.

Since γ is hermitian and positive definite, it can be diagonalised by a suitable unitary transformation U and we name the corresponding positive eigenvalues $\gamma_{\alpha'}\delta_{\alpha'\beta'} := \sum_{\alpha\beta} U_{\alpha'\alpha}\gamma_{\alpha\beta}U_{\beta\beta'}^*$. Rewriting the operators $A_\alpha := \sum_{\alpha'} U_{\alpha\alpha'}/\sqrt{\gamma_{\alpha'}}\,K_{\alpha'}$ leads to the time evolution

$$\rho^\star = \sum_\alpha K_\alpha \rho K_\alpha^\dagger \tag{1.6.9}$$

Definition & Lemma [Sch14] : The *Kraus map*

$$\rho(t + \Delta t) = \sum_\alpha K_\alpha(t, \Delta t)\rho(t)K_\alpha^\dagger(t, \Delta t) \tag{1.6.10}$$

with the *Kraus operators* $K_\alpha(t, \Delta t)$ obeying the relation

$$\mathbb{1} = \sum_\alpha K_\alpha^\dagger(t, \Delta t)K_\alpha(t, \Delta t) \tag{1.6.11}$$

is the most general time evolution that preserves positivity, self adjointness and trace of the density matrix.

In order to describe the time evolution of a system coupled to a thermal bath, we shall need the notion of the *partial trace*. This tool allows to neglect a certain part of a composed system by effectively tracing out the degrees of freedom of the subsystem. By doing so the information on this part of the system is lost. It definition is as follows.

Definition: May $\mathscr{H}$ be a Hilbert space composed out of two sub-Hilbert spaces $\mathscr{H}_1$ and $\mathscr{H}_2$ respectively. Furthermore, let $\mathcal{O} : \mathscr{H} \to \mathscr{H}$ be an operator according to

$$\mathcal{O} = \left|\psi_1\right\rangle\left\langle\phi_1\right| \otimes \left|\psi_2\right\rangle\left\langle\phi_2\right| \tag{1.6.12}$$

with $\left|\phi_i\right\rangle, \left|\psi_i\right\rangle \in \mathscr{H}_i$. The **partial trace** is then defined as

$$\operatorname{tr}_{\mathscr{H}_1}\mathcal{O} := \operatorname{tr}_{\mathscr{H}_1}\left[\left|\psi_1\right\rangle\left\langle\phi_1\right|\right]\left|\psi_2\right\rangle\left\langle\phi_2\right| \tag{1.6.13}$$

$$\operatorname{tr}_{\mathscr{H}_2}\mathcal{O} := \operatorname{tr}_{\mathscr{H}_2}\left[\left|\psi_2\right\rangle\left\langle\phi_2\right|\right]\left|\psi_1\right\rangle\left\langle\phi_1\right| \tag{1.6.14}$$

and are operators as on the reduced Hilbert spaces $\mathscr{H}_i$

$$\operatorname{tr}_{\mathscr{H}_1}\mathcal{O} : \mathscr{H}_2 \to \mathscr{H}_2 , \quad \operatorname{tr}_{\mathscr{H}_2}\mathcal{O} : \mathscr{H}_1 \to \mathscr{H}_1 . \tag{1.6.15}$$
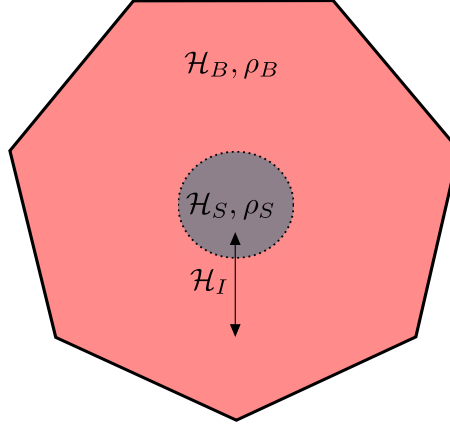
Figure 1.19: Closed quantum system composed out of a thermal bath $\mathcal{H}_B$ with density matrix ρ_B, a system $\mathcal{H}_S$ with density matrix ρ_S and an interaction $\mathcal{H}_I$ between the former and the latter.

1.6.3 Microscopic derivation of the Lindblad equation

In this section we finally pursue the derivation of the Lindblad master equation. We begin by investigating a coarse-grained approach following the compendium of [Sch14] and describe afterwards the more physically motivated approach following the introduction of [Bre07] in order to calculate the Lindblad equation for the damped harmonic oscillator with frequency ω which will be the final result of this part

$$\partial_t \rho_S = -\mathrm{i}\omega \left[a^\dagger a, \rho_S\right] + \gamma(\bar{n}+1)\left(a\rho_S a^\dagger - \frac{1}{2}\left\{a^\dagger a, \rho_S\right\}\right) + \gamma\bar{n}\left(a^\dagger \rho_S a - \frac{1}{2}\left\{aa^\dagger, \rho_S\right\}\right) \quad (1.6.16)$$

and is stated on page 41. Here, $\bar{n} = (\exp(-\omega/T)-1)^{-1}$ is the Bose-Einstein distribution indicating the occupation of the bath mode at the oscillator energy ω and $a, a^\dagger$ are the bosonic ladder operators.

Fig 1.19 visualises the situation we want to investigate: a closed quantum system is composed out of two parts, a (thermal) bath and a system whose dynamics is of our interest. The Hilbert space of such a system is the product space of the bath and system Hilbert space

$$\mathscr{H} = \mathscr{H}_S \otimes \mathscr{H}_B \ . \quad (1.6.17)$$

The Hamiltonian is thus composed out of *three* parts: the system, the bath and the interaction between the two. It reads

$$\mathcal{H} = \mathcal{H}_S + \mathcal{H}_B + \mathcal{H}_I \quad (1.6.18)$$

with the Hamiltonians

$$\mathcal{H}_S : \mathscr{H}_S \to \mathscr{H}_S \qquad \mathcal{H}_B : \mathscr{H}_B \to \mathscr{H}_B \qquad \mathcal{H}_I : \mathscr{H} \to \mathscr{H} \quad (1.6.19)$$

obeying $[\mathcal{H}_S, \mathcal{H}_B] = 0$ since they act on different Hilbert spaces and $[\mathcal{H}_S, \mathcal{H}_I] \neq 0$, $[\mathcal{H}_B, \mathcal{H}_I] \neq 0$.

Coarse-grained master equation

Our starting point is the von-Neumann equation in the interaction picture

$$\partial_t \rho = -\mathrm{i}\left[\mathcal{H}_I(t), \rho\right] \quad (1.6.20)$$

for which we can write out the formal solution in terms of the time evolution operator as

$$U(t) = \mathcal{T}\exp\left(-\mathrm{i}\int_0^t \mathrm{d}\tau \, \mathcal{H}_I(\tau)\right) \ . \quad (1.6.21)$$

One is interested in a type of dynamics that brings the system and bath at time $t = 0$ into contact with each other. Thus, we assume that the *initial condition for the density matrix factorises* according to $\rho = \rho_S^0 \otimes \rho_B^0$ and write the closed solution as

$$\rho(t) = U(t)\rho_S^0 \otimes \rho_B^0 U^\dagger(t) \ . \tag{1.6.22}$$

It is commonly assumed that the interaction between bath and system is sufficiently weak so that it is reasonable to develop the time evolution operator into a power series of the interaction Hamiltonian (*weak-coupling limit*)

$$U(t) = \mathbb{1} - \mathrm{i} \int_0^t \mathrm{d}\tau \ \mathcal{H}_I(\tau) - \iint_0^t \mathrm{d}\tau_1 \mathrm{d}\tau_2 \ \mathcal{H}_I(\tau_1)\mathcal{H}_I(\tau_2)\Theta(\tau_1 - \tau_2) + \mathrm{O}\left(\mathcal{H}_I^3\right) \tag{1.6.23}$$

In this limit we shall assume, that the bath density matrix does not evolve in time in the interaction picture. This does *not* mean that the bath is in a stationary state, since in the interaction picture, the intrinsic dynamics of the bath is already absorbed. It rather means, that the bath is large compared to the system, so that back couplings from the system into the bath do not matter. This condition is satisfied if the bath correlation functions decay much faster then the system itself relaxes.

The most general interaction Hamiltonian is assumed to have the form

$$\mathcal{H}_I = \sum_\alpha A_\alpha \otimes B_\alpha \tag{1.6.24}$$

with the *system operators* $A_\alpha : \mathscr{H}_S \to \mathscr{H}_S$ and the bath operators $B_\alpha : \mathscr{H}_B \to \mathscr{H}_B$.

Lemma [Sch14]: For the above described system composed out of a bath, a system and a interaction, one can always find a transformation $\mathcal{H}_S \mapsto \mathcal{H}_S'$, $\mathcal{H}_B \mapsto \mathcal{H}_B'$ and $B_\alpha \mapsto B_\alpha'$ in such a way that $\forall \ \alpha : \ \langle B_\alpha \rangle = 0$.
Proof: Define the transformed bath operators as

$$B_\alpha' := B_\alpha - \langle B_\alpha \rangle \mathbb{1} \ . \tag{1.6.25}$$

Obviously, they fulfil the required property $\forall \ \alpha : \ \langle B_\alpha \rangle = 0$. We then have to define

$$\mathcal{H}_S' = \mathcal{H}_S - \sum_\alpha \langle B_\alpha \rangle A_\alpha \tag{1.6.26}$$

and we found the desired map. $\square$

We now drop the prime assuming immediately $\forall \ \alpha : \ \langle B_\alpha \rangle = 0$ and insert the series expansion (1.6.23) into the time evolution of the density matrix. Taking a partial trace (see page 36) over the bath leads to

$$\rho_S(t) = \rho_S^0 + \mathrm{tr}_{\mathscr{H}_B} \iint_0^t \mathrm{d}\tau_1 \mathrm{d}\tau_2 \bigg[\mathcal{H}_I(\tau_1)\rho_S^0 \otimes \rho_B^0 \mathcal{H}_I(\tau_2)$$
$$- \Theta(\tau_1 - \tau_2)\mathcal{H}_I(\tau_1)\mathcal{H}_I(\tau_2)\rho_S^0 \otimes \rho_B^0 + \Theta(\tau_2 - \tau_1)\rho_S^0 \otimes \rho_B^0 \mathcal{H}_I(\tau_1)\mathcal{H}_I(\tau_2) \bigg] \tag{1.6.27}$$

Inserting the explicit formula (1.6.24) and introducing the bath correlation function

$$C_{\alpha\beta}(\tau_1, \tau_2) = \mathrm{tr}_{\mathscr{H}_B} \left\{ B_\alpha(\tau_1)B_\beta(\tau_2)\rho_B^0 \right\} \tag{1.6.28}$$

renders the density matrix as[23]

$$\rho_S(t) = \rho_S^0 + \iint \mathrm{d}\tau_1 \mathrm{d}\tau_2 \ C_{\alpha\beta}(\tau_1, \tau_2) \bigg[A_\beta(\tau_2)\rho_S^0 A(\tau_1)$$
$$- \Theta(\tau_1 - \tau_2)A_\alpha(\tau_1)A_\beta(\tau_2)\rho_S^0 - \Theta(\tau_2 - \tau_1)\rho_S^0 A_\alpha(\tau_1)A_\beta(\tau_2) \bigg] \ . \tag{1.6.29}$$

---

[23]We use the compact notation $\iint \mathrm{d}\tau_1 \mathrm{d}\tau_2 = \sum_{\alpha,\beta} \iint_0^t \mathrm{d}\tau_1 \mathrm{d}\tau_2$

By inserting a complete and time-independent basis $\{|n\rangle\}$ of eigenstates the Hamiltonian and defining the jump operators $L_{ab} := |a\rangle \langle b|$, one can re-write the time evolution as

$$\rho_S(t) - \rho_S^0 = -\mathrm{i} \left[\mathcal{H}_{\mathrm{eff}} \, t, \rho_S^0 \right] + t \sum_{abcd} \gamma_{ab,cd} \left(L_{ab} \rho_S^0 L_{cd}^\dagger - \frac{1}{2} \left\{ L_{cd}^\dagger L_{ab}, \rho_S^0 \right\} \right) \tag{1.6.30}$$

with the definitions

$$\mathcal{H}_{\mathrm{eff}} = \sum_{ab} \sigma_{ab}(t) L_{ab} \tag{1.6.31}$$

$$\sigma_{ab}(t) = \frac{1}{2\mathrm{i}t} \oiint \mathrm{d}\tau_1 \mathrm{d}\tau_2 \; C_{\alpha\beta}(\tau_1, \tau_2) \, \mathrm{sgn}\,(\tau_1 - \tau_2) \, \langle a | \, A_\alpha(\tau_1) A_\beta(\tau_2) \, | b \rangle \tag{1.6.32}$$

$$\gamma_{ab,cd}(t) = \frac{1}{t} \oiint \mathrm{d}\tau_1 \mathrm{d}\tau_2 \; C_{\alpha\beta}(\tau_1, \tau_2) \, \langle a | \, A_\beta(\tau_2) \, | b \rangle \, \langle c | \, A_\alpha^\dagger(\tau_1) \, | d \rangle^* \tag{1.6.33}$$

From here on, one can go over to deduce the quantum Liouville operator that generates the quantum dynamics. Therefore, one coarse-grains the desired equation as

$$\rho_S(t) = \exp\left[\mathcal{L} \, t \right] \rho_S^0 \approx \left[\mathbb{1} + \mathcal{L} \, t \right] \rho_S^0 \; . \tag{1.6.34}$$

with the Markovian generator $\mathcal{L}$. This ansatz corresponds to applying a *Markov approximation* to the system which states that the evolution of the system solely depends on its initial state [Bre07]. By applying a secular approximation that states that rapidly oscillating contributions cancel out and which has its justification in the coarse grained picture that does not resolve the typical bath correlation times, one can cast the time evolution as a generator of a dynamical semigroup [Bre07]. A secular approximation has to compare our coarse graining increment t with the typical bath correlation time and will be carried out after the next theorem.

One now deduces the coarse grained Liouville operator as

$$\mathcal{L}\rho_S = \frac{\mathrm{i}}{\hbar} \left[\mathcal{H}_{\mathrm{eff}}(t), \rho_S \right] + \sum_{abcd} \gamma_{ab,cd}(t) \left(L_{ab} \rho_S L_{cd}^\dagger - \frac{1}{2} \left\{ L_{cd}^\dagger L_{ab}, \rho_S \right\} \right) \; . \tag{1.6.35}$$

One must now specify the formulas for the effective Hamiltonian $\mathcal{H}_{\mathrm{eff}}$ and the damping matrix γ. Both of these quantities involve the two time correlation function which can be simplified as shown in the following theorem.

Theorem [Bre07]: If the stationary bath density matrix ρ_B^{st} satisfies $\quad [\mathcal{H}_B, \rho_B^{st}] = 0 \quad$ then the bath correlation function is translational invariant in time and satisfies

$$C_{\alpha\beta}(\tau_1, \tau_2) = C_{\alpha\beta}(\tau_1 - \tau_2, 0) \tag{1.6.36}$$

Proof: One starts from the definition of the bath correlation function

$$C_{\alpha\beta}(\tau_1, \tau_2) = \mathrm{tr}_{\mathscr{H}_B} \left\{ B_\alpha(\tau_1) B_\beta(\tau_2) \rho_B^0 \right\}$$

$$= \mathrm{tr}_{\mathscr{H}_B} \left\{ \mathrm{e}^{\mathrm{i}\mathcal{H}_B \tau_1} B_\alpha(0) \mathrm{e}^{-\mathrm{i}\mathcal{H}_B(\tau_1 - \tau_2)} B_\beta(0) \mathrm{e}^{-\mathrm{i}\mathcal{H}_B \tau_2} \rho_B^{st} \right\} \tag{1.6.37}$$

Since the matrix exponential commutes with the density function by assumption, we can exchange them and use the cyclic property of the trace to obtain the assertion. $\qquad \square$

As we have already mentioned, the correlation function decays on a very short time scale compared to the time scale of the intrinsic evolution of the system. We take this into account by formally sending the coarse graining increment $t \to \infty$. This limit involves the secular approximation mentioned before.

It is then a straightforward calculation to find [Sch14]

$$\mathcal{H}_{\mathrm{eff}} = \frac{1}{2\mathrm{i}} \sum_{\alpha,\beta,a,b,c} \sigma_{\alpha\beta}(E_a - E_c) \delta_{ab} \, \langle c | \, A_\beta \, | b \rangle \, \langle c | \, A_\alpha^\dagger \, | a \rangle^* \, L_{ab} \tag{1.6.38}$$

$$\gamma_{ab,cd} = \sum_{\alpha,\beta} \Gamma_{\alpha\beta} \delta_{E_b - E_a, E_d - E_c} \, \langle a | \, A_\beta \, | b \rangle \, \langle c | \, A_\alpha^\dagger \, | d \rangle^* \tag{1.6.39}$$

with the definitions

$$\sigma_{\alpha\beta} = \int_0^\infty \mathrm{d}\tau \, C_{\alpha\beta}(\tau) \, \mathrm{sgn}(\tau) \mathrm{e}^{\mathrm{i}\omega\tau} \tag{1.6.40}$$

$$\Gamma_{\alpha\beta} = \int_0^\infty \mathrm{d}\tau \, C_{\alpha\beta}(\tau) \mathrm{e}^{\mathrm{i}\omega\tau} \ . \tag{1.6.41}$$

We are now able to (i) show that the coarse grained Lindblad equation indeed can be written as a Kraus map and (ii) calculate the exact expression for a damped quantum mechanical harmonic oscillator, which will be the basis of our work later on.

Lemma [Bre07]: The $\mathrm{O}(t)$ coarse grained Lindblad equation (1.6.30) can be written as a Kraus map.

Proof: The matrix γ is positive semi-definite [Sch14] and can thus be diagonalised by a suitable unitary transformation U such that[24]

$$\gamma_{A,B} = \sum_{C,D} U_{CA}^* \gamma_C \delta_{CD} U_{DB} \tag{1.6.42}$$

We can thus re-write eq (1.6.30) using as well the definition $\bar{L}_C = \sqrt{\gamma_C} \sum_A U_{CA}^* L_A$ as

$$\rho_S(t) - \rho_S^0 = -\mathrm{i} \left[\mathcal{H}_{\mathrm{eff}} \, t, \rho_S^0 \right] + t \sum_C \bar{L}_C \rho_S^0 \bar{L}_C^\dagger - \frac{1}{2} \left\{ \bar{L}_C^\dagger \bar{L}_C, \rho_S^0 \right\} \tag{1.6.43}$$

The Kraus operators are

$$K_1 = \mathbb{1} + t \left(-\mathrm{i} + \sum_C \bar{L}_C^\dagger \bar{L}_C \right), \quad K_2 = \bar{L}_1, \quad K_3 = \bar{L}_2, \quad \dots \tag{1.6.44}$$

We have thus found the desired Kraus decomposition of the coarse-grained Lindblad evolution. $\square$

This completes the quest for the dynamics of the reduced density matrix of the system. One may summarise the result as follows:

Definition & Theorem [Sch14, Bre07, Eng02]: The dynamics of the reduced density matrix ρ_S of a small subsystem coupled to a bath is governed by the **Lindblad equation**

$$\partial_t \rho_S = \mathcal{L} \rho_S \tag{1.6.45}$$

with the Liouville operator [compare eq (1.6.35) for the form in the interaction picture]

$$\mathcal{L}\rho_S = \mathrm{i} \left[\mathcal{H}_{\mathrm{eff}} + \mathcal{H}_S, \rho_S \right] + \sum_A \gamma_A \left(\bar{L}_A \rho_S \bar{L}_A^\dagger - \frac{1}{2} \left\{ \bar{L}_A^\dagger \bar{L}_A, \rho_S \right\} \right) \tag{1.6.46}$$

It can be shown that the Lindblad equation for a thermal heat bath drives the system towards the equilibrium Gibbs state

$$\rho_G = \frac{\exp\left(-\mathcal{H}_S/T \right)}{\mathrm{tr}_S \exp\left(-\mathcal{H}_S/T \right)} \tag{1.6.47}$$

for any initial state as long as the generated quantum dynamical semigroup is *ergodic* [Bre07].

---

[24]Here capital letters refer to the double indices introduced earlier as $A = (a, b)$, etc.

1.6.4 Lindblad equation of the harmonic oscillator

In this part, we derive the coherent quantum dynamics for a single harmonic oscillator coupled to a thermal bath of bosonic modes. Thus, we have to work with the following systems

$$\mathcal{H}_S = \Omega\, a^\dagger a\,, \qquad \mathcal{H}_B = \sum_j \omega_j r_j^\dagger r_j\,, \qquad \mathcal{H}_I = \left(a \otimes \eta^\dagger + a^\dagger \otimes \eta\right) \tag{1.6.48}$$

with the bath coupling operators $\eta = \sum_j \sqrt{\gamma_j}\, r_j$ and the coupling constants γ_j. We can thus identify the system operators A_α from the previous section as $A_1 = a$ and $A_2 = a^\dagger$ and the bath operators B_α to be $B_1 = \eta^\dagger$ and $B_2 = \eta$.

In order to evaluate the damping matrix $\gamma_{ab,cd}$ we start with the matrix Γ of Fourier transforms of the bath correlation functions. Since the bath is in thermal equilibrium at a certain temperature T, the modes are occupied according to the Bose-Einstein distribution $\bar{n} = (e^{E/T} - 1)^{-1}$. We find

$$\Gamma = \sum_j \gamma_j \delta(\omega - \omega_j) \begin{pmatrix} 0 & \bar{n}(E_j) \\ \bar{n}(E_j) + 1 & 0 \end{pmatrix} \tag{1.6.49}$$

In order to avoid ambiguity between the annihilation operator a and the index a in eq (1.6.39), we will rename the index n. The damping matrix then reads

$$\gamma_{nb,cd} = \Gamma_{12}\sqrt{b+1}\sqrt{d+1}\delta_{n,b+1}\delta_{c,d+1} + \Gamma_{21}\sqrt{b}\sqrt{d}\delta_{n,b-1}\delta_{c,d-1} \tag{1.6.50}$$

where we could drop the energy selection factor $\delta_{E_b - E_n, E_d - E_c}$ since the delta functions above always connect consecutive energy levels and the energy splitting is homogeneous for the harmonic oscillator. Using the number state representation of the ladder operators

$$a = \sum_{b=0}^\infty \sqrt{b}\,|b\rangle\langle b+1| \tag{1.6.51}$$

$$a^\dagger = \sum_{b=0}^\infty \sqrt{b+1}\,|b+1\rangle\langle b| \tag{1.6.52}$$

it is a straightforward task to find the Lindblad equation of the damped harmonic oscillator to be

$$\partial_t \rho_S = -\mathrm{i}\Omega\left[a^\dagger a, \rho_S\right] + \gamma_\Omega\left[(\bar{n}+1)\left(a\rho_S a^\dagger - \frac{1}{2}\left\{a^\dagger a, \rho_S\right\}\right) + \bar{n}\left(a^\dagger\rho_S a - \frac{1}{2}\left\{aa^\dagger, \rho_S\right\}\right)\right] \tag{1.6.53}$$

This calculation will form the basis for our treatment of the quantum dynamics of the QSM.

We are interested in the slow relaxational dynamics, after a quantum quench to $g \leq g_c$ at $T = 0$, when formally the relaxation time towards the equilibrium state of the system diverge [Cug95, Hen10]. The study of the spherical model promises to yield exact and non-trivial results, which could be used as bench-marks in the study of more general models which can no longer be solved exactly. In this respect, the quantum spherical model stands out since it is one of the very few – if not the only one – non-trivial quantum model which can be studied in d>1 dimensions.

1.6.5 A glance besides Lindblad

Historically, the Lindblad equation was surely not standing alone but rather there were many approaches to open quantum systems introduced over the last decades. Some of those are reviewed in [Wei99].

Especially, we want to stress that the Lindblad type of equation is applicable only if the dynamics is Markovian and the coupling is weak. Of course there exist similar descriptions e.g. for the strong coupling limit [Sch14] or an equivalent formulation in terms of quantum Langevin equations [Gar04]. Since we started the investigation of dynamical properties with the Langevin equation and derived a failing phenomenological quantum extension, we want to state for completeness at

this point once the correct Markovian quantum Langevin equation for a particle in a potential $V = \frac{m}{2}\omega^2 q^2$

$$\dot{q}(t) = p(t)/m \tag{1.6.54}$$

$$\dot{p}(t) = -m\omega^2 q(t) - \gamma\dot{q}(t) + \zeta(t) \tag{1.6.55}$$

With the noise operator

$$\zeta(t) = \mathrm{i} \sum_n \kappa_n \sqrt{\frac{\omega_n}{2}} \left(-a_n(t_0)\mathrm{e}^{-\mathrm{i}\omega_n(t-t_0)} + a_n^\dagger(t_0)\mathrm{e}^{\mathrm{i}\omega_n(t-t_0)} \right) \tag{1.6.56}$$

where a_n and $a_n^\dagger$ are bosonic ladder operators of the bath mode associated with the frequency ω_n and κ_n is a coupling constant. Another ansatz is proposed by Bedeaux & Mazur which involves two distinct noise operators for position and momentum [Bed01].

Additionally, there exist entirely different approaches to the "system-bath" approach: One suggestion to describe open quantum systems was the modification of quantisation procedure proposed that tried to implement the open quantum system through a time dependent mass term. Such attempts are though considered to "reproduce, at best, known results only for very limited cases" [Wei99].

Another, more recent attempt is the stochastic Schrödinger equation and the postulate of non-Hamiltonian dynamics as a modification of the standard Schrödinger equation as e.g. in the quantum-state diffusion method [Gis84, Per94, Wei99].

For systems that are not described by a simple Hamiltonian, one can implement a phenomenologically motivated approach, by e.g. dynamically describing the system in terms of occupation probabilities of (measured) energy levels [Wei99].

Overview

The focus of this thesis is on the quantum relaxation of quantum systems, through the analysis of the exactly solvable spherical model. It is widely thought that '*the field of open quantum systems is still lacking non-trivial explicitly solvable models (...) Examples of explicitly solvable models of master equations for open quantum systems are limited to quite restricted models of a single particle, single spin or harmonic oscillators.*' [Pro08]. We here want to take on this challenge to study in how far the spherical model is able to provide such a system.

The Lindblad equation will be used for the description of the quantum dynamics. From a theoretical point of view, it has the attractive feature of the quantum semi-group property. On the other hand, Lindblad equations have the deserved reputation of being difficult to solve exactly. Therefore, we shall in chapter 2 present the Lindblad equation for a single spherical quantum spin. This greatly reduces the technical complexity. However, even for this simple case, mathematical methods distinct from the ones used in classical Langevin equations are required. The physical content of this solution is made apparent by re-interpreting the single-particle solution in an external field as a mean-field treatment of a many-body problem. This gives rise to a non-trivial phase diagram and a quantum analogue of the 'freezing-by-heating' effect. The heart of this thesis is in chapter 3. Here, we strive at the formulation and solution of the N-particle quantum spherical model. Therefore, we consider in detail how to construct Lindblad dissipators explicitly. In order to make this useful for future model-building, we shall present two different approaches. The first one starts from an explicit modelling of the heat bath as a gas of non-interacting boson (phonons or photons) and we prescribe the interaction with the system. Admitting the usual Markov and Born approximations, the Lindblad dissipators can be derived. The second approach is more phenomenological. It starts from the idea that physically reasonable equations of motion should not only admit the equilibrium state as a stationary solution but that furthermore, the dynamics should reduce in the classical limit to the one given by the classical Langevin equation. As we shall show, these two approaches lead to the same end result for the Lindblad dissipators. Having thus brought onto firm ground the specific form of the Lindblad dissipator used in this work, we proceed to find the solution. As expected, the dynamics of the spherical model can be reduced exactly to the solution of a single integro-differential equation for the spherical parameter, that is, the Lagrange multiplier introduced by the spherical constraint. The Lindblad equation does live up to its reputation in that this constraint equation is indeed a formidable one and its full solution remains a very difficult problem. Therefore, we seek to make progress by concentrating on two limit cases. Indeed, in the semi-classical limit, where only the leading quantum corrections are taken into account, we show that the effective dynamics reduces to the one of the classical case, up to a renormalisation of the effective temperature, which is shown to be in agreement with the known quantum equilibrium phase diagram. Having thus confirmed the internal consistency of the Lindblad equation of the quantum spherical model, we strive for new ground by considering a deep quantum quench (at zero temperature) into the ordered phase. Although this considerably simplifies the form of the spherical constraint, its asymptotic solution is still a hard problem, much beyond what would be required in the analogous classical case, and whose solution did require the development of new mathematical tools. We find that the behaviour of the solution of the spherical constraint is considerably more rich than in the classical case. Depending on the spatial dimension, several different types of dynamical long-time behaviour are found. Their consequences for the emergent dynamical scaling of the two-point correlators will be analysed in detail, with a surprising variety of quantum dynamical behaviour. In particular, it appears that simple dynamical scaling can be derived in $d = 2$ dimensions, while subtle logarithmic corrections to scaling appear for larger values of d. The core of the mathematical methods developed in this thesis can be cast as new results on the asymptotics of certain confluent hypergeometric functions in two variables. These will be presented in a comprehensive form in chapter 4. An outlook to perspectives of future work is given in chapter 5.

Chapter 2

Lindblad dynamics of a spherical quantum spin

2.1 Introduction

In this chapter, we begin our study of the dynamics of the *quantum* spherical model. The content of this chapter is taken from our publication [Wal16].

Since the system is coupled at least to an external thermal reservoir, a description convenient for an open quantum system is required. Specifically, one is faced with the task of how to write down a 'quantum version' of the Langevin equation of the spherical model ? While in the statistical mechanics community, such attempts are often considered '... *very much model-dependent and difficult to generalise*' [Cug03, p. 394], these are routinely studied by the quantum optics or mathematics communities, see e.g. [Car99, Bre07, Eng02, Sch14, Att06b, Att07, Elo17, vH15] and references therein as well as chapter 1. In these studies we reviewed in section 1.6, the classical master equation is replaced by the *Lindblad equation*, where the evolution of the time-dependent reduced density matrix of the system is described by a quantum Liouville operator involving the system's quantum Hamiltonian and additional terms which describe the coupling to the bath.

Before we shall turn to this, let us briefly recall section 1.5 [Car99] and generalising to a large number of degrees of freedom, why a straightforward-looking extension of a classical Langevin equation is insufficient for the description of coherent quantum dynamics. Consider a pre-quantum spherical model, where the dynamical variables are the spherical spin-operators $S_{\boldsymbol{n}}$ (at each site $\boldsymbol{n} \in \mathscr{L}$ of a hyper-cubic lattice $\mathscr{L} \subset \mathbb{Z}^d$, with $\mathcal{N} = |\mathscr{L}|$ sites) and the canonically conjugate momenta $P_{\boldsymbol{n}}$. By analogy with [Obe72], the Hamiltonian is

$$H = \sum_{\boldsymbol{n} \in \mathscr{L}} \left(\frac{g}{2} P_{\boldsymbol{n}}^2 + \frac{\mathcal{S}}{2} S_{\boldsymbol{n}}^2 - \sum_{j=1}^d S_{\boldsymbol{n}} S_{\boldsymbol{n}+\boldsymbol{e}_j} \right) \tag{2.1.1}$$

Herein, g is a coupling constant, $\mathcal{S}$ denotes a Lagrange multiplier, to be found self-consistently from the spherical constraint $\left\langle \sum_{\boldsymbol{n}} S_{\boldsymbol{n}}^2 \right\rangle = \mathcal{N}$, and $\boldsymbol{e}_j$ is the jth Cartesian unit vector. Taking into account the momenta, one may write down a Kramers equation [Tai06]

$$\partial_t S_{\boldsymbol{n}} = \{S_{\boldsymbol{n}}, H\} \quad , \quad \partial_t P_{\boldsymbol{n}} = \{P_{\boldsymbol{n}}, H\} - \gamma P_{\boldsymbol{n}} + \eta_{\boldsymbol{n}}(t) \tag{2.1.2}$$

with a damping parameter[1] γ and the standard centred white-noise $\eta_{\boldsymbol{n}}(t)$, with correlator

$$\left\langle \eta_{\boldsymbol{n}}(t)\eta_{\boldsymbol{m}}(t') \right\rangle = 2\gamma T \delta_{\boldsymbol{n}\boldsymbol{m}} \delta(t - t') \ . \tag{2.1.3}$$

Herein, the brackets $\{.,.\}$ denote the Poisson brackets. Eq (2.1.2) is a well-defined and interesting dynamics with non-trivial properties, such as a hidden super-symmetry [Tai06]. It might also appear as a natural starting point for going over to the dynamics of the quantum case. According to the natural-looking procedure suggested in [Shu81], one replaces in (2.1.2)

---

[1]Throughout, units are such that the Boltzmann constant $k_{\text{B}} = 1$ and the Planck constant $\hbar = 1$.

(i) the classical variables $S_{\boldsymbol{n}} \mapsto s_{\boldsymbol{n}}(t)$ and $P_{\boldsymbol{n}} \mapsto p_{\boldsymbol{n}}(t)$ by time-dependent operators $s_{\boldsymbol{n}}(t)$ and $p_{\boldsymbol{n}}(t)$, which

(ii) at the initial time $t = 0$ obey the canonical equal-time commutation relations $[s_{\boldsymbol{n}}(0), p_{\boldsymbol{m}}(0)] = \mathrm{i}\delta_{\boldsymbol{n},\boldsymbol{m}}$,

(iii) replaces the Poisson brackets $\{.,.\} \mapsto \frac{1}{\mathrm{i}}\,[.,.]$ by a commutator and

(iv) introduces a noise operator $\eta_{\boldsymbol{n}}(t) = \eta_{\boldsymbol{n}}(t)\mathbf{1}$.

Applied to the spherical model Hamiltonian (2.1.1), this procedure would lead to the quantum operator equations of motion [Shu81]

$$\partial_t s_{\boldsymbol{n}} = g p_{\boldsymbol{n}}$$

$$\partial_t p_{\boldsymbol{n}} = -\mathcal{S} s_{\boldsymbol{n}} - \gamma g p_n + \frac{1}{\mathcal{S}}\sum_{j=1}^{d}\left(s_{\boldsymbol{n}-\boldsymbol{e}_j} + s_{\boldsymbol{n}+\boldsymbol{e}_j}\right) + \eta_{\boldsymbol{n}} \tag{2.1.4}$$

However, if one defines the commutator $c_{\boldsymbol{n}}(t) := [s_{\boldsymbol{n}}(t), p_{\boldsymbol{n}}(t)]$, one promptly obtains the equation of motion

$$\partial_t c_{\boldsymbol{n}}(t) = -g\gamma\, c_{\boldsymbol{n}}(t) \tag{2.1.5}$$

Hence, $c_{\boldsymbol{n}}(t) = \mathrm{i}\, e^{-t/t_{\mathrm{deco}}}$ which means that the dynamics (2.1.4) dissipates the quantum structure on a finite time-scale, of order $t_{\mathrm{deco}} = 1/(\gamma g)$ [Car99].[2] Indeed, one may define more general quantum spherical models by adding interactions between the momenta into the Hamiltonian (2.1.1), as we have seen in section 1.3.3. At equilibrium, this is known to lead to new quantum effects, such as a re-entrant quantum phase transitions in sufficiently small dimensions $d \lesssim 2.065$, see fig 1.18 [Wal15]. However, as we shall show in appendix 2.A, a corresponding generalisation of the equations of motion (2.1.4) always leads, for times $t \gg t_{\mathrm{deco}}$, back to the well-known relaxational dynamics [Ron78, God00, Dur15] of the classical spherical model with $g = 0$. In consequence, any quantum effects of the equilibrium state are washed out by this incoherent dynamics, which does not even relax to the required equilibrium state.

If a dynamical description is sought which maintains the quantum coherence of an open quantum system with $\gamma > 0$ and $g > 0$, and evolves towards the correct quantum equilibrium state, a different approach is required. Here, we shall adopt the result of a profound analysis of the interactions of the system with its environment, see e.g. [Car99, Bre07, Eng02, Att06b, Att07, Sch14] and references therein, and shall take as our starting point the *Lindblad equation* for the time-dependent density matrix $\rho = \rho(t)$ of the system

$$\frac{\mathrm{d}\rho}{\mathrm{d}t} = -\mathrm{i}\,[\mathcal{H}, \rho] - \sum_{\alpha}\left(L_\alpha \rho L_\alpha^\dagger - \frac{1}{2}L_\alpha^\dagger L_\alpha \rho - \frac{1}{2}\rho L_\alpha^\dagger L_\alpha\right) \tag{2.1.6}$$

where the Lindblad operators L_α describe the damping through the coupling of the system to the reservoir. It is well-known that the Lindblad equation preserves the trace, the hermiticity and the positivity of the density matrix [Car99, Bre07, Sch14]. In section 2.2, we shall specify the Lindblad operators completely and shall also re-derive that the Lindblad equation dynamics preserves the canonical commutator relations between spins and momenta, at least on average.[3]

In this chapter, we shall consider a thermal reservoir of bosonic particles and the L_α will be chosen accordingly (see section 2.2). In the past, much work has been done on systems with only two energy levels per site. Remarkably, for several quantum chains, exact results on the non-equilibrium stationary states have been derived through techniques of quantum integrability [Pro11a, Kar13, Pop13, Bra13, Bat15], see [Pro15, Bra16] for recent reviews. Here, we present first results of an exploration of a quantum system where the space of states of a single site is larger. Indeed, we hope to make use of the solvability of the quantum spherical model in order to construct exact solutions of the corresponding Lindblad equation. The aim of such an approach should be

---

[2]Formally, one might introduce an 'effective Planck constant' $\hbar_{\mathrm{eff}}(t) = e^{-t/t_{\mathrm{deco}}}$ decaying to zero.

[3]From the point of view of classical dynamics, one might say that the Lindblad equation (2.1.6) automatically contains a large number of conserved quantities, corresponding to the canonical commutators.

a comparative analysis of quantum vs classical phase transitions, see [Pod14] for an example in the Ising model universality class. As a first step towards the realisation of this programme, we consider here the quantum dynamics of a *single* spherical spin, which might also be viewed as a simple mean-field solution of the dynamics of a N-body problem and to discuss the resulting phase diagram in the stationary state. Surprisingly, the resulting phase diagram appears to be re-entrant and thereby presents a quantum analogue of a mechanism, well-known from classical systems [Kat84, Hel00, Zia02, Rad03, Ehr10, Bor14], where it is often referred to as '*freezing-by-heating*' or '*getting more from pushing less*'.

This chapter is organised as follows. In section 2.2, we precisely define the single-spin quantum spherical model and derive from (2.1.6) the quantum equations of motion of several observables. We also comment on its relationship with the Dicke model. In section 2.3, the equations of motion are solved exactly at temperature $T = 0$ and for a vanishing external field. In section 2.4, an external field is included and is used to derive a quantum mean-field theory of the non-equilibrium stationary state. The rôle of the couplings g and γ on the phase diagram, as well as the corrections implied by a sufficiently small temperature $T > 0$ will be discussed. Section 2.5 gives our summary. Several appendices treat technical details of the calculations: appendix 2.A demonstrates the insufficiency of a purely phenomenological Kramers-type equation for the description of the quantum dynamics of the quantum spherical model; appendix 2.B gives the exact solution for $B = T = 0$ and appendix 2.C contains the stability analysis in the field-dependent context.

2.2 The model

2.2.1 A single spherical quantum spin

The Hamiltonian of a single spherical quantum spin (sqs), in an external magnetic field B, reads [Obe72][4]

$$\mathcal{H} = \frac{g}{2}p^2 + \frac{\mathcal{S}}{2}s^2 - Bs \tag{2.2.1}$$

with the canonical commutation relation $[s, p] = \mathrm{i}$. This is the quantum version of the classical Hamiltonian (2.1.1), reduced to a single degree of freedom. Herein, g is the quantum coupling of the system with the classical limit $g \to 0$. The *Lagrange multiplier* $\mathcal{S} = \mathcal{S}(t)$ is chosen[5] to ensure the (mean) spherical constraint [Lew52]

$$\langle s^2 \rangle = 1 . \tag{2.2.2}$$

Consequently, the term $\left(\mathcal{S}/2\, s^2\right)$ is simply an effective energy shift of the Hamiltonian.

It is convenient to go over to creation and annihilation operators, in the usual way [Obe72]

$$s = \sqrt{\frac{g}{2\omega}}\left(a^\dagger + a\right) \ , \ \ p = \mathrm{i}\sqrt{\frac{\omega}{2g}}\left(a^\dagger - a\right), \quad \text{with} \quad \omega = \omega(t) := \sqrt{\mathcal{S}(t)g} \tag{2.2.3}$$

which recasts the Hamiltonian into the form

$$\mathcal{H} = \omega(t)\left(a^\dagger a + \frac{1}{2}\right) - B\sqrt{\frac{g}{2\omega}}\left(a^\dagger + a\right) . \tag{2.2.4}$$

The spherical constraint (2.2.2) introduces a functional relationship between the (effectively time-dependent) frequency and the two-particle-operator expectation values, via

$$\omega = \omega(t) = \frac{g}{2}\left(\langle a^\dagger a^\dagger \rangle + \langle aa \rangle + 2\langle a^\dagger a \rangle + 1\right) \tag{2.2.5}$$

This condition, along with the explicit Hamiltonian (2.2.4), defines the closed system completely.

---

[4]We use a slightly different normalisation of the spherical parameter $\mathcal{S}$ here than the one we introduces in section 1.3.

[5]The time-dependence of $\mathcal{S}(t)$ is essential for a correct description of the relaxation properties [Ron78, Cug95, God00], in contrast to the approach followed in [Shu81].

If coupled to an external bath, a coherent quantum dynamics is formulated by adopting a Schrödinger picture and writing down a Lindblad equation for the time-dependent density matrix $\rho = \rho(t)$ of this open quantum system. We assume a thermal coupling to the zero-field modes [Car99, Bre07, Sch14] and consider the following Lindblad equation

$$\dot{\rho} = -\mathrm{i}\left[\mathcal{H}, \rho\right] + \gamma(n_\omega + 1)\left[a\rho a^\dagger - \frac{1}{2}\left(a^\dagger a\,\rho + \rho\,a^\dagger\,a\right)\right] + \gamma n_\omega\left[a^\dagger\rho a - \frac{1}{2}\left(aa^\dagger\,\rho + \rho\,a\,a^\dagger\right)\right] \quad (2.2.6)$$

where the bath, of given temperature T, is characterised by the Bose-Einstein statistics $n_\omega = \left(e^{\omega/T} - 1\right)^{-1}$ and γ is a coupling constant. Because of the spherical constraint (2.2.5), the frequency $\omega = \omega(t)$ must be considered as a time-dependent function. In consequence, the occupation number $n_\omega = n_{\omega(t)}$ becomes effectively time-dependent as well.

The three equations (2.2.4, 2.2.5, 2.2.6) define completely our time-dependent, open quantum model system of a single SQS. It depends on the physical parameters temperature T, magnetic field B, dissipation coupling γ and quantum coupling g. We shall consider these equations as a phenomenological ansatz and shall concentrate from now on how to extract their time-dependent behaviour.

Consequently, we deduce the closed set of equations of motion for the following averages

$$\partial_t \left\langle aa \right\rangle = -\left[\gamma + 2\mathrm{i}\omega\right]\left\langle aa \right\rangle + \mathrm{i}\sqrt{\frac{2g}{\omega}}\,B\left\langle a \right\rangle \tag{2.2.7}$$

$$\partial_t \left\langle a^\dagger a \right\rangle = -\gamma\left\langle a^\dagger a \right\rangle + \gamma n_\omega + \mathrm{i}\sqrt{\frac{g}{2\omega}}\,B\left(\left\langle a^\dagger \right\rangle - \left\langle a \right\rangle\right) \tag{2.2.8}$$

$$\partial_t \left\langle a \right\rangle = -\left[\frac{\gamma}{2} + \mathrm{i}\omega\right]\left\langle a \right\rangle + \mathrm{i}\sqrt{\frac{g}{2\omega}}\,B \tag{2.2.9}$$

where $\omega = \omega(t)$ is given by (2.2.5). Clearly, $\left\langle a^\dagger \right\rangle = \left\langle a \right\rangle^*$ and $\left\langle a^\dagger a^\dagger \right\rangle = \left\langle aa \right\rangle^*$.

In the chosen form (2.2.6) of the Lindblad equation, where the bosonic creation and annihilation operators $a^\dagger$ and a are guaranteed to be operators of physical observables are time-independent, we can now briefly comment on the preservation of the quantum coherence. Specifically, the average of their commutator becomes

$$\left\langle \left[a, a^\dagger\right] \right\rangle(t) = \operatorname{tr}\left[a, a^\dagger\right]\rho(t) = \operatorname{tr}\mathbf{1}\rho(t) = 1 \tag{2.2.10}$$

Inverting (2.2.3), it also follows that the canonical commutation relations between s and p are kept, at least on average, viz. $\left\langle [s, p] \right\rangle = \mathrm{i}$ for all times t.

Conceptually, the constraint (2.2.2) means that besides the coupling to an external thermal bath with a fixed temperature T, as described by the dissipative terms in (2.2.6), effectively there is a *second external* bath which acts on the system in a way that (2.2.2) holds true, where $\mathcal{S}$ is canonically conjugate to s^2. In principle, we could have followed the standard derivation of Lindblad equations, see [Car99, Bre07, Att07, Sch14], in order to obtain explicitly the corresponding Lindblad operators L_α, as in eq (2.1.6). We shall not carry this out here, since we expect that for a large number of degrees of freedom, this explicit construction would merely correspond to a change of the statistical ensemble. That should be analogous to a change between, say, canonical and grand canonical ensembles. In the classical spherical model, this would correspond to requiring the spherical constraint either exactly on each microscopic spin configuration, or merely on average. It is well-known that this distinction becomes unimportant for the analysis of the critical behaviour in the limit $\mathcal{N} \to \infty$ of a large number of spins, both at and far from equilibrium [Lew52, Fus02].[6]

Turning now to the analysis of the long-time behaviour following from the equations of motion (2.2.7, 2.2.8, 2.2.9), we keep in mind that the combined action of two distinct external baths may lead the system to evolve towards a *non-equilibrium* stationary state.

---

[6]Since we consider this study as preliminary work on the dynamics of the quantum spherical model with $\mathcal{N} \to \infty$ spins, we do not go further into the distinction of ensembles. In this respect, the present results on a single spherical spin should rather be viewed as some mean-field approximation of that full $\mathcal{N}$-body problem.

2.2.2 Relationship with the Dicke model

The *single-mode Dicke model* [Dic54] describes the cooperative interaction of $\mathcal{M}$ atoms in a cavity with a single mode of the radiation field. In the rotating-wave-approximation, the Dicke model Hamiltonian reads [Gar11, Ton09]

$$\mathcal{H}_D = \omega \left(S_z + \frac{\mathcal{M}+1}{2} \right) + \frac{\gamma}{\sqrt{\mathcal{M}}} \left(r^\dagger S_- + r S_+ \right) + \omega_r r^\dagger r \qquad (2.2.11)$$

Herein, each of the $\mathcal{M}$ atoms is represented by a two-level system, with ground states $|g_j\rangle$ and excited states $|e_j\rangle$, $j = 1, \ldots, \mathcal{M}$. The transitions in each atom are described in terms of spin-$\frac{1}{2}$ operators

$$S_+^{(j)} = |e_j\rangle \langle g_j| \;\;,\;\; S_-^{(j)} = |g_j\rangle \langle e_j| \;\;,\;\; S_z^{(j)} = \frac{1}{2} \left(|e_j\rangle \langle e_j| - |g_j\rangle \langle g_j| \right) \qquad (2.2.12)$$

and the collective atomic operators read $S_\pm = \sum_{j=1}^{\mathcal{M}} S_\pm^{(j)}$ and $S_z = \sum_{j=1}^{\mathcal{M}} S_z^{(j)}$. The state of the cavity (reservoir) is described by the bosonic raising and lowering operators $r^\dagger$ and r, with $\left[r, r^\dagger \right] = 1$. The two energy scales ω and ω_r, as well as the coupling γ, are taken to be constants. The Dicke model is known to undergo a continuous phase transition, from a normal to a super-radiant phase, with the order parameter $\lim_{\mathcal{M} \to \infty} \mathcal{M}^{-1} \langle r^\dagger r \rangle$. This transition either occurs at a finite critical temperature $T_c > 0$ and then is thermally driven, or else is a quantum phase transition at $T = 0$ and is driven by γ, see the reviews [Gar11, Ton09] and references therein.

Within this setup, the model can be re-written through a Holstein-Primakoff transformation [Hol40, Gar11], which replaces the collective atomic operators by a bosonic degree of freedom via

$$S_+ = a^\dagger \mathcal{M}^{1/2} \left(1 - a^\dagger a / \mathcal{M} \right)^{1/2} \;\;,\;\; S_- = \mathcal{M}^{1/2} \left(1 - a^\dagger a / \mathcal{M} \right)^{1/2} a \;\;,\;\; S_z = a^\dagger a - \mathcal{M}/2 \quad (2.2.13)$$

where we recognise the system's bosonic creation and annihilation operators $a^\dagger$ and a.

Inserting (2.2.13) into (2.2.11) and expanding this up to leading order in $a^\dagger a / \mathcal{M}$, gives in the limit $\mathcal{M} \to \infty$ the effective low-energy Hamiltonian

$$\mathcal{H}_D \approx \omega \left(a^\dagger a + \frac{1}{2} \right) + \gamma \left(r^\dagger a + r a^\dagger \right) + \omega_r r^\dagger r \qquad (2.2.14)$$

This Hamiltonian has the general form $\mathcal{H}_D = \mathcal{H}_{\rm sys} + \mathcal{H}_{\rm int} + \mathcal{H}_{\rm res}$ and describes, as a 'system', a single boson with Hamiltonian $\mathcal{H}_{\rm sys}$ analogous to (2.2.4), interacting through the term $\mathcal{H}_{\rm int}$ with a '*bosonic single-mode reservoir*' described by $\mathcal{H}_{\rm res}$. This is the usual starting point for deriving a Lindblad equation for the dynamics of the 'system' by tracing out the degrees of freedom of the 'reservoir'. Indeed, if one adopts the usual procedure of fixing the properties of the 'reservoir', for instance its temperature T, and also assumes the 'reservoir' large enough as to be not influenced by the properties of the 'system', a lengthy but standard calculation shows that the quantum dynamics of the reduced density matrix of the 'system' is given by the Lindblad equation (2.2.6) with the Hamiltonian (2.2.4), with $B = 0$ [Bre07, Car99, Sch14].

In spite of this formal analogy, the SQS and the single-mode Dicke model are still different. First, the phase transition in the Dicke model refers for the definition of the order parameter to the properties of the 'reservoir', which is traced out in the SQS. This is probably not very important, since in the low-energy Hamiltonian (2.2.14), 'system' and 'reservoir' can be exchanged according to $(a, a^\dagger) \longleftrightarrow (r, r^\dagger)$, along with $\omega \longleftrightarrow \omega_r$. In this respect, the SQS and the Dicke model are dual to each other. Second, this averaging is normally done for a fixed temperature and the assumed properties of the reservoir in general do not allow for a phase transition.[7] Third, and probably most important, the Dicke model considers the angular frequency ω as a fixed parameter, whereas in the SQS, its time-dependent value $\omega(t)$ has to be found self-consistently from the spherical constraint (2.2.5). In the next section, we shall see that this leads to an important qualitative difference in the behaviour of the two models.[8]

---

[7] We hope to return elsewhere to an exploration of the consequences of an assumed phase transition in an external reservoir.

[8] In the limit $\omega_r \to 0$, the Dicke Hamiltonian (2.2.11) becomes the one of the integrable Tavis-Cummings model, whose dynamics for an arbitrarily prescribed time-dependent $\omega = \omega(t)$ can be studied through the Bethe ansatz [Bar13].

2.3 Analytic solution in zero field and at zero temperature

We focus on the case where $B = 0$ and $T = 0$. This particular case is analytically solvable for all times t.

     Due to the vanishing field $B = 0$, the equations (2.2.7, 2.2.8) decouple from (2.2.9), such that the single-particle operators can be treated separately. We must investigate the system

$$\partial_t \langle aa \rangle = -\left[\gamma + 2\mathrm{i}\omega(t) \right] \langle aa \rangle \tag{2.3.1}$$

$$\partial_t \langle a^\dagger a \rangle = -\gamma \langle a^\dagger a \rangle \ . \tag{2.3.2}$$

Obviously, the particle-number-operator expectation value decays exponentially

$$\langle a^\dagger a \rangle = N e^{-\gamma t} \ , \qquad N \in \mathbb{R}_+ \ . \tag{2.3.3}$$

By means of this solution and the spherical constraint (2.2.5), the expectation value of the pair-annihilation operator obeys the equation

$$\partial_t \langle aa \rangle = -\left[\gamma + \mathrm{i}\left(1 + 2N e^{-\gamma t} \right) \right] \langle aa \rangle - \mathrm{i}g \left| \langle aa \rangle \right|^2 - \mathrm{i}g \langle aa \rangle^2 \ . \tag{2.3.4}$$

Separating amplitude and complex phase, via $\langle aa \rangle = R(t)e^{\mathrm{i}\Theta(t)}$, leads to

$$\dot{R}(t) = -\gamma \, R(t) \tag{2.3.5}$$

$$\dot{\Theta}(t) = -g \left[2R(t)\cos\Theta(t) + 2N e^{-\gamma t} + 1 \right] \ . \tag{2.3.6}$$

These equations allow to separate the two basic physical mechanisms and show in particular that the exponential decay is an intrinsic fact of the *classical spherical model*, whereas the time-dependent phase $\Theta(t)$ is a quantum effect of the SQS (for $g = 0$, eq (2.3.6) simply states that $\dot{\Theta} = 0$).

     The amplitude eq (2.3.5) simply gives $R = R(t) = Ae^{-\gamma t}$, with $A \in \mathbb{R}_+$.[9] However, the phase equation is more complicated. In appendix 2.B, we show that the solution of (2.3.6) is

$$\cos\Theta = \mathrm{Re}\left(-\frac{N}{A} - \mathrm{i}\sqrt{1 - \frac{N^2}{A^2}} + \frac{g}{\gamma}\left(\sqrt{1 - \frac{N^2}{A^2}} - \mathrm{i}\frac{N}{A} \right) \frac{\mathrm{i}\frac{\gamma}{g} KM(\mathscr{T}_{(1,1)}) - U(\mathscr{T}_{(1,1)})}{KM(\mathscr{T}) - U(\mathscr{T})} \right) \tag{2.3.7}$$

for $A \neq N$ and

$$\cos\Theta = -\mathrm{Re}\left(1 + \frac{\mathrm{i}}{\sqrt{A}} \, e^{\frac{\gamma}{2}t} \frac{KJ_{\mathrm{i}\frac{g}{\gamma}}\left(2\mathrm{i}\frac{g}{\gamma}\sqrt{Ae^{-\gamma t}} \right) - J_{-\mathrm{i}\frac{g}{\gamma}}\left(2\mathrm{i}\frac{g}{\gamma}\sqrt{Ae^{-\gamma t}} \right)}{KJ_{1+\mathrm{i}\frac{g}{\gamma}}\left(2\mathrm{i}\frac{g}{\gamma}\sqrt{Ae^{-\gamma t}} \right) + J_{-1-\mathrm{i}\frac{g}{\gamma}}\left(2\mathrm{i}\frac{g}{\gamma}\sqrt{Ae^{-\gamma t}} \right)} \right) \tag{2.3.8}$$

for $A = N$, respectively. Herein, the constant K is related to the initial condition, $M = M(\mathscr{T})$, $U = U(\mathscr{T})$ are Kummer's hypergeometric functions [Abr64], with the triple argument

$$\mathscr{T} := \left(-\frac{g}{2\gamma}\left(\mathrm{i} + \frac{1}{\sqrt{A^2/N^2 - 1}} \right) \ ; \ -\mathrm{i}\frac{g}{\gamma} \ ; \ 2\frac{g}{\gamma}\sqrt{A^2 - N^2} \, e^{-\gamma t} \right) \tag{2.3.9}$$

and the further abbreviation $\mathscr{T}_{(x,y)} := \mathscr{T} + (x; y; 0)$. Furthermore, $J_p(z)$ denotes the Bessel function of the first kind and order[10] p. We have checked that $-1 \leq \cos\Theta(t) \leq 1$ for all times and all ratios A/N.

     The functions (2.3.7) and (2.3.8) can be analysed in the long-time limit $t \to \infty$, respectively $e^{-\gamma t} \to 0^+$. A Taylor-series expansion in $e^{-\gamma t}$ yields, to leading order

$$\cos\Theta \simeq \mathrm{Re}\left\{ -\frac{N}{A} - \mathrm{i}\sqrt{1 - \frac{N^2}{A^2}} + \epsilon_1 \cos gt + \epsilon_2 \sin gt \right\} \tag{2.3.10}$$

---

[9] At equilibrium, it follows from the Hamiltonian (2.2.1) that $\langle aa \rangle_{\mathrm{eq}} = \langle a^\dagger a^\dagger \rangle_{\mathrm{eq}} = 0$. Hence the amplitude A can be viewed as a measure of the initial distance from the equilibrium state.

[10] Confluent hypergeometric or Bessel functions with complex indices/orders are often met in the dynamics of quantum systems, see e.g. [Gar11, Bat15, Bra16].
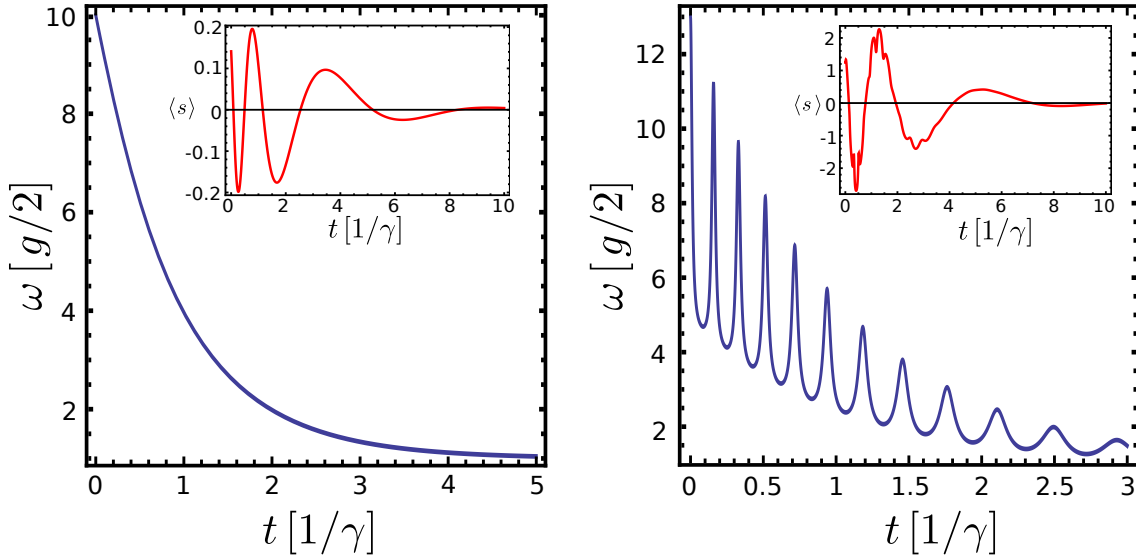
Figure 2.1: Left panel: Time-dependence of the effective frequency $\omega(t)$ (main plot) and of the magnetisation $m(t) = \langle s \rangle (t)$ (inset), for the parameters $A = N = 3$ and $g = 0.1$ in the weak quantum-coupling regime. A simple exponential decay for the frequency is seen, which leads to a time-varying oscillation frequency in the magnetisation. Right panel: analogous plots with parameters $A = N = 4$ and $g = 10$ in the strong quantum-coupling regime. Here, the exponential decay of $\omega(t)$ is modulated by strong oscillations with sharp peaks. These lead to a rather complex oscillatory behaviour in the magnetisation.

with appropriate (complex) constants ϵ_1 and ϵ_2. Thus, the long-time limit provides the expected harmonic oscillator with frequency $\Omega = g$. This asymptotic expansion reveals the oscillations at least for large times in the effective frequency $\omega(t)$ (while for all other models like the Dicke model or the Jaynes-Cummings model, the frequency ω is a constant). As the effective oscillation frequency $\omega(t)$ tends to zero for $g \to 0$, we observe here a *quantum effect* of the system.

Now, combining equations. (2.3.7, 2.3.8) with the definition of $\langle aa \rangle = R(t)e^{i\Theta(t)}$, the time-dependent effective frequency $\omega = \omega(t)$ can be reconstructed from eq (2.2.5), using also (2.3.3). Afterwards, the magnetisation $m(t) = \langle s(t) \rangle = \sqrt{\frac{g}{2\omega(t)}} \left(\langle a^\dagger \rangle + \langle a \rangle \right)$, see (2.2.3), follows by integrating eq (2.2.9). Fig 2.1 shows the resulting oscillation frequency $\omega(t)$ and the magnetisation $m(t)$, for the special case $A = N$. Already in this more simple case, we observe a distinction between (i) a *weak-quantum-coupling regime* $g \ll 1$, characterised by a simple monotonous decay of $\omega(t)$ and a simple oscillatory relaxation of $m(t)$ and (ii) a *strong-quantum-coupling regime* $g \gg 1$, where on the decay of $\omega(t)$ is superposed strongly peaked non-harmonic oscillations, which leads to a complex oscillatory behaviour of $m(t)$.

The same two regimes also arise when $A \neq N$. In fig 2.2, the behaviour in the weak-quantum-coupling regime is illustrated for choices such that either $A \ll N$, $A \simeq N$ or $A \gg N$, respectively. In this regime, we find qualitatively the same behaviour already shown in fig 2.1 for $A = N$: the effective frequency $\omega(t)$ decays monotonously (almost exponentially) and the decay of the magnetisation is a simple damped oscillation, of which the frequency decreases, towards $\omega(\infty) = g/2$.

Fig 2.3 displays the behaviour in the strong-quantum-coupling regime, again for different choices such that either $A \ll N$, $A \simeq N$ or $A \gg N$, respectively. When $A \ll N$, quantum effects, after a rapid initial drop, merely lead to a small modulation of an essentially still monotonic decay of $\omega(t)$, which in turn is not very visible in the oscillating decay of the magnetisation, see the left panel in fig 2.3. On the other hand, quantum effects do become much more pronounced whenever $A \gtrsim N$. After a clearly visible drop in $\omega(t)$ at short times, followed by a monotonous decay up to times $t \sim \mathrm{O}(1/\gamma)$, strong peaks overlay the background evolution. These are also visible in the relaxation behaviour of the magnetisation, where a secondary periodic behaviour appears, see
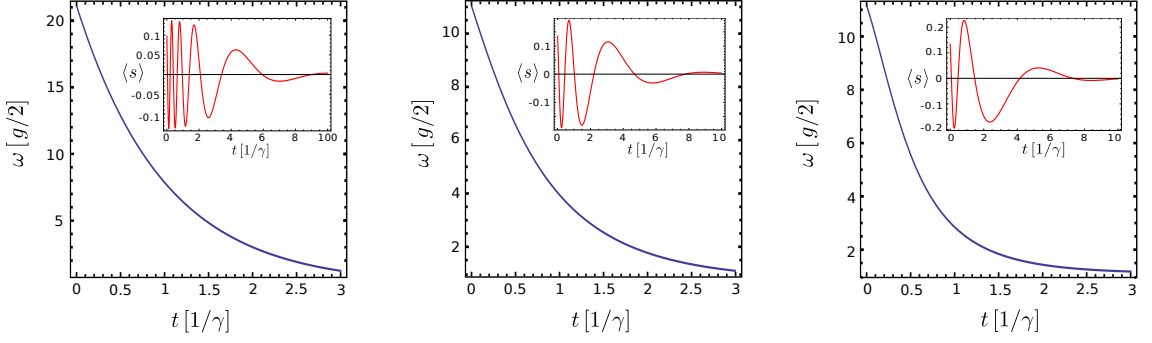
Figure 2.2: Time-dependence of the effective frequency $\omega(t)$ and of the magnetisation $m(t) = \langle s \rangle (t)$, in the weak-quantum-coupling regime with $g = 0.1$, for different ratios A/N:
Left panel: $A = 0.1$, $N = 10$ Centre panel: $A = 4$, $N = 5$ Right panel: $A = 10$, $N = 0.1$. In all cases, $\omega(t)$ decays monotonously, in analogy with the case $A = N$, see left panel in fig 2.1.
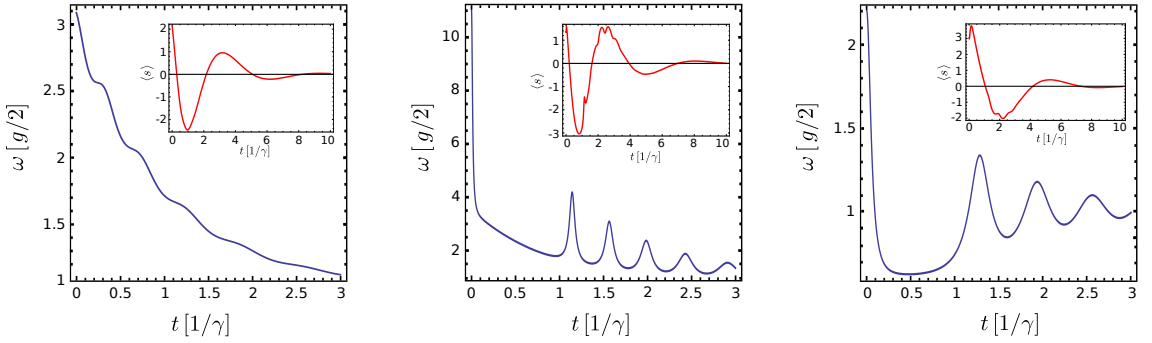
Figure 2.3: Time-dependence of the effective frequency $\omega(t)$ and of the magnetisation $m(t) = \langle s \rangle (t)$, in the strong-quantum-coupling regime for the following parameters:
Left panel: $A = 0.1$, $N = 10$ and $g = 7$, Centre panel: $A = 4$, $N = 3$, $g = 10$, Right panel: $A = 1$, $N = 0.1$, $g = 10$.

centre and right panels in fig 2.3. This is qualitatively analogous to the right panel in fig 2.1.

In order to better appreciate the rôle of the spherical constraint, let us recall the well-known behaviour of a quantum harmonic oscillator without it [Bre07, Car99, Sch14], as was also encountered in section 2.2 for the single-mode Dicke model. The Hamiltonian is again taken to be given by (2.2.4), with the fixed frequency $\omega = \omega_h = \text{cst}$. Upon coupling the system to a thermal bath, the dynamics is again described by the Lindblad equation (2.2.6). From this, the equation of motion for $\langle a \rangle$ is rapidly written down, being the analogue of (2.2.9), and solved [Bre07, Car99, Sch14]. It follows that the average magnetisation has the form

$$\langle s \rangle = e^{-\frac{\gamma}{2}t} \left(a \cos \omega_h t + b \sin \omega_h t \right) \tag{2.3.11}$$

where a, b are constants. One has a regular damped oscillation, with fixed frequency $\omega = \omega_h$. The distinct regimes of weak and strong quantum couplings seen in fig 2.1 do not appear. Although the long-time limit looks to be analogous to the one derived in eq (2.3.10) the finite-time behaviour of the single-spin spherical model allows for considerable more complexity. For example, even in the weak-coupling regime, the decrease of the oscillation frequency $\omega(t)$ is clearly visible in the non-harmonic oscillations of the magnetisation in the inset of the left panel in figs 2.1, 2.2 and 2.3.

2.4 Steady-state solution in the mean-field description

In this section, we consider the single SQS at $T = 0$ as a mean-field approximation of an N-body problem. In the most simple mean-field scheme of magnetic phase transitions, one replaces the

spin-spin interactions by an effective external magnetic field $B = B_{\text{eff}}$ [Jäg96], which is then self-consistently related to the magnetisation, by writing $B_{\text{eff}} = \kappa \langle s \rangle$ with some appropriately chosen proportionality constant κ.

We formally keep the above Lindblad equation (2.2.6) for the description of the dynamics, even if $B \neq 0$. Our main interest will be the determination of the structure of the phase diagram which means that essentially, we are going to look at the stability of the disordered phase with a vanishing magnetisation. In principle, the Lindblad operators L_α no longer couple directly to the eigenmodes of the system, and one cannot expect a relaxation to an equilibrium state [Bre07]. Rather, the relaxation should be towards some non-equilibrium steady-state (NESS) whose properties we are going to study. On the other hand, since we are mainly interested in the regime $B_{\text{eff}} \sim \langle s \rangle \ll 1$, these differences should not be very large. Also, in the quantum spherical model one expects that a mean-field approximation should correctly describe the quantum critical behaviour at $T = 0$ above the upper critical dimension, $d > d^* = 3$ [Sac01, Täu14].

2.4.1   Zero-temperature phase diagram

In order to start with the zero-temperature case ($T = 0$), we introduce the definitions

$$x_1 := \text{Re} \langle a \rangle , \ x_2 := \text{Im} \langle a \rangle , \ x_3 := \text{Re} \langle aa \rangle , \ x_4 := \text{Im} \langle aa \rangle , \ x_5 := \langle a^\dagger a \rangle \qquad (2.4.1)$$

and find from equations. (2.2.7), (2.2.8) and (2.2.9) the following set of real-valued equations of motion of the SQS in an external magnetic field B

$$\dot{x}_1 = -\frac{\gamma}{2}x_1 + \omega x_2 \qquad (2.4.2)$$

$$\dot{x}_4 = -\gamma x_4 - 2\omega x_3 + \sqrt{\frac{2g}{\omega}}Bx_1 \qquad (2.4.5)$$

$$\dot{x}_2 = -\frac{\gamma}{2}x_2 - \omega x_1 + \frac{1}{2}\sqrt{\frac{2g}{\omega}}B \qquad (2.4.3)$$

$$\dot{x}_5 = -\gamma x_5 + \sqrt{2g}x_2 \qquad (2.4.6)$$

$$\dot{x}_3 = -\gamma x_3 + 2\omega x_4 - \sqrt{\frac{2g}{\omega}}Bx_2 \qquad (2.4.4)$$

We now cast this system of equations as a self-consistent mean-field approximation by relating the external field B to the magnetisation, viz. $B = \kappa \langle s \rangle$. Then, recall (2.2.3) and also use the spherical constraint (2.2.5) in order to eliminate the variable x_5. We wish to analyse the stationary state, for which we have the system of equations

$$0 = -\frac{\gamma}{2}x_1 + \omega x_2 \qquad (2.4.7)$$

$$0 = -\gamma x_4 - 2\omega x_3 + 2g\kappa\frac{x_1^2}{\omega} \qquad (2.4.10)$$

$$0 = -\frac{\gamma}{2}x_2 - \omega x_1 + g\kappa\frac{x_1}{\omega} \qquad (2.4.8)$$

$$0 = -\gamma\frac{\omega}{g} + \gamma x_3 + \frac{\gamma}{2} + 2g\kappa\frac{x_1 x_2}{\omega} \qquad (2.4.11)$$

$$0 = -\gamma x_3 + 2\omega x_4 - 2g\kappa\frac{x_1 x_2}{\omega} \qquad (2.4.9)$$

with the five independent variables x_1, x_2, x_3, x_4 and $\omega = \omega(\infty)$.

This system has two distinct solutions for ω: one corresponds to a *disordered state*, labelled d, with frequency $\omega_{\text{d}} = g/2$ and $x_1 = x_2 = x_3 = x_4 = 0$ and the other one corresponding to a magnetically *ordered state*, labelled o, with frequency $\omega_{\text{o}}^2 = g\kappa - \gamma^2/4$ and the $x_1, \ldots, x_4$ non-vanishing. Compactly, the two physically distinct stationary states can be distinguished by their frequencies

$$\text{disordered: } \omega_{\text{d}} = \frac{g}{2} \quad ; \quad \text{ordered: } \omega_{\text{o}} = \sqrt{g\kappa - \frac{\gamma^2}{4}} \ . \qquad (2.4.12)$$

In the left panel of fig 2.4, we characterise the different stationary states by displaying the stationary frequencies ω as a function of the quantum coupling g, for several values of the dissipation coupling γ. The red (dotted) straight line corresponds to the disordered solution ω_{d}, while the other lines correspond to the ordered solution ω_{o}, for different values of the damping γ. Depending on the value of γ, we either find

- two intersections, for $0 < \gamma < 2\kappa/$, at

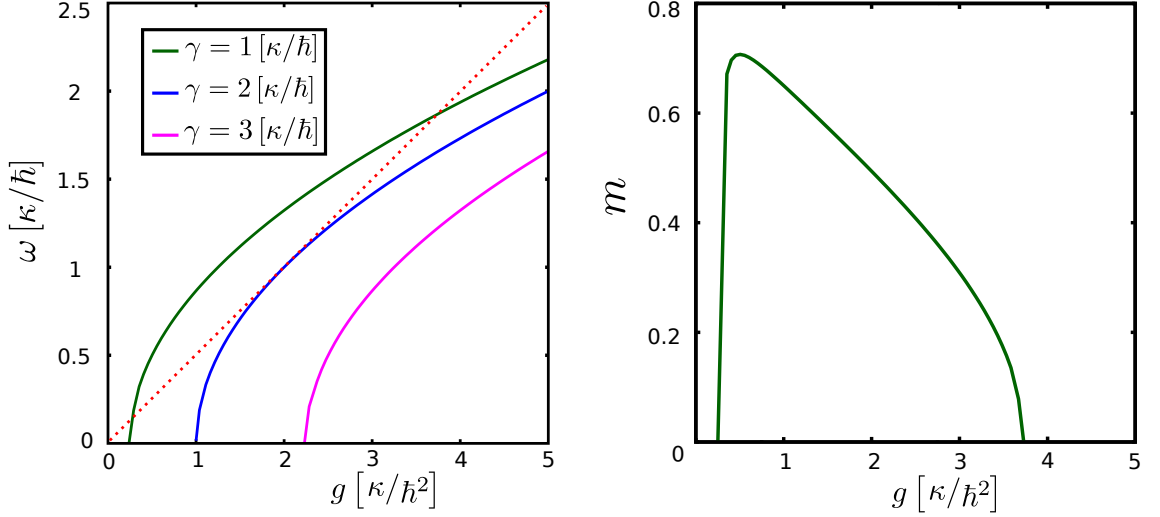$$g_{1,2} = 2\kappa \mp \sqrt{4\kappa^2 - \gamma^2} \qquad (2.4.13)$$

Figure 2.4: <u>Left panel:</u> stationary frequency ω as a function of the quantum coupling g for the two distinct steady-state solutions, for several values of γ, and for temperature $T = 0$.The full lines give ω_o, the dotted line ω_d. <u>Right panel:</u> average magnetisation m as a function of g, for $\gamma = 1$ and $T = 0$. There are two quantum critical points for $\gamma < 2\kappa$ and one multi-critical point for $\gamma = 2\kappa$.

- one intersection, for $\gamma = 2\kappa/$, at

$$g_c = 2\kappa \tag{2.4.14}$$

- no intersection, for $2\kappa < \gamma$.

It turns out that the larger of these solutions ω is stable, in the sense of a linear stability analysis of the system (2.4.2 - 2.4.6), as shown in appendix 2.C. In other words, whenever no intersections between ω_o and ω_d occur, the disordered solution, with frequency ω_d, is stable and the ordered solution, with frequency ω_o, is unstable. On the other hand, in the case of two intersections, the disordered solution, with frequency ω_d, is only stable if either $g < g_1$ or $g > g_2$, while the ordered solution ω_o is stable in the intermediate region $g_1 < g < g_2$. In this intermediate regime, there is a non-vanishing spontaneous magnetisation

$$m^2 = \langle s \rangle^2 = \frac{\gamma^2}{4\kappa g}\left(1 - \frac{g}{2\omega}\right)\left(1 + \frac{4\omega^2}{\gamma^2}\right) \;, \tag{2.4.15}$$

whose dependence on g, for a fixed value $\gamma = 1$, is shown in the right panel of fig 2.4. This makes apparent the physical origin of the labels 'ordered' and 'disordered'. Two distinct quantum phase transitions occur at g_1 and g_2, respectively. Near these quantum critical points, we can rewrite the magnetisation as follows, with $j = 1, 2$

$$m^2 \approx \frac{\gamma}{4\kappa g_j^2}\left(1 + \frac{g_j^2}{\gamma^2}\right)\frac{\sqrt{4\kappa^2 - \gamma^2}}{2\kappa - \sqrt{4\kappa^2 - \gamma^2}}\left|g - g_j\right| \;. \tag{2.4.16}$$

Recalling the standard definition of the magnetisation critical exponent, $m^2 \sim |g - g_j|^{2\beta}$, we read off the expected mean-field value $\beta = 1/2$.

The mean-field phase diagram is shown in the left panel of fig 2.5. The ordered and the disordered phases are clearly separated. For sufficiently large values of the damping constant γ, any ordered structure is simply dissipated away, for all values of the quantum coupling g. Analogously, for sufficiently large values of g, quantum disorder destroys any magnetic order. Surprisingly, we find a re-entrance of the disordered phase also when the quantum coupling becomes small enough ! This means that in order to have an ordered stationary state, a *cooperative effect* between the quantum fluctuations, parametrised by g and the dissipation, parametrised by γ, is required. This is a highly non-intuitive effect of the coherent quantum dynamics, without an analogue in the classical spherical model.
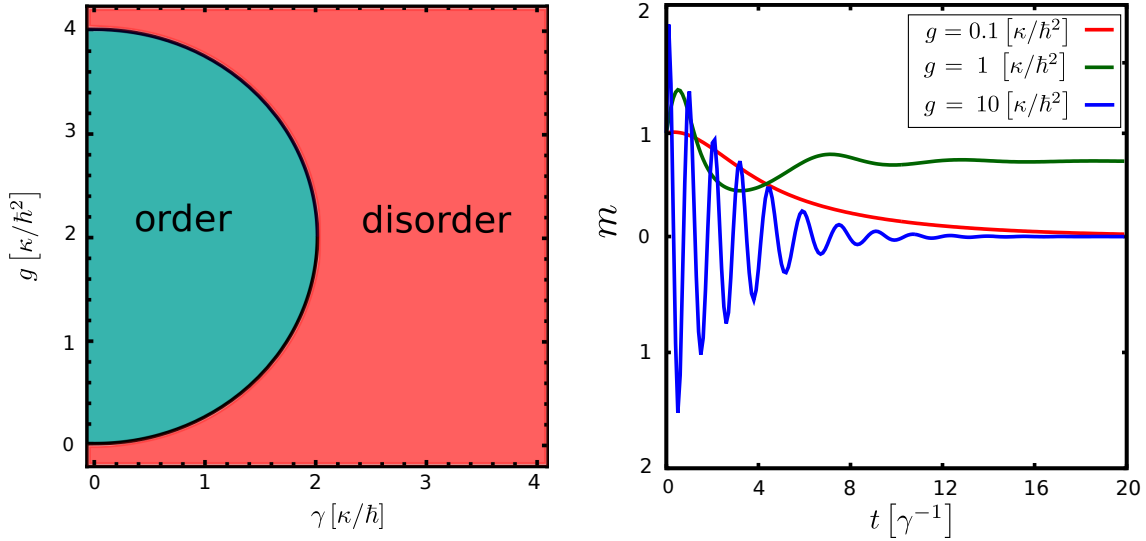
Figure 2.5: Left panel: mean-field phase diagram of the SQS at $T = 0$ with its two distinct phases. The critical line is a parabola, given by eq (2.4.13). Right panel: relaxation of the magnetisation, along the line $\gamma = 1$. In the disordered phase with $g < g_1$, there is a monotonous exponential decay (red curve), in the disordered phases with $g > g_2$, there is an oscillatory decay (blue curve). In the intermediate phase $g_1 < g < g_2$, there is a relaxation towards a magnetically ordered stationary state (green curve).

The distinction between the two regions of the disordered phase is further illustrated through the relaxation of the magnetisation, see the right panel of fig 2.5. Although the stationary magnetisation always vanishes in the disordered phase, the approach to this stationary value depends on value of the quantum coupling g. If $g > g_2$ is large enough, there are magnetisation oscillations while for $g < g_1$ small enough, the approach towards to stationary value is monotonous. Some magnetic oscillations are also seen for relaxations within the ordered phase.

To what extent could one take these results, interpreted as coming from a mean-field approximation, as a useful guide for more complex systems with stronger fluctuation effects ? The pronounced difference in the shape of the magnetisation curve $m = m(g)$, near to $g = g_1$ and $g = g_2$, respectively, might suggest that fluctuation effects might turn the continuous transition at $g = g_1$ into a first-order transition. Of course, it would be important to check if the presence of a disordered state for quantum couplings $0 < g < g_1$ remains valid beyond the mean-field approximation. However, since mean-field theory is considered as a reliable qualitative guide (and even quantitatively for the critical behaviour of the spherical model in $d > 3$ dimensions), it appears plausible that the qualitative features of the phase diagram in fig 2.5 and the different types of relaxation behaviour could reflect more than an artefact of a simple approximation scheme. To answer this questions requires a solution of the Lindblad equation of a full N-body version of the quantum spherical model in dimensions $d > 1$. We shall return to this problem in the next chapter.

2.4.2 Finite-temperature corrections

For a sufficiently small temperature $T > 0$, we shall calculate the first-order correction to the above zero-temperature solution by expanding the occupation number for $T \ll \min_{t \geq 0} \omega(t)$

$$ n_\omega = \left(e^{\omega/T} - 1 \right)^{-1} \simeq e^{-\omega/T} \ . \tag{2.4.17} $$

Since the temperature T enters explicitly only into the the average $\langle a^\dagger a \rangle$ via the equation of motion (2.2.8), it follows that the the ordered zero-temperature solution and its frequency ω_o remains unaffected by the temperature, to leading order, while the frequency of the disordered
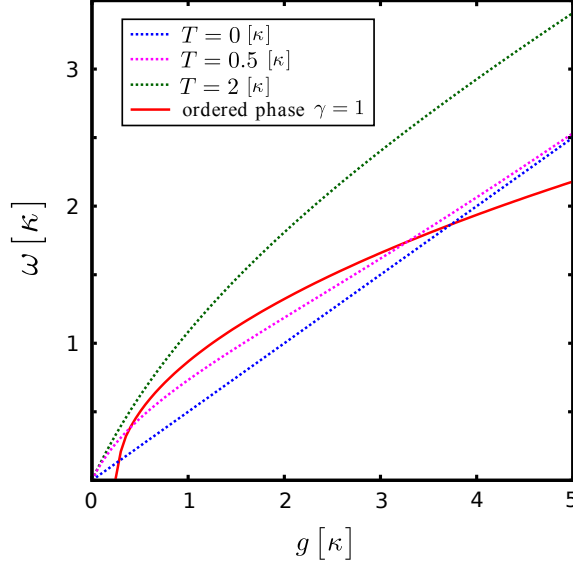
Figure 2.6: Effective frequencies ω of the different solutions of the steady-state, for a small temperature $T > 0$ and $\gamma = 1$, as a function of g. The frequency ω_{o} of the ordered phase is given by the full red line. The frequencies ω_{d} for the disordered phase is given by the dotted blue, magenta and green lines for $T/\kappa = [0, 0.5, 2]$, from bottom to top. characteristic energy κ.

solution is slightly shifted, according to

$$\omega_{\text{d}}(T, g) \approx \frac{g}{2} + T \, W \left(\frac{g}{T} e^{-g/2T} \right) \; . \tag{2.4.18}$$

where W denotes the Lambert-W function [Abr64]. In fig 2.6, we compare the the frequency ω_{o} of the ordered phase with the temperature-dependent frequencies ω_{d} of the disordered state. As the temperature T increases, the curves of $\omega_{\text{d}}(g)$ bend downwards but provided T does not grow too large, one can still find two intersections. This indicates that the topology of the phase diagram (left panel of fig 2.5) should remain unchanged for a sufficiently small temperature $T > 0$ such that the two quantum phase transitions obtained at $T = 0$ persist.

2.5   Summary

In this chapter, we have studied the coherent quantum dynamics, as described by a Lindblad equation, of a simple toy model, consisting of a single quantum oscillator which was also assumed to obey a constraint analogous to the quantum spherical model of ferromagnetism. While the low-energy modes of that model look very similar to the ones of the Dicke model (in the rotating-phase approximation), an essential difference arises from the effective time-dependence of the frequency $\omega(t)$, as determined from the spherical constraint, while in the Dicke model, the frequency is usually taken to be a constant. Our aim has been to understand better the phenomenological consequences of describing a coherent quantum dynamics of an open quantum system, coupled to a bosonic heat bath via the Lindblad equation. We have found:

1. the exact time-dependent solution, without an external field and at zero temperature, allows to distinguish two distinct relaxational regimes, of weak and of strong quantum-coupling, respectively. In the weak-quantum-coupling regime, the relaxation is dominated by the dissipation, as described by the dissipation coupling γ, whereas in the strong-quantum-coupling regime, intrinsic quantum oscillations lead to a more complex phenomenology of the relaxation of physical observables, such as the magnetisation, see fig 2.3.

2. when considering our single-spin model, in the presence of an external magnetic field, as an effective mean-field approximation of a quantum ferromagnet, the stationary state displays

a surprising structure of its phase diagram. Remarkably, it turns out that a magnetically ordered state can only arise if both quantum disorder, parametrised by the coupling g, as well as dissipation, parametrised through γ, are present. For fixed values of γ (not too small and not too large) we find *two* distinct quantum phase transitions at couplings $g_{1,2}$, such that an ordered magnetic state is stable for couplings $g_1 < g < g_2$ and is unstable otherwise, see fig 2.5.

These zero-temperature quantum phase transitions are stable under a small thermal perturbation.

For the interpretation of these quantum phase transitions, recall that the quantum coupling g plays for quantum phase transitions at $T = 0$ in d dimensions a rôle analogous to the temperature $T > 0$ in classical phase transitions in $d + 1$ dimensions [Sac01, Hen84b, Voj96, Oli06, Wal15]. Therefore, fixing a value of $\gamma < 2\kappa$ and looking at the phase diagram in fig 2.5, when increasing the value of g, starting from a small value $g \ll g_1$, we see that *increasing the quantum fluctuations leads to a magnetic ordering of the system*. Only if $g > g_2$ becomes rather large, this order will melt again. In classical systems, this phenomenon is well-known and was first observed in non-equilibrium steady-states [Kat84, Hel00, Zia02, Bor14, Alt15] (and references therein), although it was pointed out that it is not intrinsically a non-equilibrium effect [Rad03] and simple examples of it are known even when detailed balance is maintained [Zia02]. In the wide sense of order induced by larger fluctuations, names such as '*freezing-by-heating*' [Hel00] or '*getting more from pushing less*' [Zia02] have been invented for this phenomenon, although such re-entrant behaviour has been known long before in equilibrium systems [Rad03]. In non-equilibrium steady-states, this is related to the occurrence of *negative* responses. Freezing-by-heating was also observed experimentally in super-cooled water on negatively charged surfaces of the pyroelectric material $LiTaO_3$ [Ehr10]. A negative response of the system's energy with respect to the bath temperature was also reported in the Dicke model [Ros12].

Apparently we have observed a true quantum analogue of this well-known phenomenon, which one might call '*quantum order by quantum fluctuations*', since our control parameter is the quantum coupling g and not the bath temperature T.[11] A common feature of systems undergoing freezing-by-heating or their quantum analogue is that their Hamiltonians conserve the total number of quasi-particles [Kat84, Hel00, Zia02, Ros12, Bor14].[12]

In the next chapter, we shall continue and extend the study of this model along the following lines:

1. derive the N-body form of the Lindblad dissipators

2. obtain the exact spherical constraint

3. solve this constraint exactly (at least in certain special cases)

This will give access to an analysis of the quantum dynamics of an exactly solvable many-body quantum system.

---

[11]By analogy with [Ros12], this suggests that experimental observations of this effect could also use purely quantum control parameters and are not restricted to purely thermodynamical variables. However, in the SQS the average energy $\langle \mathcal{H} \rangle$ of the stationary state increases monotonically with g. At the critical points $g = g_{1,2}$ the derivative $\partial \langle \mathcal{H} \rangle / \partial g$ taken from the left is clearly smaller than its analogue taken from the right.

[12]Since there is no obvious breaking of a symmetry between a macroscopic number of ground states, there is no immediate relationship to the well-known 'order-by-disorder' phenomenon, see [Vil80, Ber07] and [Ros14] for an experimental observation in the pyrochlore magnet $Er_2Ti_2O_7$.

Appendix

2.A   Phenomenological dynamics in the quantum spherical model

The 'spin-anisotropic quantum spherical model' (saqsm) was introduced in section 1.3.3 and is defined, on a d-dimensional hyper-cubic lattice, and for a vanishing magnetic field $B = 0$, by the Hamiltonian [Wal15]

$$\mathcal{H} = \sum_{\boldsymbol{n}} \left(\frac{g}{2} p_{\boldsymbol{n}}^2 + \mathcal{S} \, s_{\boldsymbol{n}}^2 - \sum_{j=1}^{d} \left(\frac{1+\lambda}{2} \, s_{\boldsymbol{n}} s_{\boldsymbol{n}+\boldsymbol{e}_j} + \frac{1-\lambda}{2} \frac{g}{2\mathcal{S}} p_{\boldsymbol{n}} p_{\boldsymbol{n}+\boldsymbol{e}_j} \right) \right) \qquad (2.A.1)$$

with the commutation relations $[s_{\boldsymbol{n}}, p_{\boldsymbol{m}}] = \mathrm{i}\delta_{\boldsymbol{nm}}$. The spherical parameter $\mathcal{S}$ is found self-consistently from the (mean) spherical constraint $\left\langle \sum_{\boldsymbol{n}} s_{\boldsymbol{n}}^2 \right\rangle = \mathcal{N}$, where $\mathcal{N}$ is the number of lattice sites. The model's parameters are g and λ.[13] Because of the symmetry in λ [Wal15], we restrict throughout to $\lambda > 0$. The usual quantum spherical model [Obe72] is the special case $\lambda = 1$. At equilibrium, for all $\lambda \neq 0$ and $d > 1$, the model has a continuous quantum phase transition at temperature $T = 0$. The associated exponents and universal amplitude ratios are λ-independent, as expected from universality [Wal15]. Remarkably, for dimensions $1 < d \lesssim 2.065$, that phase transition is re-entrant in the sense that the critical coupling $g_c = g_c(\lambda)$ is a non-monotonous function of λ [Wal15]. The saqsm therefore allows to analyse non-trivial quantum effects on its critical behaviour. Here, we shall show that *if the dynamics is taken to be the analogue of the phenomenological 'quantum Kramers equation' (2.1.4), the system's behaviour becomes equivalent to the classical case $g = 0$, $\lambda = 1$ for sufficiently large times.*

Step 1: Generalising the procedure leading to (2.1.4) to generic values of λ, we find the 'quantum Kramers equations' of motion (with $J = 1$) [Tai06, Dur15]

$$\partial_t s_{\boldsymbol{n}} = g p_{\boldsymbol{n}} - \frac{1-\lambda}{2} \frac{g}{2\mathcal{S}(t)} \sum_{j=1}^{d} \left(p_{\boldsymbol{n}-\boldsymbol{e}_j} + p_{\boldsymbol{n}+\boldsymbol{e}_j} \right) \qquad (2.A.2)$$

$$\partial_t p_{\boldsymbol{n}} = -2 s_{\boldsymbol{n}} + \sum_{j=1}^{d} \left(\frac{1+\lambda}{2} \left(s_{\boldsymbol{n}-\boldsymbol{e}_j} + s_{\boldsymbol{n}-\boldsymbol{e}_j} \right) + \frac{1-\lambda}{2} \frac{g}{2\mathcal{S}(t)} \left(p_{\boldsymbol{n}-\boldsymbol{e}_j} + p_{\boldsymbol{n}-\boldsymbol{e}_j} \right) \right) - \gamma g p_{\boldsymbol{n}} + \eta_{\boldsymbol{n}}$$
$$(2.A.3)$$

Step 2: Using the Fourier representation (on a hyper-cubic lattice with $\mathcal{N} = N^d$ sites)

$$q_{\boldsymbol{k}} = \sum_{\boldsymbol{n}} e^{\mathrm{i}\frac{2\pi}{N}\boldsymbol{k}\cdot\boldsymbol{n}} s_{\boldsymbol{n}} \;\; , \;\; \pi_{\boldsymbol{k}} = \sum_{\boldsymbol{n}} e^{\mathrm{i}\frac{2\pi}{N}\boldsymbol{k}\cdot\boldsymbol{n}} p_{\boldsymbol{n}} \;\; , \;\; \tilde{\eta}_{\boldsymbol{k}} = \sum_{\boldsymbol{n}} e^{\mathrm{i}\frac{2\pi}{N}\boldsymbol{k}\cdot\boldsymbol{n}} \eta_{\boldsymbol{n}} \qquad (2.A.4)$$

decouples the modes and brings the equations of motion to the form

$$\partial_t q_{\boldsymbol{k}} = \frac{g}{\mathcal{S}(t)} \Lambda_2^2(t,\boldsymbol{k}) \pi_{\boldsymbol{k}} \;\; , \;\; \partial_t \pi_{\boldsymbol{k}} = -2\Lambda_1^2(t,\boldsymbol{k}) q_{\boldsymbol{k}} - \frac{g\gamma}{\mathcal{S}(t)} \Lambda_2^2(t,\boldsymbol{k}) \pi_{\boldsymbol{k}} + \tilde{\eta}_{\boldsymbol{k}}(t) \qquad (2.A.5)$$

with the following eigenvalues of the Hamiltonian [Wal15]

$$\Lambda(t,\boldsymbol{k}) = \Lambda_1(t,\boldsymbol{k}) \, \Lambda_2(t,\boldsymbol{k}) := \sqrt{\mathcal{S}(t) - \frac{1+\lambda}{2} \sum_{j=1}^{d} \cos k_j} \sqrt{\mathcal{S}(t) - \frac{1-\lambda}{2} \sum_{j=1}^{d} \cos k_j} \qquad (2.A.6)$$

If one defines $\Omega(t,\boldsymbol{k}) := \exp\left(-\int_0^t \mathrm{d}\tau \frac{g\gamma}{\mathcal{S}(\tau)} \Lambda_2^2(\tau,\boldsymbol{k}) \right)$ and denotes the convolution by $*$ (with respect to $\boldsymbol{k}$), the formal solution of (2.A.5) for the momenta reads[14]

$$\pi_{\boldsymbol{k}}(t) = \pi_{\boldsymbol{k}}(0)\Omega(t,\boldsymbol{k}) + \left(-2\Lambda_1(t,\boldsymbol{k}) q_{\boldsymbol{k}}(t) + \tilde{\eta}_{\boldsymbol{k}}(t) \right) * \Omega(t,\boldsymbol{k}) \, . \qquad (2.A.7)$$

---

[13]As in the whole work, we always re-scale the nearest-neighbour exchange energy $J = 1$.

[14](with a slight abuse of notation concerning the convolution with respect to $\boldsymbol{k}$)

Inserting this solution into the other eq (2.A.5) for $q_{\boldsymbol{k}}$, we find in the long-time limit

$$\partial_t q_{\boldsymbol{k}}(t) \approx -\frac{1}{\gamma} \left(-\Lambda_1^2(t, \boldsymbol{k}) q_{\boldsymbol{k}}(t) + \tilde{\eta}_{\boldsymbol{k}}(t)\right) * \partial_t \Omega(t, \boldsymbol{k}) , \tag{2.A.8}$$

where we dropped the contribution of the initial values of the conjugate momenta. For sufficiently large times, this is justified, since for $\lambda > 0$, the spherical parameter $\mathcal{S}(t) \geq \frac{1+\lambda}{2} d$ [Wal15], hence $\Lambda_2^2(t, \boldsymbol{k}) - \Lambda_1^2(t, \boldsymbol{k}) \geq \lambda \sum_{j=1}^d \cos k_j \approx \lambda d$ in the low-momentum limit which is relevant for the slowest modes. Therefore, the conjugate momenta decay at least as fast as

$$\pi(t) \sim \exp\left(-\frac{2\lambda}{1+\lambda} g\gamma\, t\right) = \exp\left(-\frac{2\lambda}{1+\lambda} \frac{t}{t_{\text{deco}}}\right) \tag{2.A.9}$$

whereas the decay of the slowest spin modes in the system is according to

$$q(t) \sim \exp\left(-\Lambda_1^2(t, \boldsymbol{k})/\gamma\right) \sim \exp\left(-\left[\mathcal{S}(t) - (1+\lambda)d/2\right]/\gamma + \mathrm{O}(\boldsymbol{k})^2\right) . \tag{2.A.10}$$

Step 3: We want to show how, in the long-time limit, the equation of motion (2.A.8) reduces to the Langevin equation of the classical spherical model, with $g = 0$ and $\lambda = 1$.

In order to extract the leading long-term behaviour (2.A.8), one first maps this differential equation to an algebraic one, by using the Laplace transform

$$\bar{q}_{\boldsymbol{k}}(u) := \mathcal{L}\left(q_{\boldsymbol{k}}(t)\right)(u) = \int_0^\infty \mathrm{d}t\, e^{-ut}\, q_{\boldsymbol{k}}(t) \tag{2.A.11}$$

We find

$$u\, \bar{q}_{\boldsymbol{k}}(u) - q_{\boldsymbol{k}}(0) = \frac{1}{\gamma} \left(1 - u\bar{\Omega}(u, \boldsymbol{k})\right)\, \mathcal{L}\left(-2\Lambda_1^2(t, \boldsymbol{k}) q_{\boldsymbol{k}}(t) + \tilde{\eta}_{\boldsymbol{k}}(t)\right)(u) \tag{2.A.12}$$

We shall need the large-time asymptotics of $\Omega(t, \boldsymbol{k})$, and its Laplace transform $\bar{\Omega}(u, \boldsymbol{k})$. Indeed, in the long-time limit, the integral in the exponential can be approximated by a time-independent average, as follows

$$\bar{\Omega}(u, \boldsymbol{k}) = \int_0^\infty \mathrm{d}t\, e^{-ut} e^{-\gamma \int_0^t \mathrm{d}\tau \frac{g}{\mathcal{S}(\tau)} \Lambda_2^2(\tau, \boldsymbol{k})} = \int_0^\infty \mathrm{d}t\, e^{-\left(u + t^{-1} \int_0^t \mathrm{d}\tau \frac{g\gamma}{\mathcal{S}(\tau)} \Lambda_2^2(\tau, \boldsymbol{k})\right)t}$$

$$\simeq \int_0^\infty \mathrm{d}t\, e^{-\left(u + g\gamma \left\langle \frac{1}{\mathcal{S}} \Lambda_2^2(\boldsymbol{k})\right\rangle\right)t} = \left(u + g\gamma \left\langle \frac{1}{\mathcal{S}} \Lambda_2^2(\boldsymbol{k})\right\rangle\right)^{-1} \tag{2.A.13}$$

where we define the average $\left\langle \frac{1}{\mathcal{S}} \Lambda_2^2(\boldsymbol{k})\right\rangle := t^{-1} \int_0^t \mathrm{d}\tau \frac{1}{\mathcal{S}(\tau)} \Lambda_2^2(\tau, \boldsymbol{k})$. Inserting this result into eq (2.A.12), we find

$$u\, \bar{q}_{\boldsymbol{k}}(u) - q_{\boldsymbol{k}}(0) = \frac{1}{\gamma} \frac{\left\langle \Lambda_2^2(\boldsymbol{k})/\mathcal{S}\right\rangle}{\frac{1}{\gamma g} u + \left\langle \Lambda_2^2(\boldsymbol{k})/\mathcal{S}\right\rangle} \mathcal{L}\left(-2\Lambda_1^2(t, \boldsymbol{k}) q_{\boldsymbol{k}}(t) + \tilde{\eta}_{\boldsymbol{k}}(t)\right)(u) . \tag{2.A.14}$$

Standard Tauberian theorems [Fel71, ch. XIII.5] relate the asymptotic long-time behaviour of a function $f(t)$ as $t \to \infty$ to the behaviour of its Laplace transform $\mathcal{L}(f)(u)$ as $u \to 0^+$. Therefore, in order to find the leading long-time behaviour of the spin operators $\tilde{s}_{\boldsymbol{k}}(t)$, we first analyse the leading $u \to 0^+$-behaviour of the expression (2.A.14), which gives

$$u\, \bar{q}_{\boldsymbol{k}}(u) - q_{\boldsymbol{k}}(0) \simeq \frac{1}{\gamma} \mathcal{L}\left(-2\Lambda_1^2(t, \boldsymbol{k}) q_{\boldsymbol{k}}(t) + \tilde{\eta}_{\boldsymbol{k}}(t)\right)(u) \tag{2.A.15}$$

and then, via an inverse Laplace transform, we find the sought effective long-time form of the equations of motion for the spin variables

$$\partial_t q(t, \boldsymbol{k}) \simeq -\frac{2}{\gamma} \Lambda_1^2(t, \boldsymbol{k}) q(t, \boldsymbol{k}) + \frac{1}{\gamma} \tilde{\eta}_{\boldsymbol{k}}(t)$$

$$= -\frac{2}{\gamma} \left(\mathcal{S}(t) - \frac{1+\lambda}{2} \sum_{j=1}^d \cos k_j\right) q(t, \boldsymbol{k}) + \frac{1}{\gamma} \tilde{\eta}_{\boldsymbol{k}}(t) , \tag{2.A.16}$$

which we now compare to the Langevin equation of the classical spherical model [Ron78, God00].

Indeed, if we take $\lambda = 1$, we see that (2.A.16) reproduces the classical Langevin equation if we choose

$$\gamma = 2 \ . \tag{2.A.17}$$

and renormalise the temperature $T \mapsto \gamma T$ (unimportant for a quantum phase transition at $T = 0$). Moreover, the result (2.A.16) shows that the parameter $\lambda \neq 1$ merely gives rise to a renormalisation of the time t and of the spherical parameter. Therefore, the supposed 'quantum dynamics' (2.A.2, 2.A.3) does *not* relax to the equilibrium state of the SAQSM-model (2.A.1), but rather dissipates away the non-trivial quantum effects [Wal15] on the phase boundary $g_c = g_c(\lambda)$.

2.B   Solution of the phase equation

In the main text, the phase $\Theta = \Theta(t)$ was shown to obey the equation (2.3.6), which reads

$$-\frac{\dot{\Theta}}{g} = 2A\,e^{-\gamma t}\cos\Theta + 2N\,e^{-\gamma t} + 1 \ . \tag{2.B.1}$$

and where A, N, γ and g are real constants. We shall solve this equation explicitly by mapping it to a well-known Riccati equation.

Let $y(t) := e^{\mathrm{i}\Theta(t)}$ and re-write eq (2.B.1) as

$$\frac{\mathrm{i}}{g}\dot{y}e^{\gamma t} = ye^{\gamma t} + 2Ny + A\left(y^2 + 1\right) \tag{2.B.2}$$

A change of the time-scale, according to $\tau = e^{-\gamma t}$, together with the definitions

$$Y(\tau) := y(t), \quad \mathcal{A} := \frac{g}{\mathrm{i}\gamma}A, \quad B := \frac{2gN}{\mathrm{i}\gamma}, \quad C := \frac{g}{\mathrm{i}\gamma} \ . \tag{2.B.3}$$

reduces this to the following *Riccati equation*

$$\tau\dot{Y}(\tau) + (B\tau + C)\,Y(\tau) + \mathcal{A}\tau Y^2(\tau) + \mathcal{A}\tau = 0 \tag{2.B.4}$$

which depends on the three parameters $\mathcal{A}, B, C$. A standard method for solving this kind of equation consists in mapping it to a second-order linear differential equation, by changing variables according to $\lambda Y =: \dot{u}/u$ [Pol02, sec. 1.2.2, eq (45)]. Hence

$$\tau\ddot{u} + (B\tau + C)\dot{u} + \mathcal{A}^2\tau u = 0 \ . \tag{2.B.5}$$

Next, simplify (2.B.5) by separating off an exponential, according to $u(\tau) = e^{-\delta\tau}w(\tau)$, where δ remains to be chosen. We arrive at the following equation, for the unknown function $w(\tau)$

$$\tau\ddot{w} + [C - (2\delta - B)\tau]\,\dot{w} + \left[\tau(\delta^2 - \delta B + \mathcal{A}^2) - \delta C\right]w = 0 \ . \tag{2.B.6}$$

We now choose the free parameter δ in order to render the pre-factor of w in eq (2.B.6) time-independent. This will allow us to recognise (2.B.6) as a Kummer or Bessel differential equation. In principle, one might take either of the two possibilities $\delta = B/2 \pm \sqrt{B^2/4 - \mathcal{A}^2}$. Without loss of generality, we prefer the choice $\delta = B/2 + \sqrt{B^2/4 - \mathcal{A}^2}$. Eq (2.B.6) turns into the form

$$\tau\ddot{w} + \left(C - \sqrt{B^2 - 4\mathcal{A}^2}\ \tau\right)\dot{w} + \frac{C}{2}\left(B + \sqrt{B^2 - 4\mathcal{A}^2}\ \right)w = 0 \tag{2.B.7}$$

for which we have to distinguish two different cases.

1. Case $B/2 \neq \mathcal{A}$. This case may stated alternatively by requiring $A \neq N$. We can define a rescaled time variable $T = \tau\sqrt{B^2 - 4\mathcal{A}^2}$, which reduces (2.B.7) to a *Kummer equation*

$$T\ddot{w} + (C - T)\dot{w} - \frac{C}{2}\left(1 + \frac{B}{\sqrt{B^2 - 4\mathcal{A}^2}}\right)w = 0 \tag{2.B.8}$$

A basis of solutions is given by Kummer's functions M and U [Abr64]. The general solution of (2.B.8) is consequently a linear combination of both

$$w(T) = K_1 U(\mathscr{T}) + K_2 M(\mathscr{T}) \,, \tag{2.B.9}$$

with the triplet of indices and the argument

$$\mathscr{T} := \left[-\frac{g}{2\gamma} \left(\mathrm{i} + \frac{1}{\sqrt{A^2/N^2 - 1}} \right) \;\; ; \;\; -\mathrm{i}\frac{g}{\gamma} \;\; ; \;\; 2\frac{g}{\gamma}\sqrt{A^2 - N^2}e^{-\gamma t} \right] \,. \tag{2.B.10}$$

Back-transformation to the required solution of the original first-order differential equation will introduce a relation between the two integration constants K_1 and K_2 of the second-order equation (2.B.8).

Finally, we transform this result back to our original variable $\Theta = \Theta(t)$. For this purpose, we introduce the shorthand $\mathscr{T}_{(x,y)} = \mathscr{T} + (x; y; 0)$. The phase Θ then reads

$$\cos\Theta(t) = \mathrm{Re}\left(-\frac{N}{A} - \mathrm{i}\sqrt{1 - \frac{N^2}{A^2}} + \frac{g}{\gamma}\left(\sqrt{1 - \frac{N^2}{A^2}} - \mathrm{i}\frac{N}{A} \right) \frac{\mathrm{i}\frac{\gamma}{g}KM(\mathscr{T}_{(1,1)}) - U(\mathscr{T}_{(1,1)})}{KM(\mathscr{T}) - U(\mathscr{T})} \right) \tag{2.B.11}$$

Herein, the constant K is related to the initial condition.

As a 'sanity check' of the whole procedure, we illustrate in fig 2.7 an example of the right-hand-side of eq (2.B.11). It is satisfying to see that $\cos\Theta(t)$ assumes as values the full range $[-1, 1]$, but does *not* exceed it, as it should be for a well-defined cosine function. This also holds true for all other parameter values.
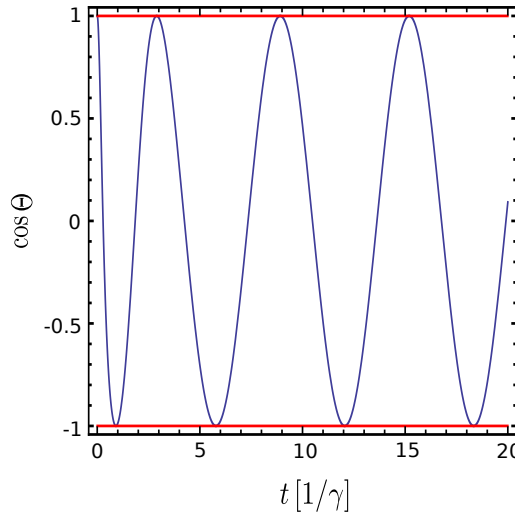
Figure 2.7: Illustration of the right-hand-side of eq (2.3.6), over against the time t, for the parameters $g/\gamma = 1$, $A = 1$, $N = 2$.

2. Case $B/2 = \mathcal{A}$. This case can also be specified by the condition $A = N$. Now, eq (2.B.7) turns into a Bessel differential equation

$$\tau\ddot{w} + C\dot{w} + \frac{BC}{2}w = 0 \tag{2.B.12}$$

with the general solution [Boa83]

$$w(\tau) = K_1\tau^{(1-C)/2}J_{1-C}\left(\mathrm{i}\sqrt{2BC\tau} \right) + K_2\tau^{(1-C)/2}J_{C-1}\left(\mathrm{i}\sqrt{2BC\tau} \right) \tag{2.B.13}$$

where $J_p(x)$ denotes the Bessel function of the first kind of order p [Abr64] (C is not an integer, see (2.B.3)). Transforming back to the original variables, we find

$$\cos\Theta(t) = -\mathrm{Re}\left(1 + \frac{\mathrm{i}}{\sqrt{A}}\,\mathrm{e}^{-\frac{\gamma}{2}t}\frac{KJ_{\mathrm{i}\frac{g}{\gamma}}\left(2\mathrm{i}\frac{g}{\gamma}\sqrt{A\,e^{-\gamma t}}\right) - J_{-\mathrm{i}\frac{g}{\gamma}}\left(2\mathrm{i}\frac{g}{\gamma}\sqrt{A\,e^{-\gamma t}}\right)}{KJ_{1+\mathrm{i}\frac{g}{\gamma}}\left(2\mathrm{i}\frac{g}{\gamma}\sqrt{A\,e^{-\gamma t}}\right) + J_{-1-\mathrm{i}\frac{g}{\gamma}}\left(2\mathrm{i}\frac{g}{\gamma}\sqrt{A\,e^{-\gamma t}}\right)}\right) \tag{2.B.14}$$

The constant K is related to the initial condition. We also checked that the function $\cos\Theta(t)$ in (2.B.14) has the full range $[-1, 1]$, in analogy with fig 2.7, as it should be.

Eqs. (2.B.11,2.B.14) are the main result of this appendix and are quoted in the main text.

2.C Linear stability of the steady state

We analyse the stability of the stationary solutions found in section 2.4 with a linear stability analysis. Consider the equations of motion (2.4.2,...,2.4.6) and use the spherical constraint to eliminate the variable x_5. The Jacobian matrix $\mathcal{J}$ of the resulting system of five equations, in the variables $x_1, \ldots, x_4, \omega$, is

$$\mathcal{J} = \begin{bmatrix} -\gamma/2 & \omega & 0 & 0 & gx_2 \\ \kappa g/\omega - \omega & -\gamma/2 & 0 & 0 & -gx_1\left(1 + g\kappa/\omega^2\right) \\ -2g\kappa x_2/\omega & -2\kappa gx_1/\omega & -\gamma & 2\omega & 2g\left(x_4 + \kappa gx_1x_2/\omega^2\right) \\ 4\kappa gx_1/\omega & 0 & -2\omega & -\gamma & -2g\left(x_3 + \kappa gx_1^2/\omega^2\right) \\ 0 & 0 & 0 & 2\omega & g\left(2x_4 - \gamma/g\right) \end{bmatrix} \tag{2.C.1}$$

Inserting the disordered solution $\omega = \omega_{\mathrm{d}}$ gives the following list of eigenvalues e_i of $\mathcal{J}$:

$$e_1 = -\gamma \tag{2.C.2}$$

$$e_2 = -\gamma - \mathrm{i}g \tag{2.C.3}$$

$$e_3 = -\gamma + \mathrm{i}g \tag{2.C.4}$$

$$e_4 = -\gamma/2 - \sqrt{\kappa g - g^2/4} \tag{2.C.5}$$

$$e_5 = -\gamma/2 + \sqrt{\kappa g - g^2/4} \tag{2.C.6}$$

In the range $g \in (0, g_1) \cup (g_2, \infty)$, with $g_{1,2}$ given by (2.4.13), all real parts of the eigenvalues are negative and thus the disordered solution is stable under small perturbations. On the other hand, for $g \in (g_1, g_2)$, the disordered solution is unstable, since the real part of the eigenvalue e_5 is positive and yields consequently an amplification of an infinitesimal perturbation.

For the ordered solution, there is no simple closed representation of the eigenvalues. However, we have checked that the numerical computation of the eigenvalues of $\mathcal{J}$ at the ordered solution $\omega = \omega_{\mathrm{d}}$ does imply linear stability of the ordered solution in the region $g \in (g_1, g_2)$ and instability outside of this region.

Chapter 3

Lindblad dynamics of the quantum spherical model

3.1 Introduction

In this chapter, we shall study the relaxational quantum dynamics of the quantum spherical model, after a quantum quench, in the limit of $\mathcal{N} \to \infty$ quantum spins. This is work done in [Wal17b].

The statistical mechanics of non-equilibrium open system continues to pose many challenges, related to the absence of a unified framework for their formulation. Here, we shall be concerned with non-equilibrium relaxations of open *quantum* systems. In the vicinity of equilibrium, linear-response theories such as the Kubo formula or the Landauer-Büttiker formalism may be used[Kub57a, Kub57b, Jeo95, Mah00]. But such approaches cannot describe the system's behaviour after a quench from one physical phase into another. Studies on the physical ageing of glassy and non-glassy systems after such quenches have led to a precise understanding of the associated phenomena and in particular have made it clear that the competition between several distinct, but equivalent, equilibrium states may prevent the system to relax to an equilibrium state at all, even if the microscopic dynamics does satisfy detailed balance [Hen09, Mar05, Sch14].

Often-used phenomenological approaches to classical dissipative systems include master equations for the probability distributions or Langevin equations for the observables. A major distinction of quantum systems with respect to classical ones is the presence of a conjugate momentum p_n for each classical observable s_n, both to be considered as operators, such that canonical commutation relations $[s_n, p_m] = i\hbar\delta_{n,m}$ should hold. From the point of view of a phenomenological classical description, this raises the requirement to re-formulate the dynamics in such a way that these prescribed conservation laws should be obeyed. Therefore, simplistic approaches such as phenomenological Kramers equations, for the observables s_n and the momenta p_m, supplemented by phenomenological damping terms, are inadequate, since they lead to the violation of the canonical commutation relations, on time-scales of the order of the inverse damping rate, such that an effectively classical dynamics remains [Car99]. The open system dynamics of a quantum system is most ideally studied using the concept of dynamical semi-groups and completely positive trace preserving (CPTP) dynamics. In the Heisenberg picture, this may be implemented using the tools of quantum Langevin equations [Gar04]. Conversely, in the Schrödinger picture, that is most readily accomplished using Lindblad master equations.

Formally, the Lindblad equation preserves the trace, the hermiticity and the positivity of the reduced density matrix ρ. On the other hand, it is not considered straightforward to write down explicit expressions for the Lindblad dissipators for generic many-body systems, although well-established formalisms exist for few-body systems, see e.g. [Bre07, Att06b, Att07, Wei99, Sch14]. Finally, if such expressions have been obtained, actually solving a Lindblad equation is far from obvious. Some results exist for one- or two-body problem, see [Bre07, Wei99, Sch14]. For *fermionic* many-body *chains*, exact solutions have been found by establishing relationships with $1D$ quantum integrability, see [Pro10, Pro11a, Kar13] and [Pro15] for a recent review. Indeed, integrable models are relevant for the understanding of a large range of experiments, see [Bat16] for a recent review.

But by their very mathematical nature, such techniques are limited to one-dimensional systems.

In order to provide insight beyond purely numerical studies, a versatile and non-trivial exactly solvable model is sought. In equilibrium statistical mechanics, the so-called *spherical model* of a ferromagnet (see section 3.2 for the precise definition) [Ber52, Lew52] has since a long time served for such purposes. In the classical formulation with ferromagnetic nearest-neighbour interactions, it undergoes a continuous phase transition at a critical temperature $T_c > 0$ for spatial dimensions $d > 2$ (d can be treated as a continuous parameter) and for $2 < d < 4$ dimensions, the critical exponents are distinct from those of mean-field theory. The standard formulation in terms of classical spins has the drawback that the third fundamental theorem of thermodynamics is not obeyed, since the specific heat $c_h = 1$ for a temperatures $T < T_c$ [Ber52]. This can be cured however, by adjoining to each spin variable s_n a canonically conjugate momentum p_n and adding a kinetic energy term, with a quantum coupling g, to the Hamiltonian H, thus arriving at the *quantum spherical model* [Obe72]. Then the specific heat c_h vanishes indeed as $T \to 0$, as it should be [Voj96, Oli06]. The model's properties near the critical temperature $T_c(g) > 0$ are the same as in the classical spherical model. However, at temperature $T = 0$, there is for $d > 1$ dimensions a quantum critical point, at some $g = g_c > 0$, which is in the same universality class as the classical model in $d + 1$ dimensions [Hen84b, Voj96, Oli06, Wal15]. The formulation of the spherical model contains the so-called 'spherical constraint'. The exact solution of the model reduces to establishing the constraint equation for the associated Lagrange multiplier which at equilibrium must be found from the solution of a transcendent equation. Turning to the dynamics, the kinetics of the classical spherical model can be described in terms of a Langevin equation, such that the spherical constraint reduces to a Volterra integral equation for the now time-dependent Lagrange multiplier [Ron78, God00]. Many aspects of the non-equilibrium dynamics of the model have been analysed in great detail, including extensions to the spherical spin glass and to the growth of interfaces [Ron78, Con94, Cug95, God00, Pic02, Dur17].

Here, we shall explore aspects of the non-equilibrium quantum dynamics of the quantum spherical model. In order to construct the Lindblad dissipators, we shall require that these are chosen such that (i) the correct quantum equilibrium state emerges as the stationary state of the dynamics and (ii) in the classical limit $g \to 0$, the correct classical Langevin dynamics should be recovered. As we shall see, this fixes the form of the Lindblad dissipators, up to the choice of an overall time scale. To do so, we recall in section 3.2 the definition of the quantum spherical model and the main properties of its equilibrium phase diagram. In section 3.3, the Lindblad dissipators will be constructed in two different ways. First, we shall follow the traditional route of system-plus-reservoir methods [Bre07, Sch14], and inspired by recent constructions of free bosonic quantum systems [Ga16, San16], we shall give an explicit description for the phonons which make up the reservoir. We also discuss how this construction must be amended to take the spherical constraint into account. In section 3.4, we derive the associated equations of motion for the observables. Independently of any specific model for the reservoir, we shall show how a comparison with the classical limit $g \to 0$ (whenever available) determines the form of the Lindblad dissipators. This also clarifies further the interpretation of the phonon reservoir model. The formal closed-form solution for spin- and momentum-correlators will be derived. The most difficult part of any spherical-model calculation is the solution of the spherical constraint, which becomes a highly non-trivial integro-differential equation. Since a full solution of this equation is very difficult, we shall focus on two special cases. First, in section 3.5, we analyse the semi-classical limit, which can be used to describe the leading quantum correction to the order-disorder phase transition at temperature $T = T_c(g)$. By construction, the Lindblad equation does preserve quantum coherence. Still, we find from the explicitly computed spin-spin correlator that to leading order in g, the dynamical critical behaviour, for temperatures $T > T_c(g)$, $T = T_c(g)$ or $T < T_c(g)$ is exactly the one of the classical dynamics, where quantum effects only manifest themselves through the appearance of a new effective temperature $T \mapsto T_{\text{eff}}(g)$. For quenches to $T \leq T_c(g)$, dynamical scaling hold with a dynamical exponent $z = 2$. Having thus confirmed the consistency of the Lindblad formalism applied to the quantum spherical model, we analyse in section 3.6 what happens for a quantum quench deeply into the ordered phase, through an exact analysis of the leading long-time and large-distance behaviour of the spin-spin and momentum-momentum correlators. It turns out that the leading long-time behaviour is independent of the dissipation rate γ. The dynamical exponent now is $z = 1$, but we do not find simple dynamical scaling. Rather, the exact
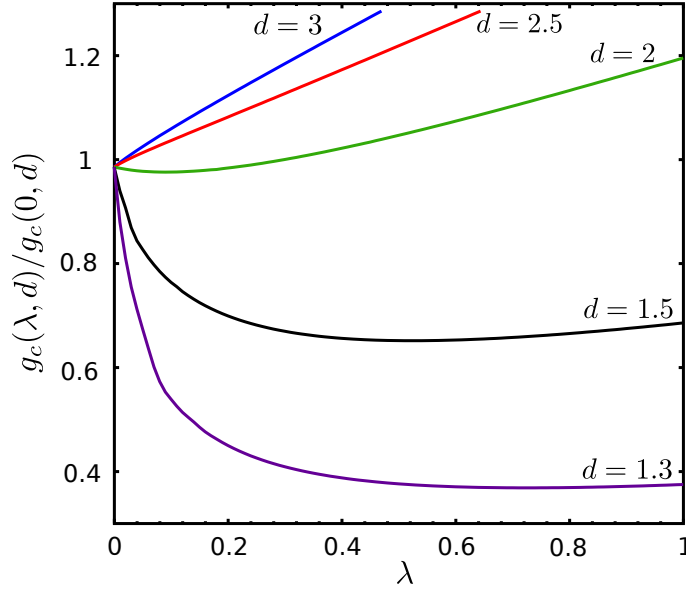
Figure 3.1: Equilibrium quantum phase diagram of the SAQSM at $T = 0$, for dimensions $d = [1.3, 1.5, 2, 2.5, 3]$, from bottom to top. We show for each dimension the critical line $g_c(\lambda)$ below which the system is a quantum ferromagnet. Above these lines order is destroyed by quantum fluctuations [Wal15].

scaling functions point towards the existence of several length scales, which differ by logarithmic factors. The technical details of the calculations are covered in several appendices.

3.2 Quantum spherical model: equilibrium

The **S**pin-**A**nisotropic **Q**uantum **S**pherical **M**odel (SAQSM) [Wal15] is defined by a set of 'spin operators' $s_{\boldsymbol{n}} = s_{\boldsymbol{n}}^{\dagger}$, attached to the sites $\boldsymbol{n}$ of a d-dimensional hyper-cubic lattice $\mathcal{L} \subset \mathbb{Z}^d$ with $\mathcal{N} = N^d$ sites. For each spin variable we define the corresponding conjugated momentum $p_{\boldsymbol{n}} = p_{\boldsymbol{n}}^{\dagger}$ [Obe72], which satisfies the canonical commutation relations

$$[s_{\boldsymbol{n}}, p_{\boldsymbol{m}}] = \mathrm{i}\,\delta_{\boldsymbol{n},\boldsymbol{m}} \tag{3.2.1}$$

Throughout, we shall use units such that $\hbar = 1$. For nearest-neighbour interactions, and with periodic boundary conditions, the Hamiltonian is

$$H = \sum_{\boldsymbol{n} \in \mathcal{L}} \left[\frac{g}{2} \left(p_{\boldsymbol{n}}^2 - \frac{1-\lambda}{2\mathcal{S}} \sum_{\langle \boldsymbol{n}, \boldsymbol{m} \rangle} p_{\boldsymbol{n}} p_{\boldsymbol{m}} \right) + \mathcal{S} \left(s_{\boldsymbol{n}}^2 - \frac{1+\lambda}{2\mathcal{S}} \sum_{\langle \boldsymbol{n}, \boldsymbol{m} \rangle} s_{\boldsymbol{n}} s_{\boldsymbol{m}} \right) \right] \tag{3.2.2}$$

where $\langle \boldsymbol{n}, \boldsymbol{m} \rangle$ are pairs of nearest-neighbour sites $\boldsymbol{m}$ and $\boldsymbol{n}$. The parameter λ describes the spin-anisotropy in the interactions (this can be seen explicitly by going over to bosonic degrees of freedom [Wal15]) and the usually studied quantum spherical model is the special case $\lambda = 1$. The parameter g is the quantum coupling, such that for $\lambda = 1$ and $g \to 0$, the spin operators become real numbers $s_{\boldsymbol{n}} \in \mathbb{R}$ and one recovers the classical spherical model [Ber52]. Finally, the *spherical parameter* $\mathcal{S}$ is a Lagrange multiplier, to be chosen self-consistently in order to satisfy the so-called mean *spherical constraint* [Lew52]

$$\sum_{\boldsymbol{n} \in \mathcal{L}} \langle s_{\boldsymbol{n}}^2 \rangle = \mathcal{N} \tag{3.2.3}$$

The quantum Hamiltonian is invariant under the duality transformation $\mathscr{D}$ given by

$$\lambda \leftrightarrow -\lambda \;\;,\;\; s_{\boldsymbol{n}} \leftrightarrow \sqrt{\frac{g}{2\mathcal{S}}}\, p_{\boldsymbol{n}} \tag{3.2.4}$$

We shall strive to find a Lindblad dissipator which will preserve this symmetry. The equilibrium phases at temperature $T = 0$, and the dimension-dependent transition lines $g_c(\lambda, d)$ are shown in fig 3.1. A re-entrant phase transition is seen for $1 < d \lesssim 2.065$ when λ is small enough, without a known counterpart in the fermionic analogues of the SAQSM [Wal15]. This illustrates the non-trivial nature of the ground state of H.

The Hamiltonian (3.2.2) is readily diagonalized. First, one goes over to to Fourier space. Define the (non-hermitian) operators $q_{\boldsymbol{k}} = q^\dagger_{-\boldsymbol{k}}$ and $\pi_{\boldsymbol{k}} = \pi^\dagger_{-\boldsymbol{k}}$, along with the inverse transformations

$$q_{\boldsymbol{k}} := \mathcal{N}^{-1/2} \sum_{n \in \mathcal{L}} s_{\boldsymbol{n}} \, \mathrm{e}^{-i\boldsymbol{n}\cdot\boldsymbol{k}} \quad , \quad \pi_{\boldsymbol{k}} := \mathcal{N}^{-1/2} \sum_{\boldsymbol{n} \in \mathcal{L}} p_{\boldsymbol{n}} \, \mathrm{e}^{i\boldsymbol{n}\cdot\boldsymbol{k}} \tag{3.2.5a}$$

$$s_{\boldsymbol{n}} = \mathcal{N}^{-1/2} \sum_{\boldsymbol{k} \in \mathcal{B}} q_{\boldsymbol{k}} \, \mathrm{e}^{i\boldsymbol{n}\cdot\boldsymbol{k}} \quad , \quad p_{\boldsymbol{n}} = \mathcal{N}^{-1/2} \sum_{\boldsymbol{k} \in \mathcal{B}} \pi_{\boldsymbol{k}} \, \mathrm{e}^{-i\boldsymbol{n}\cdot\boldsymbol{k}} \, . \tag{3.2.5b}$$

where the momentum $\boldsymbol{k}$ lies in the first *Brillouin zone* $\mathcal{B} := \{\boldsymbol{k} = (k_1 \ldots k_d) | k_i \in \{-\frac{\pi}{N} \ldots \frac{\pi}{N}\}$. These operators obey the canonical commutation relations

$$[q_{\boldsymbol{k}}, \pi_{\boldsymbol{k}'}] = i \, \delta_{\boldsymbol{k}, \boldsymbol{k}'} \tag{3.2.6}$$

and the transformation (3.2.5a) casts the Hamiltonian (3.2.2) into the form

$$H = \sum_{\boldsymbol{k} \in \mathcal{B}} \left[\frac{g}{2\mathcal{S}} \Lambda^2_{-;\boldsymbol{k}} \, \pi_{\boldsymbol{k}} \pi_{-\boldsymbol{k}} + \Lambda^2_{+;\boldsymbol{k}} \, q_{\boldsymbol{k}} q_{-\boldsymbol{k}} \right] \tag{3.2.7}$$

where

$$\Lambda_{\pm;\boldsymbol{k}} := \sqrt{\mathcal{S} + \frac{1 \pm \lambda}{4}(\omega_{\boldsymbol{k}} - 2d)} \qquad \text{with} \qquad \omega_{\boldsymbol{k}} := 2\sum_{j=1}^{d}(1 - \cos k_j) \tag{3.2.8}$$

In the same manner, the spherical constraint (3.2.3) is transformed as

$$\sum_{\boldsymbol{k} \in \mathcal{B}} \langle q_{\boldsymbol{k}} q_{-\boldsymbol{k}} \rangle = \mathcal{N} \, . \tag{3.2.9}$$

The Hamiltonian (3.2.7) is now diagonalised by introducing the *bosonic ladder operators*

$$q_k = \alpha_{\boldsymbol{k}} \frac{b_{\boldsymbol{k}} + b^\dagger_{-\boldsymbol{k}}}{\sqrt{2}} \qquad , \quad \pi_{\boldsymbol{k}} = \frac{i}{\alpha_{\boldsymbol{k}}} \frac{b^\dagger_{\boldsymbol{k}} - b_{-\boldsymbol{k}}}{\sqrt{2}}, \tag{3.2.10a}$$

$$b_{\boldsymbol{k}} = \frac{\alpha_{\boldsymbol{k}}}{\sqrt{2}} \left(\frac{q_{\boldsymbol{k}}}{\alpha^2_{\boldsymbol{k}}} + i\pi_{-\boldsymbol{k}} \right) \quad , \quad b^\dagger_{\boldsymbol{k}} = \frac{\alpha_{\boldsymbol{k}}}{\sqrt{2}} \left(\frac{q_{-\boldsymbol{k}}}{\alpha^2_{\boldsymbol{k}}} - i\pi_{\boldsymbol{k}} \right) \tag{3.2.10b}$$

where

$$\alpha_{\boldsymbol{k}} = \left(\frac{g}{2\mathcal{S}} \right)^{1/4} \sqrt{\frac{\Lambda_{-;\boldsymbol{k}}}{\Lambda_{+;\boldsymbol{k}}}} \tag{3.2.11}$$

The operators $b_{\boldsymbol{k}}$ and $b^\dagger_{\boldsymbol{k}}$ obey the usual Weyl-Heisenberg algebra $[b_{\boldsymbol{k}}, b^\dagger_{\boldsymbol{k}'}] = \delta_{\boldsymbol{k}, \boldsymbol{k}'}$. The Hamiltonian in eq (3.2.7) then becomes

$$H = \sum_{\boldsymbol{k} \in \mathcal{B}} E_{\boldsymbol{k}} \left(b^\dagger_{\boldsymbol{k}} b_{\boldsymbol{k}} + \frac{1}{2} \right) \quad , \quad E_{\boldsymbol{k}} = \sqrt{2\frac{g}{\mathcal{S}}} \, \Lambda_{+;\boldsymbol{k}} \Lambda_{-;\boldsymbol{k}} \, . \tag{3.2.12}$$

The isotropic case

For technical simplicity, we shall focus on the Lindblad equation in the isotropic case $\lambda = 1$. Then, eq (3.2.8) reduces to $\Lambda_{-;\boldsymbol{k}} = \sqrt{\mathcal{S}}$ and

$$\Lambda_{+;\boldsymbol{k}} =: \Lambda_{\boldsymbol{k}} = \sqrt{\mathcal{S} - d + \omega_{\boldsymbol{k}}/2} \tag{3.2.13}$$

The energy $E_{\boldsymbol{k}}$ in eq (3.2.12) and the parameter α_k in eq (3.2.11) simplify to

$$E_{\boldsymbol{k}} = \sqrt{2g} \cdot \Lambda_{\boldsymbol{k}} = \sqrt{g} \sqrt{2(\mathcal{S} - d) + \omega_{\boldsymbol{k}}} \quad , \quad \alpha_{\boldsymbol{k}} = \left(\frac{g}{2} \right)^{1/4} \frac{1}{\sqrt{\Lambda_{\boldsymbol{k}}}} \tag{3.2.14}$$

In the long-wavelength limit we may expand the cosines and write

$$E_k \simeq \sqrt{2g} \left[\sqrt{\mathcal{S} - d} + \frac{1}{2} \frac{k^2}{\sqrt{\mathcal{S} - d}} \right] \tag{3.2.15}$$

where $k^2 = k_1^2 + \ldots + k_d^2$. The last term in (3.2.15) represents a non-relativistic massive dispersion relation, whereas the first term represents a chemical potential term. Clearly, thermodynamic stability is realised if $\mathcal{S} \geq d$. Furthermore, the zero-momentum energy gaps vanish for $\mathcal{S} = d$. In complete analogy with the classical spherical model [Ber52], this last condition defines the critical point.

3.3   Construction of the Lindblad master equation

Now, we discuss how to describe the dynamics of the of the quantum spherical model in contact with a heat bath. We shall explicitly admit the Markov property in the dynamics and the *weak-coupling limit* of the coupling between the system and the bath. It is well-established that under these hypotheses, the most general description of the quantum dynamics of a system interacting with a reservoir is a non-unitary time-evolution of the reduced density matrix ρ, via the *Lindblad equation* [Bre07, Sch14]

$$\partial_t \rho = -\mathrm{i}\,[H, \rho] + \mathcal{D}(\rho) \tag{3.3.1}$$

Herein, the *dissipator* $\mathcal{D}(\rho)$ describes the relaxation towards equilibrium. In the case of a single harmonic oscillator, interacting with a thermal bath, made of a phonon or photon gas, at the fixed temperature T [Lin76, Bre07, Sch14]

$$\mathcal{D}(\rho) = \gamma(E) \left((\bar{n} + 1) \left[b\rho b^\dagger - \frac{1}{2}\{b^\dagger b, \rho\} \right] + \bar{n} \left[b^\dagger \rho b - \frac{1}{2}\{bb^\dagger, \rho\} \right] \right) \tag{3.3.2}$$

where E is the energy of the oscillator, b and $b^\dagger$ are the bosonic ladder operators of the system, $\{A, B\} = AB + BA$ is the anti-commutator, $\gamma(E)$ is the *damping parameter* which also depends substantially on the bath and

$$\bar{n} = \left(\mathrm{e}^{E/T} - 1 \right)^{-1} \tag{3.3.3}$$

is the Bose-Einstein occupation number at bath temperature T. This quantum master equation (3.3.1,3.3.2) preserves essential properties of the density matrix ρ, namely *trace*, *complete positivity* and *hermiticity* [Lin76]. In addition, the Schrödinger picture is used for the bosonic operators $b, b^\dagger$. Hence the commutator $[b, b^\dagger] = 1$ is time-independent and its conservation is an intrinsic property of the formalism [Car99].

For our many-body problem, further consistency requirements are necessary:

1. the quantum equilibrium state must be a stationary state of eqs (3.3.1,3.3.2),

2. this should imply that in the $g \to 0$ limit, the classical equilibrium state must be a stationary state,

3. the classical Langevin dynamics must follows in the limit $g \to 0$, for all times.

It turns out that these requirements can all be met, in an essentially unique way. The final Lindblad equation of the SAQSM will come out to read

$$\partial_t \rho = -\mathrm{i}[H, \rho] + \gamma_0 \sum_{k \in \mathcal{B}} \left[\left(\frac{1+\lambda}{2} \right)^2 \Lambda_{-;k}^2 + \left(\frac{1-\lambda}{2} \right)^2 \Lambda_{+;k}^2 \right] \frac{\Lambda_{+;k}^2 \Lambda_{-;k}^2}{\mathcal{S}^2} \times$$
$$\times \left[(\bar{n}_k + 1) \left(b_k \rho b_k^\dagger - \frac{1}{2}\{b_k^\dagger b_k, \rho\} \right) + \bar{n}_k \left(b_k^\dagger \rho b_k - \frac{1}{2}\{b_k b_k^\dagger, \rho\} \right) \right] \tag{3.3.4}$$

Herein, the only free parameter is the constant γ_0 which sets the time-scale. Clearly, the dissipator does depend on the spherical parameter $\mathcal{S}$. The derivation of (3.3.4) is made first for a free bosonic system, without taking the spherical constraint into account. At the end, through the spherical constraint which must hold at all times, $\mathcal{S} = \mathcal{S}(t)$ becomes time-dependent. This will turn out to make the solution of the spherical constraint considerably more complicated than at equilibrium (and also with respect to the classical dynamics).

Two different ways of deriving (3.3.4) will be presented:

(i) One may consider explicitly the system-reservoir coupling and go through the standard route, with the usual approximations [Bre07]. The bath properties are taken into account through the explicit time-dependent phonon (or photon) correlators. This gives a formal derivation of the Lindblad equation and will be carried out in the remainder of this section.

(ii) For the purpose of model-building, an alternative and more phenomenological approach might be useful. As we shall show in section 3.5, one may start from a generic form of the dissipator, essentially a sum of terms of the form (3.3.2) for each mode, and with yet unspecified damping constants $\gamma_{\boldsymbol{k}}$. We then derive quantum equations of motion for certain observables. Comparison of these equations of motion with the known classical $g \to 0$ limit (if available) then fixes the $\gamma_{\boldsymbol{k}}$.

At the end, both procedures lead to the same Lindblad equation (3.3.4).

3.3.1   General structure of the system-bath coupling

Now, largely following [Bre07], but with the few adaptations required for the quantum spherical model, we introduce the open-system dynamics.

For clarity, we begin treating just a single spin, say $s_{\boldsymbol{n}}$, coupled to the bath. The coupling of several spins is obtained at the end straightforwardly. As usual, the bath will be modelled by an infinite number of bosonic 'phonon' degrees of freedom, with the bath Hamiltonian

$$H_B = \sum_\ell \Omega_\ell \eta_\ell^\dagger \eta_\ell \tag{3.3.5}$$

with the bosonic operators η_ℓ and their corresponding frequencies Ω_ℓ. The system-bath interaction Hamiltonian is assumed to take the form

$$H_I = \sum_\ell f_\ell \, A_{\boldsymbol{n}} \otimes (\eta_\ell + \eta_\ell^\dagger) \tag{3.3.6}$$

where $f_\ell \in \mathbb{R}$ is a coupling constants and $A_{\boldsymbol{n}}$ is a hermitian system operator. There is a certain freedom in the choice of $A_{\boldsymbol{n}}$. Here, rather than a simplistic coupling to only the spin operator $s_{\boldsymbol{n}} = s_{\boldsymbol{n}}^\dagger$ or only to the momentum operator $p_{\boldsymbol{n}} = p_{\boldsymbol{n}}^\dagger$, we prefer a coupling which preserves the invariance under the duality transformation $\mathscr{D}$, see eq (3.2.4). The most general linear operator compatible with duality is

$$A_{\boldsymbol{n}} = \frac{1+\lambda}{2} \frac{s_{\boldsymbol{n}}}{\sqrt{g}} + \frac{1-\lambda}{2} \frac{p_{\boldsymbol{n}}}{\sqrt{2\mathcal{S}}} \; . \tag{3.3.7}$$

In the weak-coupling limit, the action of the bath is described approximately by a Lindblad equation for the reduced density matrix ρ of the system

$$\partial_t \rho = -\mathrm{i}[H, \rho] + \mathcal{D}_n(\rho) \tag{3.3.8}$$

where the first term describes the unitary evolution and $\mathcal{D}_n(\rho)$ is the Lindblad dissipator corresponding to the interaction (3.3.6). The expression for $\mathcal{D}_n(\rho)$ is most commonly derived using the method of eigenoperators [Bre07].

To make this presentation self-contained, we rapidly recall the main steps before applying it to the SAQSM. Consider a Hamiltonian H with energy levels ϵ and let $\mathscr{P}_\epsilon$ denote the corresponding projection operator onto the subspace of eigenvectors that have energy ϵ. Moreover, assume that the system-bath coupling may be described by an interaction Hamiltonian of the form $H_I = AB$,

where A and B are *hermitian* system and bath operators, respectively. Define the eigenoperator $A(\omega)$ corresponding to A via the relation

$$A(\omega) = \sum_{\epsilon,\epsilon'} \mathscr{P}_\epsilon A \mathscr{P}_{\epsilon'} \, \delta_{\epsilon'-\epsilon,\omega} \tag{3.3.9}$$

where the sum is over all distinct energies ϵ, ϵ' and $\delta_{a,b}$ is the Kronecker delta. It can be shown that

$$[H, A(\omega)] = -\omega A(\omega) \ , \ \ A^\dagger(\omega) = A(-\omega) \ . \tag{3.3.10}$$

The quantities ω represent all allowed energy differences that may be produced by the action of the operator A.

It follows that the Lindblad dissipator corresponding to the interaction $H_I = AB$ reads, in the Born-Markov and rotating wave approximations [Bre07]

$$\mathcal{D}(\rho) = \sum_\omega \Gamma(\omega) \left[A(\omega)\rho A^\dagger(\omega) - \frac{1}{2}\{A^\dagger(\omega)A(\omega), \rho\} \right] \tag{3.3.11}$$

where

$$\Gamma(\omega) = \int_{-\infty}^{\infty} \mathrm{d}t \ e^{i\omega t} \langle B(t)B(0) \rangle \tag{3.3.12}$$

is the Fourier transform of the bath correlation functions. This method therefore allows one to readily write down the dissipator corresponding to a given system-bath interaction. However, to do so we must compute the eigenoperator $A(\omega)$ from eq (3.3.9), which require the full eigenstructure of the Hamiltonian. It is also worth noting that this method also produces a Lamb-shift correction to the Hamiltonian. However, this correction is usually small and, for simplicity, will be neglected.

3.3.2 Evaluation of bath correlation functions

Returning now to our problem, the interaction Hamiltonian (3.3.6) has $A = A_{\boldsymbol{n}}$ and $B = \sum_\ell f_\ell(\eta_\ell + \eta_\ell^\dagger)$. One must compute eq (3.3.12) for this choice of B. If the bath is in thermal equilibrium at a fixed temperature T, one has

$$\langle B(t)B(0) \rangle = \sum_\ell f_\ell^2 \left(e^{-i\Omega_\ell t}[\bar{n}(\Omega_\ell) + 1] + e^{i\Omega_\ell t}\bar{n}(\Omega_\ell) \right) \tag{3.3.13}$$

with the Bose-Einstein distribution $\bar{n}$ defined in eq (3.3.3). Inserting this into eq (3.3.12) leads to

$$\Gamma(\omega) = 2\pi \sum_\ell f_\ell^2 \left(\delta_{\omega,\Omega_\ell}[\bar{n}(\Omega_\ell) + 1] + \delta_{\omega,-\Omega_\ell}\bar{n}(\Omega_\ell) \right) \tag{3.3.14}$$

If the bath frequencies Ω_ℓ vary continuously in the interval $[0,\infty)$, one may convert the sum to an integral, leading to

$$\Gamma(\omega) = \int_0^\infty \mathrm{d}\Omega \, \gamma(\Omega) \left(\delta_{\omega,\Omega}[\bar{n}(\Omega) + 1] + \delta_{\omega,-\Omega}\bar{n}(\Omega) \right) = \begin{cases} \gamma(\omega)[\bar{n}(\omega) + 1] & , \text{ if } \omega > 0 \\ \gamma(|\omega|)\bar{n}(|\omega|) & , \text{ if } \omega < 0 \end{cases} \tag{3.3.15}$$

with the associated *spectral density*

$$\gamma(\Omega) = 2\pi \sum_\ell f_\ell^2 \, \delta(\Omega - \Omega_\ell) \tag{3.3.16}$$

In order to have a definite prediction for the spectral density $\gamma(\omega)$, additional physical information about the distribution of bath frequencies is needed. In general, one expects that

$$\gamma(\Omega) \sim \Omega^\kappa \tag{3.3.17}$$

for some exponent κ. For definiteness, we shall consider the specific model where the bath bosons are phonons (assuming acoustic phonons for simplicity). Then the index ℓ is replaced by the

momentum $\boldsymbol{k}$ and the dispersion relation $\Omega_k = c|\boldsymbol{k}|$ where c is the sound velocity. Transforming the sum in eq (3.3.16) into an integral gives

$$\gamma(\Omega) \sim f(\Omega)^2 \Omega^2 \tag{3.3.18}$$

The coupling constants $f_{\boldsymbol{k}}$ are usually assumed to be proportional to the electric field (minimum coupling) [Bre07], which in turn is proportional to $\sqrt{\Omega_k}$. In the continuum limit $f \sim \sqrt{\Omega}$ such that finally

$$\gamma(\Omega) = \gamma_0 \Omega^3 \tag{3.3.19}$$

where the constant γ_0 describes the strength of the system-bath coupling. As we shall see in section 3.5, the choice $\kappa = 3$ indeed reproduces the correct classical dynamics in the $g \to 0$ limit, for all dimensions $d > 0$.

3.3.3   Calculation of the eigenoperators

To finish the construction of the dissipator (3.3.11) one must find the eigenoperators $A(\omega)$ corresponding to $A = A_{\boldsymbol{n}}$. First, use eqs (3.2.5b) and (3.2.10a) to write

$$A_{\boldsymbol{n}} = \frac{(g^{-3}/2\mathcal{S})^{\frac{1}{4}}}{\sqrt{2\mathcal{N}}} \sum_{\boldsymbol{k}\in\mathcal{B}} e^{\mathrm{i}\boldsymbol{n}\cdot\boldsymbol{k}} \left(c_{\boldsymbol{k}} b_{\boldsymbol{k}} + c_{\boldsymbol{k}}^* b_{-\boldsymbol{k}}^\dagger \right) \quad \text{with} \quad c_{\boldsymbol{k}} = \frac{1+\lambda}{2}\sqrt{\frac{\Lambda_{-;\boldsymbol{k}}}{\Lambda_{+;\boldsymbol{k}}}} + \mathrm{i}\frac{1-\lambda}{2}\sqrt{\frac{\Lambda_{+;\boldsymbol{k}}}{\Lambda_{-;\boldsymbol{k}}}} \tag{3.3.20}$$

Next we note that, due to the diagonal structure of H in eq (3.2.12), it follows that $[H, b_{\boldsymbol{k}}] = -E_{\boldsymbol{k}} b_{\boldsymbol{k}}$. Hence, comparison with eq (3.3.10) shows that $b_{\boldsymbol{k}}$ is an eigenoperator of H with allowed transition frequency $\omega = E_{\boldsymbol{k}}$. The same is true for $c_{\boldsymbol{k}} b_{\boldsymbol{k}}$ as well. The full eigenoperator therefore reads

$$A_{\boldsymbol{n}}(\omega) = \frac{(g^{-3}/2\mathcal{S})^{\frac{1}{4}}}{\sqrt{2\mathcal{N}}} \sum_{\boldsymbol{k}\in\mathcal{B}} e^{\mathrm{i}\boldsymbol{n}\cdot\boldsymbol{k}} \left(c_{\boldsymbol{k}} b_{\boldsymbol{k}} \delta_{E_{\boldsymbol{k}},\omega} + c_{\boldsymbol{k}}^* b_{-\boldsymbol{k}}^\dagger \delta_{E_{\boldsymbol{k}},-\omega} \right) \tag{3.3.21}$$

The dissipator (3.3.11) corresponding to $A_{\boldsymbol{n}}$ being coupled to the bath, will then be

$$\mathcal{D}_{\boldsymbol{n}}(\rho) = \sum_\omega \Gamma(\omega) \left[A_{\boldsymbol{n}}(\omega) \rho A_{\boldsymbol{n}}^\dagger(\omega) - \frac{1}{2} \{ A_{\boldsymbol{n}}^\dagger(\omega) A_{\boldsymbol{n}}(\omega), \rho \} \right] \tag{3.3.22}$$

This expression may be simplified further. To do that, it suffices to look only at the first term:

$$\sum_\omega \Gamma(\omega) A_{\boldsymbol{n}}(\omega) \rho A_{\boldsymbol{n}}^\dagger(\omega)$$

$$= \sum_{\omega,\boldsymbol{k},\boldsymbol{k}'} \frac{e^{\mathrm{i}\boldsymbol{n}\cdot(\boldsymbol{k}-\boldsymbol{k}')}}{2\,\mathcal{N}} \Gamma(\omega) \sqrt{\frac{g^{-3}}{2\mathcal{S}}} \left(c_{\boldsymbol{k}} b_{\boldsymbol{k}} \delta_{E_{\boldsymbol{k}},\omega} + c_{\boldsymbol{k}}^* b_{-\boldsymbol{k}}^\dagger \delta_{E_{\boldsymbol{k}},-\omega} \right) \rho \left(c_{\boldsymbol{k}'}^* b_{\boldsymbol{k}'}^\dagger \delta_{E_{\boldsymbol{k}'},\omega} + c_{\boldsymbol{k}'} b_{-\boldsymbol{k}'}^\dagger \delta_{E_{\boldsymbol{k}'},-\omega} \right)$$

Since $E_{\boldsymbol{k}} > 0$. see eq (3.2.12), the only terms which will survive the constraints imposed by the δ's are those with $E_{\boldsymbol{k}} = E_{\boldsymbol{k}'}$. Since the energies may be degenerate, this does not necessarily imply that $\boldsymbol{k} = \boldsymbol{k}'$. But if we carry out the sum over ω and use eq (3.3.15), we obtain

$$\sum_\omega \Gamma(\omega) A_{\boldsymbol{n}}(\omega) \rho A_{\boldsymbol{n}}^\dagger(\omega)$$

$$= \sqrt{\frac{g^{-3}}{8\mathcal{S}}} \sum_{\boldsymbol{k},\boldsymbol{k}'} \delta_{E_{\boldsymbol{k}},E_{\boldsymbol{k}'}} \frac{e^{\mathrm{i}\boldsymbol{n}\cdot(\boldsymbol{k}-\boldsymbol{k}')}}{\mathcal{N}} \gamma(E_{\boldsymbol{k}}) \left[c_{\boldsymbol{k}} c_{\boldsymbol{k}'}^* (\bar{n}_{\boldsymbol{k}}+1) b_{\boldsymbol{k}} \rho b_{\boldsymbol{k}'}^\dagger + c_{\boldsymbol{k}}^* c_{\boldsymbol{k}'} \bar{n}_{\boldsymbol{k}} b_{\boldsymbol{k}}^\dagger \rho b_{\boldsymbol{k}'} \right] .$$

The structure of the other terms in eq (3.3.22) will be similar. Finally, we define

$$\gamma_{\boldsymbol{k},\boldsymbol{k}'}^{(\boldsymbol{n})} = \sqrt{\frac{g^{-3}}{8\mathcal{S}}} \gamma(E_{\boldsymbol{k}}) \frac{e^{\mathrm{i}\boldsymbol{n}\cdot(\boldsymbol{k}-\boldsymbol{k}')}}{\mathcal{N}} c_{\boldsymbol{k}} c_{\boldsymbol{k}'}^* \tag{3.3.23}$$

The final single-site dissipator (3.3.22) reads

$$\mathcal{D}_{\boldsymbol{n}}(\rho) = \sum_{\boldsymbol{k},\boldsymbol{k}'} \delta_{E_{\boldsymbol{k}},E_{\boldsymbol{k}'}} \left((\bar{n}_{\boldsymbol{k}}+1)\gamma_{\boldsymbol{k},\boldsymbol{k}'}^{(\boldsymbol{n})} \left[b_{\boldsymbol{k}}\rho b_{\boldsymbol{k}'}^{\dagger} - \frac{1}{2}\{b_{\boldsymbol{k}'}^{\dagger}b_{\boldsymbol{k}},\rho\} \right] + \gamma_{\boldsymbol{k}',\boldsymbol{k}}^{(\boldsymbol{n})}\bar{n}_{\boldsymbol{k}} \left[b_{\boldsymbol{k}}^{\dagger}\rho b_{\boldsymbol{k}'} - \frac{1}{2}\{b_{\boldsymbol{k}'}b_{\boldsymbol{k}}^{\dagger},\rho\} \right] \right)$$
(3.3.24)

and describes the action of coupling a single degree of freedom to the heat bath. It couples to all normal modes $b_{\boldsymbol{k}}$. Furthermore, it is well-known that dissipators of this form will let evolve the system towards the correct thermal Gibbs state $\rho \sim e^{-H/T}$, although only a single spin was coupled to the bath [Bre07].

The information which site $\boldsymbol{n}$ is coupled to the bath is contained in the factor $\gamma_{\boldsymbol{k},\boldsymbol{k}'}^{(\boldsymbol{n})}$.

3.3.4 Effect of coupling the entire system to the bath

We now extend this to the case where all spins are coupled to the bath. In this case, for each degree of freedom, at site $\boldsymbol{n}$, we shall have a dissipator $\mathcal{D}_{\boldsymbol{n}}(\rho)$ appearing in eq (3.3.8). But if we look at eq (3.3.24) we see that n only appears in the quantities $\gamma_{\boldsymbol{k},\boldsymbol{k}'}^{(\boldsymbol{n})}$. Thus if we sum all dissipators $\mathcal{D}_n(\rho)$ we will get a result with a structure identical to eq (3.3.24), but with $\gamma_{\boldsymbol{k},\boldsymbol{k}'}^{(\boldsymbol{n})}$ replaced by

$$\sum_{\boldsymbol{n}} \gamma_{\boldsymbol{k},\boldsymbol{k}'}^{(\boldsymbol{n})} = \sqrt{\frac{g^{-3}}{8\mathcal{S}}}\gamma(E_{\boldsymbol{k}})|c_{\boldsymbol{k}}|^2\delta_{\boldsymbol{k},\boldsymbol{k}'} =: \delta_{\boldsymbol{k},\boldsymbol{k}'}\,\gamma_{\boldsymbol{k}}$$
(3.3.25)

where, using also eq (3.3.19), we find

$$\gamma_{\boldsymbol{k}} = \gamma_0 \left[\left(\frac{1+\lambda}{2}\right)^2 \Lambda_{-;\boldsymbol{k}}^2 + \left(\frac{1-\lambda}{2}\right)^2 \Lambda_{+;\boldsymbol{k}}^2 \right] \frac{\Lambda_{+;\boldsymbol{k}}^2\Lambda_{-;\boldsymbol{k}}^2}{\mathcal{S}^2}$$
(3.3.26)

Specific calculations will only be carried out for the isotropic case $\lambda = 1$. Then (3.3.26) simplifies to

$$\gamma_{\boldsymbol{k}} = \gamma_0\Lambda_{\boldsymbol{k}}^2$$
(3.3.27a)

see also eq (3.2.13). The final dissipator, after having summed over $\boldsymbol{n}$, reads

$$\mathcal{D}(\rho) = \sum_{\boldsymbol{k}\in\mathcal{B}} \gamma_{\boldsymbol{k}} \left((\bar{n}_{\boldsymbol{k}}+1)\left[b_{\boldsymbol{k}}\rho b_{\boldsymbol{k}}^{\dagger} - \frac{1}{2}\{b_{\boldsymbol{k}}^{\dagger}b_{\boldsymbol{k}},\rho\} \right] + \bar{n}_{\boldsymbol{k}}\left[b_{\boldsymbol{k}}^{\dagger}\rho b_{\boldsymbol{k}} - \frac{1}{2}\{b_{\boldsymbol{k}}b_{\boldsymbol{k}}^{\dagger},\rho\} \right] \right)$$
(3.3.27b)

This is our final result (3.3.4) for the microscopic derivation of the Lindblad dissipator.

Recall that this dissipator satisfies detailed balance, as shown in [Bre07]. Therefore, *modulo* an ergodicity assumption, the Lindblad equation (3.3.4) will thermalise the system, irrespective of the initial condition, to the unique steady-state with reduced density matrix $\rho \sim e^{-H/T}$.

This entire discussion did not take into account the spherical constraint (3.2.9). If one uses it in an *ad hoc* fashion, one would consider $\mathcal{S} = \mathcal{S}(t)$ as time-dependent. Then either the couplings to the bath or the bath properties themselves, described by $\gamma_{\boldsymbol{k}}$, $\bar{n}_{\boldsymbol{k}}$ and the operators $b_{\boldsymbol{k}}$ must be considered time-dependent. Pragmatically, one considers an effectively time-dependent dissipator $\mathcal{D}_t$ which will always have as its target state the instantaneous Hamiltonian $H = H(t)$ of the system, such that formally $\mathcal{D}_t(e^{-\beta H(t)}) = 0$. Physically, that means that the time-dependent changes in H should be slow enough, which in turn should be the case if the changes in $\mathcal{S}(t)$ should be more slow than the typical bath correlation times. Since the eventual applications we are interested in concern the slow power-law relaxations after a quantum quench into the two-phase coexistence regime with formally infinite relaxation times, we expect that these kinds of physical requirements should be satisfied.

More systematically, one should not have imposed a spherical constraint, but rather have considered a second bath in order to implement it, at least on average. Since we expect that for sufficiently long times, the effective equations of motion should become the same as those we are going to study in the next section, we have not carried out this explicitly. At the present time, we consider it more urgent to arrive at some understanding of the qualitative consequences of the equations of motion on the long-time behaviour of the non-equilibrium correlators.

3.4 Dynamical equations for observables

In this section, we shall examine the dynamical equations governing the evolution of certain important observables under the influence of the heat bath. For any observable $\mathcal{O}$, the time-dependent average $\langle \mathcal{O} \rangle = \langle \mathcal{O} \rangle (t)$ is found from

$$\frac{\mathrm{d}}{\mathrm{d}t} \langle \mathcal{O} \rangle = \mathrm{tr}\, \mathcal{O}\, \partial_t \rho + \mathrm{tr}\, \rho\, \partial_t \mathcal{O} \tag{3.4.1}$$

In principle, all quantities $\alpha_{\boldsymbol{k}}$, $E_{\boldsymbol{k}}$, $\gamma_{\boldsymbol{k}}$ and $\bar{n}_{\boldsymbol{k}}$ should be considered as being time-dependent, if the spherical constraint is taken into account. These explicit time-dependencies come from the second term on the right-hand-side in (3.4.1). For the sake of simplicity of the presentation, we shall discard it for the moment but shall re-introduce it later.

Therefore, for any observable $\mathcal{O}$ not depending explicitly on time, hence $\partial_t \mathcal{O} = 0$, inserting the Lindblad equation (3.3.8) into (3.4.1) gives

$$\frac{\mathrm{d}}{\mathrm{d}t} \langle \mathcal{O} \rangle = -\mathrm{i}\langle [\mathcal{O}, H] \rangle + \langle \bar{\mathcal{D}}(\mathcal{O}) \rangle \tag{3.4.2}$$

with the adjoint dissipator

$$\bar{\mathcal{D}}(\mathcal{O}) = \sum_{\boldsymbol{k} \in \mathcal{B}} \gamma_{\boldsymbol{k}} \left((\bar{n}_{\boldsymbol{k}} + 1)\left[b_{\boldsymbol{k}}^\dagger \mathcal{O} b_{\boldsymbol{k}} - \frac{1}{2}\{ b_{\boldsymbol{k}}^\dagger b_{\boldsymbol{k}}, \mathcal{O} \} \right] + \bar{n}_{\boldsymbol{k}}\left[b_{\boldsymbol{k}} \mathcal{O} b_{\boldsymbol{k}}^\dagger - \frac{1}{2}\{ b_{\boldsymbol{k}} b_{\boldsymbol{k}}^\dagger, \mathcal{O} \} \right] \right) \tag{3.4.3}$$

Although the form of the $\gamma_{\boldsymbol{k}}$ was discussed in the previous section, we shall keep them here in a generic form. This will allow an alternative derivation of the Lindblad equation (3.3.4).

In order to understand how this adjoint dissipator arises, consider the second term as an example, namely $\mathcal{D}_2(\rho) = \gamma \bar{n} \left(b^\dagger \rho b - \frac{1}{2}\{ b^\dagger b, \rho \} \right)$, for a single mode. Then

$$\mathrm{tr}\, \mathcal{O} \mathcal{D}_2 = \gamma \bar{n}\, \mathrm{tr}\left(\mathcal{O} b^\dagger \rho b - \frac{1}{2} \mathcal{O} b^\dagger b \rho - \frac{1}{2} \mathcal{O} \rho b^\dagger b \right)$$

$$= \gamma \bar{n}\, \mathrm{tr}\, \rho \left(b \mathcal{O} b^\dagger - \frac{1}{2} \mathcal{O} b^\dagger b - \frac{1}{2} b^\dagger b \mathcal{O} \right) = \gamma \bar{n} \left\langle b \mathcal{O} b^\dagger - \frac{1}{2} \mathcal{O} b^\dagger b - \frac{1}{2} b^\dagger b \mathcal{O} \right\rangle$$

which produces the second term in (3.4.3). The first term is obtained similarly.

For the single-particle observables $\mathcal{O} \in \{ b_{\boldsymbol{k}}, b_{\boldsymbol{k}}^\dagger, q_{\boldsymbol{k}}, \pi_{\boldsymbol{k}} \}$, we find from (3.4.1, 3.4.2, 3.4.3)

$$\frac{\mathrm{d}}{\mathrm{d}t} \langle b_{\boldsymbol{k}} \rangle = -\left(\frac{\gamma_{\boldsymbol{k}}}{2} + \mathrm{i}E_{\boldsymbol{k}} \right) \langle b_{\boldsymbol{k}} \rangle + \langle \partial_t b_{\boldsymbol{k}} \rangle \quad , \quad \frac{\mathrm{d}}{\mathrm{d}t} \langle b_{\boldsymbol{k}}^\dagger \rangle = -\left(\frac{\gamma_{\boldsymbol{k}}}{2} - \mathrm{i}E_{\boldsymbol{k}} \right) \langle b_{\boldsymbol{k}}^\dagger \rangle + \langle \partial_t b_{\boldsymbol{k}}^\dagger \rangle \tag{3.4.4a}$$

$$\frac{\mathrm{d}}{\mathrm{d}t} \langle q_{\boldsymbol{k}} \rangle = -\frac{\gamma_{\boldsymbol{k}}}{2} \langle q_{\boldsymbol{k}} \rangle + \frac{g}{\mathcal{S}} \Lambda_{-;\boldsymbol{k}}^2 \langle \pi_{-\boldsymbol{k}} \rangle \quad , \quad \frac{\mathrm{d}}{\mathrm{d}t} \langle \pi_{-\boldsymbol{k}} \rangle = -\frac{\gamma_{\boldsymbol{k}}}{2} \langle \pi_{-\boldsymbol{k}} \rangle - 2\Lambda_{+;\boldsymbol{k}}^2 \langle q_{\boldsymbol{k}} \rangle \tag{3.4.4b}$$

where we also used the fact that $E_{\boldsymbol{k}}$, $\alpha_{\boldsymbol{k}}$ and $\gamma_{\boldsymbol{k}}$ are all even in $\boldsymbol{k}$. In particular, the time-dependent magnetization is expressed as

$$M = \sum_{\boldsymbol{n} \in \mathcal{L}} \langle s_{\boldsymbol{n}} \rangle = \sqrt{\mathcal{N}}\, \langle q_{\boldsymbol{0}} \rangle \tag{3.4.5}$$

where use was made of the orthogonality of the Fourier series.

Next we turn to two-body correlators. We find, again using eqs (3.4.1, 3.4.2, 3.4.3),

$$\frac{\mathrm{d}}{\mathrm{d}t} \langle b_{\boldsymbol{k}}^\dagger b_{\boldsymbol{k}'} \rangle = \langle \partial_t b_{\boldsymbol{k}}^\dagger b_{\boldsymbol{k}'} \rangle + \left[\mathrm{i}(E_{\boldsymbol{k}} - E_{\boldsymbol{k}'}) - \frac{\gamma_{\boldsymbol{k}} + \gamma_{\boldsymbol{k}'}}{2} \right] \langle b_{\boldsymbol{k}}^\dagger b_{\boldsymbol{k}'} \rangle + \gamma_{\boldsymbol{k}} \bar{n}_{\boldsymbol{k}} \delta_{\boldsymbol{k}, \boldsymbol{k}'} \tag{3.4.6a}$$

$$\frac{\mathrm{d}}{\mathrm{d}t} \langle b_{\boldsymbol{k}} b_{\boldsymbol{k}'} \rangle = \langle \partial_t b_{\boldsymbol{k}} b_{\boldsymbol{k}'} \rangle + \left[-\mathrm{i}(E_{\boldsymbol{k}} + E_{\boldsymbol{k}'}) - \frac{\gamma_{\boldsymbol{k}} + \gamma_{\boldsymbol{k}'}}{2} \right] \langle b_{\boldsymbol{k}} b_{\boldsymbol{k}'} \rangle \tag{3.4.6b}$$

From these equations we may also compute dynamical equations for the two-point correlators

$$Q_{\boldsymbol{k}}(t) = \langle q_{\boldsymbol{k}} q_{-\boldsymbol{k}} \rangle \;\; , \;\; \Pi_{\boldsymbol{k}}(t) = \langle \pi_{\boldsymbol{k}} \pi_{-\boldsymbol{k}} \rangle \;\; , \;\; \Xi_{\boldsymbol{k}}(t) = \frac{1}{2} \langle q_{\boldsymbol{k}} \pi_{\boldsymbol{k}} + \pi_{-\boldsymbol{k}} q_{-\boldsymbol{k}} \rangle \tag{3.4.7}$$

The spherical constraint (3.2.9) then becomes in the $\mathcal{N} \to \infty$ limit

$$\sum_{\boldsymbol{k} \in \mathcal{B}} Q_{\boldsymbol{k}}(t) = \mathcal{N} \ \Leftrightarrow \ \int_{\mathcal{B}} \frac{\mathrm{d}\boldsymbol{k}}{(2\pi)^d} Q_{\boldsymbol{k}}(t) = 1 \tag{3.4.8}$$

and we find the eqs of motion for the two-point correlators

$$\frac{\mathrm{d}Q_{\boldsymbol{k}}}{\mathrm{d}t} = -\gamma_{\boldsymbol{k}} \left[Q_{\boldsymbol{k}}(t) - \frac{1}{4} \sqrt{\frac{2g}{\mathcal{S}}} \frac{\Lambda_{-;\boldsymbol{k}}}{\Lambda_{+;\boldsymbol{k}}} (2\bar{n}_{\boldsymbol{k}} + 1) \right] + 2\frac{g}{\mathcal{S}} \Lambda^2_{-;\boldsymbol{k}} \Xi_{\boldsymbol{k}}(t) \tag{3.4.9a}$$

$$\frac{\mathrm{d}\Xi_{\boldsymbol{k}}}{\mathrm{d}t} = -\gamma_{\boldsymbol{k}} \cdot \Xi_{\boldsymbol{k}}(t) + \frac{g}{\mathcal{S}} \Lambda^2_{-;\boldsymbol{k}} \cdot \Pi_{\boldsymbol{k}}(t) - 2\Lambda^2_{+;\boldsymbol{k}} \cdot Q_{\boldsymbol{k}}(t) \tag{3.4.9b}$$

$$\frac{\mathrm{d}\Pi_{\boldsymbol{k}}}{\mathrm{d}t} = -\gamma_{\boldsymbol{k}} \left[\Pi_{\boldsymbol{k}}(t) - \sqrt{\frac{\mathcal{S}}{2g}} \frac{\Lambda_{+;\boldsymbol{k}}}{\Lambda_{-;\boldsymbol{k}}} (2\bar{n}_{\boldsymbol{k}} + 1) \right] - 4\Lambda^2_{+;\boldsymbol{k}} \cdot \Xi_{\boldsymbol{k}}(t) \tag{3.4.9c}$$

At this point we would like to stress again that the canonical commutation relation $[q_{\boldsymbol{k}}, \pi_{\boldsymbol{k}'}] = \mathrm{i}\delta_{k,k'}$ is preserved due to the fact that $q_{\boldsymbol{k}}$ and $\pi_{\boldsymbol{k}'}$ are Schrödinger operators. In particular this is connected to the trace preserving property of the dynamics as

$$\partial_t \langle [q_{\boldsymbol{k}}, \pi_{\boldsymbol{k}'}] \rangle = \mathrm{tr}\left([q_{\boldsymbol{k}}, \pi_{\boldsymbol{k}'}] \dot{\rho} \right) = \mathrm{i}\delta_{k,k'} \partial_t \mathrm{tr}\, \rho = 0 \ . \tag{3.4.10}$$

Along with this, the commutation relation between the bosonic ladder operators is preserved since they present the same underlying algebra as

$$\left[b_{\boldsymbol{k}}, b^{\dagger}_{\boldsymbol{k}'} \right] = -\frac{\mathrm{i}}{2} \left(\frac{\alpha_{k'}}{\alpha_k} [q_{\boldsymbol{k}}, \pi_{\boldsymbol{k}'}] - \frac{\alpha_k}{\alpha_{k'}} [\pi_{-\boldsymbol{k}'}, q_{-\boldsymbol{k}}] \right) = \delta_{k,k'} \ . \tag{3.4.11}$$

Having completed these formal calculations, we must now take the spherical constraint (3.2.9, 3.4.8) into account. From (3.4.9a), this becomes an integro-differential equation for the time-dependent spherical parameter $\mathcal{S} = \mathcal{S}(t)$. It follows that the parameter $\alpha_{\boldsymbol{k}} = \alpha_{\boldsymbol{k}}(t)$, defined in (3.2.11), becomes time-dependent as well. It describes the transformation (3.2.10a) between the bosonic operators $b_{\boldsymbol{k}}, b^{\dagger}_{\boldsymbol{k}}$ and the spins $q_{\boldsymbol{k}}$ and momenta $\pi_{\boldsymbol{k}}$. Therefore, one must decide whether either the pair $(b_{\boldsymbol{k}}, b^{\dagger}_{\boldsymbol{k}})$ or else the pair $(q_{\boldsymbol{k}}, \pi_{\boldsymbol{k}})$ is taken to be time-independent, and hence is described by the Schrödinger picture.

We choose $(q_{\boldsymbol{k}}, \pi_{\boldsymbol{k}})$ as time-independent operators. The Lindblad formalism then implies the time-independent commutator (3.2.6). Furthermore, the equations of motion eqs (3.4.4b) and (3.4.9) remain valid. They will form the basis for our analysis of the dynamics of the quantum spherical model.

In consequence, in eqs (3.4.4a) and (3.4.6) the contributions coming from the second term in (3.4.1) must be worked out. For example, the first equation of motion in (3.4.4a) now becomes, where the dot indicates the time derivative

$$\frac{\mathrm{d}}{\mathrm{d}t} \langle b_{\boldsymbol{k}} \rangle = -\left(\frac{\gamma_{\boldsymbol{k}}}{2} + \mathrm{i}E_{\boldsymbol{k}} \right) \langle b_{\boldsymbol{k}} \rangle - \frac{\dot{\alpha}_{\boldsymbol{k}}}{\alpha_{\boldsymbol{k}}} \langle b^{\dagger}_{-\boldsymbol{k}} \rangle \tag{3.4.12}$$

The other equations can be generalised similarly, but we shall not require them in this work.

Before we analyse the dynamics produced by equations (3.4.9), we shall first consider their steady-state properties.

3.4.1 Stationary solution and equilibrium properties

The correlators in eqs (3.4.9) will relax to their stationary values, namely $\Xi_{\boldsymbol{k}}(\infty) = 0$ and

$$Q_{\boldsymbol{k}}(\infty) = \frac{1}{4} \sqrt{\frac{2g}{\mathcal{S}}} \frac{\Lambda_{-;\boldsymbol{k}}}{\Lambda_{+;\boldsymbol{k}}} (2\bar{n}_{\boldsymbol{k}} + 1), \qquad \Pi_{\boldsymbol{k}}(\infty) = \sqrt{\frac{\mathcal{S}}{2g}} \frac{\Lambda_{+;\boldsymbol{k}}}{\Lambda_{-;\boldsymbol{k}}} (2\bar{n}_{\boldsymbol{k}} + 1) \tag{3.4.13}$$
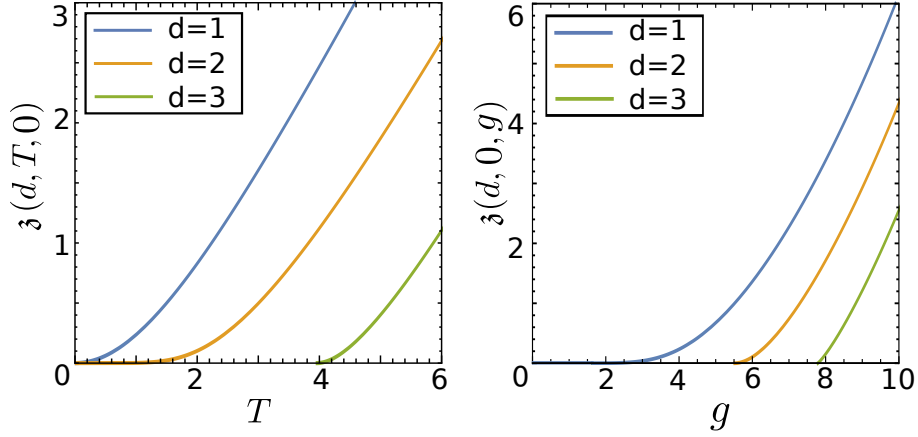
Figure 3.2: Spherical parameter $\mathfrak{z} = \mathfrak{z}(d, T, g)$ as a function of d, the temperature T and the coupling g. <u>Left panel</u>: classical limit $g = 0$. <u>Right panel</u>: quantum transition at $T = 0$.

These are precisely the equilibrium values expected from the SAQSM [Wal15]. To see that more clearly, we substitute these results into the spherical constraint (3.2.9) and find

$$1 = \sqrt{\frac{g}{8\mathcal{S}}} \frac{1}{\mathcal{N}} \sum_{\boldsymbol{k} \in \mathcal{B}} \frac{\Lambda_{-;\boldsymbol{k}}}{\Lambda_{+;\boldsymbol{k}}} (2\bar{n}_{\boldsymbol{k}} + 1) \overset{\mathcal{N} \nearrow \infty}{\longrightarrow} \sqrt{\frac{g}{8\mathcal{S}}} \int_{\mathcal{B}} \frac{\mathrm{d}\boldsymbol{k}}{(2\pi)^d} \frac{\Lambda_{-;\boldsymbol{k}}}{\Lambda_{+;\boldsymbol{k}}} \coth(E_{\boldsymbol{k}}/2T) \tag{3.4.14}$$

This is indeed the spin-anisotropic spherical constraint at equilibrium. The derivation, through a canonical transformation is given in appendix 3.A. In view of the re-entrant phase diagram for a non-isotropic interaction with $\lambda \neq 1$, this is a non-trivial check of the formalism.

We have therefore confirmed that the equilibrium state of the SAQSM is a stationary solution of the Lindblad equation. Details on the form of the $\gamma_{\boldsymbol{k}}$ are not required to verify this.

In the isotropic case $\lambda = 1$, it is useful to let $\mathfrak{z} := 2(\mathcal{S} - d)$. Then (3.4.14) reduces to the familiar form [Oli06]

$$\frac{\sqrt{g}}{2} \int_{\mathcal{B}} \frac{\mathrm{d}\boldsymbol{k}}{(2\pi)^d} \frac{1}{\sqrt{\mathfrak{z} + \omega_{\boldsymbol{k}}}} \coth\left(\frac{\sqrt{g}}{2T} \sqrt{\mathfrak{z} + \omega_{\boldsymbol{k}}}\right) = 1 . \tag{3.4.15}$$

In the following sections, we shall mainly concentrate on either the semi-classical limit $g \to 0$ or else on the the zero-temperature equilibrium limit $T = 0$. In these limit cases, the spherical constraint reduces to

$$\begin{cases} 1 - \frac{g}{12T} \simeq T \int_{\mathcal{B}} \frac{\mathrm{d}\boldsymbol{k}}{(2\pi)^d} \left[\frac{1}{\mathfrak{z} + \omega_{\boldsymbol{k}}} + \mathrm{O}\left(g^2\right) \right] & \text{, for } g \to 0 \\[2ex] 1 = \sqrt{\frac{g}{4}} \int_{\mathcal{B}} \frac{\mathrm{d}\boldsymbol{k}}{(2\pi)^d} \frac{1}{\sqrt{\mathfrak{z} + \omega_{\boldsymbol{k}}}} & \text{, for } T = 0 \end{cases} \tag{3.4.16}$$

The upper case in (3.4.16) reduces to the familiar classical form of the equilibrium spherical constraint [Ber52, Lew52], where the temperature $T \mapsto T_{\text{eff}}(g) = T/(1 - \frac{g}{12T})$ is replaced by an effective temperature. This also shows that in the $g \to 0$ limit, one recovers the classical equilibrium state. The lower case in (3.4.16) is the spherical constraint for the quantum phase transition at $T = 0$ [Hen84b, Voj96, Oli06]. For illustration, in fig 3.2 we show the Lagrange multiplier $\mathfrak{z} = \mathfrak{z}(d, T, g)$. In the classical limit $g = 0$ (left panel), the critical value $\mathfrak{z} = 0$ is reached for $d \leq 2$ only for a vanishing temperature $T = 0$ and there is no phase transition. On the other hand, for $d > 2$, the line $\mathfrak{z} = 0$ is already reached for a finite value $T = T_c(d) > 0$ which defines the critical temperature. A qualitatively analogous behaviour is seen for the quantum phase transition at $T = 0$ (right panel of fig 3.2). While for $d = 1$, the critical line $\mathfrak{z} = 0$ is only reached for $g = 0$, for any dimension $d > 1$ one finds a finite critical value $g_c(d) > 0$. A more detailed comparison reveals that the classical transition in $d + 1$ dimensions, at $g = 0$ and $T_c > 0$ and the quantum transition in d dimensions at $T = 0$ and $g_c(d) > 0$, are in the same equilibrium universality class [Hen84b, Voj96, Oli06, Wal15].

3.4.2 Formal solution of the non-equilibrium problem

To complete the microscopic derivation of the Lindblad dissipator, we now give a phenomenological discussion of how to chose the dissipator in a physically motivated fashion in order to include the correct classical many-body dynamics. To do so, we begin by writing down the formal solution of eqs (3.4.9a)-(3.4.9c). This system can be re-written in a matrix form

$$\frac{\mathrm{d}}{\mathrm{d}t} \begin{pmatrix} Q_{\boldsymbol{k}}(t) \\ \Xi_{\boldsymbol{k}}(t) \\ \Pi_{\boldsymbol{k}}(t) \end{pmatrix} = -m_{\boldsymbol{k}}^{\lambda}(t) \begin{pmatrix} Q_{\boldsymbol{k}}(t) \\ \Xi_{\boldsymbol{k}}(t) \\ \Pi_{\boldsymbol{k}}(t) \end{pmatrix} + \boldsymbol{u}_{\boldsymbol{k}}^{\lambda}(t) \tag{3.4.17}$$

with the matrices

$$m_{\boldsymbol{k}}^{\lambda}(t) = \begin{pmatrix} \gamma_{\boldsymbol{k}}(t) & -2\frac{g}{\mathcal{S}}\Lambda_{-;\boldsymbol{k}}^{2} & 0 \\ 2\Lambda_{+;\boldsymbol{k}}^{2} & \gamma_{\boldsymbol{k}}(t) & -\frac{g}{\mathcal{S}}\Lambda_{-;\boldsymbol{k}}^{2} \\ 0 & 4\Lambda_{+;\boldsymbol{k}}^{2} & \gamma_{\boldsymbol{k}}(t) \end{pmatrix} \; , \; \boldsymbol{u}_{\boldsymbol{k}}^{\lambda} = \gamma_{\boldsymbol{k}}(t)(2\bar{n}_{\boldsymbol{k}}+1)\begin{pmatrix} -\sqrt{\frac{g}{8\mathcal{S}}}\frac{\Lambda_{-;\boldsymbol{k}}}{\Lambda_{+;\boldsymbol{k}}} \\ 0 \\ \sqrt{\frac{\mathcal{S}}{2g}}\frac{\Lambda_{+;\boldsymbol{k}}}{\Lambda_{-;\boldsymbol{k}}} \end{pmatrix} \; . \tag{3.4.18}$$

Here we suppressed the explicit time-dependence of the spherical parameter $\mathcal{S} = \mathcal{S}(t)$ of $\Lambda_{\pm;\boldsymbol{k}} = \Lambda_{\pm;\boldsymbol{k}}(t)$ for readability of the equation. Some more comments are in order:

- For a phenomenological discussion the damping rates $\gamma_{\boldsymbol{k}}$ were left unspecified. Since spin-anisotropy is a quantum-mechanical effect, this discussion must be carried out in the isotropic case $\lambda = 1$. Only at the end, we shall compare with the dissipator (3.3.27) derived form microscopic consideration in section 3.3.

- The time-dependence of the spherical parameter $\mathcal{S}(t)$ is to be found self-consistently from the formal solution and the spherical constraint $\sum_{\boldsymbol{k} \in \mathcal{B}} Q_{\boldsymbol{k}}(t) = \mathcal{N}$.

- Already the isotropic case $\lambda = 1$ turns out to be considerably more difficult than the classical non-equilibrium dynamics, so that we leave the non-isotropic case $\lambda \neq 1$ for future work.

Concentrating from now on on the isotropic case $\lambda = 1$, we can simplify the matrices (3.4.18) by using the relations (3.2.13, 3.3.27a) and find

$$m_{\boldsymbol{k}}(t) = \begin{pmatrix} \gamma_{\boldsymbol{k}}(t) & -2g & 0 \\ 2\Lambda_{\boldsymbol{k}}^{2} & \gamma_{\boldsymbol{k}}(t) & -g \\ 0 & 4\Lambda_{\boldsymbol{k}}^{2} & \gamma_{\boldsymbol{k}}(t) \end{pmatrix} \; , \; \boldsymbol{u}_{\boldsymbol{k}}^{\lambda} = \gamma_{\boldsymbol{k}}(t)(2\bar{n}_{\boldsymbol{k}}+1)\begin{pmatrix} \frac{1}{4}\frac{\sqrt{2g}}{\Lambda_{\boldsymbol{k}}} \\ 0 \\ \frac{\Lambda_{\boldsymbol{k}}}{\sqrt{2g}} \end{pmatrix} \; . \tag{3.4.19}$$

Choice of the damping parameters

For $\lambda = 1$, a well-defined classical limit $g \to 0$ exists. Then, the equation of motion for the spin correlator $Q_{\boldsymbol{k}}$ decouples and leads to (recall $\mathfrak{z} = 2(\mathcal{S} - d)$)

$$\frac{\mathrm{d}}{\mathrm{d}t}Q_{\boldsymbol{k}}(t) = -\gamma_{\boldsymbol{k}}(t)Q_{\boldsymbol{k}}(t) + \gamma_{\boldsymbol{k}}(t)\frac{T}{\mathfrak{z}(t) + \omega_{\boldsymbol{k}}} \; . \tag{3.4.20a}$$

We stress that this equation of motion is qualitatively different from the classical Kramers equation (see [Wal16] for more details) since thermal fluctuations occur not just in the equation of motion of the momenta but already in the equation for the spins. The second term of the r.h.s. of eq (3.4.20a) comes from the assumed Lindblad dissipator and generates a coherent quantum dynamics. For an initial state at infinite temperature $Q_{\boldsymbol{k}}(0) = 1$. Then the formal solution of (3.4.20a) reads

$$Q_{\boldsymbol{k}}(t) = \mathrm{e}^{-\int_0^t \mathrm{d}\tau\, \gamma_{\boldsymbol{k}}(\tau)}\left(1 + T\int_0^t \mathrm{d}t'\, \frac{\gamma_{\boldsymbol{k}}(t')}{\mathfrak{z}(t') + \omega_{\boldsymbol{k}}}\, \mathrm{e}^{\int_0^{t'} \mathrm{d}\tau\, \gamma_{\boldsymbol{k}}(\tau)}\right) \tag{3.4.20b}$$

We now compare this with the known dynamics of the classical model [God00, eq (2.18)]. The spin-spin correlator obeys the following equation of motion, which can be derived from the Langevin equation of the classical spherical model

$$\frac{\mathrm{d}}{\mathrm{d}t}Q_{\boldsymbol{k}}(t) = -2\bigl(\mathfrak{z}(t) + \omega_{\boldsymbol{k}}\bigr)Q_{\boldsymbol{k}}(t) + 2T \tag{3.4.21a}$$

and has the solution

$$Q_{\boldsymbol{k}}(t) = \mathrm{e}^{-2t\omega_{\boldsymbol{k}} - 2\int_0^t \mathrm{d}\tau\,\mathfrak{z}(\tau)}\left(1 + 2T\int_0^t \mathrm{d}t'\,\mathrm{e}^{-2t'\omega_{\boldsymbol{k}} - 2\int_0^{t'}\mathrm{d}\tau\,\mathfrak{z}(\tau)}\right) \tag{3.4.21b}$$

Our requirement that the $g \to 0$ limit should reduce to the classical Langevin equation means that eqs (3.4.20) and (3.4.21) must be consistent. This is achieved if we choose

$$\gamma_{\boldsymbol{k}}(t) = 2\Lambda_{\boldsymbol{k}}^2(t) = 2\left(\mathfrak{z}(t) + \omega_{\boldsymbol{k}}\right) \tag{3.4.22}$$

and includes an implicit fixing of the time-scale in the classical dynamics [God00]. Remarkably, the condition (3.4.22) is identical to the result eq (3.3.27a) obtained from the microscopic derivation of the Lindblad dissipator (3.3.27), up to a choice of the overall damping constant γ_0. In particular, this sheds a different light on the heuristic argument we used above in order to fix the phenomenological exponent $\kappa = 3$.

Therefore, we have seen that *the requirements of reproducing (i) the correct quantum equilibrium state and (ii) the full classical dynamics in the limit $g \to 0$ are enough to fix the precise form of the Lindblad dissipator, up to an overall choice of the time scale.*

Closed formal solution

With the final choice (3.4.22), we return to the dynamics for $g \neq 0$, but keep $\lambda = 1$. The formal solution of eq (3.4.17) is

$$\begin{pmatrix} Q_{\boldsymbol{k}}(t) \\ \Xi_{\boldsymbol{k}}(t) \\ \Pi_{\boldsymbol{k}}(t) \end{pmatrix} = \mathrm{e}^{M_{\boldsymbol{k}}(t)}\begin{pmatrix} Q_{\boldsymbol{k}}(0) \\ \Xi_{\boldsymbol{k}}(0) \\ \Pi_{\boldsymbol{k}}(0) \end{pmatrix} + \gamma\int_0^t \mathrm{d}\tau\,\mathrm{e}^{M_{\boldsymbol{k}}(t) - M_{\boldsymbol{k}}(\tau)}(2n_{\boldsymbol{k}}(\tau) + 1)\begin{pmatrix} \sqrt{\frac{g}{2}}\Lambda_{\boldsymbol{k}} \\ 0 \\ \sqrt{\frac{2}{g}}\Lambda_{\boldsymbol{k}}^3 \end{pmatrix} \tag{3.4.23}$$

where

$$M_{\boldsymbol{k}}(t) = \int_0^t \mathrm{d}\tau\,m_{\boldsymbol{k}}(\tau) = -\bigl(Z(t) + t\omega_{\boldsymbol{k}}\bigr)\begin{pmatrix} \gamma & 0 & 0 \\ 1 & \gamma & 0 \\ 0 & 2 & \gamma \end{pmatrix} + gt\begin{pmatrix} 0 & 2 & 0 \\ 0 & 0 & 1 \\ 0 & 0 & 0 \end{pmatrix} \tag{3.4.24}$$

and we defined the integrated spherical parameter

$$Z(t) := \int_0^t \mathrm{d}\tau\,\mathfrak{z}(\tau) \tag{3.4.25}$$

At equilibrium, thermodynamic stability requires $\mathfrak{z} = \mathfrak{z}_{\mathrm{eq}} \geq 0$, as we have seen in section 3.2.

Here, we are interested in the non-equilibrium dynamics after the systems undergoes a quench from an initial disordered state to a state characterised by certain values of (T, g). Since then the initial values $\langle q_{\boldsymbol{k}}\rangle(0) = \langle\pi_{\boldsymbol{k}}\rangle(0) = 0$, the noise-averaged global magnetisation remains zero at all times, although fluctuations around this will be present. We therefore focus on two-body correlators. By analogy with classical dynamics we expect that if that quench goes towards a state in the disordered phase, with a single ground state of the Hamiltonian H, a rapid relaxation, with a finite relaxation time, should occur towards that quantum equilibrium state. For sufficiently large times, $\mathfrak{z}(t) > 0$ is expected. On the other hand, for quenches either onto a critical point or

else into the ordered phase (with at least two distinct, but equivalent ground states), the formal relaxation times become infinite. Then $\mathfrak{z}(t)$ may evolve differently. For the classical spherical model, quenched from a fully disordered high-temperature state to a temperature T, one finds for long times the leading behaviour [Ron78, God00, Pic04]

$$Z^{\mathrm{cl}}(t) \sim \frac{\mathcal{F}}{2}\ln t \ , \quad \mathcal{F} = \begin{cases} -\frac{1}{2}(4-d) & ; \ \text{if } T = T_c \text{ and } d < 4 \\ 0 & ; \ \text{if } T = T_c \text{ and } d > 4 \\ -\frac{d}{2} & ; \ \text{if } T < T_c \end{cases} \tag{3.4.26}$$

In contrast to the equilibrium situation, this is non-positive and by itself gives a clear indication that after a quench to $T \leq T_c$, the system never reaches equilibrium. In the next two sections, we shall work out what happens in the case of quantum dynamics. As we shall show, $Z(t) < 0$ for non-equilibrium quantum quenches, but the time-dependence can be quite different from the classical result, in particular for quenches deep into the ordered phase.

In order to study what happens after a quench from the disordered phase, the system must be prepared by choosing initial two-point correlators. For a quantum initial state, this requires $\Xi_{\boldsymbol{k}}(0) = 0$ and $Q_{\boldsymbol{k}}(0) =: \mathcal{A}_k$ and $\Pi_{\boldsymbol{k}}(0) = \mathcal{C}_k$, where $\mathcal{A}_{\boldsymbol{k}} = \mathcal{A}_{\boldsymbol{k}}(T_0, g_0)$ and $\mathcal{C}_{\boldsymbol{k}} = \mathcal{C}_{\boldsymbol{k}}(T_0, g_0)$ are chosen to specify the initial state further. The quench amounts to changing $T_0 \mapsto T$ and $g_0 \mapsto g$ to their final values which are kept fixed during the system's evolution. The two-point correlators are found from the system (3.4.23) by evaluating the matrix exponential which finally gives

$$Q_{\boldsymbol{k}}(t) = \mathrm{e}^{-\frac{\gamma}{g}\Delta_t}\left[\mathcal{A}_{\boldsymbol{k}}\cos^2\sqrt{t\Delta_t} + \mathcal{C}_{\boldsymbol{k}}g^2 t\frac{\sin^2\sqrt{t\Delta_t}}{\Delta_t}\right]$$
$$+ \frac{\gamma}{2}\int_0^t \mathrm{d}\tau\,\sqrt{\Delta_\tau'}\left(\left[\frac{\cos\sqrt{t\Delta_t}\sin\sqrt{\tau\Delta_\tau}}{\sqrt{\Delta_\tau/(\tau\Delta_\tau')}} - \frac{\sin\sqrt{t\Delta_t}\cos\sqrt{\tau\Delta_\tau}}{\sqrt{\Delta_t/(t\Delta_\tau')}}\right]^2\right.$$
$$\left. + \left[\cos\sqrt{t\Delta_t}\cos\sqrt{\tau\Delta_\tau} - \frac{\sin\sqrt{t\Delta_t}\sin\sqrt{\tau\Delta_\tau}}{\sqrt{(\Delta_t/t)/(\Delta_\tau/\tau)}}\right]^2\right)\mathrm{e}^{\frac{\gamma}{g}(\Delta_\tau - \Delta_t)}\coth\frac{\sqrt{\Delta_\tau'}}{2T} \tag{3.4.27a}$$

$$\Pi_{\boldsymbol{k}}(t) = \mathrm{e}^{-\frac{\gamma}{g}\Delta_t}\left[\mathcal{A}_{\boldsymbol{k}}g^2 t\frac{\sin^2\sqrt{t\Delta_t}}{\Delta_t} + \mathcal{C}_{\boldsymbol{k}}\cos^2\sqrt{t\Delta_t}\right]$$
$$+ \frac{\gamma}{2g^2}\int_0^t \mathrm{d}\tau\,\sqrt{\Delta_\tau'}\left(\left[\frac{\sin\sqrt{t\Delta_t}\sin\sqrt{\tau\Delta_\tau}}{\sqrt{t/\Delta_t}} + \frac{\cos\sqrt{t\Delta_t}\cos\sqrt{\tau\Delta_\tau}}{\sqrt{\tau/\Delta_\tau}}\right]^2\right.$$
$$\left. + \left[\frac{\sin\sqrt{t\Delta_t}\cos\sqrt{\tau\Delta_\tau}}{\sqrt{t/\Delta_t}} - \frac{\cos\sqrt{t\Delta_t}\sin\sqrt{\tau\Delta_\tau}}{\sqrt{\tau/\Delta_\tau}}\right]^2\right)\mathrm{e}^{\frac{\gamma}{g}(\Delta_\tau - \Delta_t)}\coth\frac{\sqrt{\Delta_\tau'}}{2T} \tag{3.4.27b}$$

$$\Xi_{\boldsymbol{k}}(t) = \mathrm{e}^{-\frac{\gamma}{g}\Delta_t}\left[\frac{\mathcal{C}_{\boldsymbol{k}}g}{\sqrt{\Delta_t}} - \mathcal{A}_{\boldsymbol{k}}\sqrt{\Delta_t}\right]\sin 2\sqrt{t\Delta_t} + \frac{\gamma}{g}\int_0^t \mathrm{d}\tau\,\mathrm{e}^{\frac{\gamma}{g}(\Delta_\tau - \Delta_t)}\coth\frac{\sqrt{\Delta_\tau'}}{2T}$$
$$\times \sqrt{\Delta_\tau}\sqrt{\frac{t}{\tau}}\left[\frac{\cos\sqrt{t\Delta_t}\cos\sqrt{\tau\Delta_\tau}}{\sqrt[4]{(\Delta_\tau/\tau)/(\Delta_t/t)}} + \frac{\sin\sqrt{t\Delta_t}\sin\sqrt{\tau\Delta_\tau}}{\sqrt[4]{(\Delta_t/t)/(\Delta_\tau/\tau)}}\right]\left[\frac{\sin\sqrt{t\Delta_t}\cos\sqrt{\tau\Delta_\tau}}{\sqrt[4]{(\Delta_\tau/\tau)/(\Delta_t/t)}}\right.$$
$$\left. + \frac{\cos\sqrt{t\Delta_t}\sin\sqrt{\tau\Delta_\tau}}{\sqrt[4]{(\Delta_t/t)/(\Delta_\tau/\tau)}}\right] + \frac{\tau\Delta_\tau'}{\sqrt{\Delta_\tau}}\sqrt{\frac{t}{\tau}}\left[\frac{\sin\sqrt{t\Delta_t}\cos\sqrt{\tau\Delta_\tau}}{\sqrt[4]{(\Delta_\tau/\tau)/(\Delta_t/t)}} - \frac{\cos\sqrt{t\Delta_t}\sin\sqrt{\tau\Delta_\tau}}{\sqrt[4]{(\Delta_t/t)/(\Delta_\tau/\tau)}}\right] \times$$
$$\times \left[\frac{\cos\sqrt{t\Delta_t}\sin\sqrt{\tau\Delta_\tau}}{\sqrt[4]{(\Delta_\tau/\tau)/(\Delta_t/t)}} - \frac{\sin\sqrt{t\Delta_t}\cos\sqrt{\tau\Delta_\tau}}{\sqrt[4]{(\Delta_t/t)/(\Delta_\tau/\tau)}}\right]\right) \tag{3.4.27c}$$

with the definition (the $\boldsymbol{k}$-dependence is suppressed for readability)

$$\Delta_t := g(Z(t) + t\omega_{\boldsymbol{k}}) \tag{3.4.28}$$

and the notation $\Delta'_t = \frac{\mathrm{d}\Delta_t}{\mathrm{d}t}$. We remind that the commutation relations are conserved quantities in this formalism.

Eqs (3.4.27a, 3.4.27b, 3.4.27c) give the full solution of the quantum problem and must be evaluated by using the the spherical constraint (3.4.8), viz. $\int_{\mathcal{B}} \frac{\mathrm{d}\boldsymbol{k}}{(2\pi)^d} Q_{\boldsymbol{k}}(t) = 1$. This leads to a formidable integro-differential equation for spherical parameter $\mathfrak{z}(t)$.

Remark on the relaxation towards equilibrium

In order to arrive at the first understanding of the correlator (3.4.27a), let us assume that there exists a *finite* relaxation time t_r such that the system is stationary for times $t \geq t_r$. For such times, we can write $\mathfrak{z} = \mathfrak{z}_\infty \simeq Z(t)/t$. Furthermore, the integration in (3.4.27a) can be split according to $[0, t] = [0, t_r] \cup [t_r, t]$. In the limit $t \to \infty$ we would have

$$Q_{\boldsymbol{k}}(\infty) = \frac{1}{2} \frac{\sqrt{g}}{\sqrt{\mathfrak{z}_\infty + \omega_{\boldsymbol{k}}}} \coth\left[\frac{\sqrt{g}}{2T}\sqrt{\mathfrak{z}_\infty + \omega_{\boldsymbol{k}}}\right] \tag{3.4.29}$$

and this is consistent with the equilibrium correlator eq (3.4.13). We can then conclude:
If the system relaxes towards a stationary state with a positive spherical parameter $\mathfrak{z}_\infty > 0$, this stationary state has to be the unique thermodynamic equilibrium.

3.5   Semi-classical limit

Eqs. (3.4.27) contain two contributions of a different physical nature. The first one contains the contributions from the fluctuations in the initial state, while the second one describes the fluctuations generated by the coupling to the external bath. These contributions appear far too formidable to yield to a direct approach. We therefore restrict to the study of two limiting cases. In this section, we shall present a quasi-classical limit designed to reduce the complexity of the interaction with the bath considerably, so that it can be treated. In the next section, we consider a quench deep into the ordered phase, where the bath interactions are expected to produce only sub-leading term in the long-time limit.

The spin-spin correlator, eq (3.4.27a), contains complicated terms depending on Δ_t, which in turn depends on the quantum coupling g. This suggests that a semi-classical description should mean that the quantum fluctuations generated by such terms should be small and could be achieved by letting $\Delta_t \to 0$. Simplifying, eq (3.4.27a) would then reduce to

$$Q_{\boldsymbol{k}}(t) \simeq \frac{\mathrm{e}^{-\gamma t \omega_{\boldsymbol{k}}}}{G(t)} + \gamma\sqrt{\frac{g}{4}} \int_0^t \mathrm{d}\tau\, \frac{G(\tau)}{G(t)} \mathrm{e}^{-\gamma(t-\tau)\omega_{\boldsymbol{k}}} \sqrt{\mathfrak{z}(\tau) + \omega_{\boldsymbol{k}}} \coth\left[\frac{\sqrt{g}}{2T}\sqrt{\mathfrak{z}(\tau) + \omega_{\boldsymbol{k}}}\right] \tag{3.5.1}$$

with the definition

$$G(t) = \mathrm{e}^{\gamma Z(t)} \tag{3.5.2}$$

Inserted into the spherical constraint $\int_{\mathcal{B}} \frac{\mathrm{d}\boldsymbol{k}}{(2\pi)^d} Q_{\boldsymbol{k}}(t) = 1$, this gives a still complicated integro-differential equation for $G(t)$. Manageable expressions can be found by expanding the thermal occupation. We introduce as a small parameter

$$\varepsilon = \sqrt{\frac{g}{T}}\;. \tag{3.5.3}$$

which measures the relative importance of quantum and thermal fluctuations. For $\varepsilon \to 0$

$$\coth\left(\varepsilon\sqrt{\frac{\mathfrak{z}(\tau) + \omega_{\boldsymbol{k}}}{4T}}\right) = \frac{1}{\varepsilon}\sqrt{\frac{4T}{\mathfrak{z}(\tau) + \omega_{\boldsymbol{k}}}} + \frac{\varepsilon}{3}\sqrt{\frac{\mathfrak{z}(\tau) + \omega_{\boldsymbol{k}}}{4T}} + \mathrm{O}(\varepsilon^3) \tag{3.5.4}$$

The first term in this expansion reproduces the classical model while the higher-order terms give successive quantum corrections.

3.5.1 Classical limit

Stopping at the first term in the expansion (3.5.4) and choosing $Q_{\boldsymbol{k}}(0) = 1$ for an infinite-temperature initial state gives the classical spin-spin correlator

$$Q_{\boldsymbol{k}}(t) = \frac{1}{G(t)} \left(e^{-\gamma t \omega_{\boldsymbol{k}}} + \gamma T \int_0^t d\tau \, G(\tau) e^{-\gamma(t-\tau)\omega_{\boldsymbol{k}}} \right) \tag{3.5.5}$$

From the spherical constraint eq (3.4.8), in the $\mathcal{N} \to \infty$ limit, one finds a Volterra integral equation for $G(t)$

$$G(t) = F(t) + \gamma T \int\limits_0^t d\tau \, G(\tau) F(t - \tau) = F(t) + \gamma T (F \star G)(t) \tag{3.5.6}$$

where $\star$ denotes a convolution and with the integral kernel

$$F(t) = \int_{\mathcal{B}} \frac{d\boldsymbol{k}}{(2\pi)^d} \, e^{-\gamma t \omega_{\boldsymbol{k}}} = \left(e^{-2\gamma t} I_0(2\gamma t) \right)^d \tag{3.5.7}$$

and $I_0(x)$ is a modified Bessel function [Abr64]. Up to a rescaling $\frac{1}{2} \gamma T \mapsto T$ of temperature, this reproduces the dynamical spherical constraint of the classical model, see [God00, eq (2.23)]. Of course, this was to be expected from our derivation of the Lindblad dissipator (3.3.27).

For a deep quench to temperatures $T \ll T_c(d)$ (or $T = 0$), the solution of (3.5.6) trivially is $G(t) \simeq F(t)$, up to corrections to scaling. As we shall see in section 3.6, the solution of the analogous deep *quantum* quench is far from being trivial.

3.5.2 Leading quantum correction

New insight beyond the classical model is found if one includes the first quantum correction from the expansion (3.5.4) in eq (3.5.1). We then get

$$Q_{\boldsymbol{k}}(t) \simeq \frac{e^{-\gamma t \omega_{\boldsymbol{k}}}}{G(t)} + \gamma \int_0^t d\tau \left[T + \frac{g}{12T} (\mathfrak{z}(\tau) + \omega_{\boldsymbol{k}}) \right] \frac{G(\tau)}{G(t)} \, e^{-\gamma(t-\tau)\omega_{\boldsymbol{k}}} \tag{3.5.8}$$

The spherical constraint (3.4.8) becomes again a Volterra-integral equation for $G(t)$. This is seen as follows. From the definitions (3.5.7) and (3.5.2) we have

$$\frac{dF(t)}{dt} = -\gamma \int_{\mathcal{B}} \frac{d\boldsymbol{k}}{(2\pi)^d} \, \omega_{\boldsymbol{k}} \, e^{-\gamma t \omega_{\boldsymbol{k}}} \quad , \quad \frac{dG(t)}{dt} = \gamma \mathfrak{z}(t) G(t)$$

Integrating (3.5.8) gives

$$G(t) = F(t) + \gamma T \, (G \star F)(t) + \frac{g}{12T} \int_0^t d\tau \left[\frac{dG(\tau)}{d\tau} F(t - \tau) + G(\tau) \frac{dF(t - \tau)}{d\tau} \right]$$

$$= F(t) + \gamma T \, (G \star F)(t) + \frac{g}{12T} \int_0^t d\tau \frac{d}{d\tau} \left(G(\tau) F(t - \tau) \right)$$

and using the initial values $G(0) = F(0) = 1$, this can be recast as

$$G(t) \left(1 - \frac{g}{12T} \right) = F(t) \left(1 - \frac{g}{12T} \right) + \gamma T \, (G \star F)(t)$$

The spherical constraint can now be written as

$$G(t) = F(t) + \gamma T^\star \int_0^t d\tau \, G(\tau) F(t - \tau) \tag{3.5.9}$$

which is identical to the classical constraint eq (3.5.6), if one introduces an effective temperature

$$T^\star = T^\star(g) = \frac{T}{1 - \frac{g}{12T}} \simeq T \left(1 + \frac{g}{12T} \right) \tag{3.5.10}$$
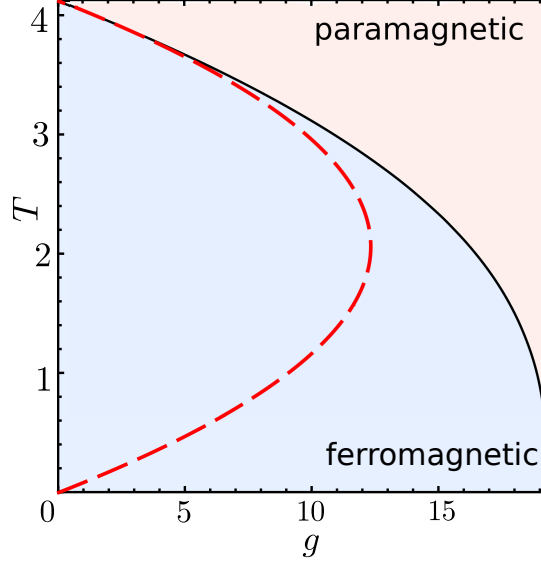
Figure 3.3: Phase diagram of the isotropic quantum spherical model in $d = 3$ dimensions. The black curve is the exact critical line [Oli06] which separates the paramagnetic and ferromagnetic phases. The red curve shows the critical line $T_c^\star(g)$ according to eq (3.5.10), to first order in g.

Remarkably, $T^\star(g) = T_{\text{eff}}(g)$ is exactly the effective temperature found in section 3.4 for the semi-classical *equilibrium* quantum spherical model, see eq (3.4.16). In fig 3.3 we show the phase diagram of the $3D$ isotropic quantum spherical model ($\lambda = 1$) There is an ordered ferromagnetic and a disordered paramagnetic phase. The quantum phase transition occurs on the horizontal axis $T = 0$ and the purely thermal phase transition is on the vertical axis $g = 0$. Clearly, the effective temperature $T^\star(g)$ reproduces the exact critical line to first order in g. As expected, quantum fluctuations reduce the critical temperature $T_c(g) \leq T_c(0)$ with respect to the value of the classical model.

The identity $T_{\text{eff}}(g) = T^\star(g)$ of the effective temperatures from the equilibrium and dynamical analysis corroborates the correctness of our proposed Lindblad formalism. On the other hand, we see that the effective long-time dynamics of the *semi-classical* spherical model becomes purely classical, although the underlying microscopic dynamics is described by a Lindblad equation and explicitly preserves quantum coherence. Quantum effects on the dynamics will only appear in second or higher order in g.

3.5.3   Equal-time spin-spin correlator

The analysis of the Volterra equation (3.5.9) is standard (see appendix 3.B for details).

We have already seen that the formal expression for the single-time spin-spin correlator is

$$Q_{\boldsymbol{k}}(t) = \frac{e^{-\gamma t \omega_{\boldsymbol{k}}}}{G(t)} + \frac{g}{12T}\left[1 - \frac{e^{-\gamma t \omega_{\boldsymbol{k}}}}{G(t)}\right] + \frac{\gamma T}{G(t)}\int_0^t \mathrm{d}\tau\, G(\tau) e^{-\gamma(t-\tau)\omega_{\boldsymbol{k}}} \tag{3.5.11}$$

Its long-time behaviour depends both on the dimension d and on the effective temperature $T^\star = T^\star(g)$.

1. $T^\star > T_c^\star$. This corresponds to the paramagnetic phase at equilibrium and in particular to $d < 2$. The system relaxes within a finite time-scale τ_{eq} towards its (quantum) equilibrium state. For $d > 2$, the critical temperature $T_c^\star > 0$ and

$$\gamma \tau_{\text{eq}} \overset{T^\star \to T_c^\star}{\simeq} \left[\frac{T_c^{\star 2}}{T^\star - T_c^\star}\frac{|\Gamma(1 - \frac{d}{2})|}{(4\pi)^{\frac{d}{2}}}\right]^{2/(d-2)}. \tag{3.5.12}$$

The limiting correlation function becomes rapidly constant in time and takes essentially an Ornstein-Zernicke form

$$Q_{\boldsymbol{k}}(t) \to Q_{\boldsymbol{k}}(\infty) = \frac{g}{12T} + \frac{T}{\omega_{\boldsymbol{k}} + \xi_{\mathrm{eq}}^{-2}} \tag{3.5.13}$$

with the *equilibrium correlation length* $\xi_{\mathrm{eq}}^2 = \gamma\tau_{\mathrm{eq}}$. We also note a hard-core term, absent in the classical limit $g \to 0$ and which in direct space would give a contribution $\sim \frac{g}{12T}\delta(\boldsymbol{r})$.

2. $\underline{T^\star < T_c^\star}$. For $d > 2$ dimensions, the critical point $T_c^\star > 0$ and there is a ferromagnetic phase. In the scaling limit where $t \to \infty$ and $\boldsymbol{k} \to \boldsymbol{0}$ such that $\omega_{\boldsymbol{k}}t$ remains finite, we find the dynamical scaling form

$$Q_{\boldsymbol{k}}(t) \simeq \frac{g}{12T} + \mathrm{e}^{-\gamma t \boldsymbol{k}^2}(4\pi\gamma t)^{d/2}\left(1 - \frac{g}{12T}\right)m^2 \tag{3.5.14}$$

Fourier-transforming to direct space gives the spin-spin correlator

$$C(t, \boldsymbol{r}) \simeq \frac{g}{12T}\delta(\boldsymbol{r}) + \left(1 - \frac{g}{12T}\right)m^2\,\mathrm{e}^{-\frac{r^2}{4\gamma t}} \tag{3.5.15}$$

and with the short-hand $m^2 = 1 - \frac{T^\star}{T_c^\star} \simeq 1 - \frac{T}{T_c}$, sufficiently close to the critical point. Indeed, up to the hard-core term, and a small g-dependent modification of the scaling amplitude, this has the same long-time behaviour as the classical spherical model [Ron78, God00] to which one reverts when taking the limit $g \to 0$. The Gaussian shape of the time-space correlator is a known property of the spherical model.

3. $\underline{T^\star = T_c^\star}$. For quenches onto the critical line, we find the dynamical scaling form

$$Q_{\boldsymbol{k}}(t) = \begin{cases} \frac{g}{12T_c} + \frac{2\gamma T_c}{d-2}t\,{}_1F_1\left(1, \frac{d}{2}; -\gamma\omega_{\boldsymbol{k}}t\right) & ;\ \text{if } 2 < d < 4 \\ \frac{g}{12T_c} + \frac{T_c}{\omega_{\boldsymbol{k}}}\left(1 - e^{-\gamma\omega_{\boldsymbol{k}}t}\right) & ;\ \text{if } 4 < d \end{cases} \tag{3.5.16}$$

Apart from the hard-core term, this agrees with what is known in the classical model.

In particular, we recover for $T^\star \leq T_c^\star$ the dynamics exponent $z = 2$, characteristic for diffusive dynamics of the basic degrees of freedom.

3.6   Disorder-driven dynamics after a deep quench

We now turn to a different quench where quantum effects should be dominant for the long-time behaviour. The two-point correlators (3.4.9) contain contributions (i) from the fluctuations of the initial state and (ii) fluctuations which come from the exchange with the bath. In classical systems, the second term dominates for quenches onto the critical point, but only generates corrections to scaling for quenches into the two-phase coexistence region, where the first contribution dominates. Indeed, for classical systems the long-time scaling behaviour in the entire two-phase region is the same as for the deep quenches to zero temperature $T = 0$. We anticipate that a similar result should also hold true for quantum systems, quenched deeply into the ordered phase with $g \ll g_c(d)$. At temperatures $T = 0$, this is possible for dimensions $d > 1$, where $g_c(d) > 0$. Therefore, instead of eqs (3.4.9) or their formal solutions (3.4.27), we shall rather consider the correlators

$$Q_{\boldsymbol{k}}(t) = \mathrm{e}^{-\frac{\gamma}{g}\Delta_t}\left[\mathcal{A}_{\boldsymbol{k}}\cos^2\sqrt{t\Delta_t} + \mathcal{C}_{\boldsymbol{k}}g^2 t\frac{\sin^2\sqrt{t\Delta_t}}{\Delta_t}\right] \tag{3.6.1a}$$

$$\Pi_{\boldsymbol{k}}(t) = \mathrm{e}^{-\frac{\gamma}{g}\Delta_t}\left[\mathcal{A}_{\boldsymbol{k}}g^2 t\frac{\sin^2\sqrt{t\Delta_t}}{\Delta_t} + \mathcal{C}_{\boldsymbol{k}}\cos^2\sqrt{t\Delta_t}\right] \tag{3.6.1b}$$

$$\Xi_{\boldsymbol{k}}(t) = \mathrm{e}^{-\frac{\gamma}{g}\Delta_t}\left[\frac{\mathcal{C}_{\boldsymbol{k}}g}{\sqrt{\Delta_t}} - \mathcal{A}_{\boldsymbol{k}}\sqrt{\Delta_t}\right]\sin 2\sqrt{t\Delta_t} \tag{3.6.1c}$$

along with $\Delta_t := g(Z(t) + t\omega_{\boldsymbol{k}})$. The terms neglected therein, with respect to (3.4.9), should for weak bath coupling γ and for a quench deep into the ordered phase only account for corrections to the leading scaling we seek. In our exploration of the coherent dynamics of the quantum spherical model, we conjecture that this is so and we shall inquire in particular if dynamical behaviour distinct from the one found in the quasi-classical case can be obtained.

As we shall see, and in contrast to the classical model, the solution of the dynamics is non-trivial.

3.6.1   Spherical Constraint and Asymptotic Behaviour of the Spherical Parameter

Accepting the reduced form (3.6.1) for the two-point correlators, we concentrate on their dissipative dynamics, dominated by the *initial* disorder. The spherical constraint simplifies to

$$1 = \int_{\mathcal{B}}\frac{\mathrm{d}\boldsymbol{k}}{(2\pi)^d}\,\mathrm{e}^{-\gamma(Z(t)+t\omega_k)}\left(\mathcal{A}_{\boldsymbol{k}}\cos^2\sqrt{t\Delta_t} + \mathcal{C}_{\boldsymbol{k}}gt\frac{\sin^2\sqrt{t\Delta_t}}{Z(t)+t\omega_{\boldsymbol{k}}}\right) \tag{3.6.2}$$

and the initial conditions are characterised by the constants $\mathcal{C}_{\boldsymbol{k}}$ and $\mathcal{A}_{\boldsymbol{k}}$. This is still a difficult integro-differential equation without an obvious solution.

Initial conditions

Consider a strongly disordered equilibrium initial state, situated far away from criticality. Then the equilibrium correlators are known [Wal15]. Especially, $\Xi_{\boldsymbol{k}}(0) = 0$ and the spherical parameter $\mathfrak{z}_0 \gg 1$. We call this an *infinitely disordered state*. Such states are characterised by an equal occupation number of all modes $\boldsymbol{k}$, such that the equilibrium correlators eq (3.4.13) simplify to

$$Q_{\boldsymbol{k}}(0) \simeq \sqrt{\frac{g_0}{4\mathfrak{z}_0}}\coth\left(\sqrt{\frac{\mathfrak{z}_0 g_0}{4T_0^2}}\right)\overset{!}{=} 1 \quad,\quad \Pi_{\boldsymbol{k}}(0) \simeq \sqrt{\frac{\mathfrak{z}_0}{4g_0}}\coth\left(\sqrt{\frac{\mathfrak{z}_0 g_0}{4T_0^2}}\right) = \frac{\mathfrak{z}_0}{g_0} =: \mathcal{C} \tag{3.6.3}$$

where the first relation follows from the spherical constraint. Hence the single constant $\mathcal{C}$ characterises the infinitely disordered initial state. Since $\mathfrak{z}(T_0, g_0)$ is defined self-consistently by the spherical constraint, no explicit expression $\mathcal{C}(g_0, T_0)$ is available. Solving (3.6.3) numerically, the parameter $\mathcal{C} = \mathcal{C}(g_0/T_0)$ is traced in fig 3.4. Two limit cases can be identified, which are both obtained for $\mathfrak{z}_0 \gg 1$.
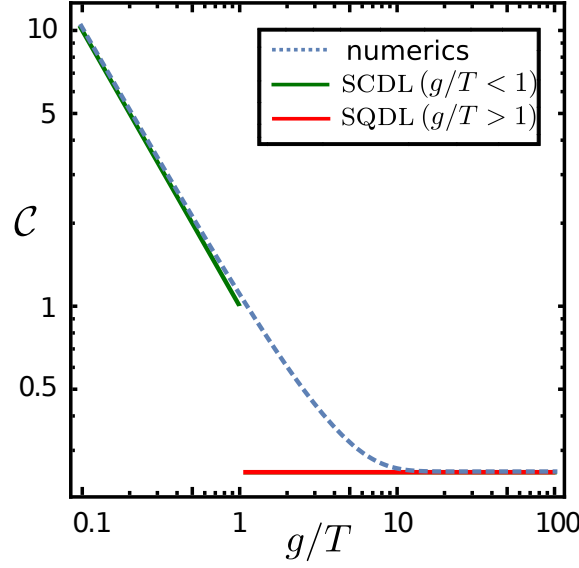
Figure 3.4: The initial parameter $\mathcal{C} = \mathcal{C}(g_0/T_0)$ and the two limits of SCDL and SQDL.

1. the strong classical-disorder limit (SCDL), defined by the condition $g_0 \ll T_0^2$, along with $\mathfrak{z}_0 \gg 1$. A first-order Taylor series of coth gives

$$\mathcal{C} \simeq \frac{T_0}{g_0} \gg 1 \tag{3.6.4}$$

The SCDL is obtained when $\mathcal{C}$ is becoming large and positive.

2. the strong quantum-disorder limit (SQDL), defined by the condition $g_0 \gg T_0^2$, along with $\mathfrak{z}_0 \gg 1$. An asymptotic expansion now gives

$$\mathcal{C} \simeq \frac{1}{4} \tag{3.6.5}$$

which is the smallest admissible value for $\mathcal{C}$ for an quantum *equilibrium* initial state.

Clearly, more general initial conditions interpolate between the limiting cases eqs (3.6.4,3.6.5). It is conceptually significant that initial momentum correlators *must* be present.

At first sight, one might have appealed to an analogy with classical initial disordered states and expected that $\mathcal{C} = 0$ would be possible, but fig 3.4 shows that such a state does not correspond to a quantum disordered equilibrium state. Choosing $\mathcal{C} = 0$ means that one is considering an 'artificial' initial state, inconsistent with the laws of quantum mechanics.

We consequently parametrise our disordered initial state by

$$Q_{\boldsymbol{k}}(0) = 1, \qquad \Pi_{\boldsymbol{k}}(0) = \mathcal{C} \tag{3.6.6}$$

and then quench the system to temperature $T = 0$ and a small coupling $g \ll g_c(T)$ far below the quantum critical point.

3.6.2 The spin-spin correlator

Our first task is to solve the spherical constraint. This requires in turn to cast the spin-spin correlator into a more manageable form. In the deep-quench scenario just defined, the spin-spin correlator becomes

$$Q_{\boldsymbol{k}}(t) = \mathrm{e}^{-\gamma(Z(t)+t\omega_{\boldsymbol{k}})} \left[\cos^2\left(\sqrt{gt(Z(t)+t\omega_{\boldsymbol{k}})} \right) + \frac{\mathcal{C}gt}{Z(t)+\omega_{\boldsymbol{k}}} \sin^2\left(\sqrt{gt(Z(t)+t\omega_{\boldsymbol{k}})} \right) \right] \tag{3.6.7}$$

Recall from the classical dynamics that $Z^{cl}(t) \simeq -\frac{d}{2}\ln t$ for $t \to \infty$ at $T = 0$. In order to prepare for the possibility that $Z(t) < 0$ also in the quantum case, it will turn out to be advantageous to rewrite the correlator in terms of a hypergeometric function[1]

$$Q_{\boldsymbol{k}}(t) = \frac{1}{2}\left[1 + \frac{\mathcal{C}gt}{Z + t\omega_{\boldsymbol{k}}} + \left(1 - \frac{\mathcal{C}gt}{Z + t\omega_{\boldsymbol{k}}}\right){}_0F_1\left(\frac{1}{2}; -gt(Z + t\omega_{\boldsymbol{k}})\right)\right]\mathrm{e}^{-\gamma(Z + t\omega_{\boldsymbol{k}})}$$

$$= \left[1 + \frac{1}{2}\left(1 - \frac{\mathcal{C}gt}{Z + t\omega_{\boldsymbol{k}}}\right)\sum_{n=1}^{\infty}\frac{(-gt)^n}{\left(\frac{1}{2}\right)_n}\frac{(Z + t\omega_{\boldsymbol{k}})^n}{\Gamma(n+1)}\right]\mathrm{e}^{-\gamma(Z+t\omega_{\boldsymbol{k}})} \tag{3.6.8}$$

where $(a)_n = \frac{\Gamma(a+n)}{\Gamma(a)}$ denotes the Pochhammer symbol. The evaluation of the spherical constraint becomes more simple if all dependence on $\boldsymbol{k}$ is brought into the exponential. This will allow to derive factorised representations which in turn will permit to rewrite the expressions where the dimension d becomes a parameter which then can be generalised and considered as real $d \in \mathbb{R}$. This is easily achieved as

$$Q_{\boldsymbol{k}}(t) = \left[1 + \frac{1}{2}\sum_{n=1}^{\infty}\left(\partial_\gamma^n + \mathcal{C}gt\partial_\gamma^{n-1}\right)\frac{1}{\left(\frac{1}{2}\right)_n}\frac{(gt)^n}{n!}\right]\mathrm{e}^{-\gamma(Z+t\omega_{\boldsymbol{k}})} \tag{3.6.9}$$

3.6.3   The spherical constraint

We recall that the spherical constraint (3.4.8), written as $1 = \int_{\mathcal{B}}\frac{\mathrm{d}\boldsymbol{k}}{(2\pi)^d}Q_{\boldsymbol{k}}$, and define[2]

$$\mathfrak{f}(\gamma) := \int_{\mathcal{B}}\frac{\mathrm{d}\boldsymbol{k}}{(2\pi)^d}\mathrm{e}^{-\gamma(Z+t\omega_{\boldsymbol{k}})} = \mathrm{e}^{-\gamma Z}\left(\mathrm{e}^{-2\gamma t}I_0(2\gamma t)\right)^d \overset{t\to\infty}{\simeq} \mathrm{e}^{-\gamma Z}(4\pi\gamma t)^{-\frac{d}{2}} \tag{3.6.10}$$

Thus, we can rewrite the constraint using eq (3.6.9) as[3]

$$1 = \mathfrak{f}(\gamma) + \sum_{n=1}^{\infty}\frac{(gt)^n}{2}\Gamma\begin{bmatrix}\frac{1}{2} \\ n+\frac{1}{2} & n+1\end{bmatrix}\left(\partial_\gamma^n + \mathcal{C}gt\partial_\gamma^{n-1}\right)\mathfrak{f}(\gamma) \tag{3.6.11}$$

It is shown in appendix 3.C that in the long-time limit, the derivative can be written as

$$\partial_\gamma^n\mathfrak{f}(\gamma) \simeq (-1)^n\mathfrak{f}(\gamma)\sum_{k=0}^n\Gamma\begin{bmatrix}n+1 & \frac{d}{2}+k \\ \frac{d}{2} & n-k+1 & k+1\end{bmatrix}\gamma^{-k}Z^{n-k} \tag{3.6.12}$$

At this point, we have achieved a first goal: d merely enters as a parameter and from now, we can treat it as continuous by means of an analytic continuation. Consequently, the spherical constraint can be cast in the form

$$1 = \frac{\mathfrak{f}(\gamma)}{2}\left(1 + \mathfrak{s}_1 + \mathfrak{s}_2\right) \tag{3.6.13}$$

---

[1] We suppress the explicit time-dependence of $Z = Z(t)$.

[2] In the short-hand $\mathfrak{f} = \mathfrak{f}(\gamma)$, the dependence on Z and t is suppressed.

[3] We use throughout the notation $\Gamma\begin{bmatrix}a_1 & \cdots & a_n \\ b_1 & \cdots & b_m\end{bmatrix} = \frac{\Gamma(a_1)\cdots\Gamma(a_n)}{\Gamma(b_1)\cdots\Gamma(b_m)}$.

with the two double sums (see appendix 3.D for the derivation)

$$
\mathfrak{s}_1 := \sum_{n=0}^{\infty} \sum_{k=0}^{n} \Gamma \begin{bmatrix} \frac{1}{2} & \frac{d}{2}+k & \\ n+\frac{1}{2} & \frac{d}{2} & n-k+1 & k+1 \end{bmatrix} \left(-\frac{gt}{\gamma} \right)^n (\gamma Z)^{n-k}
$$

$$
= \Phi_3 \left(\frac{d}{2}; \frac{1}{2}; -gtZ, -\frac{g}{\gamma} t \right) \tag{3.6.14}
$$

$$
\mathfrak{s}_2 := -\gamma \mathcal{C} g t \sum_{n=1}^{\infty} \sum_{k=0}^{n-1} \Gamma \begin{bmatrix} \frac{1}{2} & \frac{d}{2}+k & \\ n+\frac{1}{2} & \frac{d}{2} & n-k & k+1 \end{bmatrix} \frac{1}{n} \left(-\frac{gt}{\gamma} \right)^n (\gamma Z)^{n-1-k}
$$

$$
= 2\mathcal{C} g^2 t^2 \int_0^1 \mathrm{d}w \; \Phi_3 \left(\frac{d}{2}; \frac{3}{2}; -\frac{gt}{\gamma} w, -gtZw \right) \tag{3.6.15}
$$

that can be expressed in terms of the Humbert function Φ_3 [Hum20, Hum22]. In terms of this function the spherical constraint reads

$$
1 = \frac{\mathfrak{f}(\gamma)}{2} \left[1 + \Phi_3 \left(\frac{d}{2}; \frac{1}{2}; -gtZ, -\frac{g}{\gamma} t \right) + 2\mathcal{C} g^2 t^2 \int_0^1 \mathrm{d}w \; \Phi_3 \left(\frac{d}{2}; \frac{3}{2}; -\frac{gt}{\gamma} w, -gtZw \right) \right] \tag{3.6.16}
$$

and we shall study the mathematical properties of the Humbert function thoroughly in chapter 4.

The function Φ_3 is a confluent of one of Appell's generalizations F_3 [App26], of Gauss' hypergeometric function, to two independent variables [Sri85]. The analysis of the spherical constraint requires the asymptotics of these functions when the absolute values of both arguments become simultaneously large. Since no information on these appears to be known in the mathematical literature, we shall derive it, as is outlined in appendix 3.D. Indeed, very similar methods can be applied to different, but related confluents of the Appell function F_3. These will be discussed at length in chapter 4. For our purposes, we simply state the main result: both sums can be expressed *exactly* as Laplace convolutions

$$
\mathfrak{s}_1 = \Gamma \begin{bmatrix} \frac{1}{2} & \\ \frac{1}{2}-\epsilon & \epsilon \end{bmatrix} \sqrt{t} \int_0^t \mathrm{d}v \; \frac{{}_1F_1 \left(\frac{d}{2}; \frac{1}{2}-\epsilon; -\frac{g}{\gamma} v \right)}{v^{\frac{1}{2}-\epsilon}} \frac{{}_0F_1 \left(; \epsilon; -gZ(t-v) \right)}{(t-v)^{1-\epsilon}} \tag{3.6.17}
$$

$$
\mathfrak{s}_2 = \mathcal{C} g^2 t^{3/2} \Gamma \begin{bmatrix} \frac{1}{2} & \\ \frac{3}{2}-\epsilon & \epsilon \end{bmatrix} \int_0^1 \mathrm{d}w \int_0^t \mathrm{d}v \; \frac{{}_1F_1 \left(\frac{d}{2}; \frac{3}{2}-\epsilon; -\frac{g}{\gamma} wv \right)}{v^{\epsilon-\frac{1}{2}}} \frac{{}_0F_1 \left(; \epsilon; -gZw(t-v) \right)}{(t-v)^{1-\epsilon}} \tag{3.6.18}
$$

(where $0 < \epsilon < \frac{1}{2}$ in $\mathfrak{s}_1$ and $0 < \epsilon < \frac{3}{2}$ in $\mathfrak{s}_2$). In appendix 3.D, we first show how these integrals can be de-convoluted and then how their asymptotic limit for $t \to \infty$ can be found, using Tauberian theorems [Fel71]. We then arrive at the following expression for the spherical constraint

$$
1 \simeq \frac{\mathfrak{f}(\gamma)}{2} \left\{ 1 + \left[1 + \mathcal{C} \frac{gt}{Z} \left(e^{\gamma Z} - 1 \right) \right] \left(\frac{\gamma}{gt} \right)^{\frac{d}{2}} \frac{{}_0F_1 \left(\frac{1-d}{2}; -gtZ \right)}{\Gamma \left(\frac{1-d}{2} \right) / \sqrt{\pi}} \right.
$$

$$
\left. + \gamma \mathcal{C} gt \left[\frac{{}_1F_1 \left(1; 2 - \frac{d}{2}; \gamma Z \right)}{\frac{d}{2} - 1} + \left(\frac{gt}{\gamma} \right)^{1-\frac{d}{2}} \frac{{}_1F_2 \left(1 - \frac{d}{2}; 2 - \frac{d}{2}, \frac{3-d}{2}; -gtZ \right) e^{\gamma Z}}{\left(1 - \frac{d}{2} \right) \Gamma \left(\frac{3-d}{2} \right) / \sqrt{\pi}} \right] \right\} \tag{3.6.19}
$$

and recall $\mathfrak{f}(\gamma)$ from (3.6.10). This representation, which depends on the initial condition through the parameter $\mathcal{C}$ and contains the dimension d as a continuous parameter, will be the basis of our analysis of the physics contained in quantum spherical constraint.

We must solve this equation for $Z = Z(t)$, in the asymptotic limit $t \to \infty$, and for fixed parameters γ, g and $\mathcal{C}$ and for a given dimension $d > 1$. The most simple case is given by the initial condition $\mathcal{C} = 0$ and serves as an illustration on how to solve the spherical constraint. We
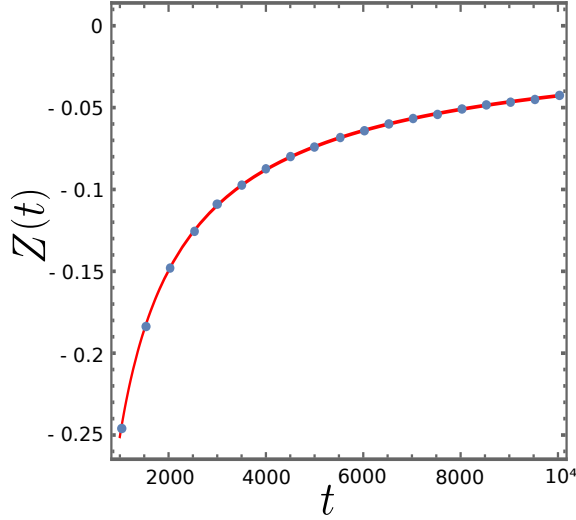
Figure 3.5: Time-dependence of the integrated Lagrange multiplier $Z(t)$, in $d = 2$ dimensions and for the parameters $g = 0.2$, $\gamma = 0.1$ and $\mathcal{C} = 0$. The full curve is the asymptotic form eq (3.6.21) and the dots come from solving numerically (3.6.19).

then have

$$2e^{\gamma Z} (4\pi\gamma t)^{d/2} = 1 + \left(\frac{\gamma}{gt}\right)^{d/2} \frac{{}_0F_1\left(\frac{1-d}{2}; -gtZ\right)}{\Gamma\left(\frac{1-d}{2}\right)/\sqrt{\pi}}$$

$$= 1 + \gamma^{d/2} (\pi gt)^{1/2} \left(\frac{|Z|}{gt}\right)^{(d+1)/4} I_{-(d+1)/2}\left(2\sqrt{gt|Z|}\right) \qquad (3.6.20)$$

where we anticipated that the solution is negative $Z = -|Z(t)| < 0$ and I_ν is a modified Bessel function [Abr64]. To illustrate this point, we display in fig 3.5 a typical of the numerical solution $Z = Z(t)$ of (3.6.19) with $\mathcal{C} = 0$. Indeed, the solution is negative and we also observe that $Z(t) \to$ for $t \to \infty$. The asymptotic form of I_ν then leads to the following simplified form

$$2 (4\pi g)^{d/2} = \left(\frac{\gamma^2 |Z|}{gt}\right)^{d/4} e^{2\sqrt{gt|Z|}}$$

which has the solution

$$|Z(t)| = \frac{d^2}{16gt} W^2\left(\frac{\pi}{d} 16^{\frac{1+d}{d}} gt^2\right) \simeq \frac{d^2}{16g} \frac{\ln^2 t}{t} \qquad (3.6.21)$$

where $W = W_0$ denotes the principal branch of the Lambert-W function [Cor96].[4] The agreement with the numerical solution is illustrated in fig 3.5. Clearly, this solution applies to all values of d and is distinct from the classical result (3.4.26). The logarithmic factor indicates corrections to a simple power-law scaling. We also notice that it is independent of the coupling γ between the system and the bath.

Any equilibrium initial state must have $\mathcal{C} \geq \frac{1}{4}$. Clearly, eq (3.6.19) with $\mathcal{C} \neq 0$ is still too complicated for an explicit solution. However, it turns out that a case distinction between the dimensions $1 < d < 2$, $d = 2$ and $d > 2$ leads to more manageable forms. The details of the calculations are given in appendices 3.E for $d = 2$ and 3.F for $d \neq 2$. Here, we quote the results.
A. For $d > 2$, $Z = -|Z(t)| < 0$ turns out to be negative, in such a way that $t|Z|$ becomes large for large t. We have the equation

$$2\,e^{\gamma Z}(4\pi\gamma t)^{d/2} \simeq 1 + \frac{1}{2}\gamma^{d/2}\left(1 + \mathcal{C}\frac{gt}{|Z|}\right)\left(\frac{|Z|}{gt}\right)^{\frac{d}{4}} e^{2\sqrt{gt|Z|}} \qquad ;\ \text{for } d > 2 \qquad (3.6.22a)$$

---

[4]Asymptotically, $W(x) \simeq \ln x - \ln\ln x + \mathrm{o}(1)$ for $x \to \infty$.

B. For $d = 2$, we find again $Z = -|Z(t)| < 0$ for large times, but now such that $t|Z| \to \varphi$ tends to a constant. This constant is given by the transcendent equation

$$\frac{4\pi}{\mathcal{C}g^2} = \varphi \; {}_2F_3\left(1, 1; \frac{3}{2}, 2, 2; g\varphi\right) \quad ; \text{ for } d = 2 \tag{3.6.22b}$$

C. Finally, for $1 < d < 2$, the integrated Lagrange multiplier $Z = Z(t) > 0$ becomes positive for large enough times and it increases with increasing t beyond any bound. Its value is determined from

$$2\left(4\pi\gamma t\right)^{d/2} = \frac{\mathcal{C}gt}{Z}e^{-\gamma Z} \tag{3.6.22c}$$
$$+ \; \frac{d\mathcal{C}\gamma^{d/2}}{2}\left(\frac{Z}{gt}\right)^{d/4-1}\left[\frac{3(d+2)(4-d)}{64}\frac{\cos\left(2\sqrt{gtZ} + \frac{\pi d}{4}\right)}{Z} - \frac{\sin\left(2\sqrt{gtZ} + \frac{\pi d}{4}\right)}{\sqrt{gtZ}}\right]$$
$$; \text{ for } 1 < d < 2$$

However, we also find an intermediate regime, with large but not enormous times, where $Z(t) < 0$ is still negative. In that regime the effective behaviour is analogous to the one found above for $d > 2$.

Summarising, for large times, the leading asymptotics of the solutions of eqs (3.6.22) become

$$|Z(t)| \simeq \begin{cases} \frac{(d-2)^2}{4g}\frac{\ln^2 t}{t} & , \quad d > 2 \\ \varphi \; t^{-1} & , \quad d = 2 \\ \left(1 - \frac{d}{2}\right)\gamma^{-1}\ln t & , \quad \frac{4}{3} < d < 2 \end{cases} \tag{3.6.23}$$

where φ is given by (3.6.22b). Recall that $Z(t)$ is negative for $d \geq 2$ and positive for $1 < d < 2$. More precisely, for $\frac{4}{3} < d < 2$, the large-time behaviour is given by

$$Z(t) \simeq \left(1 - \frac{d}{2}\right)\gamma^{-1}\ln\gamma t + \mathcal{B}(d)\cos\left(2\sqrt{gtZ} + \frac{\pi d}{4}\right)\frac{t^{1-3d/4}}{\ln^{2-d/4}\gamma t} \tag{3.6.24}$$

and where $\mathcal{B}(d)$ is a known dimension-dependent amplitude. Hence the oscillatory term can no longer be treated as a mere correction for $d < \frac{4}{3}$.[5]

The intermediate regime seen for dimensions $1 < d < 2$ for large, but not enormous times where $Z(t) < 0$, is effectively described by $|Z(t)| \approx \frac{(d-2)^2}{4g}\frac{\ln^2 t}{t}$.

In fig 3.6, we illustrate the solution for $d > 2$.

Several comments are in order:

1. Although the toy initial condition $\mathcal{C} = 0$ does indeed reproduce one instance of the long-time behaviour found from the physically more sensible equilibrium initial states with $\mathcal{C} \geq \frac{1}{4}$, it does not capture the full complexity of possible behaviours.

2. For equilibrium initial states, in $d = 2$ dimensions there is a qualitative change in the long-time behaviour of the solution $Z(t)$.

3. For $d < 2$ where the SAQSM undergoes a quantum phase transition at $T = 0$ but where the thermal critical temperature $T_c(d) = 0$ vanishes, the behaviour of $Z(t)$ is analogous to the one of the classical solution (3.4.26), although with the opposite sign. The Lagrange multiplier $\mathfrak{z}(t) \sim t^{-1}$ has a simple algebraic behaviour.

   Very large times are required to see this regime. In addition, we find an intermediate regime of large, but not enormous times, where the system behaves effectively as for dimensions $d > 2$, up to an amplitude.

---

[5]The occurrence of such a second 'critical dimension' which a qualitative change in the systems' behaviour is a little reminiscent of the classical reaction-diffusion process reactions $2A \to \emptyset$ and $A \to 3A$, which has the critical dimensions $d_c = 2$ and $d'_c \simeq \frac{4}{3}$ [Car96a, Car98].
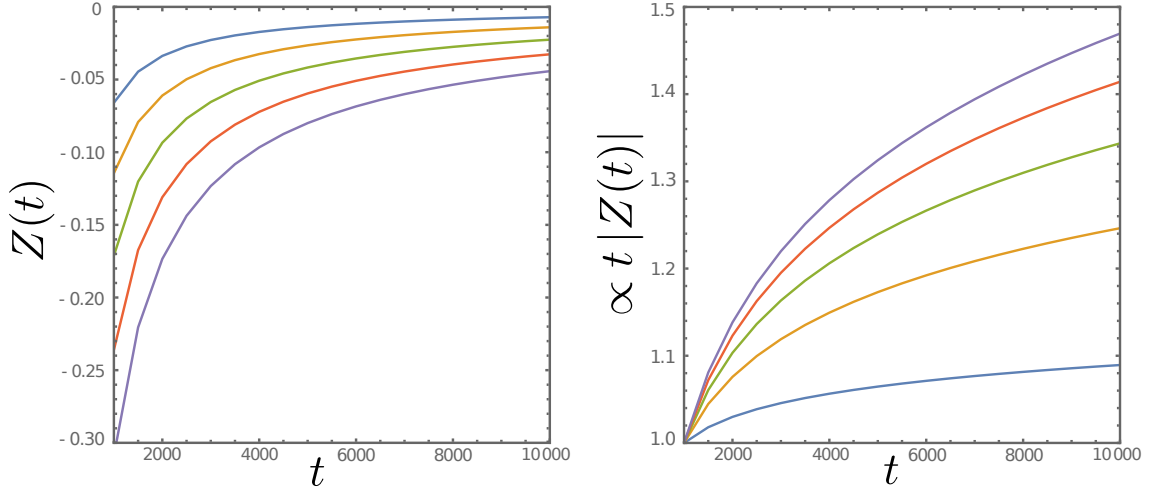
Figure 3.6: Left panel: Integrated Lagrange multiplier $Z(t)$ as a function of time t obtained by solving eq (3.6.19) numerically, for $d = [2.1, 2.4, 2.7, 3, 3.3]$, from top to bottom, and for the parameters $\gamma = 1$, $g = 0.2$, $\mathcal{C} = 1$.
Right panel: Integrated Lagrange multiplier $t|Z(t)|$, normalised to unity at $t = 1000$, as a function of time and for $d = [2.1, 2.4, 2.7, 3, 3.3]$, from bottom to to top, and the same parameters.

4. For $d > 2$ where the system also has a finite critical temperature $T_c(d) > 0$, strong logarithmic corrections modify the leading scaling behaviour, which is distinct from the classical one.

5. The case $d = 2$ is intermediate between the two, with a simple power-law scaling behaviour $|Z(t)| \sim t^{-1}$.

6. Surprisingly, the influence of the coupling of the coupling γ with the bath is also dimension-dependent. For $d \geq 2$ dimensions, γ disappears from the leading long-time behaviour of $Z(t)$, while it is present for $d < 2$. Therefore, for $d \geq 2$ dimensions, as well as in the intermediate regime for $d < 2$, the limit $\gamma \to 0$ can be formally taken.

The physical meaning of these properties will be understood by analysing the behaviour of the two-point correlators.

3.6.4   Correlation Function and relevant Length scales

For the deep-quench dynamics the spin-spin correlation function in Fourier space reads

$$Q_k(t) = \frac{1}{2}\left[1 + \frac{\mathcal{C}gt}{Z + t\omega_{\boldsymbol{k}}} + \left(1 - \frac{\mathcal{C}gt}{Z + t\omega_{\boldsymbol{k}}}\right) {}_0F_1\left(\frac{1}{2}, -gt(Z + t\omega_{\boldsymbol{k}})\right)\right] e^{-\gamma(Z + t\omega_{\boldsymbol{k}})} \qquad (3.6.25)$$

We are now interested in transforming this expression back to real space and studying the large-distance behaviour of the correlation. This is routinely revealed by a small $|\boldsymbol{k}|$ expansion and in fig 3.7 we see on the $2D$ example that such an expansion is more than reasonable in the asymptotic limit $t \to \infty$. We consequently write $\omega_{\boldsymbol{k}} \approx |\boldsymbol{k}|^2 = k^2$ and observe that Q_k solely depends on k. This leads to the following simplified expression for the d dimensional inverse Fourier transform

$$f(R) \propto R^{1-\frac{d}{2}} \int_0^\infty \mathrm{d}k\, k^{\frac{d}{2}} J_{\frac{d}{2}-1}(kR)\hat{f}(k) \qquad (3.6.26)$$

A. We start the investigation with the case $d = 2$. In fig 3.7 we show a typical structure factor Q_k in 2D for different times and observe that the distribution is peaked around the zero momentum mode $k = 0$ and the peak sharpens for larger times. One can argue that the main contribution is given by the interval $[0, k^*]$ where k^* is the mode where the argument of the hypergeometric
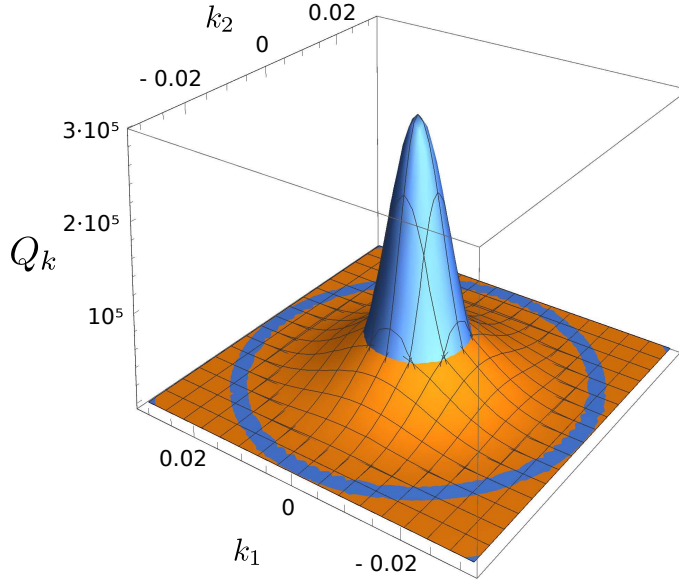
Figure 3.7: Structure factor Q_k in $d = 2$ dimensions shown in the first Brillouin zone for the parameter values $c = 1; g = 0.1; \gamma = 0.1; t = 500$ (orange); 1000 (blue). We observe that the function is sharply peaked around the centre of the Brillouin zone with the peak sharpening with time increasing.

function changes signs and $_0F_1$ reduces from an exponential contribution to a geometric function at this point. We can thus write correlation function as

$$C(R) \propto \int_0^{k^*} \mathrm{d}k \ \frac{1}{2}\left[1 + \frac{\mathcal{C}gt}{Z + tk^2} + \left(1 - \frac{\mathcal{C}gt}{Z + tk^2}\right) {}_0F_1\left(\frac{1}{2}, -gt(Z + tk^2)\right)\right] \mathrm{e}^{-\gamma(Z + tk^2)} \quad (3.6.27)$$

By introducing the *scaling variable* $\varrho := \sqrt{\varphi}\frac{R}{t}$ where φ is the solution to eq (3.6.22b), we find in a straightforward fashion using the variable transform $\mu = \frac{|Z| - tk^2}{|Z|}$ the scaling form

$$C(R) \propto \mathcal{C}g \int_0^1 \mathrm{d}\mu \ \frac{{}_0F_1\left(; \frac{1}{2}; g\varphi\mu\right) - 1}{\mu} J_0\left(\varrho\sqrt{1 - \mu}\right) =: \mathcal{C}g\mathcal{W}(\varrho) \quad (3.6.28)$$

This makes explicit the dynamical scaling behaviour of the spin-spin correlator. In fig 3.8 we show the behaviour of the scaling function $\mathcal{W}$ for different ranges of ϱ. For small ϱ the scaling function decays in a Gaussian fashion (left hand side) while it shows decaying oscillations for larger values. It is instructive to compare with the dynamical scaling seen in the classical spherical model, quenched to temperature $T \ll T_c(d)$. For a purely relaxational dynamics without any conservation law (model A), dynamical scaling is found [Ron78, God00], whereas in the case of a conserved order-parameter (model B), the existence to two logarithmically distinct length scale was established long ago [Con89]. This logarithmic breaking of scale-invariance for conserved dynamics was later shown to be a peculiarity of the spherical model, see e.g. [Maz06]. The quantum dynamics we are considering here actually has an infinite number of prescribed conservation laws, namely all canonical commutators between the spherical spins s_n and their conjugate moment p_n. Our finding that at least for $d = 2$ a standard dynamical scaling is found clearly suggests that the quantum mechanical spherical model should not be considered to be as special as its classical counterpart. Any breaking of dynamical scaling which we may find for different values cannot be as readily dismissed as a specific model property but could rather be a typical feature for more general models.

B. In the case $d > 2$ the treatment is similar to the case $d = 2$ since the argument of the hypergeometric function presents once again a change of signs. However we have to respect that φ is no longer a constant but diverges logarithmically as it is shown in eq (3.6.23). This leads to
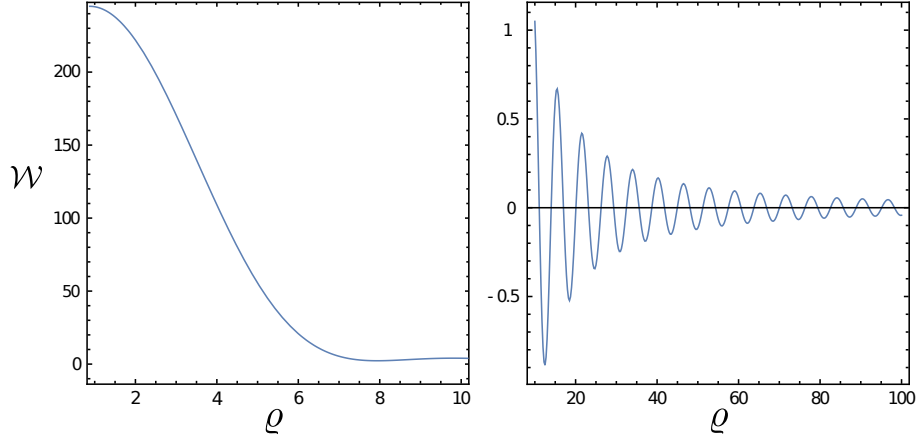
Figure 3.8: Illustration of the scaling function $\mathcal{W}$ in $d = 2$ dimensions for different ranges of the scaling variable ϱ.

a modified multi-scaling behaviour

$$C(R) \propto \mathcal{C}gR^{2-d} \int_0^1 \mathrm{d}\mu \; \frac{{}_0F_1\left(;\frac{1}{2};\frac{(d-2)^2}{4}\mu\ln^2 t\right) - 1}{\mu} \left(\varrho\sqrt{1-\mu}\right)^{\frac{d}{2}-1} J_{\frac{d}{2}-1}\left(\varrho\sqrt{1-\mu}\right) \quad (3.6.29)$$
$$=: \mathcal{C}gR^{2-d}\mathcal{V}(\varrho, t)$$

since $\varrho \simeq \frac{\frac{d}{2}-1}{\sqrt{g}} R\ln(t)/t$ which is illustrated in fig 3.9. The explicit logarithmic terms do break simple scale-invariance and point towards the existence of several length scales, which are distinguished by logarithmic factors. We observe a behaviour in terms of ρ which is is qualitatively not too different from the case $d = 2$. However, the functional dependence on ρ changes strongly when the time is increased which is a manifest of breaking of simple scaling behaviour.

Phenomenologically, this looks analogous to the well-known behaviour of the classical spherical model with conserved order-parameter (model B) [Con89] but here we obtain this breaking of dynamical scaling by a mere change of the dimension d. Such a feature has never been seen before, to the best of our knowledge.
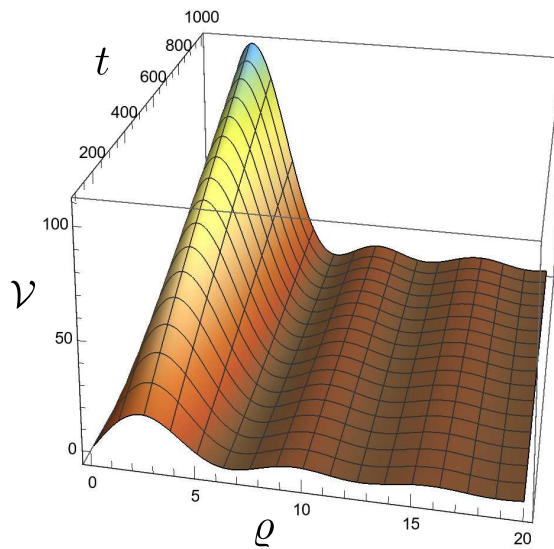
Figure 3.9: Functional dependence of the correlation function for $d = 3$ and $g = 0.1$. We do not find a single scaling function but rather find a dependence on the variable ϱ and the time t.

C. In $\frac{4}{3} < d < 2$ spatial dimensions the situation is different since the spherical parameter is $Z > 0$ positive and there is no intrinsic cut-off for the integral. We investigate first the structure factor Q_k by pointing out that the contribution $\propto \mathcal{C}gt$ is leading for large times.

$$Q_{\boldsymbol{k}} \simeq \frac{1}{2}\frac{\mathcal{C}gt}{Z+tk^2}\left[1 - {}_0F_1\left(;\frac{1}{2};-gt(Z+tk^2)\right)\right]\mathrm{e}^{-\gamma(Z+tk^2)} \tag{3.6.30}$$

This expression can be rewritten as

$$Q_{\boldsymbol{k}} \simeq \mathcal{C}g^2t^2\,{}_1F_2\left(1;\frac{3}{2},2;-gt(Z+tk^2)\right)\mathrm{e}^{-\gamma(Z+tk^2)} \tag{3.6.31}$$

and its Fourier transform is readily cast in the form[6]

$$C(R) \propto \frac{\mathcal{C}g^2}{R^{\frac{d}{2}-1}}\int_0^\infty \mathrm{d}\mu\,\mu^{\frac{d-2}{4}}J_{\frac{d}{2}+1}\left(\sqrt{\mu}R/t\right){}_1F_2\left(1;\frac{3}{2},2;-g(tZ+\mu)\right)\mathrm{e}^{-\gamma\mu/t}\,. \tag{3.6.32}$$

We observe that the integral is exponentially cut off and thus only small μ values contribute. Thus, we can omit the μ contribution in ${}_1F_2$ since $tZ \to \infty$ and the integral can be evaluated explicitly [Pru86, eq (2.12.9.3)]

$$C(R) \propto \frac{\mathcal{C}g}{(2\gamma)^{d/2}}\frac{\sin^2\left(\sqrt{gtZ}\right)}{Z}\mathrm{e}^{-\frac{R^2}{4\gamma t}} \tag{3.6.33}$$

Having completed the analysis of the spin correlation function we mention that the momentum correlation function can be obtained from the spin correlator by simply exchanging $\mathcal{A}_{\boldsymbol{k}}$ and $\mathcal{C}_{\boldsymbol{k}}$ in eq (3.6.1). We thus expect a qualitatively analogous behaviour.

Now we studied the real space correlation function and want to investigate the *relevant length scale* given by

$$L^2(t) \propto -\left.\frac{\partial_k^2 Q_k}{Q_k}\right|_{k=0} \tag{3.6.34}$$

This is readily evaluated to

$$L^2 \propto \frac{2t}{Z}\left(\frac{\mathcal{C}gt\left[1+\gamma Z-(1+\gamma Z){}_0F_1\left(\frac{1}{2},-gtZ\right)-2gtZ{}_0F_1\left(\frac{3}{2},-gtZ\right)\right]}{\mathcal{C}gt\left[1-{}_0F_1\left(\frac{1}{2},-gtZ\right)\right]+Z\left[1+{}_0F_1\left(\frac{1}{2},-gtZ\right)\right]}\right.$$
$$\left.+\frac{\gamma Z^2\left[1+{}_0F_1\left(\frac{1}{2};-gtZ\right)+2\frac{g}{\gamma}t{}_0F_1\left(\frac{3}{2},-gtZ\right)\right]}{\mathcal{C}gt\left[1-{}_0F_1\left(\frac{1}{2},-gtZ\right)\right]+Z\left[1+{}_0F_1\left(\frac{1}{2},-gtZ\right)\right]}\right) \tag{3.6.35}$$

For a vanishing quantum coupling the relevant length scale reduces to a purely diffusive behaviour introduced by the heat bath

$$L_\gamma^2 \propto 2\gamma t\,. \tag{3.6.36}$$

The length scale allows to read of the dynamical exponent z according to $L^2 \propto t^{2/z}$ and we deduce from eq (3.6.35) $z=2$ as expected for the classical dynamics [God00, Hen10].

In order to evaluate the intrinsic length scale taking into account the quantum effects, we have to once more distinguish the cases

A. $\underline{d=2}$: Here Z is negative and we can rewrite the hypergeometric functions as hyperbolic functions. Moreover the correlation function obeys a clean scaling behaviour and we find

$$L^2 \simeq 2t\left(\gamma + \sqrt{\frac{gt}{|Z|}}\right) = 2\gamma t + 2\sqrt{\frac{g}{\varphi}}t^2 \tag{3.6.37}$$

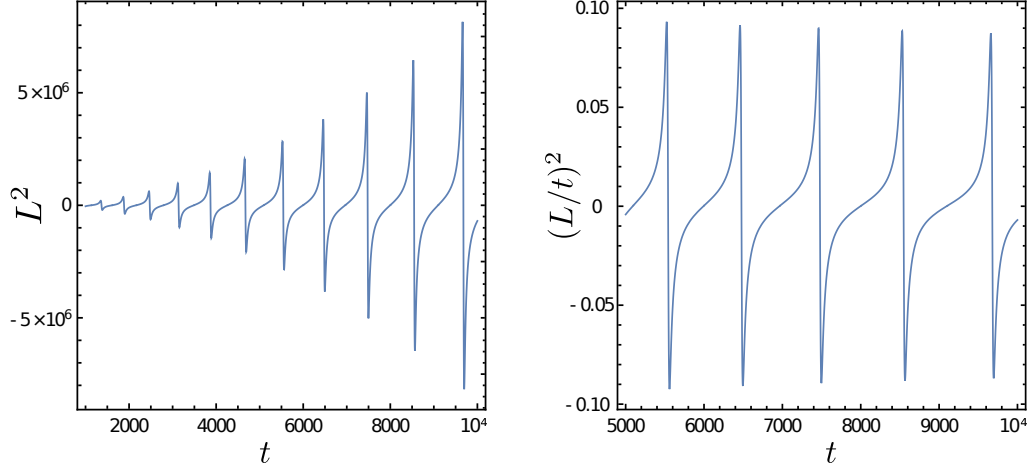[6]One simply uses the change of variables $\mu = t^2k^2$.

Figure 3.10: <u>left panel</u>: effective characteristic length L^2 for $d = 1.5$, $\gamma = 1$, $g = 0.1$ and $\mathcal{C} = 1$. <u>right panel</u>: $(L/t)^2$ for the same parameters as in the left panel.

indicating a crossover from *diffusive* to *ballistic transport*. The dynamical critical exponent crosses from $z = 2$ to $z = 1$ as we expect for a true quantum dynamics[7] [Dut15, Cal06].

B. <u>$d > 2$</u>: This case can be treated analogously to the case **A** since Z is still negative. Nevertheless, we do not have a clean scaling behaviour and logarithmic corrections are present in the long-time limit. The length scale reads

$$L^2 \simeq 2t \left(\gamma + \sqrt{\frac{gt}{|Z|}} \right) = 2\gamma t + 2g(d-2)\frac{t^2}{\ln t} \tag{3.6.38}$$

and up to logarithmic corrections, we observe the same diffusive to ballistic crossover as for $d = 2$ with $z = 1$.

C. <u>$\frac{4}{3} < d < 2$</u>: In this case, the spherical parameter is positive and the hypergeometric functions reduce to trigonometric contributions. The length scale then reduces to

$$L^2 \simeq 2\gamma t - 2\sqrt{\frac{gt}{Z}} \frac{\mathcal{C}gt^2 \sin 2\sqrt{gtZ}}{\mathcal{C}gt \sin^2 \sqrt{gtZ} + Z\cos^2 \sqrt{gtZ}} \tag{3.6.39}$$

and can be recast up to a removable singularity as

$$L^2 \simeq 2\gamma t - 4\mathcal{C}gt^2 \sqrt{\frac{gt}{Z}} \frac{\tan \sqrt{gtZ}}{\mathcal{C}gt \tan^2 \sqrt{gtZ} + Z} \tag{3.6.40}$$

This length scale shows an oscillatory behaviour which is shown in the left panel of fig 3.10 to which we shall come back later. For now we want to focus on the right panel where we show L^2/t^2 as a function of time. We see that the peaks are rather constant and $|L/t|$ remains bound for all times what indicates that the dynamical exponent should be $z \geq 1$. The specific value of z will depend strongly on the specific time window.

Furthermore, we observe a strong kinked oscillatory behaviour that even renders L^2 negative. This can be better understood by referring to simple correlation functions as

$$C_1 = \mathrm{e}^{-R/\xi} \cos(R/\Lambda), \qquad C_2 = \mathrm{e}^{-(R/\xi)^2} \cos(R/\Lambda) \tag{3.6.41}$$

---

[7]An exception from the fast ballistic transport are many-body localized systems where information spreads much slower[Pal10, Bas06]. Such slow transport has as well been observed in translation-invariant $1D$ quantum lattice models [Mic17].
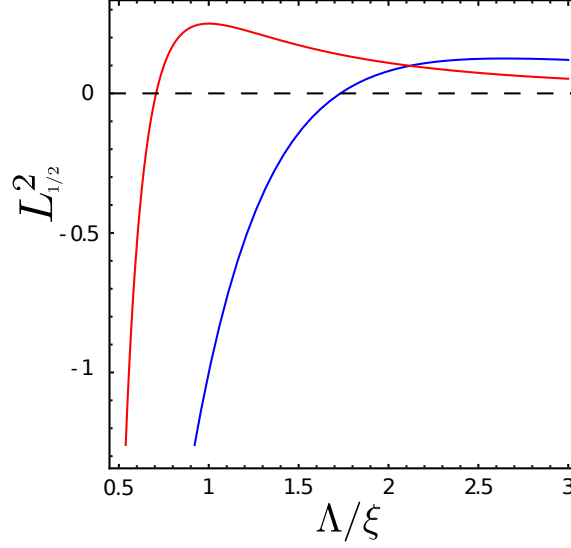
Figure 3.11: Effective squared length scale $L_i^2(t)$, $i = 1, 2$ as a function of Λ/ξ for a modulated exponential correlator (blue) and a modulated Gaussian correlator (red) introduced in eq (3.6.41).

For simplicity, we refer to $d = 1$ here, since dimensionality is not changing the key aspect and it is straightforward to generalise the calculation. The characteristic length scale L_i^2 with $i = 1, 2$ associated with the correlation function C_i is readily obtained

$$L_1^2 \simeq 2\Lambda^2 \frac{(\Lambda/\xi)^2 - 3}{(1 + (\Lambda/\xi)^2)^2}, \qquad L_2^2 \simeq \frac{\Lambda^2}{4} \frac{1}{(\Lambda/\xi)^2} \left(2 - \frac{1}{(\Lambda/\xi)^2} \right) . \qquad (3.6.42)$$

While the overall time-dependence of this effective length scale can still be used to extract the dynamical exponent from the scaling relation $L_i^2(t) \sim t^{2/z}$, the sign of the amplitude does depend on the ratio Λ/ξ. This change of sign, according to eq (3.6.42), is illustrated in fig 3.11.

Such a change of signs can thus be attributed to an oscillating correlation length and the competition between the two distinct length scales ξ and Λ. Since L itself becomes imaginary it is thus not adequate any longer to interpret it as a length scale, but we can still deduce the dynamical exponent as shown before. The oscillatory nature of eq (3.6.39) indicates consequently a competition between different length scales in the system.

3.6.5 Dynamic Susceptibility

By means of eq (3.6.23) we can calculate the dynamic susceptibility which is essentially proportional to Q_0

$$\chi \propto Q_0 = \frac{1}{2} \left[1 + \frac{\mathcal{C}gt}{Z} + \left(1 - \frac{\mathcal{C}gt}{Z} \right) {}_0F_1 \left(\frac{1}{2}, -gtZ \right) \right] e^{-\gamma Z} . \qquad (3.6.43)$$

We find for the leading contribution for large times

$$\chi(t) \propto \begin{cases} \mathcal{C}g/\varphi \sinh^2(\sqrt{g\varphi}) \, t^2, & d = 2 \\[2ex] \frac{\mathcal{C}g^2}{(d-2)^2} \, t^d / \ln^2 t, & d > 2 \\[2ex] \frac{\mathcal{C}g\gamma}{2-d} \frac{t^{2-\frac{d}{2}}}{\ln t} \sin^2 \left(\sqrt{g/\gamma(1 - d/2)t \ln t} \right), & \frac{4}{3} < d < 2 \end{cases} \qquad (3.6.44)$$

In general, for systems with simple scaling, one expects $\chi(t) \sim L(t)^d \sim t^{d/z}$, or said in words, the susceptibility is proportional to the volume explored up to time t [God00]. In $d = 2$ dimensions, this expectation, is fully confirmed by our exact solution, since

$$\chi_{2D}(t) \propto t^2 \propto L^2 \qquad (3.6.45)$$

and in particular, we see once more that indeed $z = 1$, in contrast to classical dynamics. For dimensions, $d > 2$, this scaling expectation for $\chi(t)$ is again confirmed, but only up to logarithmic corrections. In addition, the effective length scale $L_{\text{eff}}(t) \sim t \, (\ln t)^{-2/d}$ is different from the length scale extracted above from the second moment.

Finally, for $d < 2$, not only does the exponent of the leading time-dependence deviate from the expected value (to say nothing on the logarithmic correction) which sends $\chi(t) \to 0$ for large times, but furthermore, a strong time-dependent modulation of $\chi(t)$ is found. We can understand this as a further justification of the strong competition between different length scales as we already discussed in the previous section.

3.6.6   Crossed Correlations

We now want to study the crossed correlation term and which reads

$$\Xi_{\boldsymbol{k}}(t) = \; \mathrm{e}^{-\frac{\gamma}{g}\Delta_t} \left[\frac{\mathcal{C}g}{\sqrt{\Delta_t}} - \sqrt{\Delta_t} \right] \sin 2\sqrt{t\Delta_t} \tag{3.6.46}$$

with $\Delta_t = g(Z(t) + t\omega_{\boldsymbol{k}})$.

A. For $d = 2$ we know that $Z < 0$ and thus Δ_t changes signs from negative to positive for after a time t^* for fixed $k \neq 0$. Consequently, all $\Xi_{\boldsymbol{k}} \to 0$ for $\boldsymbol{k} \neq 0$ due to the exponential damping. For the zero mode we find

$$\Xi_0 \simeq \mathcal{C}\sqrt{\frac{g}{\varphi}} \sinh(2\sqrt{g\varphi})\sqrt{t} \quad \overset{t\to\infty}{\to} \quad \infty \tag{3.6.47}$$

and see a diverging crossed correlation. This is a strong indicator that the system will not relax towards its thermal equilibrium but will rather stay in a non-equilibrium state for all times. This looks analogous to what happens in systems undergoing physical ageing, but we have not yet achieved all results needed to test the three defining properties of physical ageing (slow dynamics, breaking of time-translation invariance, dynamical scaling) [Cug95, Hen10]. We hope to return to an analysis of physical ageing in the quantum spherical model elsewhere.

B. For $d > 2$ the situation is up to logarithmic corrections similar to $d = 2$. We find immediately

$$\Xi_0 \simeq \frac{\mathcal{C}g}{d-2} \frac{t^{d-\frac{3}{2}}}{\ln t} \tag{3.6.48}$$

while all non-zero mode crossed correlations vanish in the asymptotic limit.

C. In $\frac{4}{3} < d < 2$ the behaviour is qualitative different. While it remains true, that all non-zero mode crossed correlations vanish, we find for the zero mode

$$\Xi_0 \propto t^{\frac{d}{2}-1}\ln t \tag{3.6.49}$$

which decays to zero and thus at least indicates that a relaxation into thermal equilibrium is possible. Moreover we observe that in this scenario the solution $Z(t)$ depends on the bath quantity γ while for $d \geq 2$ the bath scales entirely out. All these observations point towards the fact that *the actual bath coupling becomes less important in higher dimensional open quantum dynamics.*

3.7   Conclusions

We studied the QSM as a simple exactly solvable model in order to explore exact quantum dynamics and compare classical to quantum dynamical properties. We used certain consistency criteria, namely (i) the quantum equilibrium is a stationary state of the chosen dynamics and (ii) the classical Langevin dynamics is included in the limit $g \to 0$ in order to construct the precise form of the Lindblad master equation. The QSM has then proven to reduce just as in equilibrium the

full N-body problem to a single integro-differential equation. The full solution of this equation is still an open and exceptionally hard problem.

We have focussed in this chapter on two special cases. First, we considered weak quantum dynamics and calculated the leading quantum corrections to the classical dynamics. It turns out that the effective quantum dynamics is classical and quantum effects only renormalise the temperature. This is a further justification of the formalism we set up to describe the open quantum dynamics of the spherical model.

Second, we studied the true quantum dynamics driven by the initial disorder for a quantum quench across the critical point and deep into the ordered phase. In order to carry out this analysis, we explored new mathematical methods that are related to asymptotic expansions of confluent hypergeometric functions in two variables. We shall present further details on this connection in the next chapter. It turns out that the long-time behaviour of the integrated spherical parameter $Z(t)$ is extremely complex to deduce and that it depends on the spatial dimension in a non-trivial fashion.

$$|Z(t)| \simeq \begin{cases} \frac{(d-2)^2}{4g} \frac{\ln^2 t}{t} & , \quad d > 2 \\ \varphi \, t^{-1} & , \quad d = 2 \\ \left(1 - \frac{d}{2}\right) \gamma^{-1} \ln t & , \quad \frac{4}{3} < d < 2 \end{cases} \tag{3.7.1}$$

This behaviour is qualitatively different from the classical case where simply $|Z| \propto \ln t$.

Due to this strong dependence on the dimensionality of the system, we observed prominent differences in the scaling behaviour. In $d = 2$ dimensions we find a regular scaling with a unique characteristic length scale. Thus, the QSM is able to reliably predict general qualitative properties. In $d \neq 2$ dimensions, we find strong logarithmic corrections which destroy a simple scaling behaviour. One might be tempted to view these corrections as a peculiarity of the SM [Con89] but since we find a clean scaling in $d = 2$ dimensions we are not convinced by simply dismissing the logarithmic corrections as a feature specific to the SM. Below $d = 2$ we find additionally strong time dependent modulations in terms of the distance R.

Furthermore, the analysis of the leading time dependence of the characteristic length scale L^2 and of the time-dependent susceptibility $\chi(t)$ fully confirmed simple dynamic scaling in $d = 2$ and else *several* different length scales.

All these results depend on the conjecture that the integral term in eq (3.4.27a) is irrelevant. Testing this remains a difficult open problem.

We thus conclude that, to the extend as the QSM is a reliable guide for collective quantum dynamical behaviour, we would expect $2D$ quantum systems to show simple dynamical scaling, whereas in $3D$ quantum systems it should only be possible to find small time-dependent windows with effective time-dependent exponents. To what extent such an expectation is born out in more general quantum models remains an important challenge for the future.

Appendix

3.A   Equilibrium quantum spherical constraint

We present the exact derivation of the quantum spherical constraint in the equilibrium SAQSM, by diagonalising the Hamiltonian via canonical transformations. Consider the following Hamiltonian, with bosonic operators a_n such that $[a_n, a_m^\dagger] = \delta_{n,m}$

$$H = \sum_{n,m \in \mathcal{L}} \left[a_n^\dagger A_{nm} a_m - \frac{1}{2} \left(a_n B_{nm} a_m + \text{h.c.} \right) \right] + \sum_{n \in \mathcal{L}} C_n \left(a_n + a_n^\dagger \right) \tag{3.A.1}$$

which for a specific choice of the matrices A, B reduces to the Hamiltonian (3.2.2) of the SAQSM. In addition, the vector $\boldsymbol{C}$ allows to consider the effects of an external field. We shall present an exact derivation of the equilibrium spherical constraint, which should also arise from the stationary state ($t \to \infty$ limit) of the dynamics. Many aspects of the treatment are analogous to the one of free fermion Hamiltonians, see e.g. [Lie61, Hen99]. For the sake of notational simplicity, we only treat the $1D$ case explicitly, the generalisation to any $d > 1$ being obvious.

Define the harmonic oscillator ladder operators [Wal15]

$$s_n = \left(\frac{g}{8\mathcal{S}} \right)^{1/4} \left(a_n + a_n^\dagger \right) \quad , \quad p_n = -\mathrm{i} \left(\frac{\mathcal{S}}{2g} \right)^{1/4} \left(a_n - a_n^\dagger \right) \tag{3.A.2}$$

and the spherical constraint is then

$$\mathcal{N}\sqrt{\frac{8\mathcal{S}}{g}} = \sum_{n \in \mathcal{L}} \left(\langle a_n a_n \rangle + \langle a_n^\dagger a_n^\dagger \rangle + 2\langle a_n^\dagger a_n \rangle + 1 \right)$$

$$= \left| \langle \boldsymbol{a} \rangle \right|^2 + \left| \langle \boldsymbol{a}^\dagger \rangle \right|^2 + 2\langle \boldsymbol{a}^\dagger \cdot \boldsymbol{a} \rangle + \mathcal{N} \; , \tag{3.A.3}$$

where we have introduced the vector $\boldsymbol{a} = (a_1, a_2, \ldots, a_{\mathcal{N}-1}, a_{\mathcal{N}})$ and its element-wise adjoint. We now apply the canonical transformation, used for the diagonalisation in [Wal15]

$$\boldsymbol{a} = \boldsymbol{r} + v^t \boldsymbol{b} - w^t \boldsymbol{b}^\dagger \tag{3.A.4}$$

to the spherical constraint and find

$$\mathcal{N}\sqrt{\frac{8\mathcal{S}}{g}} = 4\left| \boldsymbol{r} \right|^2 + 4\boldsymbol{r} \cdot (v-w)^t \left\langle \boldsymbol{b} + \boldsymbol{b}^\dagger \right\rangle$$

$$+ \sum_{lmn} (v_{ml}v_{nl} - 2v_{ml}w_{nl} + w_{ml}w_{nl}) \langle b_m b_n \rangle$$

$$+ \sum_{lmn} (w_{ml}w_{nl} - 2w_{ml}v_{nl} + v_{ml}v_{nl}) \left\langle b_m^\dagger b_n^\dagger \right\rangle$$

$$+ \sum_{lmn} (2v_{ml}v_{nl} - v_{ml}w_{nl} + w_{ml}v_{nl}) \left\langle b_m^\dagger b_n \right\rangle$$

$$+ \sum_{lmn} (2w_{ml}w_{nl} - v_{ml}w_{nl} + w_{ml}v_{nl}) \left\langle b_n b_m^\dagger \right\rangle + \mathcal{N} \tag{3.A.5}$$

Following [Wal15], we define the matrix

$$\underline{\Psi} := (v - w)^t \tag{3.A.6}$$

with the eigenvectors $\boldsymbol{\Psi}_n$ of $(A - B)(A + B)$ as column entries, see (3.A.1). Analogously, we define

$$\underline{\Phi} := (A + B)\underline{\Psi} \tag{3.A.7}$$

(for a full analysis of the diagonalisation of H via canonical transformations, see [Wal15, app. A]).

Since $[b_n, b_m] = [b_n^\dagger, b_m^\dagger] = 0$, we can exchange the indices m and n in line 2 and 3 of eq (3.A.5) to find the same prefactor for $\langle b_m b_n \rangle$ and $\langle b_m^\dagger b_n^\dagger \rangle$. In the fifth line we use the commutation relation to achieve a normal order and estimate the prefactor of $\langle b_m^\dagger b_n \rangle$ from this and the fourth line. We find

$$2\mathcal{N}\sqrt{\frac{\mathcal{S}}{g}} = \mathcal{N} + 4\,|\boldsymbol{r}|^2 + 4\boldsymbol{r}\cdot\underline{\underline{\Psi}}\left\langle \boldsymbol{b} + \boldsymbol{b}^\dagger \right\rangle + \sum_n \left(|\boldsymbol{\Psi}_n|^2 - \boldsymbol{\Psi}_n\cdot\boldsymbol{\Phi}_n \right)$$
$$+ \sum_{mn} \boldsymbol{\Psi}_m\cdot\boldsymbol{\Psi}_n \left(\left\langle \widehat{b_m b_n} \right\rangle + \left\langle b_m^\dagger b_n^\dagger \right\rangle + 2\left\langle b_m^\dagger b_n \right\rangle \right)$$

Using the property $\boldsymbol{\Phi}_n\cdot\boldsymbol{\Psi}_n = 1$ [Wal15], we can rewrite the spherical constraint as

$$\frac{\mathcal{N}}{2}\sqrt{\frac{\mathcal{S}}{g}} = |\boldsymbol{r}|^2 + \boldsymbol{r}\cdot\underline{\underline{\Psi}}\left\langle \boldsymbol{b} + \boldsymbol{b}^\dagger \right\rangle + \sum_{mn} \frac{\boldsymbol{\Psi}_m\cdot\boldsymbol{\Psi}_n}{4} \left(\langle b_m b_n \rangle + \langle b_m^\dagger b_n^\dagger \rangle + 2\langle b_m^\dagger b_n \rangle + \delta_{nm} \right) \qquad (3.A.8)$$

Finally, we use the orthogonality of the eigenvectors of Toeplitz matrices to find

$$\frac{\mathcal{N}}{2}\sqrt{\frac{\mathcal{S}}{g}} = |\boldsymbol{r}|^2 + \boldsymbol{r}\cdot\underline{\underline{\Psi}}\left\langle \boldsymbol{b} + \boldsymbol{b}^\dagger \right\rangle + \sum_n \frac{|\boldsymbol{\Psi}_n|^2}{4} \left(\langle b_n b_n \rangle + \langle b_n^\dagger b_n^\dagger \rangle + 2\langle b_n^\dagger b_n \rangle + 1 \right) \qquad (3.A.9)$$

For systems without an external magnetic field $\boldsymbol{r} = \boldsymbol{0}$ which we shall admit from now on. The absolute value of the eigenvectors was found in [Wal15] to be

$$|\boldsymbol{\Psi}_n|^2 = \frac{\Lambda_k^-}{\Lambda_k^+} = \sqrt{\frac{\mathcal{S} - \frac{1-\lambda}{2}\cos k}{\mathcal{S} - \frac{1+\lambda}{2}\cos k}} \qquad (3.A.10)$$

With this result we can write the final result, in zero external field

$$\sqrt{\frac{8}{g}}\sqrt{\mathcal{S}} = \int_{\mathcal{B}} \frac{\mathrm{d}k}{2\pi} \frac{\Lambda_{-,k}}{\Lambda_{+,k}} \left(\langle b_k b_k \rangle + \left\langle b_k^\dagger b_k^\dagger \right\rangle + 2\left\langle b_k^\dagger b_k \right\rangle + 1 \right) \qquad (3.A.11)$$

which is easily generalised to d dimensions.

In equilibrium, the off-diagonal averages $\langle b_k b_k \rangle = \left\langle b_k^\dagger b_k^\dagger \right\rangle \to 0$ decay to zero and the number operator $\left\langle b_k^\dagger b_k \right\rangle$ is given by the thermal occupation of the corresponding mode

$$\sqrt{\frac{8}{g}}\,\mathcal{S}^{1/2} = \int_{\mathcal{B}} \frac{\mathrm{d}\boldsymbol{k}}{(2\pi)^d} \frac{\Lambda_{-,k}}{\Lambda_{+,k}} \left(2n_k + 1 \right) \qquad (3.A.12)$$

which is equivalent to eq (3.4.14) in the main text.

3.B Analysis of the Volterra equation

Solving the linear Volterra equation (3.5.9), at an effective temperature $T^\star$, is standard, e.g. [Ron78, Cug95, God00]. Define the Laplace transform

$$\overline{f}(p) = \int_0^\infty \mathrm{d}t\, f(t)\mathrm{e}^{-pt} \qquad (3.B.1)$$

such that the Laplace-transformed equation (3.5.9) reads simply

$$\overline{G}(p) = \frac{\overline{F}(p)}{1 - \gamma T^\star\,\overline{F}(p)} \qquad (3.B.2)$$

Tauberian theorems [Fel71] permit to extract the long-time behaviour of $G(t)$ from the behaviour of $\overline{G}(p)$ for $p \to 0$. We require $\overline{F}(p) = \overline{F}_{\mathrm{uni}}(p) + \overline{F}_{\mathrm{reg}}(p)$, for p small, conveniently decomposed into an universal and a regular part, which have been derived countless times before

$$\overline{F}_{\mathrm{uni}}(p) \stackrel{p\to 0}{\approx} \frac{\Gamma\left(1 - \frac{d}{2}\right)}{\gamma(4\pi)^{\frac{d}{2}}} \left(\frac{p}{\gamma}\right)^{\frac{d}{2}-1} \quad,\quad \overline{F}_{\mathrm{reg}}(p) = \frac{1}{\gamma}\left(A_1 - A_2\frac{p}{\gamma} + A_3\left(\frac{p}{\gamma}\right)^2 \mp \ldots \right) \qquad (3.B.3)$$

where the last expansion can only be carried to the point where the coefficients

$$A_n = \int_{\mathcal{B}} \frac{\mathrm{d}\boldsymbol{k}}{(2\pi)^d} \frac{1}{\omega_{\boldsymbol{k}}^n} \; . \tag{3.B.4}$$

exist. For example, even A_1 does not exist for $d \leq 2$ and A_2 only exists for $d > 4$. We conclude that

$$\bar{F}(p) \overset{p\to 0}{\approx} \frac{1}{\gamma}
\begin{cases}
\Gamma\left(1 - \frac{d}{2}\right)(4\pi)^{-\frac{d}{2}}\,(p/\gamma)^{\frac{d}{2}-1} & , \;\; \text{if } 0 < d < 2 \\
A_1 - \left|\Gamma\left(1 - \frac{d}{2}\right)\right|(4\pi)^{-\frac{d}{2}}\,(p/\gamma)^{\frac{d}{2}-1} & , \;\; \text{if } 2 < d < 4 \\
A_1 - A_2\,p/\gamma\; - \left|\Gamma\left(1 - \frac{d}{2}\right)\right|(4\pi)^{-\frac{d}{2}}\,(p/\gamma)^{\frac{d}{2}-1} & , \;\; \text{if } 4 < d < 6
\end{cases} \tag{3.B.5}$$

In the last, we included the regular term which dominates for $d < 6$. Inserting into (3.B.2) gives $\overline{G}(p)$ which in turn must inserted into the generic expression (3.5.11) for the spin-spin correlator, which we repeat here for convenience

$$Q_{\boldsymbol{k}}(t) = \frac{\mathrm{e}^{-\gamma t \omega_{\boldsymbol{k}}}}{G(t)} + \frac{g}{12T}\left[1 - \frac{\mathrm{e}^{-\gamma t \omega_{\boldsymbol{k}}}}{G(t)}\right] + \gamma T \frac{1}{G(t)} \int_0^t \mathrm{d}\tau\, G(\tau)\mathrm{e}^{-\gamma(t-\tau)\omega_{\boldsymbol{k}}} \tag{3.B.6}$$

We shall now study the three cases from (3.B.5) separately.

3.B.1 $0 < d < 2$

In this case, $\overline{F}(p)$ is a monotonous and surjective function on the interval $(0, \infty)$, hence the equation $1 - \gamma T^\star \overline{F}(p) = 0$ always has a solution at $p = p_0$. Hence $\overline{G}(p)$ has a simple pole at some $p_0 = t_{\mathrm{eq}}^{-1}$, for all $T^\star > 0$. The leading long-time behaviour of $G(t)$ is exponential, with the explicit relaxation time

$$G(t) \sim \mathrm{e}^{t/t_{\mathrm{eq}}} \;\; , \;\; t_{\mathrm{eq}} = \gamma^{-1}\left[T^\star \Gamma\left(1 - \frac{d}{2}\right)(4\pi)^{-d/2}\right]^{-\frac{2}{d-2}} \tag{3.B.7}$$

Inserting this into (3.B.6) leads straightforwardly to (3.5.13).

3.B.2 $2 < d < 4$

Since for dimensions $d > 2$ the coefficient A_1 is finite, its value can be used to define a critical temperature

$$T_c^\star = \frac{1}{A_1} \tag{3.B.8}$$

Then three distinct situations can arise: (i) The case $T^\star > T_c^\star$ is treated analogously to the case $d < 2$. Here, the relaxation time is modified, because the phase transition does occurs at finite temperature, according to

$$t_{\mathrm{eq}} = \gamma^{-1}\left[\frac{T^\star - T_c^\star}{T^\star T_c^\star}|\Gamma\left(1 - \frac{d}{2}\right)|(4\pi)^{-d/2}\right]^{-\frac{2}{d-2}} \tag{3.B.9}$$

but the correlator retains the form (3.5.13). (ii) For $T > T_c$ we have to analyse eq (3.B.2) carefully. Define the short-hand

$$m^2 = 1 - T^\star/T_c^\star \tag{3.B.10}$$

and expand $\overline{G}(p)$ to lowest non-trivial order in p to find

$$\bar{G}(p) = \frac{1}{\gamma}\frac{A_1 - (4\pi)^{-d/2}\left|\Gamma\left(1 - \frac{d}{2}\right)\right|(p/\gamma)^{d/2-1}}{m^2 + T^\star(4\pi)^{-d/2}\left|\Gamma\left(1 - \frac{d}{2}\right)\right|(p/\gamma)^{d/2-1}}$$

$$\overset{p\to 0}{\simeq} \frac{1}{\gamma}\left[\frac{A_1}{m^2} - \frac{(4\pi)^{-d/2}}{m^4}\left|\Gamma\left(1 - \frac{d}{2}\right)\right|\left(\frac{p}{\gamma}\right)^{\frac{d}{2}-1}\right] + \ldots \tag{3.B.11}$$

The Tauberian theorem then gives the long-time behaviour of $G(t)$ by a formal inverse Laplace transform ($\delta(t)$ is the Dirac distribution)

$$G(t) \simeq \frac{1}{m^2 \gamma T_c^\star} \delta(t) + \frac{(4\pi\gamma t)^{-d/2}}{m^4}, \text{ for } t \to \infty \text{ and } 2 < d < 4 \tag{3.B.12}$$

The singular term therein, of course, does not appear in the long-time limit, but is required to evaluate the correlator. Following [Hen15], we insert into (3.B.6) and obtain

$$
\begin{aligned}
Q_{\boldsymbol{k}}(t) &= e^{-\gamma\omega_{\boldsymbol{k}}t} m^4 (4\pi\gamma t)^{d/2} \left(1 - \frac{g}{12T}\right) + \frac{g}{12T} \\
&\quad + e^{-\gamma\omega_{\boldsymbol{k}}t} m^4 (4\pi\gamma t)^{d/2} \frac{\gamma T}{m^2 \gamma T_c^\star} + \gamma T t^{d/2} \mathscr{L}^{-1} \left(\Gamma(1-d/2) p^{1-d/2} \frac{1}{p + \gamma\omega_{\boldsymbol{k}}}\right)(t) \\
&= e^{-\gamma\omega_{\boldsymbol{k}}t} m^4 (4\pi\gamma t)^{d/2} \left(1 - \frac{g}{12T} + \frac{1}{m^2} \frac{T}{T_c^\star}\right) + \frac{g}{12T} \\
&\quad + \gamma T\, t \frac{1}{1 - d/2}\, {}_1F_1\left(1, 2 - \frac{d}{2}; -\gamma\omega_{\boldsymbol{k}}t\right) \\
&= e^{-\gamma\omega_{\boldsymbol{k}}t} m^2 (4\pi\gamma t)^{d/2} \left(1 - \frac{g}{12T}\right) + \frac{g}{12T} \\
&\quad + \frac{\gamma T}{1 - d/2} t\, e^{-\gamma\omega_{\boldsymbol{k}}t}\, {}_1F_1\left(1 - \frac{d}{2}, 2 - \frac{d}{2}; \gamma\omega_{\boldsymbol{k}}t\right)
\end{aligned} \tag{3.B.13}
$$

Herein, in the first two lines the terms proportional to T come from the integral in (3.B.6). The first of those in the contribution from the singular term in (3.B.12) and the other is cast into an inverse Laplace transformation. In the next step, this inverse transformation is found using [Pru92b, eq (2.1.2.1)] and the coefficient of the other term is simplified using the definitions of m^2 and of $T^\star$. Finally, we used the identity [Abr64, eq (13.1.27)]. We are interested in the limit $\boldsymbol{k} \to \boldsymbol{0}$, $t \to \infty$ such that $\omega_{\boldsymbol{k}} t$ remains finite. Then the last term is sub-dominant and we arrive at (3.5.14). (iii) For $T^\star = T_c^\star = 1/A_{1,,}$, the leading terms in small-p expansion are

$$\bar{G}(p) = \frac{1}{\gamma} \left(\frac{1}{T_c^\star}\right)^2 \frac{(4\pi)^{d/2}}{\left|\Gamma(1 - \frac{d}{2})\right|} \left(\frac{p}{\gamma}\right)^{1-d/2} - \frac{1}{\gamma T_c^\star} \tag{3.B.14}$$

hence

$$G(t) = G_d t^{d/2-2} - \frac{1}{\gamma T_c^\star} \delta(t) \tag{3.B.15}$$

where G_d is a known constant whose value will not be required. Inserting into (3.B.6) and taking into account the contribution of the singular term in the integral gives

$$
\begin{aligned}
Q_{\boldsymbol{k}}(t) &= \frac{e^{-\gamma\omega_{\boldsymbol{k}}t} t^{2-d/2}}{G_d} \underbrace{\left(1 - \frac{g}{12T_c} - \frac{T_c}{T_c^\star}\right)}_{=0} + \frac{g}{12T_c} + \gamma T_c t^{2-d/2} \Gamma(d/2 - 1) \mathscr{L}^{-1}\left(p^{1-d/2} \frac{1}{p + \gamma\omega_{\boldsymbol{k}}}\right)(t) \\
&= \frac{g}{12T_c} + \frac{\gamma T}{d/2 - 1} t\, {}_1F_1\left(1, \frac{d}{2}; -\gamma\omega_{\boldsymbol{k}}t\right)
\end{aligned} \tag{3.B.16}
$$

Herein, the firm term vanishes because of the definition of $T^\star$ and we re-used [Pru92b, eq (2.1.2.1)]. This gives the first eq (3.5.16).

3.B.3 $d > 4$

The discussion is analogous to the previous ones. At $T^\star = T_c^\star$, expansion gives for small p gives $\overline{G}(p) \simeq \frac{1}{T_c^{\star 2} A_2} \frac{1}{p} - \frac{1}{\gamma T_c^\star}$, hence

$$G(t) \simeq -\frac{1}{\gamma T_c^\star} \delta(t) + \frac{1}{T_c^{\star 2} A_2} \tag{3.B.17}$$

Inserting this into (3.B.6) leads to

$$Q_{\boldsymbol{k}}(t) = T_c^{\star 2} A_2 e^{-\gamma \omega_{\boldsymbol{k}} t} \underbrace{\left(1 - \frac{g}{12 T_c} + \frac{T_c}{T_c^{\star}}\right)}_{=0} + \frac{g}{12 T_c} + \frac{T_c}{\omega_{\boldsymbol{k}}} \left(1 - e^{-\gamma \omega_{\boldsymbol{k}} t}\right) \tag{3.B.18}$$

where we used again the definition of $T^{\star}$ and have thus found the second eq (3.5.16). Finally, below criticality, we must expand up to the first universal term. We obtain for p small (as it stands, this holds for $d < 6$, but extensions are obvious)

$$\bar{G}(p) \simeq \frac{1}{\gamma} \frac{A_1 - A_2 \frac{p}{\gamma} - |\mathcal{F}|_1 \left(\frac{p}{\gamma}\right)^{d/2-1}}{m^2 + T^{\star} A_2 \frac{p}{\gamma} + \gamma T^{\star} |\mathcal{F}_1 \left(\frac{p}{\gamma}\right)^{d/2-1}} \simeq \frac{1}{\gamma} \left(\frac{A_1}{m^2} - \frac{A_2}{m^4} \frac{p}{\gamma}\right) - \frac{|\mathcal{F}|_1}{m^4} \left(\frac{p}{\gamma}\right)^{d/2-1} \tag{3.B.19}$$

which gives for large times

$$G(t) \simeq \frac{1}{m^2 \gamma T_c^{\star}} \delta(t) - \frac{A_2}{m^4 \gamma^2} \delta'(t) + \frac{(4\pi \gamma t)^{-d/2}}{m^4} \tag{3.B.20}$$

and from which one readily arrives again at eq (3.5.14).

We remark that the small-p expansions must be carried up to including (i) eventual constant terms and (ii) the leading universal contribution. The first contribution is required for the correct evaluation of the correlator (unless one prefers to derive sum rules instead, as carried out in [God00]) and the second contribution gives the leading time-dependence.

We did not discuss the case $d = 4$ explicitly, although this can be done without much extra difficulty [Has06, Ebb08]. Below criticality, there is no dimension-dependent singularity and one may simply set $d = 4$ in the final result (3.5.14) and at criticality, additional logarithmic singularities will appear.

3.C   Proof of an identity

We prove the asymptotic identity eq (3.6.12).
Lemma: *The function* $\mathfrak{f}(\gamma) = e^{-\gamma Z}(4\pi\gamma t)^{-d/2}$ *obeys for all* $d > 0$ *and all* Z, t *the identity*

$$\partial_\gamma^n \mathfrak{f}(\gamma) = (-1)^n \mathfrak{f}(\gamma) \sum_{k=0}^n \Gamma \begin{bmatrix} n+1 & \frac{d}{2}+k \\ \frac{d}{2} & n-k+1 & k+1 \end{bmatrix} \gamma^{-k} Z^{n-k} \tag{3.C.1}$$

Proof: This proceeds via mathematical induction, with the habitual two steps.

• Basis $n = 1$: it suffices to calculate the first derivative and compare with (3.C.1). We find straightforwardly, in both cases

$$\partial_\gamma \mathfrak{f}(\gamma) = -\mathfrak{f}(\gamma) \left[Z + \frac{d}{2\gamma} \right]$$

• Step $n \to n+1$: We write

$$\partial_\gamma^{n+1} \mathfrak{f}(\gamma) = \partial_\gamma \partial_\gamma^n \mathfrak{f}(\gamma)$$

and use the expression (3.C.1) to find

$$\partial_\gamma^{n+1} \mathfrak{f}(\gamma) = (-1)^{n+1} \mathfrak{f}(\gamma) \sum_{k=0}^n \Gamma \begin{bmatrix} n+1 & \frac{d}{2}+k \\ \frac{d}{2} & k+1 & n-k+1 \end{bmatrix} \gamma^{-k} Z^{n-k} \left\{ Z + \frac{d}{2\gamma} + \frac{k}{\gamma} \right\}$$

Shifting the index n to $n+1$ produces

$$\partial_\gamma^{n+1} \mathfrak{f}(\gamma) = \qquad (-1)^{n+1} \mathfrak{f}(\gamma) \sum_{k=0}^{n+1} \left\{ \Gamma \begin{bmatrix} n+2 & \frac{d}{2}+k \\ \frac{d}{2} & k+1 & n-k+2 \end{bmatrix} \gamma^{-k} Z^{n+1-k} \times \right.$$
$$\left. \times \left[1 - \frac{k}{n+1} \right] \left[1 + \frac{d}{2Z\gamma} + \frac{k}{Z\gamma} \right] \right\}$$

Herein, the first line is already the sought expression for the $(n+1)^{\text{st}}$ derivative. It only remains to show that the residual terms

$$\sum_{k=0}^{n+1} \Gamma \begin{bmatrix} n+2 & \frac{d}{2}+k \\ \frac{d}{2} & k+1 & n-k+2 \end{bmatrix} \gamma^{-k} Z^{n+1-k} \left\{ \frac{d}{2Z\gamma} + \frac{k}{Z\gamma} - \frac{k}{n+1} \left[1 + \frac{d}{2Z\gamma} + \frac{k}{Z\gamma} \right] \right\} \tag{3.C.2}$$

cancel. For simplicity we omit non-zero multiplicative factors and consider[8]

$$\sum_{k=0}^{n+1} \Gamma \begin{bmatrix} \frac{d}{2}+k \\ k+1 & n-k+2 \end{bmatrix} (\gamma Z)^{-k} \left[\left(\frac{d}{2}+k \right)(n+1-k) + k\gamma Z \right]$$
$$= \sum_{k=0}^n \Gamma \begin{bmatrix} \frac{d}{2}+k+1 \\ k+1 & n-k+1 \end{bmatrix} (\gamma Z)^{-k} - \sum_{k=1}^n \Gamma \begin{bmatrix} \frac{d}{2}+k \\ k & n-k+2 \end{bmatrix} (\gamma Z)^{-k-1} = 0$$

which completes the proof. $\qquad\qquad\qquad\qquad\qquad\qquad\qquad\qquad\qquad\qquad\qquad\square$

---

[8]In (3.C.2), bring the curly bracket to the common denominator, which does not depend on k and hence can be dropped.

3.D   Asymptotic analysis of some double series

In the main text, we introduced two double series

$$\mathfrak{s}_1 := \sum_{n=0}^{\infty}\sum_{k=0}^{n} \Gamma \begin{bmatrix} \frac{1}{2} & \frac{d}{2}+k & \\ n+\frac{1}{2} & \frac{d}{2} & n-k+1 & k+1 \end{bmatrix} \left(-\frac{gt}{\gamma}\right)^n (\gamma Z)^{n-k} \tag{3.D.1}$$

$$\mathfrak{s}_2 := -\gamma \mathcal{C} gt \sum_{n=1}^{\infty}\sum_{k=0}^{n-1} \Gamma \begin{bmatrix} \frac{1}{2} & \frac{d}{2}+k & \\ n+\frac{1}{2} & \frac{d}{2} & n-k & k+1 \end{bmatrix} \frac{1}{n}\left(-\frac{gt}{\gamma}\right)^n (\gamma Z)^{n-1-k} \tag{3.D.2}$$

and we require their asymptotic behaviour for $t \gg 1$ large, where Z is either being kept fixed or varies slowly with t.

1. We start our analysis with the treatment of $\mathfrak{s}_1$. Begin with (3.D.1) and exchange the order of summation, followed by a shift in the second summation variable. This results in

$$\mathfrak{s}_1 = \sum_{k=0}^{\infty}\sum_{n=k}^{\infty} \Gamma \begin{bmatrix} \frac{1}{2} & \frac{d}{2}+k & \\ n+\frac{1}{2} & \frac{d}{2} & n-k+1 & k+1 \end{bmatrix} \left(-\frac{gt}{\gamma}\right)^n (\gamma Z)^{n-k}$$

$$= \sum_{k=0}^{\infty}\sum_{n=0}^{\infty} \Gamma \begin{bmatrix} \frac{1}{2} & \frac{d}{2}+k & \\ n+k+\frac{1}{2} & \frac{d}{2} & n+1 & k+1 \end{bmatrix} \left(-\frac{gt}{\gamma}\right)^{n+k} (\gamma Z)^n \tag{3.D.3a}$$

$$= \frac{\Gamma(\frac{1}{2})}{\Gamma(\frac{d}{2})} \sum_{k=0}^{\infty}\sum_{n=0}^{\infty} \frac{\Gamma(k+\frac{d}{2})}{\Gamma(k+n+\frac{1}{2})} \frac{(-gt/\gamma)^k}{k!} \frac{(-gtZ)^n}{n!} \tag{3.D.3b}$$

Recalling the definition of the Humbert function [Hum20, Hum22]

$$\Phi_3\left(\beta; \gamma; x, y\right) = \sum_{m=0}^{\infty}\sum_{n=0}^{\infty} \frac{(\beta)_m}{(\gamma)_{m+n}} \frac{x^m}{m!} \frac{y^n}{n!}$$

we can identify $\mathfrak{s}_1 = \Phi_3\left(\frac{d}{2}; \frac{1}{2}; -gtZ, -\frac{gt}{\gamma}\right)$, as stated in (3.6.14) in the main text. Sums such as (3.D.3) would be easy to evaluate if they would factorise, but in fact they are coupled by the factor $\Gamma\left(n+k+\frac{1}{2}\right)$ in the denominator. In order to achieve a factorisation, we use the following identity, which involves Euler's Beta function, with an arbitrary constant $0 < \epsilon < \frac{1}{2}$

$$\frac{1}{\Gamma\left(n+k+\frac{1}{2}\right)} = \frac{B(n+\epsilon, \frac{1}{2}+k-\epsilon)}{\Gamma(\epsilon+n)\Gamma(\frac{1}{2}-\epsilon+k)} = \frac{t^{\frac{1}{2}-n-k}}{\Gamma(\epsilon+n)\Gamma(\frac{1}{2}-\epsilon+k)} \int_0^t \mathrm{d}x\, x^{k-\epsilon-\frac{1}{2}}(t-x)^{n+\epsilon-1}$$
$$\tag{3.D.4}$$

which is obtained from eqs (6.2.1) and (6.2.2) in [Abr64]. Now, insert this identity into (3.D.3a) such that the sums over n and k decouple. We then find

$$\mathfrak{s}_1 = \Gamma \begin{bmatrix} \frac{1}{2} & \\ \frac{1}{2}-\epsilon, & \epsilon \end{bmatrix} \sqrt{t}\, (\mathfrak{u}_1 \star \mathfrak{v}_1)\,(t) \tag{3.D.5}$$

with the functions

$$\mathfrak{u}_1(x) = x^{-\frac{1}{2}-\epsilon}{}_1F_1\left(\frac{d}{2}; \frac{1}{2}-\epsilon; -\frac{g}{\gamma}x\right) \quad,\quad \mathfrak{v}_1(x) = x^{\epsilon-1}{}_0F_1\left(\epsilon; -gZx\right) \tag{3.D.6}$$

Inserting the functions from (3.D.6) then gives the exact representation of $\mathfrak{s}_1$ as a Laplace convolution, stated in (3.6.17) in the main text, where the Laplace transform is defined as

$$\overline{\mathfrak{h}}(p) := \mathscr{L}(\mathfrak{h})(p) = \int_0^{\infty} \mathrm{d}x\, \mathfrak{h}(x)\mathrm{e}^{-px} \ , \tag{3.D.7}$$

The *Laplace convolution theorem* states $(\mathfrak{u}_1 \star \mathfrak{v}_1)(t) = \mathscr{L}^{-1}\left(\overline{\mathfrak{u}}_1(p)\overline{\mathfrak{v}}_1(p)\right)(t)$.

In addition, combining the representation (3.6.17,3.D.5) with the Laplace convolution theorem gives access to the large-t asymptotics of $\mathfrak{s}_1$, via a Tauberian theorem [Fel71]: *find the small-p behaviour for $\bar{\mathfrak{u}}_1(p)$ and $\bar{\mathfrak{v}}_1(p)$ and then carry out the inverse Laplace transform.* Therefore, we use eq (3.38.1.1) from [Pru92a] and find

$$\bar{\mathfrak{u}}_1(p) = \Gamma\left(\frac{1}{2} - \epsilon\right) p^{\epsilon - \frac{1}{2}} \left(1 + \frac{g}{\gamma p}\right)^{-d/2}, \qquad \bar{\mathfrak{v}}_1(p) = \Gamma(\epsilon) p^{-\epsilon} \mathrm{e}^{-\frac{gZ}{p}} \tag{3.D.8}$$

The small-p expansion of the product $\bar{\mathfrak{u}}_1(p)\bar{\mathfrak{v}}_1(p)$ yields[9]

$$\mathfrak{s}_1 \overset{p \searrow 0}{\simeq} \sqrt{\pi t} \left(\frac{\gamma}{g}\right)^{\frac{d}{2}} \mathscr{L}^{-1}\left(p^{\frac{d-1}{2}} \mathrm{e}^{-\frac{gZ}{p}}\right)(t) \tag{3.D.9}$$

and the inverse Laplace transform can be extracted from eq (2.2.2.1) in [Pru92b]

$$\mathfrak{s}_1 \simeq \sqrt{\pi} \left(\frac{\gamma}{gt}\right)^{\frac{d}{2}} \frac{{}_0F_1\left(\frac{1-d}{2}; -gtZ\right)}{\Gamma\left(\frac{1-d}{2}\right)} \tag{3.D.10}$$

2. For $\mathfrak{s}_2$ our approach is analogous. Starting from (3.D.2), we shift variables and exchange the order of summation to arrive at

$$\mathfrak{s}_2 = -\gamma\mathcal{C}gt \sum_{n=1}^{\infty} \sum_{k=1}^{n} \Gamma\begin{bmatrix} \frac{1}{2} & \frac{d}{2} - 1 + k & & \\ n + \frac{1}{2} & \frac{d}{2} & n - k + 1 & k \end{bmatrix} \frac{1}{n} \left(-\frac{gt}{\gamma}\right)^n (\gamma Z)^{n-k}$$

$$= -\gamma\mathcal{C}gt \sum_{k=1}^{\infty} \sum_{n=k}^{\infty} \Gamma\begin{bmatrix} \frac{1}{2} & \frac{d}{2} - 1 + k & & \\ n + \frac{1}{2} & \frac{d}{2} & n - k + 1 & k \end{bmatrix} \frac{1}{n} \left(-\frac{gt}{\gamma}\right)^n (\gamma Z)^{n-k}$$

$$= -\gamma\mathcal{C}gt \sum_{k=0}^{\infty} \sum_{n=0}^{\infty} \Gamma\begin{bmatrix} \frac{1}{2} & \frac{d}{2} + k & & \\ n + 1 & \frac{d}{2} & n + k + \frac{3}{2} & k + 1 \end{bmatrix} \frac{1}{n + k + 1} \left(-\frac{gt}{\gamma}\right)^{n+k} (\gamma Z)^n$$

$$= \gamma\mathcal{C}g^2 t^2 \int_0^{\infty} \mathrm{d}v\, \mathrm{e}^{-v} \sum_{k=0}^{\infty} \sum_{n=0}^{\infty} \Gamma\begin{bmatrix} \frac{1}{2} & \frac{d}{2} + k \\ \frac{d}{2} & n + k + \frac{3}{2} \end{bmatrix} \frac{(-gt\mathrm{e}^{-v}/\gamma)^k}{k!} \frac{(-gtZ\mathrm{e}^{-v})^n}{n!} \tag{3.D.11}$$

With the definition of the Humbert function Φ_3 from above, we can also identify $\mathfrak{s}_2 = 2\mathcal{C}g^2 t^2 \int_0^1 \mathrm{d}w\, \Phi_3\left(\frac{d}{2}; \frac{3}{2}; -\frac{gt}{\gamma}w, -gtZw\right)$, as stated in (3.6.15) in the main text.

The two sums can be decoupled via the identity, with $0 < \epsilon < \frac{3}{2}$

$$\frac{1}{\Gamma\left(n + k + \frac{3}{2}\right)} = \frac{t^{\frac{1}{2} - n - k}}{\Gamma(\epsilon + n)\Gamma(\frac{3}{2} - \epsilon + k)} \int_0^t \mathrm{d}x\, x^{k - \epsilon - \frac{3}{2}} (t - x)^{n + \epsilon - 1} \tag{3.D.12}$$

such that we finally recast the double sum into an integrated convolution

$$\mathfrak{s}_2 = \mathcal{C}g^2 t^{\frac{3}{2}} \Gamma\begin{bmatrix} \frac{1}{2} & \\ \frac{3}{2} - \epsilon & \epsilon \end{bmatrix} \int_0^1 \mathrm{d}w\, (\mathfrak{u}_2 \star \mathfrak{v}_2)(t) \tag{3.D.13}$$

with

$$\mathfrak{u}_2(x) = x^{\frac{1}{2} - \epsilon}\, {}_1F_1\left(\frac{d}{2}, \frac{3}{2} - \epsilon, -\frac{g}{\gamma}wx\right) \quad , \quad \mathfrak{v}_2(x) = x^{\epsilon - 1}\, {}_0F_1\left(\epsilon, -gZwx\right) \tag{3.D.14}$$

---

[9]Here we explicitly treat the quantum case $g \neq 0$. Admitting $g = 0$ leads to a different small-p expansion that results in the well-known classical zero-temperature quench dynamics [God00]

as stated in (3.6.18) in the main text. Finally, the asymptotics for $t \to \infty$ is found as before from a Tauberian theorem. The Laplace transforms of the above functions read [Pru92a, (3.38.1.1)]

$$\bar{\mathfrak{u}}_2(p) = \Gamma\left(\frac{3}{2} - \epsilon\right) p^{\epsilon - \frac{3}{2}} \left(1 + \frac{gw}{\gamma p}\right)^{-\frac{d}{2}} \quad , \quad \bar{\mathfrak{v}}_2(p) = \Gamma(\epsilon) p^{-\epsilon} e^{-gZ\frac{w}{p}} \tag{3.D.15}$$

Inserting leads to the expression

$$\mathfrak{s}_2 = \qquad \mathcal{C}g^2\sqrt{\pi t^3}\mathscr{L}^{-1}\left(p^{\frac{d-3}{2}}\int_0^1 \mathrm{d}w \left(p + \frac{g}{\gamma}w\right)^{-\frac{d}{2}} e^{-gwZ/p}\right)(t) \tag{3.D.16}$$

The w-integration can be expressed exactly as an incomplete Gamma function [Abr64]

$$\mathfrak{s}_2 = \gamma\mathcal{C}g\sqrt{\pi t^3}(\gamma Z)^{\frac{d}{2}-1}e^{\gamma Z}\mathscr{L}^{-1}\left[\Gamma\left(1 - \frac{d}{2}, \gamma Z\right)\frac{1}{\sqrt{p}} - \frac{1}{\sqrt{p}}\Gamma\left(1 - \frac{d}{2}, Z\frac{g}{p} + \gamma Z\right)\right](t) \tag{3.D.17}$$

Since we now want to study this expression in the $p \to 0$ limit, it is adequate to use an asymptotic expansion for the last term, which we extract from eq [Abr64, (6.5.30)]

$$\Gamma(a, x+y) \overset{x\to\infty}{\simeq} \Gamma(a,x) - e^{-x}x^{a-1}\left(1 - e^{-y}\right) \tag{3.D.18}$$

In order to evaluate the inverse Laplace transform, we consult eqs (2.2.2.1), (3.10.2.2) and (2.1.1.3) in [Pru92b] and find

$$\mathfrak{s}_2 \simeq \gamma\mathcal{C}gt\left\{\frac{{}_1F_1\left(1; 2 - \frac{d}{2}; \gamma Z\right)}{\frac{d}{2} - 1} + \sqrt{\pi}\left(\frac{\gamma}{gt}\right)^{\frac{d}{2}-1}\left[\frac{{}_1F_2\left(1 - \frac{d}{2}; 2 - \frac{d}{2}, \frac{3-d}{2}; -gtZ\right)}{\left(1 - \frac{d}{2}\right)\Gamma\left(\frac{3-d}{2}\right)} e^{\gamma Z}\right.\right.$$

$$\left.\left. + \frac{e^{\gamma Z} - 1}{gtZ}\frac{{}_0F_1\left(\frac{1-d}{2}; -gtZ\right)}{\Gamma\left(1 - \frac{d}{2}\right)}\right]\right\} \tag{3.D.19}$$

Finally, combining eqs (3.D.10,3.D.19) and inserting into the constraint (3.6.13), we arrive at the asymptotic form (3.6.19) of the spherical constraint.

Similar methods can be applied to find the asymptotics of several confluents of Appell's hypergeometric function F_3 [App26, Sri85], when both arguments become large as we show in the following chapter.
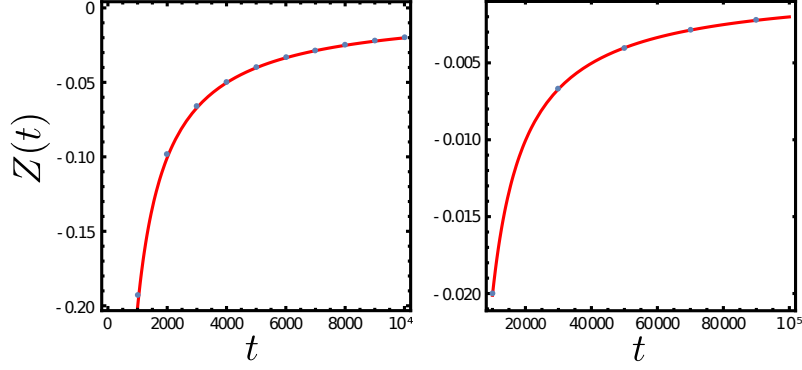
Figure 3.12: Solution $Z(t)$ of the spherical constraint for $d = 2$, $g = 0.1$, $\gamma = 1$ and $\mathcal{C} = 1/4$. The full curve is from (3.E.5) and the dots are numerical data. The left and right panel display different intervals for t.

3.E Spherical constraint in two spatial dimensions

The constraint (3.6.13) requires a special analysis in two spatial dimensions, due to apparent divergences in eq (3.D.19) for $d \to 2$. We carry this out by writing $d = 2(1 + \varepsilon)$ and studying the limit $\varepsilon \to 0$. We want to show that eq (3.D.19) is indeed well-defined in the $d \to 2$ limit and to find this limit.

The critical sum is $\mathfrak{s}_2$, which is straightforwardly written as

$$\mathfrak{s}_2 \simeq \mathcal{C}gt\gamma \left[e^{\gamma Z} \left(\frac{1}{\varepsilon} - \frac{{}_1F_2\left(-\varepsilon; 1, \frac{1}{2}; -gtZ\right)}{\varepsilon} \right) + \frac{e^{\gamma Z} - 1}{gtZ} \sqrt{\pi} \, \frac{{}_0F_1\left(-\frac{1}{2}; -gtZ\right)}{\Gamma\left(-\frac{1}{2}\right)} \right] \tag{3.E.1}$$

The limit where ε goes to zero can be taken using the formula

$$\lim_{\varepsilon \to 0} \left(\frac{1}{\varepsilon} - \frac{{}_1F_2\left(-\varepsilon; 1, \frac{1}{2}; x\right)}{\varepsilon} \right) = 2x \, {}_2F_3\left(1, 1; \frac{3}{2}, 2, 2; x\right) \tag{3.E.2}$$

and renders the sum $\mathfrak{s}_2$ into the form

$$\mathfrak{s}_2 \simeq \mathcal{C}gt\gamma \left[-e^{\gamma Z} 2gtZ \, {}_2F_3\left(1, 1; \frac{3}{2}, 2, 2; -gtZ\right) - 2\frac{e^{\gamma Z} - 1}{gtZ} \, {}_0F_1\left(-\frac{1}{2}; -gtZ\right) \right] \tag{3.E.3}$$

Recalling (3.D.10), we can now study the constraint (3.6.13) in $2D$. Solving the spherical constraint numerically, see fig 3.12, we remark that the observations $Z = -|Z| < 0$ and $Z \to 0$ still hold true in the long-time limit $t \to \infty$. However, an asymptotic expansion for $t|Z| \to \infty$ fails. Therefore, we must consider $t|Z| =: \varphi \to$ cst. and proceed to determine this constant. Asymptotically, the constraint (3.6.13) reads

$$8\pi\gamma t \simeq 1 - \sqrt{\frac{1}{4t}\frac{\gamma}{g}} \, {}_0F_1\left(-\frac{1}{2}; g\varphi\right) + \mathcal{C}g\gamma t \left[2g\varphi \, {}_2F_3\left(1, 1; \frac{3}{2}, 2, 2; g\varphi\right) - \frac{2\gamma}{gt} \, {}_0F_1\left(-\frac{1}{2}; g\varphi\right) \right] \tag{3.E.4}$$

where we replaced $e^{\gamma Z} \mapsto 1$. We also observe that the first and the last term on the right-hand site are sub-dominant. For the constant φ we thus find the transcendental equation

$$\frac{4\pi}{\mathcal{C}g^2} = \varphi \, {}_2F_3\left(1, 1; \frac{3}{2}, 2, 2; g\varphi\right) \tag{3.E.5}$$

which is eq (3.6.22b) in the main text. It always has an unique solution since the image of the right-hand side is $\mathbb{R}^+$ and the function is monotonous. The spherical parameter then reads $Z \simeq -\varphi/t$.

In the limit of an extreme SCDL with $\mathcal{C} \to \infty$, see fig 3.4, we have simply $\varphi\mathcal{C} = 4\pi g^{-2}$. The opposite limit of an extreme SQDL with $\mathcal{C} = \frac{1}{4}$ gives an upper bound for the admissible values of φ.
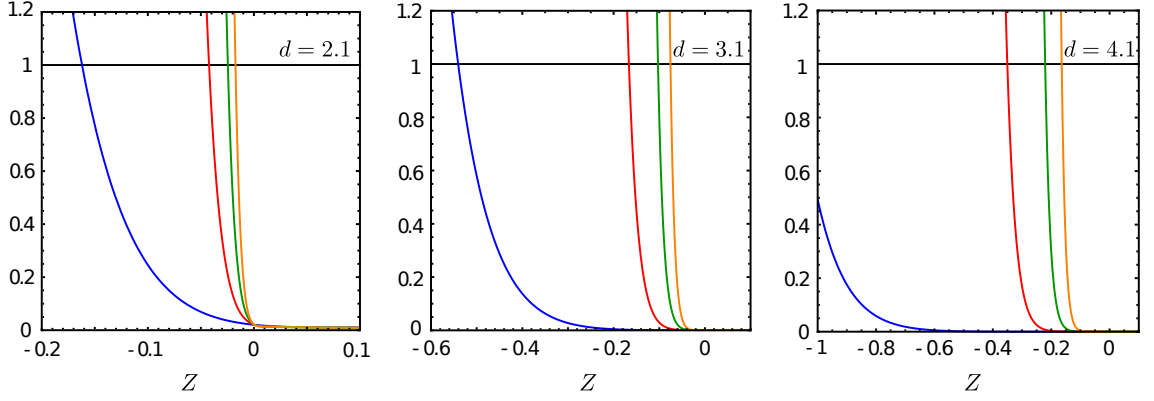
Figure 3.13: Solving the constraint eq (3.6.19) as a function of Z: the LHS is shown in black and the RHS is shown for different times $t = [1000, 4000, 7000, 10000]$ corresponding to the blue, red, green and orange lines, from left to right. The other parameters are $\mathcal{C} = 1$, $\gamma = 0.1$ and $g = 0.1$. Different frames correspond to different dimensions: left panel $d = 2.1$, middle panel $d = 3.1$, right panel $d = 4.1$.

3.F   Analysis of the spherical constraint for $d \neq 2$

We present the asymptotic analysis of the spherical constraint (3.6.19) in generic dimensions $d \neq 2$.

3.F.1 $d > 2$

In order to define the goals of an asymptotic analysis, we first consider the qualitative behaviour of the numerical solution $Z = Z(t)$, illustrated in fig 3.13. Therein, both the left-hand side (LHS) and the right-hand-side (RHS) are displayed as a function of Z, for certain values of t, and for typical values of $\mathcal{C}$, g and γ. The solution $Z = Z(t)$ is given by the intersections of the black and one of the coloured lines, respectively. For large times and for dimensions $d > 2$, the numerical examples suggest the following properties, which we shall need for our further analysis:

1. The solution to the spherical constraint is *unique* and *negative*, which is clear from fig 3.13.[10]

2. In the asymptotic limit where $t \to \infty$, the solution tends to $Z \to 0^-$. This is apparent in fig 3.13 and further shown in the left panel of fig 3.6 in the main text.

3. the decay of Z is slower than $\mathrm{O}(t^{-1})$, such that $t|Z(t)|$ still increases with t, as further illustrated in the right panel of fig 3.6.

In fig 3.6 in the main text, the time-dependence of $Z(t)$ is further illustrated for the generic spatial dimensions $d \neq 2$. The qualitative shape of these curves does not depend much on the specific values of the other parameters. Therefore, these examples suggest that the sought long-time behaviour can be obtained by studying the asymptotics for $t|Z(t)| \to \infty$ in (3.6.19), at least when $d \neq 2$. A more detailed study further suggests that this growth is more slow than any power-law.

Therefore, we need the following expansions of the various hypergeometric functions in (3.6.19)

---

[10]We have checked numerically that $Z < 0$ f or times up to $t \approx 10^{51}$.

for $t|Z(t)| \gg 1$ and $|Z(t)| \ll 1$. This is achieved by the asymptotic identities [Wol17]

$$_1F_2\left(1-\frac{d}{2};2-\frac{d}{2},\frac{3-d}{2};gt|Z|\right) \simeq -\left(1-\frac{d}{2}\right)\frac{\Gamma(\frac{3}{2}-\frac{d}{2})}{\Gamma(-\frac{1}{2})}\frac{e^{2\sqrt{gt|Z|}}}{(gt|Z|)^{1-d/4}} \tag{3.F.1a}$$

$$_0F_1\left(\frac{1-d}{2};gt|Z|\right) \simeq -\frac{\Gamma(\frac{1}{2}-\frac{d}{2})}{\Gamma(-\frac{1}{2})}(gt|Z|)^{d/4}\,e^{2\sqrt{gt|Z|}} \tag{3.F.1b}$$

$$_1F_1\left(1;2-\frac{d}{2};\gamma Z\right) \simeq 1+\frac{\gamma Z}{2-\frac{d}{2}} \tag{3.F.1c}$$

which simplify the constraint (3.6.19) to the following form

$$e^{\gamma Z}(4\pi\gamma t)^{d/2} \simeq \frac{1}{2}+\left(1+\mathcal{C}gt\gamma\left[1+\frac{1}{\gamma|Z|}\right]\right)\left(\frac{\gamma^2|Z|}{gt}\right)^{\frac{d}{4}}\frac{e^{2\sqrt{gt|Z|}}}{4}+\frac{\gamma\mathcal{C}gt}{d-2}\left[1+\frac{4}{d-4}\gamma|Z|\right] \tag{3.F.2}$$

Herein, the last term on the right-hand site is sub-dominant. We can therefore neglect it and arrive at the following final form of the constraint

$$2\,e^{\gamma Z}(4\pi\gamma t)^{d/2} \simeq \left[1+\frac{\gamma^{\frac{d}{2}}}{2}\left(1+\mathcal{C}\frac{gt}{|Z|}\right)\left(\frac{|Z|}{gt}\right)^{\frac{d}{4}}e^{2\sqrt{gt|Z|}}\right] \tag{3.F.3}$$

which is eq (3.6.22a) in the main text. As before in the toy case where $\mathcal{C}=0$ and analysed in the main text, the constraint can be solved explicitly in terms of W-functions, but some care is needed to select the correct real-valued branch [Cor96], which is either W_0 or W_{-1}, such that positive values for $|Z(t)|$ are produced. We find

$$t|Z(t)| \simeq \frac{(d-4)^2}{16g}\begin{cases} W_{-1}^2\left(\frac{2g}{d-4}\left[\frac{(8\pi)^d}{\mathcal{C}^2}\right]^{\frac{1}{d-4}}t^{2\frac{d-2}{d-4}}\right) &,\quad d<4 \\[3mm] \left(\frac{2}{d-4}\right)^2\ln^2\left(\frac{(8\pi t)^2}{\mathcal{C}}\right) &,\quad d=4 \\[3mm] W_0^2\left(\frac{2g}{d-4}\left[\frac{(8\pi)^d}{\mathcal{C}^2}\right]^{\frac{1}{d-4}}t^{2\frac{d-2}{d-4}}\right) &,\quad d>4 \end{cases} \tag{3.F.4}$$

The leading behaviour is found from the known asymptotics of the W-function[11] to be

$$|Z(t)| \simeq \frac{(d-2)^2}{4g}\frac{\ln^2 t}{t} \tag{3.F.5}$$

for all dimensions $d>2$. This asymptotic result does neither depend explicitly on the initial condition $\mathcal{C}$ nor on the coupling γ to the bath.

3.F.2 $\quad 1<d<2$

Again, we try to identify the correct mathematical setting by looking at some numerical solutions of the constraint (3.6.19). We illustrate in fig 3.14 some typical behaviour, for several values of d. Clearly, the left panel shows that for $d<2$ the qualitative behaviour is different from what was seen for $d>2$. We observe as generic features

1. For large enough times, the solution to the spherical constraint becomes *positive*.

2. In the asymptotic limit $t\to\infty$, the solution $Z(t)$ grows beyond all bounds, but its growth is very slow compared to t.

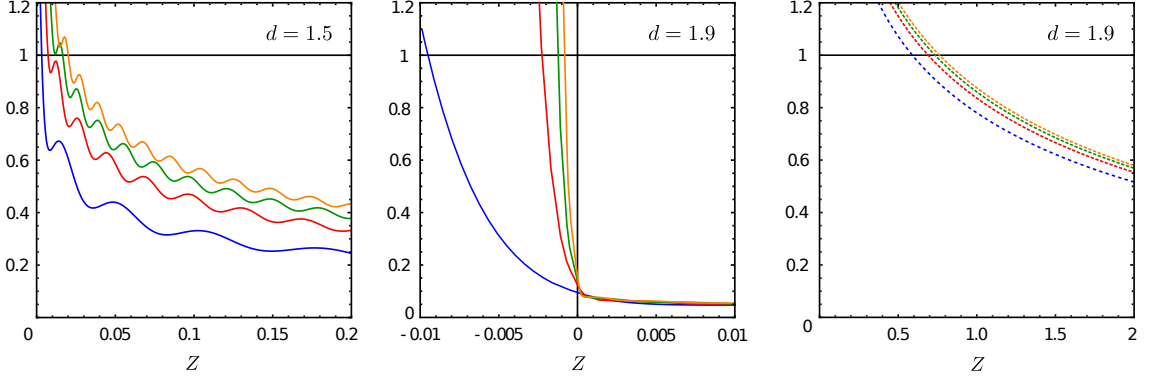[11]One uses $W_{-1}(x) \simeq \ln(-x)-\ln(-\ln(-x))+\mathrm{o}(1)$ for $x\to 0^-$ [Cor96].

Figure 3.14: Solving the constraint eq (3.6.19) as a function of Z: the LHS is shown in black and the RHS is shown for different times $t = [10000, 40000, 70000, 100000]$ corresponding to the blue, red, green and orange lines, from left to right, in the left and middle panels. In the right panel, the RHS with $t = [1, 4, 7, 10] \cdot 10^{40}$ corresponds to the blue, red, green and orange dashed lines, from left to right. The other parameters are $\mathcal{C} = 1$, $\gamma = 0.1$ and $g = 0.1$. Different frames correspond to different dimensions: left panel $d = 1.5$, middle and right panels $d = 1.9$.

3. Strong oscillations are superposed onto this growth, the frequency of whom apparently increase with t, while the amplitude decreases.

4. There is a regime of large intermediate times, where the solution $Z = -|Z(t)| < 0$ is negative and qualitatively behaves as seen above for dimensions $d > 2$. This is illustrated in the middle panel of fig 3.14, which is very similar to fig 3.13. In the right panel, it is further shown that for truly enormous times the final true asymptotic regime with $Z > 0$ is reached.

Therefore, for intermediate times, we can take over the analysis for $d > 2$ and recover eq (3.F.5) as an effective description.[12] One can estimate the order of the time-scale $t_\times$ where this crossover happens by setting $Z = 0$ in the constraint (3.6.19). For $d = 2 - \varepsilon$ dimensions, we find $t_\times \approx \frac{\gamma}{g} e^{8\pi/\mathcal{C}g}$ which for the chosen parameters can become very large indeed.

In order to find the true final asymptotics for really large values of t, we must re-analyse (3.6.19) in the limit where $t \to \infty$ and $Z \gg 1$. We then require the following asymptotic expansions [Wol17]

$$
\begin{aligned}
{}_1F_1\left(1; 2 - \frac{d}{2}; \gamma Z\right) &= \left(1 - \frac{d}{2}\right) e^{\gamma Z} (\gamma Z)^{d/2-1} \left[\Gamma\left(1 - \frac{d}{2}\right) - \Gamma\left(1 - \frac{d}{2}, \gamma Z\right)\right] \\
&\simeq \left(1 - \frac{d}{2}\right) e^{\gamma Z} (\gamma Z)^{d/2-1} \Gamma\left(1 - \frac{d}{2}\right) - \left(1 - \frac{d}{2}\right)(\gamma Z)^{-1}
\end{aligned}
\tag{3.F.6a}
$$

$$
\begin{aligned}
\frac{{}_0F_1\left(\frac{1-d}{2}; -gtZ\right)}{\Gamma(1 - d/2)} &= (gtZ)^{(d+1)/4} J_{-(d+1)/4}\left(2\sqrt{gtZ}\right) \\
&\simeq \frac{(gtZ)^{(d+1)/4}}{\pi^{1/2}} \left[\cos\left(2\sqrt{gtZ} + \frac{\pi d}{4}\right)\left(1 - \frac{d(d+2)[(d+1)^2 - 9]}{512}\frac{1}{gtZ}\right)\right. \\
&\left. - \sin\left(2\sqrt{gtZ} + \frac{\pi d}{4}\right)\frac{d(d+2)}{16}\frac{1}{\sqrt{gtZ}}\right]
\end{aligned}
\tag{3.F.6b}
$$

---

[12]Eq. (3.F.4) with $d < 4$ applies.

$$\frac{{}_1F_2\left(1-\frac{d}{2};2-\frac{d}{2},\frac{3}{2}-\frac{d}{2};-gtZ\right)}{\Gamma(\frac{3}{2}-\frac{d}{2})(1-\frac{d}{2})\pi^{-1/2}} \simeq \Gamma\left(1-\frac{d}{2}\right)(gtZ)^{d/2-1}$$

$$+\cos\left(2\sqrt{gtZ}+\frac{\pi d}{4}\right)(gtZ)^{d/4-1}\left[-1+\frac{d(d+2)(d^2-14d+56)}{512}\frac{1}{gtZ}\right]$$

$$+\sin\left(2\sqrt{gtZ}+\frac{\pi d}{4}\right)(gtZ)^{d/4-3/2}\frac{d(d-6)}{16} \tag{3.F.6c}$$

and where J_ν is a Bessel function and $\Gamma(a,x)$ an incomplete Gamma function [Abr64]. Inserting these expansions into (3.6.19), several leading terms cancel. The constraint takes the form

$$2\left(4\pi\gamma t\right)^{d/2} = \frac{\mathcal{C}gt}{Z}\,\mathrm{e}^{-\gamma Z}$$

$$+\ \frac{d\mathcal{C}\gamma^{d/2}}{2}\left(\frac{Z}{gt}\right)^{d/4-1}\left[\frac{3(d+2)(4-d)}{64}\frac{\cos\left(2\sqrt{gtZ}+\frac{\pi d}{4}\right)}{Z}-\frac{\sin\left(2\sqrt{gtZ}+\frac{\pi d}{4}\right)}{\sqrt{gtZ}}\right] \tag{3.F.7}$$

which is eq (3.6.22) in the main text. In order to solve this equation, consider first only the first term on the right-hand side. If one assumes that asymptotically $\mathrm{e}^{\gamma Z}\sim t^\alpha$, matching the left-hand side with the right-hand side gives $\alpha=1-\frac{d}{2}$. Then, the second term on the right-hand side is of the order $t^{1-d/4+\alpha}$, up to logarithmic or oscillating factors. If $\alpha<d/4$, this second term merely generates a correction. This is so for $d>\frac{4}{3}$. Similarly, the third term is of the order $t^{1/2-d/4+\alpha}$, hence it only generates a finite-time correction for $d>1$.

Hence, for $\frac{4}{3}<d<2$, it is enough to concentrate on the first term on the right-hand-side in (3.F.7). Analogously to previous cases, the constraint is solved via the Lambert-W function

$$\gamma Z = W\left(\frac{\mathcal{C}g}{2^{d+1}\pi^{d/2}}\,(\gamma t)^{1-d/2}\right) \simeq \left(1-\frac{d}{2}\right)\ln\gamma t+\mathrm{O}(\ln\ln t) \tag{3.F.8}$$

For a better approximation, one can re-inject this solution into the second and third terms on the right-hand-side of (3.F.7). Then one obtains an oscillatory correction, of the form quoted in the main text.

Chapter 4

On the asymptotics of hypergeometric functions in two variables

4.1 Introduction and definitions

This chapter presents a mathematical analysis of the asymptotics of certain confluents of the Appell hypergeometric function F_3 in two variables. This work is contained in [Wal17a].

Hypergeometric functions, usually denoted by $_pF_q(z)$, and of which Gauss' hypergeometric function $_2F_1(z)$ is the most important special case, have been studied very thoroughly and have found numerous applications in almost all fields of science, see e.g. [Bai32, Bat53, Mat73, Abr64, Sla66, Buc69, Ask92, Olv10, Mat10] and references therein. A little more than a century old, hypergeometric functions of two variables [App80a, App80b, App80c, App26, Hum20, Hum22] have also received a lot of scientific interest and recently, many new applications in many different fields of mathematics and physics are being discovered see for example [Fle03, Shp07, Kni12]. It is often convenient to define these functions via double power series. Most of the mathematical studies of these functions are either focussed on the analysis of domains of convergence, or on relating special cases to other known functions or else to derive functional relationships between different hypergeometric functions of two variables, see e.g. [App26, Bat53, Bat54, Sri85, Olv10, Cho11, Liu14, Bry17a, Bry17b]. Relatively little seems yet to be known on the asymptotic behaviour of such double series, in contrast to the classic study of Wright [Wri35, Wri40, Wri52] on the asymptotics of $_pF_q(z)$ when $|z| \to \infty$. Here, we shall present results on the leading asymptotics of some hypergeometric functions when the absolute values of both variables become large simultaneously. The main tool to derive these are Eulerian and (inverse) Laplacian integral representations, and a Tauberian theorem [Wid46, Fel71]. The results are stated as theorems in section 4.3, see eqs (4.3.1, 4.3.2, 4.3.3, 4.3.6, 4.3.8).

We shall consider the third Appell series F_3

$$F_3(\alpha, \alpha', \beta, \beta'; \gamma; x, y) = \sum_{m=0}^{\infty} \sum_{n=0}^{\infty} \frac{(\alpha)_m (\beta)_m (\alpha')_n (\beta')_n}{(\gamma)_{n+m}} \frac{x^m}{m!} \frac{y^n}{n!} \tag{4.1.1}$$

where $(\alpha)_m = \Gamma(\alpha + m)/\Gamma(\alpha)$ denotes the Pochhammer symbol for $-\alpha \notin \mathbb{N}$. We shall also study

the confluent forms (Humbert functions)

$$\Xi_1(\alpha, \alpha', \beta; \gamma; x, y) = \sum_{m=0}^{\infty} \sum_{n=0}^{\infty} \frac{(\alpha)_m (\beta)_m (\alpha')_n}{(\gamma)_{m+n}} \frac{x^m}{m!} \frac{y^n}{n!} \tag{4.1.2a}$$

$$\Xi_2(\alpha, \alpha'; \gamma; x, y) = \sum_{m=0}^{\infty} \sum_{n=0}^{\infty} \frac{(\alpha)_m (\beta)_m}{(\gamma)_{m+n}} \frac{x^m}{m!} \frac{y^n}{n!} \tag{4.1.2b}$$

$$\Phi_2(\beta, \beta'; \gamma; x, y) = \sum_{m=0}^{\infty} \sum_{n=0}^{\infty} \frac{(\beta)_m (\beta')_n}{(\gamma)_{m+n}} \frac{x^m}{m!} \frac{y^n}{n!} \tag{4.1.2c}$$

$$\Phi_3(\beta; \gamma; x, y) = \sum_{m=0}^{\infty} \sum_{n=0}^{\infty} \frac{(\beta)_m}{(\gamma)_{m+n}} \frac{x^m}{m!} \frac{y^n}{n!} \ . \tag{4.1.2d}$$

Throughout, we shall implicitly assume that the parameters $\alpha, \alpha', \beta, \beta', \gamma, \ldots$ are such that any singularity in the coefficients is avoided, without restating this explicitly. While the series F_3 converges for $\max(|x|, |y|) < 1$, the series Ξ_1 and Ξ_2 converge for $|x| < 1$ and $|y| < \infty$ and Φ_2 and Φ_3 converge for $|x| < \infty$ and $|y| < \infty$ [Sri85]. For reduction formulæ to hypergeometric functions of a single variable, see [Bry17a, Bry17b]. We shall also be interested in the series

$$\Phi_2^{(i)}(\beta, \beta'; \gamma, \lambda; x, y) := \sum_{m=0}^{\infty} \sum_{n=0}^{\infty} \frac{(\beta)_m (\beta')_n}{(\gamma)_{m+n}} \frac{1}{m+n+\lambda} \frac{x^m}{m!} \frac{y^n}{n!} \tag{4.1.3a}$$

$$\Phi_3^{(i)}(\beta; \gamma, \lambda; x, y) := \sum_{m=0}^{\infty} \sum_{n=0}^{\infty} \frac{(\beta)_m}{(\gamma)_{m+n}} \frac{1}{m+n+\lambda} \frac{x^m}{m!} \frac{y^n}{n!} \tag{4.1.3b}$$

which for $-\lambda \notin \mathbb{N}$ converge for $|x| < \infty$ and $|y| < \infty$. Clearly, for $\lambda = \gamma$, one has

$$\Phi_2^{(i)}(\beta, \beta'; \gamma, \gamma; x, y) = \frac{1}{\gamma} \Phi_2(\beta, \beta'; \gamma + 1; x, y) \ , \ \ \Phi_3^{(i)}(\beta; \gamma, \gamma; x, y) = \frac{1}{\gamma} \Phi_3(\beta; \gamma + 1; x, y) \tag{4.1.4}$$

and for $\lambda = 1$ these series may be rewritten as Kampé de Fériet series [Sri85]

$$\Phi_3^{(i)}(\beta; \gamma, 1; x, y) = \int_0^1 \mathrm{d}w \ \Phi_3(\beta; \gamma; xw, yw) = F_{2;0;0}^{1;1;0} \left(\begin{array}{ccc} (1); & (\beta); & - \\ (\gamma, 2); & -; & - \end{array} \middle| x, y \right) \tag{4.1.5a}$$

$$\Phi_2^{(i)}(\beta, \beta'; \gamma, 1; x, y) = \int_0^1 \mathrm{d}w \ \Phi_2(\beta, \beta'; \gamma; xw, yw) = F_{2;0;0}^{1;1;1} \left(\begin{array}{ccc} (1); & (\beta); & (\beta') \\ (\gamma, 2); & -; & - \end{array} \middle| x, y \right) \tag{4.1.5b}$$

such that $\Phi_2^{(i)}$, $\Phi_3^{(i)}$ might be called 'integrated Humbert functions'. We are interested in situations where both $|x|$ and $|y|$ become large. We shall therefore substitute $x \mapsto tx$ and $y \mapsto ty$ and study the limit $t \to \infty$ where $x, y \in \mathbb{R}$ will be kept fixed and non-zero.

In section 4.2 the integral and inverse Laplace representations of the Humbert functions and integrated Humbert functions are derived, which will be used in section 4.3 to derive the asymptotic forms. Section 4.4 briefly outlines an application to many-body quantum dynamics and the connection to chapter 3.

4.2   Integral representations

The starting point for the derivation of the asymptotics of the series (4.1.1, 4.1.2) will the following Eulerian integral representations. Throughout, the parameters $\alpha, \beta, \gamma \ldots$ of the functions, as well as x, y, are assumed constants and such that all series and integrals considered exist.

Lemma 1. *The functions defined in (4.1.1, 4.1.2) have the integral representations*[1]

$$\Phi_3(\beta;\gamma;tx,ty) = \Gamma\begin{bmatrix}\gamma\\\gamma-\varepsilon\ \varepsilon\end{bmatrix}\int_0^\infty \mathrm{d}u\frac{u^{\varepsilon-1}}{(1+u)^\gamma}\,{}_1F_1\left(\beta;\gamma-\varepsilon;\frac{tx}{1+u}\right){}_0F_1\left(\varepsilon;\frac{tyu}{1+u}\right)$$

$$(4.2.1a)$$

$$\Phi_2(\beta,\beta';\gamma;tx,ty) = \Gamma\begin{bmatrix}\gamma\\\gamma-\varepsilon\ \varepsilon\end{bmatrix}\int_0^\infty \mathrm{d}u\frac{u^{\varepsilon-1}}{(1+u)^\gamma}\,{}_1F_1\left(\beta;\gamma-\varepsilon;\frac{tx}{1+u}\right){}_1F_1\left(\beta';\varepsilon;\frac{tyu}{1+u}\right)$$

$$(4.2.1b)$$

$$\Xi_2(\alpha,\beta;\gamma;tx,ty) = \Gamma\begin{bmatrix}\gamma\\\gamma-\varepsilon\ \varepsilon\end{bmatrix}\int_0^\infty \mathrm{d}u\frac{u^{\varepsilon-1}}{(1+u)^\gamma}\,{}_2F_1\left(\alpha,\beta;\gamma-\varepsilon;\frac{tx}{1+u}\right){}_0F_1\left(\varepsilon;\frac{tyu}{1+u}\right)$$

$$(4.2.1c)$$

$$\Xi_1(\alpha,\beta,\beta';\gamma;tx,ty) = \Gamma\begin{bmatrix}\gamma\\\gamma-\varepsilon\ \varepsilon\end{bmatrix}\int_0^\infty \mathrm{d}u\frac{u^{\varepsilon-1}}{(1+u)^\gamma}\,{}_2F_1\left(\alpha,\beta;\gamma-\varepsilon;\frac{tx}{1+u}\right){}_1F_1\left(\beta';\varepsilon;\frac{tyu}{1+u}\right)$$

$$(4.2.1d)$$

$$F_3(\alpha,\alpha',\beta,\beta';\gamma;tx,ty) = \Gamma\begin{bmatrix}\gamma\\\gamma-\varepsilon\ \varepsilon\end{bmatrix}\int_0^\infty \mathrm{d}u\frac{u^{\varepsilon-1}}{(1+u)^\gamma}\,{}_2F_1\left(\alpha,\beta;\gamma-\varepsilon;\frac{tx}{1+u}\right){}_2F_1\left(\alpha',\beta';\varepsilon;\frac{tyu}{1+u}\right)$$

$$(4.2.1e)$$

and where ε is a fixed constant, which satisfies $0 < \varepsilon < \gamma$.

Proof: We illustrate the technique for the example $\Phi_2 = \Phi_2(\beta,\beta';\gamma;tx,ty)$. The double series (4.1.2c) is decoupled by using the decomposition $m+n+\gamma = (m+\gamma-\varepsilon)+(n+\varepsilon)$ and the identity [Abr64, (6.2.1)] involving the Euler Beta function

$$\frac{1}{\Gamma(m+n+\gamma)} = \frac{1}{\Gamma(n+\varepsilon)\Gamma(m+\gamma-\varepsilon)}\frac{\Gamma(n+\varepsilon)\Gamma(m+\gamma-\varepsilon)}{\Gamma(m+n+\gamma)}$$

$$= \frac{1}{\Gamma(n+\varepsilon)\Gamma(m+\gamma-\varepsilon)}\int_0^\infty \mathrm{d}u\,\frac{u^{n+\varepsilon-1}}{(1+u)^{m+n+\gamma}} \qquad (4.2.2)$$

Inserting this into the definition (4.1.2c) gives, because the series are absolutely convergent

$$\Phi_2 = \int_0^\infty \mathrm{d}u \sum_{m=0}^\infty \sum_{n=0}^\infty \frac{\Gamma(\gamma)(\beta)_m}{\Gamma(m+\gamma-\varepsilon)}\frac{(\beta')_n}{\Gamma(n+\varepsilon)}\frac{1}{m!\,n!}\left(\frac{xt}{1+u}\right)^m\left(\frac{ytu}{1+u}\right)^n\frac{u^{\varepsilon-1}}{(1+u)^\gamma}$$

$$= \Gamma\begin{bmatrix}\gamma\\\gamma-\varepsilon\ \varepsilon\end{bmatrix}\int_0^\infty \mathrm{d}u\frac{u^{\varepsilon-1}}{(1+u)^\gamma}\sum_{m=0}^\infty \frac{(\beta)_m}{(\gamma-\varepsilon)_m\,m!}\left(\frac{xt}{1+u}\right)^m\sum_{n=0}^\infty\frac{(\beta')_n}{(\gamma-\varepsilon)_n\,n!}\left(\frac{ytu}{1+u}\right)^n$$

$$= \Gamma\begin{bmatrix}\gamma\\\gamma-\varepsilon\ \varepsilon\end{bmatrix}\int_0^\infty \mathrm{d}u\frac{u^{\varepsilon-1}}{(1+u)^\gamma}\,{}_1F_1\left(\beta;\gamma-\varepsilon;\frac{tx}{1+u}\right){}_1F_1\left(\beta';\varepsilon;\frac{tyu}{1+u}\right)$$

as asserted in (4.2.1b). The other identities (4.2.1) are proven similarly. $\qquad\square$

Comment 1. Eqs. (4.2.1) are not immediately useful for obtaining the $t\to\infty$ asymptotics, since a naïve substitution of the asymptotic forms of the ${}_pF_q$ would lead to divergent integrals.

---

[1]We use throughout the notation $\Gamma\begin{bmatrix}a_1\ \cdots\ a_n\\b_1\ \cdots\ b_m\end{bmatrix} = \frac{\Gamma(a_1)\cdots\Gamma(a_n)}{\Gamma(b_1)\cdots\Gamma(b_m)}$.

Comment 2. Recall the following definitions of further double hypergeometric series [Sri85]

$$F_2(a, b, b'; c, c'; x, y) = \sum_{m=0}^{\infty} \sum_{n=0}^{\infty} \frac{(a)_{m+n}(b)_m(b')_n}{(c)_m(c')_n} \frac{x^m}{m!} \frac{y^n}{n!} \tag{4.2.3a}$$

$$\Psi_1(a, b; c, c'; x, y) = \sum_{m=0}^{\infty} \sum_{n=0}^{\infty} \frac{(a)_{m+n}(b)_m}{(c)_m(c')_n} \frac{x^m}{m!} \frac{y^n}{n!} \tag{4.2.3b}$$

$$\Psi_2(a; c, c'; x, y) = \sum_{m=0}^{\infty} \sum_{n=0}^{\infty} \frac{(a)_{m+n}}{(c)_m(c')_n} \frac{x^m}{m!} \frac{y^n}{n!} \tag{4.2.3c}$$

By using $\Gamma(z) = \int_0^\infty \mathrm{d}u\, u^{z-1} e^{-u}$, one may derive in a way similar to Lemma 1 the identities

$$F_2(a, b, b'; c, c'; x, y) = \frac{1}{\Gamma(a)} \int_0^\infty \mathrm{d}u\, e^{-u}\, u^{a-1}\, {}_1F_1(b; c; xu) {}_1F_1(b'; c'; yu) \tag{4.2.4a}$$

$$\Psi_1(a, b; c, c'; x, y) = \frac{1}{\Gamma(a)} \int_0^\infty \mathrm{d}u\, e^{-u}\, u^{a-1}\, {}_1F_1(b; c; xu) {}_0F_1(c'; yu) \tag{4.2.4b}$$

$$\Psi_2(a; c, c'; x, y) = \frac{1}{\Gamma(a)} \int_0^\infty \mathrm{d}u\, e^{-u}\, u^{a-1}\, {}_0F_1(c; xu) {}_0F_1(c'; yu) \tag{4.2.4c}$$

see also [Sri85, (9.4.29)]. However, there is no known way to render these as convolutions, which will become our main tool to analyse the $t \to \infty$ asymptotics of the functions in Lemma 1.
In the next lemma, we shall use the short-hand $\Phi_3 := \Phi_3(\beta; \gamma; xt, yt)$ and similarly for the other functions defined in (4.1.1, 4.1.2).

Lemma 2. *The integral representations (4.2.1) for the functions in (4.1.1,4.1.2) take the form*

$$\Phi_3 = \Gamma \begin{bmatrix} \gamma \\ \gamma-\varepsilon\ \varepsilon \end{bmatrix} t^{1-\gamma} \int_0^t \mathrm{d}v\, v^{\gamma-\varepsilon-1}\, {}_1F_1\left(\beta; \gamma-\varepsilon; xv\right)\, {}_0F_1\left(\varepsilon; y(t-v)\right)(t-v)^{\varepsilon-1} \tag{4.2.5a}$$

$$\Phi_2 = \Gamma \begin{bmatrix} \gamma \\ \gamma-\varepsilon\ \varepsilon \end{bmatrix} t^{1-\gamma} \int_0^t \mathrm{d}v\, v^{\gamma-\varepsilon-1}\, {}_1F_1\left(\beta; \gamma-\varepsilon; xv\right)\, {}_1F_1\left(\beta'; \varepsilon; y(t-v)\right)(t-v)^{\varepsilon-1} \tag{4.2.5b}$$

$$\Xi_2 = \Gamma \begin{bmatrix} \gamma \\ \gamma-\varepsilon\ \varepsilon \end{bmatrix} t^{1-\gamma} \int_0^t \mathrm{d}v\, v^{\gamma-\varepsilon-1}\, {}_2F_1\left(\alpha, \beta; \gamma-\varepsilon; xv\right)\, {}_0F_1\left(\varepsilon; y(t-v)\right)(t-v)^{\varepsilon-1} \tag{4.2.5c}$$

$$\Xi_1 = \Gamma \begin{bmatrix} \gamma \\ \gamma-\varepsilon\ \varepsilon \end{bmatrix} t^{1-\gamma} \int_0^t \mathrm{d}v\, v^{\gamma-\varepsilon-1}\, {}_2F_1\left(\alpha, \beta; \gamma-\varepsilon; xv\right)\, {}_1F_1\left(\beta'; \varepsilon; y(t-v)\right)(t-v)^{\varepsilon-1} \tag{4.2.5d}$$

$$F_3 = \Gamma \begin{bmatrix} \gamma \\ \gamma-\varepsilon\ \varepsilon \end{bmatrix} t^{1-\gamma} \int_0^t \mathrm{d}v\, v^{\gamma-\varepsilon-1}\, {}_2F_1\left(\alpha, \beta; \gamma-\varepsilon; xv\right)\, {}_2F_1\left(\alpha', \beta'; \varepsilon; y(t-v)\right)(t-v)^{\varepsilon-1} \tag{4.2.5e}$$

and where ε is a fixed constant, which satisfies $0 < \varepsilon < \gamma$.[2]

Proof. To be specific, we present but the example of Φ_2. Indeed, the change of variables $v = t/(1+u)$ transforms (4.2.1b) into (4.2.5b). The other functions are treated similarly. □

In consequence, if we use $\mathscr{F}$ as a generic symbol for any of the functions in (4.2.5), one has

$$\mathscr{F} = \Gamma \begin{bmatrix} \gamma \\ \gamma-\varepsilon\ \varepsilon \end{bmatrix} t^{1-\gamma} \int_0^t \mathrm{d}v\, \mathscr{F}_1(v)\mathscr{F}_2(t-v) = \Gamma \begin{bmatrix} \gamma \\ \gamma-\varepsilon\ \varepsilon \end{bmatrix} t^{1-\gamma} \mathscr{L}^{-1}\left(\overline{\mathscr{F}_1(p)}\,\overline{\mathscr{F}_2(p)}\right)(t) \tag{4.2.6}$$

where $\overline{f}(p) = \mathscr{L}\left(f(v)\right)(p) = \int_0^\infty \mathrm{d}v e^{-pv} f(v)$ denotes the Laplace transform. The functions $\mathscr{F}_{1,2}(v)$ are readily read off from eqs (4.2.5) and are listed in tab 4.1.

---

[2]Eq (4.2.5e) was already given in [Sri85, (9.4.16)].

Table 4.1: Functions $\mathscr{F}_1$ and $\mathscr{F}_2$ that are contained in the convolution integral of the Humbert functions.

function	$\mathscr{F}_1(v)$	$\mathscr{F}_2(v)$
Φ_3	$v^{\gamma-\varepsilon-1}\,{}_1F_1\left(\beta;\gamma-\varepsilon;xv\right)$	$v^{\varepsilon-1}\,{}_0F_1\left(\varepsilon;yv\right)$
Φ_2	$v^{\gamma-\varepsilon-1}\,{}_1F_1\left(\beta;\gamma-\varepsilon;xv\right)$	$v^{\varepsilon-1}\,{}_1F_1\left(\beta';\varepsilon;yv\right)$
Ξ_2	$v^{\gamma-\varepsilon-1}\,{}_2F_1\left(\alpha,\beta;\gamma-\varepsilon;xv\right)$	$v^{\varepsilon-1}\,{}_0F_1\left(\varepsilon;yv\right)$
Ξ_1	$v^{\gamma-\varepsilon-1}\,{}_2F_1\left(\alpha,\beta;\gamma-\varepsilon;xv\right)$	$v^{\varepsilon-1}\,{}_1F_1\left(\beta';\varepsilon;yv\right)$
F_3	$v^{\gamma-\varepsilon-1}\,{}_2F_1\left(\alpha,\beta;\gamma-\varepsilon;xv\right)$	$v^{\varepsilon-1}\,{}_2F_1\left(\alpha',\beta';\varepsilon;yv\right)$

Table 4.2: Laplace Transforms of the convolution integrals from Lemma 2. <u>Note</u>: the entries for Φ_2 and Φ_3 are contained in [Bat54].

function $\mathscr{F}(t)$	Laplace transform $\overline{\mathscr{F}(t)}(p)$
$t^{\gamma-1}\,\Phi_3(\beta;\gamma;-xt,-yt)$	$\Gamma(\gamma)\,p^{\beta-\gamma}(p+x)^{-\beta}e^{-y/p}$
$t^{\gamma-1}\,\Phi_2(\beta,\beta';\gamma;-xt,-yt)$	$\Gamma(\gamma)\,p^{\beta+\beta'-\gamma}(p+x)^{-\beta}(p+y)^{-\beta'}$
$t^{\gamma-1}\,\Xi_2(\alpha,\beta;\gamma;-xt,-yt)$	$\Gamma(\gamma)\,x^{-\alpha}p^{\alpha-\gamma}U(\alpha;1+\alpha-\beta;p/x)e^{-y/p}$
$t^{\gamma-1}\,\Xi_1(\alpha,\beta,\beta';\gamma;-xt,-yt)$	$\Gamma(\gamma)\,x^{-\alpha}p^{\alpha+\beta'-\gamma}(p+y)^{-\beta'}U(\alpha;1+\alpha-\beta;p/x)$
$t^{\gamma-1}\,F_3(\alpha,\alpha',\beta,\beta';\gamma;-xt,-yt)$	$\Gamma(\gamma)\,\dfrac{p^{\alpha+\alpha'-\gamma}}{x^\alpha y^{\alpha'}}U(\alpha;1+\alpha-\beta;\tfrac{p}{x})U(\alpha';1+\alpha'-\beta';\tfrac{p}{y})$

Next, we require the following list of Laplace transforms, taken from [Pru92a, eqs 3.38.1.1, 3.35.1.3, 3.38.1.1, 3.37.1.2] combined with [Abr64, eqs (13.1.10, 13.1.33)]

$$\mathscr{L}\left(v^{a-1}\,{}_0F_1\left(a;-yv\right)\right)(p) = \Gamma(a)p^{-a}e^{-y/p} \tag{4.2.7a}$$

$$\mathscr{L}\left(v^{b-1}\,{}_1F_1\left(a;b;-yv\right)\right)(p) = \Gamma(b)p^{a-b}(p+y)^{-a} \tag{4.2.7b}$$

$$\mathscr{L}\left(v^{c-1}\,{}_2F_1\left(a,b;c;-yv\right)\right)(p) = \Gamma(c)p^{a-c}y^{-a}U\left(a;1+a-b;\frac{p}{y}\right) \tag{4.2.7c}$$

where U denotes the Tricomi function [Abr64]. Combining these with the integral forms (4.2.6) gives

Lemma 3. *The Laplace transforms of the functions in Lemma 2 are given by the tab 4.2, where U denotes the Tricomi function.*

Corollary 1. Applying eq (4.2.2), the Kampé de Fériet series

$$F_{1;q;q'}^{0;p;p'}\left(\begin{matrix}-;&(\alpha_p);&(\alpha_{p'}')\\\gamma;&(\beta_q);&(\beta_{q'}')\end{matrix}\,\middle|\,-tx,-ty\right) = \sum_{m,n=0}^{\infty}\frac{(\alpha_1)_m\cdots(\alpha_p)_m}{(\beta_1)_m\cdots(\beta_q)_m}\frac{(\alpha_1')_n\cdots(\alpha_{p'}')_n}{(\beta_1')_n\cdots(\beta_{q'}')_n}\frac{(-t)^{m+n}}{(\gamma)_{m+n}}\frac{x^m}{m!}\frac{y^n}{n!}$$

$$= \Gamma\begin{bmatrix}\gamma\\\gamma-\varepsilon\;\varepsilon\end{bmatrix}\int_0^\infty du\,\frac{u^{\varepsilon-1}}{(1+u)^\gamma}\,{}_pF_{q+1}\left(\begin{matrix}\alpha_1,\ldots,\alpha_p\\\beta_1,\ldots,\beta_q,\gamma-\varepsilon\end{matrix};\frac{-tx}{1+u}\right)\,{}_{p'}F_{q'+1}\left(\begin{matrix}\alpha_1',\ldots,\alpha_{p'}'\\\beta_1',\ldots,\beta_{q'}',\varepsilon\end{matrix};\frac{-tyu}{1+u}\right)$$

$$= \Gamma(\gamma)t^{1-\gamma}\mathscr{L}^{-1}\left(s^{-\gamma}\,{}_pF_q\left((\alpha_p);(\beta_q);-\frac{x}{s}\right)\,{}_{p'}F_{q'}\left((\alpha_{p'}');(\beta_{q'}');-\frac{y}{s}\right)\right)(t) \tag{4.2.8}$$

contains all functions treated here explicitly as special cases. For the derivation of (4.2.8), we used the identity [Pru92a, (3.38.1.1)]

$$\mathscr{L}\left(v^{\mu-1}\,_pF_{q+1}\left((a_p);(b_q),\mu;-\omega v\right)\right)(s) = \Gamma(\mu)s^{-\mu}\,_pF_q\left((a_p);(b_q);-\frac{\omega}{s}\right) \tag{4.2.9}$$

For $q = q' = 0$ and $p = p'$, eq (4.2.8) reduces to the Lauricella function $F_B^{(p)}$ in two variables. Furthermore, for $p = p' = q = q' = 0$, one has an addition theorem

$$_0F_1(\gamma; x+y) = \sum_{m,n=0}^{\infty}\frac{1}{(\gamma)_{m+n}}\frac{x^m}{m!}\frac{y^n}{n!}$$

$$= \Gamma\left[\begin{matrix}\gamma\\\gamma-\varepsilon\ \varepsilon\end{matrix}\right]\int_0^{\infty}\mathrm{d}u\,\frac{u^{\varepsilon-1}}{(1+u)^{\gamma}}\,_0F_1\left(\gamma-\varepsilon;\frac{x}{1+u}\right)\,_0F_1\left(\varepsilon;\frac{yu}{1+u}\right) \tag{4.2.10}$$

We now turn to the variants $\Phi_3^{(i)}$ and $\Phi_2^{(i)}$ defined in eq (4.1.3). Since $\Phi_2^{(i)}$ is symmetric under the permutation $(x,\beta)\leftrightarrow(y,\beta')$, we can set $x > y$ without restriction of the generality.

Lemma 4. *The following integral representations of the functions (4.1.3) hold, with $x > y$ for $\Phi_2^{(i)}$ and $x = y$ for the symmetric function $\Phi_2^{(i,s)}$*

$$\Phi_3^{(i)} = \Phi_3^{(i)}(\beta;\gamma,1;-tx,-ty) = \int_0^1\mathrm{d}w\,\Phi_3(\beta;\gamma;-txw,-tyw)$$

$$= \Gamma\left[\begin{matrix}\gamma\\\gamma-\varepsilon\ \varepsilon\end{matrix}\right]\int_0^1\mathrm{d}w\int_0^{\infty}\mathrm{d}u\,\frac{u^{\varepsilon-1}}{(1+u)^{\gamma}}\,_1F_1\left(\beta;\gamma-\varepsilon;-\frac{txw}{1+u}\right)\,_0F_1\left(\varepsilon;-\frac{tywu}{1+u}\right)$$

$$= \Gamma(\gamma)t^{1-y}\frac{e^{y/x}}{x}\left(\frac{y}{x}\right)^{\beta-1}\mathscr{L}^{-1}\left(p^{1-\gamma}\left[\Gamma\left(1-\beta,\frac{y}{x}\right)-\Gamma\left(1-\beta,\frac{y}{x}+\frac{y}{p}\right)\right]\right)(t) \tag{4.2.11a}$$

$$\Phi_2^{(i)} = \Phi_2^{(i)}(\beta,\beta';\gamma,1;-tx,-ty) = \int_0^1\mathrm{d}w\,\Phi_2(\beta,\beta';\gamma;-txw,-tyw)$$

$$= \Gamma\left[\begin{matrix}\gamma\\\gamma-\varepsilon\ \varepsilon\end{matrix}\right]\int_0^1\mathrm{d}w\int_0^{\infty}\mathrm{d}u\,\frac{u^{\varepsilon-1}}{(1+u)^{\gamma}}\,_1F_1\left(\beta;\gamma-\varepsilon;-\frac{txw}{1+u}\right)\,_1F_1\left(\beta';\varepsilon;-\frac{tywu}{1+u}\right)$$

$$= \frac{\Gamma(\gamma)t^{1-\gamma}x^{\beta'-1}}{(1-\beta)(x-y)^{-\beta'}}\mathscr{L}^{-1}\left(p^{\beta+\gamma}(p+x)^{1-\beta}\,_2F_1\left(1-\beta,\beta';2-\beta;-\frac{(p+x)y}{p(x-y)}\right)\right.$$

$$\left.-p^{1-\gamma}\,_2F_1\left(1-\beta,\beta';2-\beta;-\frac{y}{(x-y)}\right)\right)(t) \tag{4.2.11b}$$

$$\Phi_2^{(i,s)} = \Phi_2^{(i)}(\beta,\beta';\gamma,1;-tx,-tx) = \int_0^1\mathrm{d}w\,\Phi_2(\beta,\beta';\gamma;-txw,-txw)$$

$$= \frac{\Gamma(\gamma)t^{1-\gamma}}{(1-\beta-\beta')x}\mathscr{L}^{-1}\left(p^{\beta+\beta'-\gamma}(p+x)^{1-\beta-\beta'}-p^{1-\gamma}\right)(t) \tag{4.2.11c}$$

where $\Gamma(a,x)$ is the incomplete Gamma-function.

Proof. Starting from (4.1.3b), the extra denominator is turned into an auxiliary integral

$$\Phi_3^{(i)} = \int_0^{\infty}\mathrm{d}v\sum_{m,n=0}^{\infty}e^{-v(m+n+1)}\frac{(\beta)_m}{(\gamma)_{m+n}}\frac{(-tx)^m}{m!}\frac{(-ty)^n}{n!}$$

and the decoupling of the two series proceeds via (4.2.2) as in the proof of Lemma 1. A change of variables $w = e^{-v}$ and Lemma 1 give the second line in (4.2.11a). The same change of variables

as in Lemma 2 then gives, using also (4.2.7)

$$\Phi_3^{(i)} = \Gamma(\gamma)t^{1-\gamma}\mathscr{L}^{-1}\left(p^{\beta-\gamma}\underbrace{\int_0^1 dw\,(p+xw)^{-\beta}e^{-yw/p}}_{=:\,\mathcal{M}}\right)(t)$$

The integral $\mathcal{M}$ is found as follows, reducing it to incomplete Gamma functions [Abr64]

$$\mathcal{M} = \frac{1}{x}\int_p^{x+p} da\,a^{-\beta}\exp\left[-\frac{y}{x}\frac{a-p}{p}\right] = \frac{e^{y/x}}{x}\left(\frac{px}{y}\right)^{1-\beta}\int_{y/x}^{y/x+y/p} db\,b^{-\beta}e^{-b}$$

$$= \frac{e^{y/x}}{x}\left(\frac{px}{y}\right)^{1-\beta}\left[\Gamma\left(1-\beta,\frac{y}{x}\right)-\Gamma\left(1-\beta,\frac{y}{x}+\frac{y}{p}\right)\right]$$

and inserting into $\Phi_3^{(i)}$ gives the last assertion (4.2.11a).

Turning to $\Phi_2^{(i)}$, the procedure to go from (4.1.3a) to the second line of (4.2.11b) is analogous. Changing variables as before and re-using (4.2.7), we arrive at

$$\Phi_2^{(i)} = \Gamma(\gamma)t^{1-\gamma}\mathscr{L}^{-1}\left(p^{\beta+\beta'-\gamma}\underbrace{\int_0^1 dw\,(p+xw)^{-\beta}(p+yw)^{-\beta'}}_{=:\,\mathcal{N}}\right)(t)$$

which is still symmetric under the simultaneous exchanges $(x,\beta)\leftrightarrow(y,\beta')$, as it should be. To evaluate this, recall the following identity on the incomplete Beta function [Abr64, (6.6.8),(15.3.4)]

$$I(a,b,\xi) := \int_0^\xi du\,\frac{u^{a-1}}{(1+u)^b} = \frac{\xi^a}{a}\,_2F_1(a,b;1+a;-\xi)$$

Then we can evaluate the integral $\mathcal{N}$, now using $x > y$

$$\mathcal{N} = x^{-\beta}y^{-\beta'}\int_0^1 dw\,\left(w+\frac{p}{x}\right)^{-\beta}\left(w+\frac{p}{y}\right)^{-\beta'}$$

$$= x^{-\beta}y^{-\beta'}\left(\frac{p(x-y)}{xy}\right)^{1-\beta-\beta'}\int_{y/(x-y)}^{(p+x)y/(p(x-y))} db\,b^{-\beta}(1+b)^{-\beta'}$$

$$= x^{-\beta}y^{-\beta'}\left(\frac{p(x-y)}{xy}\right)^{1-\beta-\beta'}\left[I\left(1-\beta,\beta',\frac{(p+x)y}{p(x-y)}\right)-I\left(1-\beta,\beta',-\frac{y}{(x-y)}\right)\right]$$

$$= x^{-\beta}y^{-\beta'}\left(\frac{p(x-y)}{xy}\right)^{1-\beta-\beta'}\frac{1}{1-\beta}\left[\left(\frac{(p+x)y}{p(x-y)}\right)^{1-\beta}\,_2F_1\left(1-\beta,\beta';2-\beta;-\frac{(p+x)y}{p(x-y)}\right)\right.$$

$$\left.-\left(\frac{y}{x-y}\right)^{1-\beta}\,_2F_1\left(1-\beta,\beta';2-\beta;-\frac{y}{x-y}\right)\right]$$

and inserting this into the above expression for $\Phi_2^{(i)}$ gives the last assertion (4.2.11b). Finally, in the symmetric case $x = y$ we have

$$\Phi_2^{(i,s)} = \Gamma(\gamma)t^{1-\gamma}\mathscr{L}^{-1}\left(p^{\beta+\beta'-\gamma}\int_0^1 dw\,(p+xw)^{-\beta-\beta'}\right)(t)$$

and straightforward integration gives the assertion (4.2.11c).   □

Corollary 2. *For $x > 0$, one has the identity*

$$\int_0^1 dw\,w^{\lambda-1}(1-w)^{\mu-1}\Phi_2(\beta,\beta';\gamma;-xtw,-xtw) = \frac{\Gamma(\lambda)\Gamma(\mu)}{\Gamma(\lambda+\mu)}\,_2F_2\left(\beta+\beta',\lambda;\mu+\lambda,\gamma;-xt\right)\ (4.2.12)$$

Proof. The lines of calculation are by now well-established

$$\int_0^1 dw \, w^{\lambda-1} (1-w)^{\mu-1} \Phi_2(\beta,\beta';\gamma;-xtw,-xtw)$$

$$= \Gamma(\gamma) t^{1-\gamma} \mathscr{L}^{-1} \left(p^{\beta+\beta'-\gamma} \int_0^1 dw \, w^{\lambda-1} (1-w)^{\mu-1} (p+xw)^{-\beta-\beta'} \right)(t)$$

$$= \Gamma \begin{bmatrix} \gamma & \lambda & \mu \\ & \lambda+\mu & \end{bmatrix} t^{1-\gamma} \mathscr{L}^{-1} \left(p^{-\gamma} \, _2F_1 \left(\beta+\beta',\lambda;\mu+\lambda;-\frac{x}{p} \right) \right)(t)$$

$$= \Gamma \begin{bmatrix} \lambda & \mu \\ & \lambda+\mu \end{bmatrix} \, _2F_2 \left(\beta+\beta',\lambda;\mu+\lambda,\gamma;-xt \right)$$

where in the third line, the integral representation [Abr64, (15.3.1)] of $_2F_1$ was used and in the forth line, [Pru92b, (3.35.1.10)], or else (4.2.9), was applied. $\square$

4.3 Asymptotic expansions

We shall use a Tauberian theorem for the asymptotic evaluations: *the behaviour of a function $f(t)$ for $t \to \infty$ is related to the one of its Laplace transform $\overline{f}(p)$ for $p \to 0$* [Wid46], [Fel71, ch. XIII]. Therefore, it is sufficient to analyse the behaviour of the representations as inverse Laplace transformations from Lemmas 3 and 4 in section 2 for $p \to 0$, before inverting.

Theorem 1. *The Humbert function $\Phi_2 = \Phi_2(\beta,\beta';\gamma;-tx,-ty)$ has the following leading asymptotic behaviour for $t \to \infty$, with $x,y \neq 0$ being kept fixed*

$$\Phi_2 \simeq \begin{cases} \frac{\Gamma(\gamma)}{\Gamma(\gamma-\beta-\beta')} (tx)^{-\beta} (ty)^{-\beta'} & ; \text{ for } x>0, \, y>0 \\[2mm] \frac{\Gamma(\gamma)}{\Gamma(\beta')} e^{-yt} (t(|y|+x))^{-\beta} (t|y|)^{\beta+\beta'-\gamma} & ; \text{ for } x>0, \, y<0 \\[2mm] \frac{\Gamma(\gamma)}{\Gamma(\beta)} e^{-xt} (t(y+|x|))^{-\beta'} (t|x|)^{\beta+\beta'-\gamma} & ; \text{ for } x<0, \, y>0 \\[2mm] \frac{\Gamma(\gamma)}{\Gamma(\beta)} e^{-|x|t} (t|x|)^{\beta+\beta'-\gamma} (t|x-y|)^{-\beta'} & ; \text{ for } x<y<0 \\[2mm] \frac{\Gamma(\gamma)}{\Gamma(\beta')} e^{-|y|t} (t|y|)^{\beta+\beta'-\gamma} (t|y-x|)^{-\beta'} & ; \text{ for } y<x<0 \\[2mm] \frac{\Gamma(\gamma)}{\Gamma(\beta+\beta')} e^{-|x|t} (t|x|)^{\beta+\beta'-\gamma} & ; \text{ for } y=x<0 \end{cases} \tag{4.3.1}$$

and neither γ, β, β', $\beta+\beta'$ nor $\gamma-\beta-\beta'$ are non-positive integers.

Only the signs of β, β' and of $\beta+\beta'-\gamma$ will influence the qualitative behaviour of the leading asymptotic terms, for $t \to \infty$.

Proof. The starting point is the representation of Φ_2 as an inverse Laplace transformation in Lemma 3. For $x>0$ and $y>0$, the leading term for $p \to 0$ is

$$\Phi_2 \simeq \Gamma(\gamma) t^{1-\gamma} \mathscr{L}^{-1} \left(p^{\beta+\beta'-\gamma} x^{-\beta} y^{-\beta} \right)(t)$$

and direct evaluation [Pru92b, (2.1.1.1)] gives the assertion. Next, for $x>0$ and $y<0$, one first makes the shift $q=p-y$ and second takes the leading term for $q \to 0$. Then

$$\Phi_2 = \Gamma(\gamma) t^{1-\gamma} e^{-|y|t} \mathscr{L}^{-1} \left((q+|y|)^{\beta+\beta'-\gamma} (q+|y|+x)^{-\beta} q^{-\beta'} \right)(t)$$

$$\overset{q\to 0}{\simeq} \Gamma(\gamma) t^{1-\gamma} e^{-|y|t} \mathscr{L}^{-1} \left(|y|^{\beta+\beta'-\gamma} (|y|+x)^{-\beta} q^{-\beta'} \right)(t)$$

and direct evaluation gives the assertion. For $x<0$ and $y>0$ one merely has to permute $(x,\beta) \leftrightarrow (y,\beta')$. Finally, for $x<0$ and $y<0$

$$\Phi_2 = \Gamma(\gamma) t^{1-\gamma} \mathscr{L}^{-1} \left(p^{\beta+\beta'-\gamma} (p-|x|)^{-\beta} (p-|y|)^{-\beta'} \right)(t)$$

If $x < y < 0$, or $|x| > |y|$, one makes the shift $q = p - |x|$ and the stated result follows as before. If $y < x < 0$, one merely permutes $(x, \beta) \leftrightarrow (y, \beta')$. For $x = y < 0$, the shift $q = p - |x|$ and expansion in q to lowest order gives the stated result. $\qquad\square$

Theorem 2. *The Humbert function $\Phi_3 = \Phi_3(\beta; \gamma; -tx, -ty)$ has the following asymptotic behaviour for $t \to \infty$, with $x, y \neq 0$ being kept fixed*

$$
\Phi_3 \simeq \begin{cases}
\Gamma(\gamma)(tx)^{-\beta}(ty)^{(1+\beta-\gamma)/2} J_{\gamma-\beta-1}(2\sqrt{yt}) & ; \text{ for } x > 0,\, y > 0 \\[2mm]
\Gamma(\gamma)(tx)^{-\beta}(t|y|)^{(1+\beta-\gamma)/2} I_{\gamma-\beta-1}(2\sqrt{|y|t}) & ; \text{ for } x > 0,\, y < 0 \\[2mm]
\frac{\Gamma(\gamma)}{\Gamma(\beta)}(t|x|)^{\beta-\gamma} e^{-y/|x|-|x|t} & ; \text{ for } x < 0
\end{cases}
\tag{4.3.2}
$$

where J_ν is a Bessel function and I_ν the corresponding modified Bessel function and neither γ nor β are non-positive integers.

The qualitative behaviour of the leading asymptotic term is only influenced by the signs of β and $\beta - \gamma$.

Proof. Use the representation of Φ_3 as an inverse Laplace transformation in Lemma 3. For $x > 0$, simply retain the lowest order in $p \to 0$ and use (4.2.7a). Expressing the hypergeometric function $_0F_1$ as a Bessel or a modified Bessel function, respectively, gives the assertion for $y > 0$ and $y < 0$. For $x < 0$, make the shift $q = p - |x|$ such that

$$
\Phi_3 = \Gamma(\gamma) t^{1-\gamma} e^{-|x|t} \mathscr{L}^{-1}\left((q+|x|)^{\beta-\gamma} q^{-\beta} e^{-y/(q+|x|)} \right)(t)
$$

$$
\overset{q \to 0}{\simeq} \Gamma(\gamma) t^{1-\gamma} e^{-|x|t} \mathscr{L}^{-1}\left(|x|^{\beta-\gamma} q^{-\beta} e^{-y/|x|} \right)(t)
$$

and re-use $\Gamma(\beta)\mathscr{L}^{-1}\left(q^{-\beta}\right)(t) = t^{\beta-1}$ [Pru92b, (2.1.1.1)]. $\qquad\square$

Theorem 3. *The Humbert function $\Xi_2 = \Xi_2(\alpha, \beta; \gamma; -tx, -ty)$ has the following asymptotic behaviour for $t \to \infty$, with $x, y \neq 0$ being kept fixed*

$$
\Xi_2 \simeq \begin{cases}
\frac{\Gamma(\alpha)\Gamma(\alpha-\beta)}{\Gamma(\alpha)}(tx)^{-\beta}(ty)^{-(\gamma-\beta-1)/2} J_{\gamma-\beta-1}(2\sqrt{yt}) & ; \text{ for } x > 0,\, y > 0 \text{ and } \alpha > \beta \\[2mm]
\frac{\Gamma(\alpha)\Gamma(\alpha-\beta)}{\Gamma(\alpha)}(tx)^{-\beta}(t|y|)^{-(\gamma-\beta-1)/2} I_{\gamma-\beta-1}(2\sqrt{|y|t}) & ; \text{ for } x > 0,\, y < 0 \text{ and } \alpha > \beta \\[2mm]
\frac{\Gamma(\gamma)}{\Gamma(\alpha)}(tx)^{-\alpha}(ty)^{-(\gamma-\alpha-1)/2} \left[\frac{\pi}{2} Y_{\gamma-\alpha-1}(2\sqrt{yt}) \right. \\
\qquad \left. + J_{\gamma-\alpha-1}(2\sqrt{|y|t}) \left[\frac{1}{2}\ln(tx) + \ln(x/y) - \psi(\alpha) - 2C_E \right] \right] & ; \text{ for } x > 0,\, y > 0 \text{ and } \alpha = \beta \\[2mm]
\frac{\Gamma(\gamma)}{\Gamma(\alpha)}(tx)^{-\alpha}(t|y|)^{-(\gamma-\alpha-1)/2} I_{\gamma-\alpha-1}(2\sqrt{|y|t}) \\
\qquad \times \left[\frac{1}{2}\ln(tx) + \ln(x/|y|) - \psi(\alpha) - 2C_E \right] & ; \text{ for } x > 0,\, y < 0 \text{ and } \alpha = \beta \\[2mm]
\frac{\Gamma(\alpha)\Gamma(\beta-\alpha)}{\Gamma(\beta)}(tx)^{-\alpha}(ty)^{-(\gamma-\alpha-1)/2} J_{\gamma-\alpha-1}(2\sqrt{yt}) & ; \text{ for } x > 0,\, y > 0 \text{ and } \alpha < \beta \\[2mm]
\frac{\Gamma(\alpha)\Gamma(\beta-\alpha)}{\Gamma(\beta)}(tx)^{-\alpha}(t|y|)^{-(\gamma-\alpha-1)/2} I_{\gamma-\alpha-1}(2\sqrt{|y|t}) & ; \text{ for } x > 0,\, y < 0 \text{ and } \alpha < \beta
\end{cases}
$$

$$
\tag{4.3.3}
$$

where J_ν and Y_ν are the Bessel and Neuman functions, respectively, I_ν is a modified Bessel function, $\psi(x)$ is the digamma function and $C_E \simeq 0.5772\ldots$ is Euler's constant [Abr64]. For $x < 0$, the function Ξ_2 has a cut.

Proof. In order to apply the inverse Laplace representation of Lemma 3, the small-p expansion

$$U\left(\alpha; 1+\alpha-\beta; \frac{p}{x}\right) \simeq \begin{cases} \frac{\Gamma(\alpha-\beta)}{\Gamma(\alpha)}\left(\frac{p}{x}\right)^{\beta-\alpha} & ; \text{ for } \alpha > \beta \\ -\frac{1}{\Gamma(\alpha)}\left[\ln\frac{p}{x} + \psi(\alpha) + 2C_E\right] & ; \text{ for } \alpha = \beta \\ \frac{\Gamma(\beta-\alpha)}{\Gamma(\beta)} & ; \text{ for } \alpha < \beta \end{cases}$$

according to eqs (13.5.6)-(13.5.12) in [Abr64] is required, for $\alpha - \beta \notin (-1)\cdot\mathbb{N}$. For $x > 0$ and $\alpha > \beta$, to lowest order in $p \to 0$, this gives $\Xi_2 \simeq \frac{\Gamma(\gamma)\Gamma(\alpha-\beta)}{\Gamma(\alpha)}t^{1-\gamma}x^{-\beta}\mathscr{L}^{-1}\left(p^{-(\gamma-\beta)}e^{y/p}\right)(t)$ and using (4.2.7a) gives the assertion. For $x > 0$ and $\alpha < \beta$ the result follows from the symmetry in α and β. For $\alpha = \beta$ and $y > 0$, expansion to lowest order in $p \to 0$ gives

$$\begin{aligned}
\Xi_2 &\simeq -\frac{\Gamma(\gamma)}{\Gamma(\alpha)}t^{1-\gamma}x^{-\alpha}\bigg[\mathscr{L}^{-1}\left((\psi(\alpha) + 2C_E - \ln x)\,p^{-(\gamma-\alpha)}e^{-y/p}\right)(t) \\
&\quad + \mathscr{L}^{-1}\left(p^{-(\gamma-\alpha)}\ln p\; e^{-y/p}\right)(t)\bigg] \\
&= -\frac{\Gamma(\gamma)}{\Gamma(\alpha)}t^{1-\gamma}x^{-\alpha}\bigg[\left(\psi(\alpha) + 2C_E - \ln x - \frac{1}{2}\ln\frac{t}{y}\right)\left(\frac{t}{y}\right)^{\frac{1}{2}(\gamma-\alpha-1)}J_{\gamma-\alpha-1}(2\sqrt{yt}) \\
&\quad - \left(\frac{t}{y}\right)^{\frac{1}{2}(\gamma-\alpha-1)}\frac{\partial J_{\nu-1}(2\sqrt{yt})}{\partial\nu}\bigg|_{\nu=\gamma-\alpha}\bigg]
\end{aligned} \tag{4.3.4}$$

re-using (4.2.7a) and [Pru92b, (2.5.7.3)]. For $z \to \infty$, one has asymptotically $\frac{\partial J_\nu(z)}{\partial\nu} \simeq \frac{\pi}{2}Y_\nu(z)$ [Abr64, (9.25,9.26)]. Collecting terms leads to the stated result. For $y < 0$ and $\alpha = \beta$ one has analogously

$$\begin{aligned}
\Xi_2 &\simeq -\frac{\Gamma(\gamma)}{\Gamma(\alpha)}t^{1-\gamma}x^{-\alpha}\bigg[\mathscr{L}^{-1}\left((\psi(\alpha) + 2C_E - \ln x)\,p^{-(\gamma-\alpha)}e^{|y|/p}\right)(t) \\
&\quad + \mathscr{L}^{-1}\left(p^{-(\gamma-\alpha)}\ln p\; e^{|y|/p}\right)(t)\bigg] \\
&= -\frac{\Gamma(\gamma)}{\Gamma(\alpha)}t^{1-\gamma}x^{-\alpha}\bigg[\left(\psi(\alpha) + 2C_E - \ln x - \frac{1}{2}\ln\frac{t}{y}\right)\left(\frac{t}{y}\right)^{\frac{1}{2}(\gamma-\alpha-1)}I_{\gamma-\alpha-1}(2\sqrt{yt}) \\
&\quad - \left(\frac{t}{y}\right)^{\frac{1}{2}(\gamma-\alpha-1)}\frac{\partial I_{\nu-1}(2\sqrt{yt})}{\partial\nu}\bigg|_{\nu=\gamma-\alpha}\bigg]
\end{aligned} \tag{4.3.5}$$

and from the asymptotic form [Abr64, (9.7.1)] for $I_\nu(z)$ for $z \to \infty$, we see that $\frac{\partial I_\nu(z)}{\partial\nu} \simeq -\frac{\nu}{z}I_\nu(z)$ merely gives a sub-leading correction. Collecting terms we complete the list of assertions if $x > 0$. For $x < 0$, the inverse Laplace representation in Lemma 3 has a cut. $\square$

Theorem 4. *The integrated Humbert function $\Phi_3^{(i)} = \Phi_3^{(i)}(\beta; \gamma, 1; -tx, -ty)$ has the following leading asymptotic behaviour for $t \to \infty$, with $x, y \neq 0$ being kept fixed*

$$\Phi_3^{(i)} \simeq \begin{cases} \frac{\gamma-1}{xt}\left[\Gamma(1-\beta)\,(y/x))^{\beta-1} - \frac{1}{1-\beta}\,{}_1F_1(1; 2-\beta; y/x)\right] & ; \text{ for } x, y > 0 \text{ and } \beta + \gamma > \frac{3}{2} \\ \frac{\Gamma(\gamma)}{\sqrt{\pi}}(yt)^{-\frac{1}{2}(\beta+\gamma+\frac{1}{2})}\left(\frac{y}{x}\right)^\beta \cos\left(2\sqrt{yt} + \frac{\pi}{2}\left(\beta-\gamma-\frac{1}{2}\right)\right) & ; \text{ for } x, y > 0 \text{ and } \beta + \gamma < \frac{3}{2} \\ \frac{\Gamma(\gamma)}{2\sqrt{\pi}}(|y|t)^{-\frac{1}{2}(\beta-\gamma-\frac{1}{2})}(xt)^{-\beta}\exp\left(2\sqrt{|y|t}\right) & ; \text{ for } x > 0,\ y < 0 \end{cases} \tag{4.3.6}$$

where neither γ nor $1 - \beta$ are non-positive integers.

Proof. We begin with the integral representation (4.2.11a) of Lemma 4. The leading term for $p \to 0$ is found from the asymptotic identity [Abr64, (6.5.30)] for $x \to \infty$

$$\Gamma(a, x+y) - \Gamma(a, x) \simeq -e^{-x}x^{a-1}\left(1 - e^{-y}\right)$$

In order to invert $\mathscr{L}$, we also need the identities (4.2.7a) and [Pru92b, (3.10.2.2)]

$$\mathscr{L}^{-1}\left(p^{-\mu}\Gamma\left(\nu,\frac{a}{p}\right)\right)(t) = \frac{\Gamma(\nu)}{\Gamma(\mu)}t^{\mu-1} - \frac{a^{\nu}t^{\mu+\nu-1}}{\nu\Gamma(\mu+\nu)}\,{}_1F_2\left(\nu;\nu+1,\mu+\nu;-at\right)$$

Then, for $p \to 0$ (here, $x > 0$ is assumed)

$$\Phi_3^{(i)} \simeq \frac{\Gamma(\gamma)}{t^{\gamma-1}}\frac{e^{y/x}}{x}\left(\frac{y}{x}\right)^{\beta-1}\mathscr{L}^{-1}\left(\frac{\Gamma\left(1-\beta,\frac{y}{x}\right)}{p^{\gamma-1}} - \frac{\Gamma\left(1-\beta,\frac{y}{p}\right)}{p^{\gamma-1}} + \frac{e^{-y/p}}{p^{\gamma-1}}\left(\frac{p}{y}\right)^{\beta}\left(1-e^{-y/x}\right)\right)(t)$$

$$= \frac{\Gamma(\gamma)}{t^{\gamma-1}}\frac{e^{y/x}}{x}\left(\frac{y}{x}\right)^{\beta-1}\left[\frac{\Gamma(1-\beta,y/x)-\Gamma(1-\beta)}{\Gamma(\gamma-1)} + \frac{1-e^{-y/x}}{\Gamma(\gamma-\beta-1)(yt)^{\beta}}\,{}_0F_1(\gamma-\beta-2;-yt)\right.$$
$$\left.+ \frac{(yt)^{\beta-1}}{(1-\beta)\Gamma(\gamma-\beta)}\,{}_1F_2(1-\beta;2-\beta,\gamma-\beta;-yt)\right]$$

Further evaluation is simplified by the identity, taken from [Abr64, (6.5.3,6.5.12)]

$$\left(\frac{y}{x}\right)^{-(1-\beta)}\left[\Gamma(1-\beta)-\Gamma\left(1-\beta,\frac{y}{x}\right)\right] = \frac{1}{1-\beta}\,{}_1F_1\left(1-\beta;2-\beta;-\frac{y}{x}\right)$$

and this gives

$$\Phi_3^{(i)} \simeq \Gamma(\gamma)\frac{e^{y/x}}{xt}\left[\frac{{}_1F_1(1-\beta;2-\beta;-y/x)}{(\beta-1)\Gamma(\gamma-1)}\right.$$
$$\left.+ \frac{{}_1F_2(1-\beta;2-\beta,\gamma-\beta;-yt)}{(1-\beta)\Gamma(\gamma-\beta)(xt)^{\beta-1}} + \frac{1}{(xt)^{\beta}}\frac{x}{y}\frac{1-e^{-y/x}}{\Gamma(\gamma-\beta-1)}\,{}_0F_1(\gamma-\beta-2;-yt)\right] \qquad (4.3.7)$$

We can now distinguish the two cases $y > 0$ and $y < 0$. For $y > 0$, recall the asymptotic identity [Wol17, (07.22.06.0011.01)]

$${}_1F_2(a_1;b_1,b_2;-y) \overset{y\to\infty}{\simeq} \Gamma\begin{bmatrix}b_1 & b_2 \\ \frac{1}{2} & a_1\end{bmatrix}y^{\frac{1}{2}(a_1-b_1-b_2+\frac{1}{2})}\cos\left(\frac{\pi}{2}(a_1-b_1-b_2+\frac{1}{2})+2\sqrt{y}\right)\left(1+\mathrm{O}(y^{-\frac{1}{2}})\right)$$
$$+ \Gamma\begin{bmatrix}b_1 & b_2 \\ b_1-a_1 & b_2-a_1\end{bmatrix}y^{-a_1}\left(1+\mathrm{O}(y^{-1})\right)$$

Also, the function ${}_0F_1$ can be expressed in terms of Bessel functions J_ν [Abr64]. Inserting into (4.3.7) the above expansion and using the asymptotics of J_ν [Abr64] leads to

$$\Phi_3^{(i)} \simeq \frac{\gamma-1}{xt}\left[\Gamma(1-\beta)\left(\frac{y}{x}\right)^{\beta-1} - \frac{1}{1-\beta}\,{}_1F_1\left(1;2-\beta;\frac{y}{x}\right)\right]$$
$$+ \frac{\Gamma(\gamma)}{\sqrt{\pi}}\left(\frac{y}{x}\right)^{\beta}(yt)^{-\frac{1}{2}(\beta+\gamma+\frac{1}{2})}\cos\left(2\sqrt{yt}+\frac{\pi}{2}\left(\beta-\gamma-\frac{1}{2}\right)\right)$$

Herein, the first line dominates for $\beta+\gamma > \frac{3}{2}$ and the second line for $\beta+\gamma < \frac{3}{2}$. This is the first part of the assertion. For $y = -|y| < 0$, recall the asymptotic form [Wol17, (07.22.06.0005.01)]

$${}_1F_2(a_1;b_1,b_2;y) \overset{y\to\infty}{\simeq} \frac{\Gamma(b_1)\Gamma(b_2)}{2\sqrt{\pi}\,\Gamma(a_1)}y^{\frac{1}{2}(a_1-b_1-b_2+\frac{1}{2})}e^{2\sqrt{y}}$$

and now express ${}_0F_1$ in terms of a modified Bessel function I_ν [Abr64]. Insertion into (4.3.7) and using the known asymptotic behaviour leads to

$$\Phi_3^{(i)} \simeq \frac{\Gamma(\gamma)}{2\pi^{1/2}}\frac{(|y|t)^{-\frac{1}{2}(\beta-\gamma-\frac{1}{2})}}{(xt)^{\beta}}e^{2\sqrt{|y|t}} + \frac{\gamma-1}{\beta-1}\frac{1}{xt}\,{}_1F_1\left(1;2-\beta;-\frac{|y|}{x}\right)$$

Clearly, the second term is always sub-dominant. This completes the proof. $\qquad\qquad\square$

Theorem 5. *The integrated Humbert function* $\Phi_2^{(i)} = \Phi_2^{(i)}(\beta, \beta'; \gamma, 1; -tx, -ty)$ *has the following leading asymptotic behaviour for* $t \to \infty$, *with* $x > y > 0$ *being kept fixed*

$$\Phi_2^{(i)} \simeq \frac{\Gamma(\gamma)}{(1-\beta)\Gamma(\gamma-\beta)} \frac{(xt)^{\beta'-\beta}}{((x-y)t)^\beta} \, {}_2F_2\left(1-\beta, \beta'; 2-\beta, \gamma-\beta; -\frac{xy}{x-y}t\right)$$

$$+ \frac{\gamma-1}{\beta-1}\frac{1}{xt}\left(\frac{x}{x-y}\right)^{\beta'} {}_2F_1\left(1-\beta, \beta'; 2-\beta; -\frac{y}{x-y}\right) \tag{4.3.8}$$

Herein, none of γ, $\gamma - \beta$ *or* $1 - \beta$ *is a non-positive integer. For* $y > x > 0$, *one permutes* (x, β) *and* (y, β').

Proof. We begin with the integral representation (4.2.11b) of Lemma 4. For $p \to 0$, this simplifies into

$$\Phi_2(i) \overset{p\to 0}{\simeq} \frac{\Gamma(\gamma)}{1-\beta}\frac{t^{1-\gamma}}{(x-y)^{\beta'}x^{1-\beta'}} \, \mathscr{L}^{-1}\left(\frac{x^{1-\beta}}{p^{\gamma-\beta}} \, {}_2F_1\left(1-\beta, \beta'; 2-\beta; -\frac{xy}{x-y}\frac{1}{p}\right)\right.$$

$$\left. - p^{\gamma-1} \, {}_2F_1\left(1-\beta, \beta'; 2-\beta; -\frac{y}{x-y}\right)\right)(t)$$

We need the identity [Pru92b, (3.35.1.10)]

$$\mathscr{L}^{-1}\left(p^\nu \, {}_2F_1\left(a, b; c; -\frac{\omega}{p}\right)\right)(t) = \frac{t^{\nu-1}}{\Gamma(\nu)} \, {}_2F_2(a, b; c, \nu; -\omega t)$$

Then straightforward algebra leads to the assertion. For $y > x > 0$, it is enough to exchange $\beta \leftrightarrow \beta'$ and $x \leftrightarrow y$. $\square$

More explicit asymptotics of ${}_2F_2$ can be found in [Wri40, Wri52].

The expressions derived in this section can be checked numerically. However, the convergence towards the given asymptotics is in general quite slow.

Finally, it is now straightforward to obtain the asymptotics of the special Kampé de Fériet series (4.2.8), by using the known asymptotics of the hypergeometric functions ${}_pF_q(z)$ [Wri40, Wri52].

4.4   An example from physics

The quantum spherical model [Hen84b, Voj96, Oli06] is a simple exactly solvable model of quantum phase transitions, in d spatial dimensions, with a non-trivial quantum critical behaviour at zero temperature (that is, the model cannot be described by a simple mean-field approximation, at least for $1 < d < 3$), see e.g. [Sac01, Dut15]. Its main formal characteristic is the 'spherical constraint'. As shown in chapter 3 and [Wal17b], if coherent and dissipative quantum dynamics of the model is formulated in terms of a Lindblad equation, it can be shown that the canonical quantum commutation relations are maintained, in spite of the dissipation, at least on average. As we have seen in the previous chapter, if the system is deep in the ordered phase, the spherical constraint takes the form $\mathscr{I}_1 + \mathscr{I}_2 = 1$, where

$$\mathscr{I}_1 = \int_\mathcal{B} \frac{d\boldsymbol{k}}{(2\pi)^d} \, e^{-\gamma(Z+t\omega_{\boldsymbol{k}})} \; = \; \left(e^{-2\gamma t}I_0(2\gamma t)\right)^d \overset{t\to\infty}{\simeq} \; e^{-\gamma Z}\left(4\pi\gamma t\right)^{-d/2} \tag{4.4.1}$$

$$\mathscr{I}_2 = \frac{1}{2}\int_\mathcal{B} \frac{d\boldsymbol{k}}{(2\pi)^d} \, \left(1 - \frac{Cgt}{Z+t\omega_{\boldsymbol{k}}}\right)(1-\cos 2\vartheta_{\boldsymbol{k}}) \, e^{-\gamma(Z+t\omega_{\boldsymbol{k}})} \tag{4.4.2}$$

where $Z = Z(t)$ is the integrated spherical Lagrange multiplier whose long-time behaviour as $t \to \infty$ is sought. Furthermore, $\omega_{\boldsymbol{k}} = 2(d - \cos k_1 - \ldots - \cos k_d)$ is the lattice dispersion relation on a d-dimensional hypercubic lattice with nearest-neighbour interactions, $\mathcal{B} = [-\pi, \pi]^d$ is the Brillouin zone, $\vartheta_{\boldsymbol{k}} = \sqrt{gt\,(Z+t\omega_{\boldsymbol{k}})}$, and the constants g, γ and C are the quantum coupling and the dissipative coupling with the external bath, respectively, or characterise the quantum equilibrium

initial condition. The sum $\mathscr{I}_2$ can be evaluated by expanding the cosine and integrating termwise. Then the spherical constraint can be rewritten in the form (see eqs (3.6.13, 3.6.14, 3.6.15))

$$e^{\gamma Z}(4\pi\gamma t)^{d/2} = \frac{1}{2}\Phi_3\left(\frac{d}{2};\frac{3}{2};-gZt,-\frac{g}{\gamma}t\right) + Cg^2t^2\int_0^1 \mathrm{d}w\,\Phi_3\left(\frac{d}{2};\frac{3}{2};-\frac{g}{\gamma}tw,-gZtw\right) \qquad (4.4.3)$$

For the physically interesting long-time behaviour of $Z = Z(t)$ for $t \to \infty$, the asymptotics of the Humbert function Φ_3 and of the integrated Humbert function $\Phi_3^{(i)}$ are required. In contrast to the original formulation in eqs (4.4.1,4.4.2), the reformulation in eq (4.4.3) contains the spatial dimension d merely as a parameter. This allows to discuss also the model's behaviour at non-integer dimensions $d \in \mathbb{R}$, which often provides useful physical insight.

We refer back to chapter 3 for the properties of the solutions of this equation.

Chapter 5

Outlook and perspectives

5.1 Perspectives for the spherical model

Our present studies into the quantum dynamics of the QSM only represent first explorations into a potentially very rich topic. We now mention several possible extensions of the present work.

5.1.1 Quantum ageing

The *quantum regression theorem* [Lax63, Gar04] allows an extension of the equations of motion for single operator correlation functions to two-point correlation functions. It will allow us to deduce from eq (3.4.4b) a closed system of equations for the two-time correlators $\langle q_{\boldsymbol{k}}(t+\tau)q_{-\boldsymbol{k}}(t)\rangle$, $\langle \pi_{\boldsymbol{k}}(t+\tau)\pi_{-\boldsymbol{k}}(t)\rangle$ and $\langle\{q_{\boldsymbol{k}}(t+\tau)\pi_{\boldsymbol{k}}(t)\}\rangle$ that we should be able to treat similarly to the one in eq (3.4.23). Since we already know the solution of the spherical constraint in the deep quench scenario, presented in section 3.6 we can aim at studying critical dynamical effects as ageing. The extensive studies of effect like ageing in the classical spherical model [God00, Hen10] should serve us as a guide on how to organise the studies of true quantum ageing in the spherical model.

5.1.2 Heat transport in spherical quantum chains and layers

Non-equilibrium steady state (NESS) density operators are important to describe the dynamics of boundary driven quantum chains and quantum transport phenomena. Generally, quantum transport can lead to surprising features such as the violation of the Wiedemann-Franz law [Fil16] and thus a careful investigation of dynamical properties is needed. Exactly solvable models provide a tool how to systematically analyse these systems. Here, mainly the Heisenberg spin-1/2 chain [Pro11a, Pro11b, Pro12], the Fermi-Hubbard chain [Pop15, Pro14] and the Lai-Sutherland spin-1 chain [Ili14] are studied. Since we succeeded to describe the dynamics of the QSM, we have all the tools to generalise these studies to our model. Once more the main focus here is going to be the analytical character of the solution which will give important physical insights to the underlying mechanisms. Moreover, the SM should again allow to overcome the constraint of $1D$ chains and extend the formalism to 2D layers, higher dimensional ($d > 2$) quantum systems or even fractal dimensional setups (for results in transport problems in 1D quantum chains see e.g. [Lan15a, Lan16a, Pro11a]).

5.1.3 Connection to the Bose-Hubbard model

The Bose-Hubbard model represents the bosonic analogue of the famous Fermi-Hubbard model, which is believed to be the basic toy model explaining several exotic materials in condensed matter such as, e.g., the high-T_c cuprate superconductors. The Bose-Hubbard model describes e.g. Cooper pairs of electrons undergoing Josephson tunnelling between superconducting islands, helium atoms moving on a substrate, or ultracold atoms in an optical lattice [Sac01] and is thus a *fundamental system* to describe various experimental setups. Moreover, extended version such as the competing long and short range Bose Hubbard model [Lan16b] or the multi-mode Bose-Hubbard model for

quantum dipolar gases [Car17] show that one can extend the model in order to describe more general setups. Since already the mean-field phase diagram reveals interesting properties of the transition between a Mott insulator and a superfluid [Fis89] this system became a *standard model* to describe this kind of phase transitions. As we mention in section 5.2, we are already studying quench dynamics in this model but apart from that, there are many interesting open questions:

- The Hamiltonian of the Bose Hubbard model and the one of the SM are formally similar and there are many aspects that seem to immediately relate. The main differences are the on-site repulsion in the Bose-Hubbard model and the spherical constraint in the SM. One could raise the question how far this analogy can be pushed and whether there exists a spherical approximation to the Bose-Hubbard model that might allow for analytic investigation and a straightforward extension to higher dimension.

- It is possible to connect the studies on this model to the heat transport questions raised in the previous section (compare in 1D [RI07]).

5.1.4 Dicke Model

The Dicke Model, as we already discussed in chapter 2 on page 49 has striking similarities to the SQS. Usually it is studied in a Holstein Primakoff approximation, that bosonises the many-body fermionic degrees of freedom in a single bosonic one. Moreover, the Dicke model is one of the prototypical models to study light-matter interaction in a many-body quantum system. It thus seems natural to explore the (superradiant) phase transition in this model or even apply a non-equilibrium dynamics to it analogue to the mean-field SQS and compare it to our former work. As clear as the similarities might seem, the Dicke model effectively differs from our SQS and thus it is not clear what results such dynamics can produce. Here it is most important to stress that the Dicke phase transition refers usually to a bath property. In this respect a Lindblad description in which the bath is assumed to be constant is not adequate and there have to be new tools developed in order to compare the dynamical processes accurately.

5.2 Bose Hubbard project

During this thesis, we also worked [Wal17c] on the experiment [Lan16b] which we already presented briefly in section 1.2.3.

Our aim is to better understand the Mott insulator (MI) to charge density wave (CDW) transition which corresponds to the shaded region in the right panel of fig 1.13. Without introducing in great detail into the theory of ultracold atoms and optical lattices[1], we simply refer to the result stated in [Lan16b] that the $2D$ system observed in the experiment can be described by the bosonic Hamiltonian on a $2D$ square lattice

$$\mathcal{H} = \sum_{i=1}^{K} \frac{U_s}{2} n_i (n_i - 1) - \frac{U_\ell}{K} \Theta^2 - \lambda \sum_{\langle i,j \rangle} (b_i^\dagger b_j + b_j^\dagger b_i) \ . \tag{5.2.1}$$

Here b_i is the annihilation operator at site $i \in \{1, \ldots, K\}$ and $n_i = b_i^\dagger b_i$ is the bosonic number operator. U_s is the short-ranged repulsive interaction, λ is the hopping parameter describing nearest-neighbour interaction. U_ℓ is the long-range interaction which depends on the imbalance operator $\Theta = \sum_{i \in e} n_i - \sum_{i \in o} n_i$. Here the square lattice is divided into even (e) and odd (o) square sub-lattices. The long range term is induced by the cavity and favours a chequerboard pattern in the lattice.

In the experiment independent control over the parameters U_ℓ and U_s was achieved and the phase diagram could therefore be measured as shown in fig 1.13.

The MI and CDW phases appear when $\lambda/U_s \ll 1$ and are thus essentially determined by the competition between U_s and U_ℓ. In the particular limit of $\lambda \to 0$ the Hamiltonian becomes diagonal

---

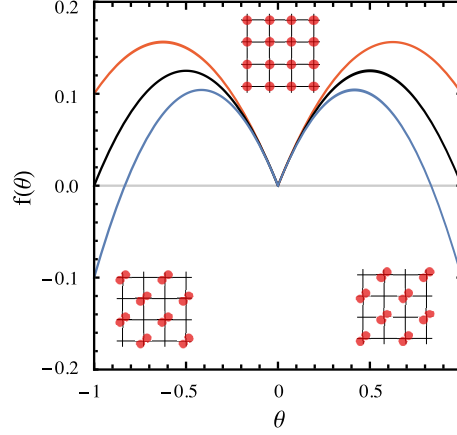[1] For reviews we refer to [Blo05, Lew07] and references therein.

Figure 5.1: The Landau free energy from eq (5.2.3) for filling $\rho = \mathcal{N}/K = 1$ and different values of U_ℓ/U_s: black $U_\ell/U_s = 0.5$, orange $U_\ell/U_s = 0.4$, blue $U_\ell/U_s = 0.6$. The system undergoes a first order quantum phase transition at $U_\ell/U_s = 1/2$, from a MI phase corresponding to a minimum at $\theta = 0$ to a CDW phase whose minimum is at $\theta = \pm 1$.

in the Fock basis and the partition function may be computed exactly at zero temperature in the canonical ensemble with $\mathcal{N}$ bosons in the lattice.

As a result, we obtain the *exact* Landau free energy in the canonical ensemble

$$f(\theta) = \frac{U_s}{2}\left[\varphi(\rho + \theta) + \varphi(\rho - \theta)\right] - U_\ell\theta^2 \tag{5.2.2}$$

where $\theta = \langle\Theta\rangle/K$ is the order parameter, $\rho = \mathcal{N}/K$ and $\varphi(\rho) = \lfloor\rho\rfloor\left[\rho - (\lfloor\rho\rfloor + 1)/2\right]$, with $\lfloor x \rfloor$ being the floor function. When $\rho = 1$ this acquires the particularly simple form

$$f(\theta) = \frac{U_s|\theta|}{2} - U_\ell\theta^2 \tag{5.2.3}$$

This result is shown in fig 5.1 for different values of U_ℓ/U_s.

Apart from the GL theory we investigate quantum dynamical properties of the transition by using a variational ansatz similar to a Gutzwiller mean-field theory [Gut63, Gut65, Kot86, Vol84]. In the standard Gutzwiller approximation one uses basis wave functions that are localised on the lattice vertices and constructs a superposition out of them. This was done numerically for the present system in [Flo17]. Our variational Ansatz is in contrast based on the eigenstates of the imbalance operator Θ which are not local and naturally reflect the symmetry of both phases.

Publication list

1) S. Wald and M. Henkel, *Quantum phase transition in the spin-anisotropic quantum spherical model*, J. Stat. Mech. (2015) P07006.

2) S. Wald and M. Henkel, *Lindblad dynamics of a quantum spherical spin*, J. Phys. A: Math. Theor. 49 (2016) 125001 **IOPSelect**.

3*) S. Wald, G.T. Landi and M. Henkel, *Lindblad dynamics of the quantum spherical model.*

4*) S. Wald, A. Timpanaro, G. Morigi and G.T. Landi, *Aspects of the Mott Insulator to Charge Density Wave transition in an extended Bose-Hubbard Model.*

5*) S. Wald and M. Henkel, *On integral representations and asymptotics of some hypergeometric functions in two variables.*

- the symbol * indicates works in preparation and their working titles

List of Figures

129

List of Tables

Bibliography

[Abr64]   Abramowitz M and Stegun IA, *Handbook of Mathematical Functions with Formulas, Graphs, and Mathematical Tables*, Dover, New York, 9th ed. (1964).

[Alb02]   Albert R and Barabási AL, *Rev Mod Phys*, **74**:47 (2002), `arXiv:cond-mat/0106096`.

[Alt15]   Altaner B *et al.*, *Phys Rev E*, **92**:042133 (2015).

[AN93]   Als-Nielsen J *et al.*, *Journal of Physics: Condensed Matter*, **5**:7871 (1993).

[And69]   Andrews T, *Philosophical Transactions of the Royal Society of London*, **159**:575 (1869).

[And13]   Ando Y, *Journal of the Physical Society of Japan*, **82**:102001 (2013), `arXiv:1304.5693`.

[App80a] Appell P, *Comptes rendus Acad Sci Paris*, **90**:296 (1880).

[App80b] Appell P, *Comptes rendus Acad Sci Paris*, **90**:731 (1880).

[App80c] Appell P, *Comptes rendus Acad Sci Paris*, **90**:977 (1880).

[App26]   Appell P and de Fériet J, *Fonctions hypergéométriques et hypersphériques: polynomes d'Hermite*, Gauthier-Villars (1926).

[Ask92]   Askey R, *SIAM Review*, **34**:503 (1992).

[Att06a] Attal S and Pautrat Y, *Annales Henri Poincaré*, **7**:59 (2006).

[Att06b] Attal S *et al.*, *Open Quantum Systems II: The Markovian Approach*, Lecture Notes in Mathematics, Springer (2006).

[Att07]   Attal S and Joye A, *Journal of Functional Analysis*, **247**:253 (2007), `arXiv:math-ph/0612055`.

[Bab16]   Babkevich P *et al.*, *Phys Rev Lett*, **116**:197202 (2016), `arXiv:1605.03443`.

[Bai32]   Bailey W, *Generalised hypergeometric series*, Cambridge University Press, Cambridge (1932).

[Bar13]   Barmettler P *et al.*, *EPL (Europhysics Letters)*, **104**:10004 (2013), `arXiv:1201.4416`.

[Bas06]   Basko D *et al.*, *Annals of Physics*, **321**:1126 (2006), `arXiv:cond-mat/0506617`.

[Bat53]   Bateman H and Erdélyi A, *Higher transcendental functions*, no. v. 1 in Higher Transcendental Functions, McGraw-Hill, New York (1953).

[Bat54]   Bateman H and Erdélyi A, *Table of integral transforms*, vol. 1, McGraw-Hill, New York (1954).

[Bat15]   Batchelor MT and Zhou HQ, *Phys Rev A*, **91**:053808 (2015), `arXiv:1408.3816`.

[Bat16]   Batchelor MT and Foerster A, *Journal of Physics A: Mathematical and Theoretical*, **49**:173001 (2016), `arXiv:1510.05810`.

[Bax71]   Baxter RJ, *Phys Rev Lett*, **26**:832 (1971).

[Bax82]   Baxter RJ, *Exactly solved models in statistical mechanics*, Academic Press, London (1982).

[Bed01]   Bedeaux D and Mazur P, *Physica A: Statistical Mechanics and its Applications*, **298**:81 (2001), statistical Thermodynamics and Colloid Science.

[Ber65]   Bernard C, *Introduction à l'étude de la médecine expérimentale*, J. B. Baillière (1865).

[Ber52]   Berlin TH and Kac M, *Phys Rev*, **86**:821 (1952).

[Ber07]   Bergman D *et al.*, *Nature Physics*, **3**:487 (2007), arXiv:cond-mat/0612001.

[Ber09]   Berche B *et al.*, *J Phys Studies*, **13**:3201 (2009), arXiv:0905.1886.

[Bet31]   Bethe H, *Zeitschrift für Physik*, **71**:205 (1931).

[Bie13]   Bienzobaz P and Salinas S, *Revista Brasileira de Ensino de Física*, **35**:3311 (2013).

[Bin83]   Binder K, in C Domb and J Lebowitz, eds., *Critical behaviour at surfaces*, *Phase transitions and critical phenomena*, vol. 8, Academic Press, London (1983).

[Bit96]   Bitko D *et al.*, *Phys Rev Lett*, **77**:940 (1996).

[Blo05]   Bloch I, *Nat Phys*, **1**:23 (2005).

[Blo08]   Bloch I *et al.*, *Rev Mod Phys*, **80**:885 (2008), arXiv:0704.3011.

[Boa83]   Boas ML, *Mathematical Methods in the Physical Sciences*, Wiley, New York (1983).

[Bor14]   Borchers N *et al.*, *Phys Rev E*, **90**:062113 (2014), arXiv:1411.6180.

[Bra00]   Brankov Ǐ *et al.*, *Theory of Critical Phenomena in Finite-size Systems: Scaling and Quantum Effects*, Series in modern condensed matter physics, World Scientific (2000).

[Bra13]   Braak D, *Journal of Physics B: Atomic, Molecular and Optical Physics*, **46**:224007 (2013), arXiv:1304.2529.

[Bra16]   Braak D, *Analytical Solutions of Basic Models in Quantum Optics*, 75–92, Springer Japan, Tokyo (2016), arXiv:1509.05748.

[Bre07]   Breuer H and Petruccione F, *The Theory of Open Quantum Systems*, Oxford University Press, Oxford (2007).

[Bri37]   Bridgman PW, *The Journal of Chemical Physics*, **5**:964 (1937).

[Bro28]   Brown R, *Philosophical Magazine*, **4**:161 (1828).

[Bru67]   Brush S, *Rev Mod Phys*, **39**:883 (1967).

[Bry17a]   Brychkov YA, *Integral Transforms and Special Functions*, **28**:22 (2017).

[Bry17b]   Brychkov YA *et al.*, *Integral Transforms and Special Functions*, **28**:350 (2017).

[Buc69]   Buchholz H, *The confluent hypergeometric function with special emphasis on its applications*, Springer tracts in natural philosophy, Springer (1969).

[Bun55]   Bundy FP *et al.*, *Nature*, **176**:51 (1955).

[Bur87]   Burkhardt TW and Guim I, *Phys Rev B*, **35**:1799 (1987).

[Cal02]   Calabrese P and Celi A, *Phys Rev B*, **66**:184410 (2002).

[Cal06]   Calabrese P and Cardy J, *Phys Rev Lett*, **96**:136801 (2006), arXiv:cond-mat/0601225.

[Cam14]   Campostrini M *et al.*, *Phys Rev B*, **89**:094516 (2014), arXiv:1401.0788.

[Car96a] Cardy J and Täuber UC, *Phys Rev Lett*, **77**:4780 (1996), `arXiv:cond-mat/9609151`.

[Car96b] Cardy JL, *Scaling and Renormalisation in Statistical Physics*, Cambridge University Press, Cambridge (1996).

[Car98] Cardy JL and Täuber UC, *Journal of Statistical Physics*, **90**:1 (1998), `arXiv:cond-mat/9704160`.

[Car99] Carmichael H, *Statistical Methods in Quantum Optics 1: Master Equations and Fokker-Planck Equations*, Physics and Astronomy Online Library, Springer, Heidelberg (1999).

[Car03] Caracciolo, S *et al.*, *Eur Phys J B*, **34**:205 (2003), `arXiv:cond-mat/0304297`.

[Car17] Cartarius F *et al.*, *Phys Rev A*, **95**:063603 (2017), `arXiv:1704.00948`.

[Cha96] Chakrabarti B *et al.*, *Quantum Ising Phases and Transitions in transverse Ising Models*, Lecture notes in physics: Monographs, Springer (1996).

[Cho11] Choi J and Hasanov A, *Computers & Mathematics with Applications*, **61**:663 (2011).

[Col10] Coldea R *et al.*, *Science*, **327**:177 (2010), `arXiv:1103.3694`.

[Con89] Coniglio A and Zannetti M, *EPL (Europhysics Letters)*, **10**:575 (1989).

[Con94] Coniglio A *et al.*, *Phys Rev E*, **50**:1046 (1994), `arXiv:cond-mat/9405003`.

[Cor96] Corless RM *et al.*, *Advances in Computational Mathematics*, **5**:329 (1996).

[Cug95] Cugliandolo LF and Dean DS, *Journal of Physics A: Mathematical and General*, **28**:4213 (1995), `arXiv:cond-mat/9502075`.

[Cug03] Cugliandolo LF, in JLB et al, ed., *Slow Relaxations and Non-Equilibrium Dynamics in Condensed Matter (Les Houches LXXVII)*, 367–521, Springer, Heidelberg (2003).

[Dag94] Dagotto E, *Rev Mod Phys*, **66**:763 (1994), `arXiv:cond-mat/9311013`.

[Dal99] Dalfovo F *et al.*, *Rev Mod Phys*, **71**:463 (1999).

[Dau02] Dauxois T *et al.*, in *Dynamics and Thermodynamics of Systems with Long Range Interactions*, Lecture Notes in Physics, Springer Berlin Heidelberg (2002), `arXiv:cond-mat/0208455`.

[DF97] Di Francesco P *et al.*, *Conformal Field Theory*, Graduate Texts in Contemporary Physics, Springer (1997).

[Dic54] Dicke RH, *Phys Rev*, **93**:99 (1954).

[Die83] Diehl H, in C Domb and J Lebowitz, eds., *Field-theoretical approach to critical behaviour at surfaces*, *Phase transitions and critical phenomena*, vol. 10, 76, Academic Press, London (1983).

[dlT22] de la Tour C, *Ann Chim Phys*, **21**:127 (1822).

[Dom96] Domb C, *The Critical Point: A Historical Introduction To The Modern Theory Of Critical Phenomena*, Taylor & Francis (1996).

[Dro15] Drozdov AP *et al.*, *Nature*, **525**:73 (2015), letter, `arXiv:1506.08190`.

[Dur15] Durang X *et al.*, *Phys Rev E*, **91**:062118 (2015), `arXiv:1309.5750`.

[Dur17] Durang X and Henkel M (2017), `arXiv:1708.08237`.

[Dut15] Dutta A *et al.*, *Quantum Phase Transitions in Transverse Field Spin Models: From Statistical Physics to Quantum Information*, Cambridge University Press (2015), `arXiv:1012.0653`.

[Ebb08]   Ebbinghaus M *et al.*, *The European Physical Journal B*, **63**:85 (2008), `arXiv:0709.3220`.

[Ehr10]   Ehre D *et al.*, *Science*, **327**:672 (2010).

[Ein05]   Einstein A, *Annalen der Physik*, **322**:549 (1905).

[Elm96]   Elmers HJ *et al.*, *Journal of Applied Physics*, **79**:4984 (1996).

[Elo17]   Elouard C *et al.*, *Nature Quantum Information*, **3**:9 (2017), `arXiv:1507.00312`.

[Eng02]   Englert BG and Morigi G, in A Buchleitner and K Hornberger, eds., *Coherent Evolution in Noisy Environments*, 55–106, Springer, Heidelberg (2002).

[Fel71]   Feller W, *An Introduction to Probability Theory and Its Applications*, vol. 2, Wiley, New York (1971).

[Fey65]   Feynman R and Hibbs A, *Quantum mechanics and path integrals*, International series in pure and applied physics, McGraw-Hill (1965).

[Fil16]   Filippone M *et al.*, *Phys Rev A*, **93**:011602 (2016), `arXiv:1410.5841`.

[Fis89]   Fisher MPA *et al.*, *Phys Rev B*, **40**:546 (1989).

[Fle03]   Fleischer J *et al.*, *Nuclear Physics B*, **672**:303 (2003), `arXiv:hep-ph/0307113`.

[Flo17]   Flottat T *et al.*, *Phys Rev B*, **95**:144501 (2017), `arXiv:1701.01624`.

[Fra78]   Fradkin E and Susskind L, *Phys Rev D*, **17**:2637 (1978).

[Fus02]   Fusco N and Zannetti M, *Phys Rev E*, **66**:066113 (2002), `arXiv:cond-mat/0210502`.

[Ga16]   Guimarães PH *et al.*, *Phys Rev E*, **94**:032139 (2016), `arXiv:1609.03885`.

[Gao94]   Gao L *et al.*, *Phys Rev B*, **50**:4260 (1994).

[Gar04]   Gardiner C and Zoller P, *Quantum Noise: A Handbook of Markovian and Non-Markovian Quantum Stochastic Methods with Applications to Quantum Optics*, Springer Series in Synergetics, Springer (2004).

[Gar11]   Garraway BM, *Philosophical Transactions of the Royal Society of London A: Mathematical, Physical and Engineering Sciences*, **369**:1137 (2011).

[Ger63]   Gersch HA and Knollman GC, *Phys Rev*, **129**:959 (1963).

[Gis84]   Gisin N, *Phys Rev Lett*, **52**:1657 (1984).

[God00]   Godrèche C and Luck JM, *Journal of Physics A: Mathematical and General*, **33**:9141 (2000), `arXiv:cond-mat/0001264`.

[God02]   Godrèche C and Luck JM, *Journal of Physics: Condensed Matter*, **14**:1589 (2002), `arXiv:cond-mat/0109212`.

[Gre02]   Greiner M *et al.*, *Nature*, **415**:39 (2002).

[Gut63]   Gutzwiller MC, *Phys Rev Lett*, **10**:159 (1963).

[Gut65]   Gutzwiller MC, *Phys Rev*, **137**:A1726 (1965).

[Has06]   Hase MO and Salinas SR, *Journal of Physics A: Mathematical and General*, **39**:4875 (2006), `arXiv:cond-mat/0512286`.

[Has10]   Hasan MZ and Kane CL, *Rev Mod Phys*, **82**:3045 (2010), `arXiv:1002.3895`.

[Hei28]   Heisenberg W, *Zeitschrift für Physik*, **49**:619 (1928).

[Hei15]   Heil C and Boeri L, *Phys Rev B*, **92**:060508 (2015), `arXiv:1507.02522`.

[Hel00]   Helbing D *et al.*, *Phys Rev Lett*, **84**:1240 (2000), `arXiv:cond-mat/9904326`.

[Hen84a] Henkel M, *Journal of Physics A: Mathematical and General*, **17**:L795 (1984).

[Hen84b] Henkel M and Hoeger C, *Zeitschrift für Physik B Condensed Matter*, **55**:67 (1984).

[Hen87a] Henkel M, *Journal of Physics A: Mathematical and General*, **20**:3969 (1987).

[Hen87b] Henkel M, *Journal of Physics A: Mathematical and General*, **20**:995 (1987).

[Hen99]   Henkel M, *Conformal Invariance and Critical Phenomena*, Texts and monographs in physics, Springer (1999).

[Hen01]   Henkel M and Schollwöck U, *Journal of Physics A: Mathematical and General*, **34**:3333 (2001), `arXiv:cond-mat/001006`.

[Hen09]   Henkel M *et al.*, *Non-Equilibrium Phase Transitions: Volume 1: Absorbing Phase Transitions*, Theoretical and Mathematical Physics, Springer, Heidelberg (2009).

[Hen10]   Henkel M and Pleimling M, *Non-Equilibrium Phase Transitions: Volume 2: Ageing and Dynamical Scaling Far from Equilibrium*, Theoretical and Mathematical Physics, Springer, Heidelberg (2010).

[Hen15]   Henkel M and Durang X, *Journal of Statistical Mechanics: Theory and Experiment*, **2015**:P05022 (2015), `arXiv:1501.07745`.

[Hir82]   Hirakawa K, *Journal of Applied Physics*, **53**:1893 (1982).

[Hof96]   Hofstetter W and Henkel M, *Journal of Physics A: Mathematical and General*, **29**:1359 (1996), `arXiv:cond-mat/9512137`.

[Hoh77]   Hohenberg PC and Halperin BI, *Rev Mod Phys*, **49**:435 (1977).

[Hoh15]   Hohenberg P and Krekhov A, *Physics Reports*, **572**:1 (2015), an introduction to the Ginzburg–Landau theory of phase transitions and nonequilibrium patterns.

[Hol40]   Holstein T and Primakoff H, *Phys Rev*, **58**:1098 (1940).

[Hol01]   Holleman AF and Wiberg E, *Inorganic Chemistry*, Academic Press (2001).

[Hua01]   Huang K, *Introduction to Statistical Physics*, Taylor & Francis (2001).

[Hum20]   Humbert P, *C R Acad Sci, Paris*, **171**:490 (1920).

[Hum22]   Humbert P, *Proceedings of the Royal Society of Edinburgh*, **41**:73–96 (1922).

[Ili14]   Ilievski E and Prosen T, *Nuclear Physics B*, **882**:485 (2014), `arXiv:1402.0342`.

[Jäg96]   Jäger E and Perthel R, *Magnetische Eigenschaften von Festkörpern*, Akademie Verlag, Berlin (1996).

[Jeo95]   Jeon S, *Phys Rev D*, **52**:3591 (1995).

[Jos77]   José JV *et al.*, *Phys Rev B*, **16**:1217 (1977).

[Jos78]   José JV *et al.*, *Phys Rev B*, **17**:1477 (1978).

[Joy72]   Joyce GS, in C Domb, M Green and J Lebowitz, eds., *Phase Transitions and Critical Phenomena*, vol. 2, 375, Academic Press, London (1972).

[Kad09]   Kadanoff LP, *Journal of Statistical Physics*, **137**:777 (2009), `arXiv:0906.0653`.

[Kar00]   Karevski D, *Journal of Physics A: Mathematical and General*, **33**:L313 (2000), `arXiv:cond-mat/0009038`.

[Kar09]   Karevski D and Platini T, *Phys Rev Lett*, **102**:207207 (2009).

[Kar13]   Karevski D *et al.*, *Phys Rev Lett*, **110**:047201 (2013), `arXiv:1211.7010`.

[Kat62]   Katsura S, *Phys Rev*, **127**:1508 (1962).

[Kat84]   Katz S *et al.*, *Journal of Statistical Physics*, **34**:497 (1984).

[Ken06a] Kenna R *et al.*, *Phys Rev Lett*, **96**:115701 (2006), `arXiv:cond-mat/0605162`.

[Ken06b] Kenna R *et al.*, *Phys Rev Lett*, **97**:155702 (2006), `arXiv:cond-mat/0608127`).

[Kib80]   Kibble T, *Physics Reports*, **67**:183 (1980).

[Kir15]   Kirkpatrick TR and Belitz D, *Phys Rev B*, **91**:214407 (2015), `arXiv:1503.04175`.

[Kni12]   Kniehl BA and Tarasov OV, *Nuclear Physics B*, **854**:841 (2012), `arXiv:1108.6019`.

[Kob00]   Kobe S, *Brazilian Journal of Physics*, **30**:649 (2000).

[Kog79]   Kogut JB, *Rev Mod Phys*, **51**:659 (1979).

[Kot86]   Kotliar G and Ruckenstein AE, *Phys Rev Lett*, **57**:1362 (1986).

[Kra95]   Kravchenko SV *et al.*, *Phys Rev B*, **51**:7038 (1995), `arXiv:cond-mat/9412103`.

[Kra12]   Kraemer C *et al.*, *Science*, **336**:1416 (2012).

[Kub57a] Kubo R, *Journal of the Physical Society of Japan*, **12**:570 (1957).

[Kub57b] Kubo R *et al.*, *Journal of the Physical Society of Japan*, **12**:1203 (1957).

[Lan08]   Langevin P, *C R Acad Sci (Paris)*, **146**:530 (1908).

[Lan15a] Landi GT and Karevski D, *Phys Rev B*, **91**:174422 (2015), `arXiv:1501.07732`.

[Lan15b] Lang G *et al.*, *Phys Rev A*, **91**:063619 (2015), `https://arxiv.org/abs/1503.08038`.

[Lan16a] Landi GT and Karevski D, *Phys Rev E*, **93**:032122 (2016), `arXiv:1412.4230`.

[Lan16b] Landig R *et al.*, *Nature*, **532**:476 (2016), `arXiv:1511.00007`.

[Lan17]   Lang G *et al.* (2017), `arXiv:1609.08865`.

[Lax63]   Lax M, *Phys Rev*, **129**:2342 (1963).

[Leg01]   Leggett AJ, *Rev Mod Phys*, **73**:307 (2001).

[Leg03]   Leggett AJ, *Rev Mod Phys*, **75**:1083 (2003).

[Lew52]   Lewis HW and Wannier GH, *Phys Rev*, **88**:682 (1952).

[Lew07]   Lewenstein M *et al.*, *Advances in Physics*, **56**:243 (2007), `arXiv:cond-mat/0606771`.

[Lie61]   Lieb E *et al.*, *Annals of Physics*, **16**:407 (1961).

[Lin76]   Lindblad G, *Comm Math Phys*, **48**:119 (1976).

[Liu14]   Liu H and Wang W, *Journal of Mathematical Analysis and Applications*, **409**:100 (2014).

[Ma97]   Ma Yq and Figueiredo W, *Phys Rev B*, **55**:5604 (1997).

[Ma00]   Ma S, *Modern Theory Of Critical Phenomena*, Advanced Books Classics, Avalon Publishing (2000).

[Mah00]   Mahan G, *Many-Particle Physics*, Physics of Solids and Liquids, Springer (2000).

[Map98]   Maple M, *Journal of Magnetism and Magnetic Materials*, **177**:18 (1998), `arXiv:cond-mat/9802202`.

[Mar05]   Marro J and Dickman R, *Nonequilibrium Phase Transitions in Lattice Models*, Aléa-Saclay, Cambridge University Press (2005).

[Mat73]   Mathai A and Saxena R, *Generalized hypergeometric functions with applications in statistics and physical sciences*, Lecture notes in mathematics, Springer, Heidelberg (1973).

[Mat10]   Mathai A *et al.*, *The H-Function: Theory and Applications*, Springer New York (2010).

[Maz06]   Mazenko GF, *Nonequilibrium Statistical Mechanics*, Wiley-VCH Verlag GmbH (2006).

[McC71]   McCoy BM *et al.*, *Phys Rev A*, **4**:2331 (1971).

[Mic17]   Michailidis AA *et al.* (2017), `arXiv:1706.05026`.

[New06]   Newburgh R *et al.*, *American Journal of Physics*, **74**:478 (2006).

[Nie95]   Nieuwenhuizen TM, *Phys Rev Lett*, **74**:4293 (1995), `arXiv:cond-mat/9408056`.

[Nis11]   Nishimori H and Ortiz G, *Elements of Phase Transitions and Critical Phenomena*, Oxford Graduate Texts, Oxford University Press, Oxford (2011).

[Obe72]   Obermair G, in JI Budnick and MP Kawars, eds., *Dynamical Aspects of Critical Phenomena*, 137, Academic Press, New York (1972).

[Oli06]   Oliveira MH *et al.*, *Phys Rev B*, **74**:184101 (2006).

[Olv10]   Olver FW *et al.*, *NIST Handbook of Mathematical Functions*, Cambridge University Press, New York, NY, USA, 1st ed. (2010).

[Onn11]   Onnes HK, *Proc K Ned Akad Wet*, **13**:1107 (1911).

[Ons44]   Onsager L, *Phys Rev*, **65**:117 (1944).

[Pal10]   Pal A and Huse DA, *Phys Rev B*, **82**:174411 (2010), `arXiv:1010.1992`.

[Pap07]   Papon P *et al.*, *The Physics of Phase Transitions: Concepts and Applications*, Advanced Texts in Physics, Springer Berlin Heidelberg (2007).

[Pea77]   Pearce PA and Thompson CJ, *Journal of Statistical Physics*, **17**:189 (1977).

[Pei36]   Peierls R, *Mathematical Proceedings of the Cambridge Philosophical Society*, **32**:477–481 (1936).

[Per09]   Perrin J, *Annales de Chimie et de Physique*, **18**:5 (1909).

[Per94]   Percival IC, *Proceedings of the Royal Society of London A: Mathematical, Physical and Engineering Sciences*, **447**:189 (1994).

[Per17]   Perakis F *et al.*, *Proceedings of the National Academy of Sciences* (2017).

[Pet02]   Pethick C and Smith H, *Bose-Einstein Condensation in Dilute Gases*, Cambridge University Press (2002).

[Pic02]   Picone A and Henkel M, *Journal of Physics A: Mathematical and General*, **35**:5575 (2002), `arXiv:cond-mat/0203411`.

[Pic04]   Picone A and Henkel M, *Nuclear Physics B*, **688**:217 (2004), `arXiv:cond-mat/0402196`.

[Pit03]   Pitaevskii L and Stringari S, *Bose-Einstein Condensation*, International Series of Monographs on Physics, Clarendon Press (2003).

[Pod14]   Podolsky D *et al.*, *Phys Rev B*, **89**:214408 (2014), `arXiv:1403.2422`.

[Pol87]   Polyakov AM, *Gauge Fields and Strings*, Contemporary concepts in physics, Taylor & Francis (1987).

[Pol02]   Polyanin AD and Zaitsev VF, *Handbook of Exact Solutions for Ordinary Differential Equations*, Chapman and Hall, London, 2nd ed. (2002).

[Pop13]   Popkov V *et al.*, *Phys Rev E*, **88**:062118 (2013), `arXiv:1310.1315`.

[Pop15]   Popkov V and Prosen T, *Phys Rev Lett*, **114**:127201 (2015), `arXiv:1501.02230`.

[Pre04]   Predel B *et al.*, *Phase Diagrams and Heterogeneous Equilibria: A Practical Introduction*, Engineering Materials and Processes, Springer Berlin Heidelberg (2004).

[Pri84]   Privman V and Fisher ME, *Phys Rev B*, **30**:322 (1984).

[Pri93]   Privman V *et al.*, in C Domb, M Green and J Lebowitz, eds., *Phase Transitions and Critical Phenomena*, vol. 14, Academic Press, London (1993).

[Pro08]   Prosen T, *New Journal of Physics*, **10**:043026 (2008), `arXiv:0801.1257`.

[Pro10]   Prosen T, *Journal of Statistical Mechanics: Theory and Experiment*, **2010**:P07020 (2010), `arXiv:1005.0763`.

[Pro11a] Prosen T, *Phys Rev Lett*, **106**:217206 (2011), `arXiv:1103.1350`.

[Pro11b] Prosen Tcv, *Phys Rev Lett*, **107**:137201 (2011), `arXiv:1106.2978`.

[Pro12]   Prosen T, *Physica Scripta*, **86**:058511 (2012), `arXiv:1205.3126`.

[Pro14]   Prosen Tcv, *Phys Rev Lett*, **112**:030603 (2014), `arXiv:1310.4420`.

[Pro15]   Prosen T, *Journal of Physics A: Mathematical and Theoretical*, **48**:373001 (2015), `arXiv:1504.00783`.

[Pru86]   Prudnikov A and Marichev O, *Integrals and Series: Special functions*, Gordon and Breach Science Publishers (1986).

[Pru92a] Prudnikov A and Marichev O, *Integrals and Series: Direct Laplace transforms*, 4, Gordon and Breach Science Publishers (1992).

[Pru92b] Prudnikov A and Marichev O, *Integrals and Series: Inverse Laplace transforms*, Gordon and Breach Science Publishers (1992).

[Rad03]   Radzihovsky L and Clark NA, *Phys Rev Lett*, **90**:189603 (2003), `arXiv:cond-mat/0212315`.

[RI07]   Romero-Isart O *et al.*, *Journal of Physics A: Mathematical and Theoretical*, **40**:8019 (2007), `arXiv:quant-ph/0703177`.

[Ron78]   Ronca G, *The Journal of Chemical Physics*, **68**:3737 (1978).

[Ros12]   Rossatto DZ *et al.*, *Phys Rev A*, **86**:035802 (2012), `arXiv:1210.0239`.

[Ros14]   Ross KA *et al.*, *Phys Rev Lett*, **112**:057201 (2014), `arXiv:1401.1176`.

[Sac01]   Sachdev S, *Quantum Phase Transitions*, Cambridge University Press (2001).

[Sac11]   Sachdev S and Keimer B, *Physics Today*, **64**:29 (2011), `arXiv:1102.4628`.

[San16]   Santos JP and Landi GT, *Phys Rev E*, **94**:062143 (2016), `arxiv:1610.05126`.

[Sch05]   Schulman L, *Techniques and Applications of Path Integration*, Wiley (2005).

[Sch14]   Schaller G, *Open Quantum Systems Far from Equilibrium*, *Lecture Notes in Physics*, vol. 881, Springer International Publishing (2014).

[SG04]   Serral Gracià R and Nieuwenhuizen TM, *Phys Rev E*, **69**:056119 (2004), `arXiv:cond-mat/0304150`.

[Shp07] Shpot MA, *Journal of Mathematical Physics*, **48**:123512 (2007), `arXiv:0711.2742`.

[Shu81] Shukla P and Singh S, *Phys Rev B*, **23**:4661 (1981).

[Sla66] Slater L, *Generalized Hypergeometric Functions*, Cambridge University Press, Cambridge (1966).

[Som49] Sommerfeld A, *Albert Einstein: Philosopher-Scientist*, **VII**:105 (1949).

[Son97] Sondhi SL *et al.*, *Rev Mod Phys*, **69**:315 (1997), `arXiv:cond-mat/9609279`.

[Sre79] Srednicki M, *Phys Rev B*, **20**:3783 (1979).

[Sri85] Srivastava H and Karlsson P, *Multiple Gaussian hypergeometric series*, Ellis Horwood series in mathematics and its applications: Statistics and operational research, E. Horwood (1985).

[Sta68] Stanley HE, *Phys Rev*, **176**:718 (1968).

[Str07] Strogatz S, *Nonlinear Dynamics And Chaos*, Studies in nonlinearity, Sarat Book House (2007).

[Suz71] Suzuki M, *Progress of Theoretical Physics*, **46**:1337 (1971).

[Tai06] Tailleur J *et al.*, *Journal of Statistical Physics*, **122**:557 (2006), `arXiv:cond-mat/0503545`.

[Tar08] Taroni A *et al.*, *Journal of Physics: Condensed Matter*, **20**:275233 (2008), `arXiv:0802.0480`.

[Täu14] Täuber UC, *Critical Dynamics*, Cambridge University Press, Cambridge (2014).

[Ton09] Tonchev NS *et al.*, *J Optoel Adv Mat*, **11**:1142 (2009).

[vD10] van Delft D, *Physics Today*, **63**:38 (2010).

[vH15] van Horssen M and Garrahan JP, *Phys Rev E*, **91**:032132 (2015), `arXiv:1411.7913`.

[Vil80] Villain, J *et al.*, *J Phys France*, **41**:1263 (1980).

[Voj96] Vojta T, *Phys Rev B*, **53**:710 (1996).

[Voj03] Vojta M, *Reports on Progress in Physics*, **66**:2069 (2003), `arXiv:cond-mat/0309604`.

[Vol84] Vollhardt D, *Rev Mod Phys*, **56**:99 (1984).

[Wac07] Waclaw B, *PhD thesis* (2007), `arXiv:0704.3702`.

[Wal15] Wald S and Henkel M, *Journal of Statistical Mechanics: Theory and Experiment*, **2015**:P07006 (2015), `arXiv:cond-mat/0309604`.

[Wal16] Wald S and Henkel M, *Journal of Physics A: Mathematical and Theoretical*, **49**:125001 (2016), `arXiv:1511.03347`.

[Wal17a] Wald S and Henkel M (2017), `arXiv:1707.06275`.

[Wal17b] Wald S *et al.* (2017), `arXiv:1707.06273`.

[Wal17c] Wald S *et al.* (2017), `arXiv:17xx.yyyyy`.

[Wei99] Weiss U, *Quantum Dissipative Systems*, *Series in modern condensed matter physics*, vol. 10, World Scientific, 2nd ed. (1999).

[Wen15] Wendenbaum P *et al.*, *Phys Rev A*, **91**:040303 (2015).

[Wes86] Westerholt K, *Journal of Magnetism and Magnetic Materials*, **54**:721 (1986).

[Wes87]   Westerholt K, *Journal of Magnetism and Magnetic Materials*, **66**:253 (1987).

[Wid46]   Widder D, *The Laplace transform*, Princeton mathematical series, Princeton university press, Princeton, 2nd ed. (1946).

[Wil75]   Wilson KG, *Rev Mod Phys*, **47**:773 (1975).

[Wol17]   Wolfram functions (2017).

[Wri35]   Wright EM, *Journal of the London Mathematical Society*, **s1-10**:286 (1935).

[Wri40]   Wright EM, *Proceedings of the London Mathematical Society*, **s2-46**:389 (1940).

[Wri52]   Wright EM, *J London Math Soc*, **27**:254 (1952).

[Yeo92]   Yeomans J, *Statistical Mechanics of Phase Transitions*, Oxford University Press (1992).

[Zam89]   Zamolodchikov AB, *International Journal of Modern Physics A*, **04**:4235 (1989).

[Zia02]   Zia RKP *et al.*, *American Journal of Physics*, **70**:384 (2002), `arXiv:cond-mat/0108502`.